Short Term, Low Strain Radial Tensile Stiffness of a Triaxial Geogrid with Integral Junctions

by

Paul Stowell

A thesis submitted in fulfilment of the degree of Master of Philosophy

Volume II

University of Nottingham
Nottingham, UK

2020

List of Tables

Table 1.1 Examples of geotextile manufacturers by category.

Table 1.2 Examples of geogrid manufacturers by category.

Table 3.1 Typical index properties for uniaxial (RE500 series) geogrids

Table 3.2 Typical performance properties for uniaxial (RE500 series) geogrids

Table 3.3 Mean test data results for all four testing directions of a Tensar TX160 as plotted in Figs 3.25. to Fig 3.28.

Table 4.1 Theoretical percentage open area of TX geogrids

Table 4.2 Basic dimensions of the TX150 geogrid

Table 4.3 Basic dimensions of the TX160 geogrid

Table 4.4 Basic dimensions of the TX170 geogrid

Table 4.5 Basic dimensions of the TX180 geogrid

Table 4.6 Characteristics and Properties of TX150 according to the EOTA TR41:2012

Table 4.7 Characteristics and Properties of TX160 according to the EOTA TR41:2012

Table 4.8 Characteristics and Properties of TX170 according to the EOTA TR41:2012

Table 4.9 Characteristics and Properties of TX180 according to the EOTA TR41:2012

Table 4.10 Properties of TX150 according to CE Marking for reinforcement specifications

Table 4.11 Properties of TX160 according to CE Marking for reinforcement specifications

Table 4.12 Properties of TX170 according to CE Marking for reinforcement specifications

Table 4.13 Properties of TX180 according to CE Marking for reinforcement specifications

Table 5.1 Mean properties of TX160 (Batch Ref: 056218, TAP 1 Year) as determined in the four directions and tested in accordance with the EOTA TR41:2012

Table 5.2 Mean properties of TX160 (Batch Ref: 059839, TAP 1 Week) as determined in the four directions and tested in accordance with the EOTA TR41:2012

Table 5.3 Batch Ref: 056218 tested at a strain rate of 20% of gauge length straight off production tested by QC

Table 5.4 Batch Ref: 056218 tested at a strain rate of 20% of gauge length TAP for 1 year

Table 5.5 Batch Ref: 056218 Secant Stiffness at 0.5%

Table 5.6 Batch Ref: 056218 Secant Stiffness at 2%

Table 5.7 Batch Ref: 059839 tested at a strain rate of 20% of gauge length straight after production

Table 5.8 Batch Ref: 059839 tested at a strain rate of 20% of gauge length TAP 1 week

Table 5.9 Batch Ref: 059839 Secant Stiffness at 0.5%

Table 5.10 Batch Ref: 059839 Secant Stiffness at 2%

Table 5.11 Batch Ref: 056218 tested at a strain rate of 2% of gauge length TAP 1 year

Table 5.12 Batch Ref: 056218 tested at a strain rate of 0.2% of gauge length TAP 1 year

Table 5.13 Batch Ref: 056218 tested at a strain rate of 0.02% of gauge length TAP for 1 year

Table 6.1 Calculations of Applied Load/m at Outer Clamps, Average Load/m Over Gauge Length and Radius at Average Load/m for all radial test specimens tested at 0°, 30°, 60° and 90° directions at four different loads

Table 6.2 Calculated local load/m and local strains for 30kg load tested in the 0° direction

Table 6.3 Calculated local load/m and local strains for 30kg load tested in the 60° direction

Table 6.4 Calculated local load/m and local strains for 30kg load tested in the 90° direction

Table 6.5 Calculated local load/m and local strains for 30kg load tested in the 30° direction

Table 6.6 Calculated local load/m and local strains for 40kg load tested in the 0° direction

Table 6.7 Calculated local load/m and local strains for 40kg load tested in the 60° direction

Table 6.8 Calculated local load/m and local strains for 40kg load tested in the 90° direction

Table 6.9 Calculated local load/m and local strains for 40kg load tested in the 30° direction

Table 6.10 Calculated local load/m and local strains for 50kg load tested in the 0° direction

Table 6.11 Calculated local load/m and local strains for 50kg load tested in the 60° direction

Table 6.12 Calculated local load/m and local strains for 50kg load tested in the 90° direction

Table 6.13 Calculated local load/m and local strains for 50kg load tested in the 30° direction

Table 6.14 Calculated local load/m and local strains for 60kg load tested in the 0° direction

Table 6.15 Calculated local load/m and local strains for 60kg load tested in the 60° direction

Table 6.16 Calculated local load/m and local strains for 60kg load tested in the 90° direction

Table 6.17 Calculated local load/m and local strains for 60kg load tested in the 30° direction

Table 7.1 Upper and lower gradients of CRS, Radial Creep, and Uniaxial Creep testing with and without an assumed locked-in stress

List of Figures

Fig 1.1 Examples of geotextile fabrics. To the left are non-woven examples. To the right are woven geotextile fabrics, in which you can see the weave pattern, Study.com (2017)

Fig 1.2 Examples of the three major categories of geogrids, Koerner (2009)

Fig 1.3 Outward radial load distribution of triaxial geogrids, Tensar International Limited (2018)

Fig 2.1 Principal of the Netlon Process, after Mercer (1986)

Fig 2.2 Biplanar junctions produced by the Netlon Process, after Mercer (1986)

Fig 2.3 The Tensar Process, after Mercer (1986).

Fig 2.4 Specification for Tensar SR2, after Paul (1994).

Fig 2.5 Schematic alignment of molecular orientation in a biaxially stretched junction, after Mercer (1986)

Fig 2.6 A grooved polymer sheet prepared for biaxial orientation, after Paul (1984)

Fig 2.7 Specification for Tensar SS1, after Paul (1994)

Fig 2.8 Specification for Tensar SS2, after Paul (1994)

Fig 2.9 Specification for Tensar SS3, after Paul (1994)

Fig 2.10 Diabolo shaped punch, after Paul (1994)

Fig 2.11 Diabolo punched sheet showing two yield zones upon stretching, after Mercer (1986)

Fig 2.12 Specification for Tensar SR80, after Paul (1994)

Fig 2.13 Specifications for the Tensar RE series geogrids, Tensar International Limited (no date)

Fig 2.14 Specification for the Tensar RE500 Series geogrids, Tensar International Limited (no date)

Fig 2.15 Specification for Tensar AR1, after Paul (1994).

Fig 2.16 Specification for Tensar SS30, Tensar International Limited (no date)

Fig 2.17 Specification for Tensar SSLA30, Tensar International Limited (no date)

Fig 2.18 Polar diagram of ultimate strength response, after Walsh (2006)

Fig 2.19 Polar diagram of secant modulus response calculated at maximum load, after Walsh (2006)

Fig 2.20 Polar diagram of grid strength at 2% strain response, after Walsh (2006)

Fig 2.21 TriAx punch geometry, Walsh (2006)

Fig 2.22 Typical TriAx geometry upon stretching the repeat cluster in Fig 2.21, Tensar Technologies Limited (2004)

Fig 2.23 “Across the flats” (AF) dimension of the initial TriAx, Walsh (2006)

Fig 2.24 TX160 technical data, Tensar International Limited (no date)

Fig 2.25 TX170-G technical data, Tensar International Limited (no date)

Fig 2.26 TX190L technical data, Tensar International Limited (no date)

Fig 2.27 TX130S technical data, Tensar International Limited (no date)

Fig 3.1 Isometric view and half section of the clamps used to determine the load-strain properties

Fig 3.2 Typical load-strain curve for a Tensar SR2 geogrid, after McGown (1984)

Fig 3.3 Typical load-strain curves for a Tensar RE560 geogrid

Fig 3.4 Creep performance of Tensar SR2 geogrids at 20°C when subjected to a range of loads, after McGown (1984)

Fig 3.5 Creep performance of Tensar RE560 at 40°C when subjected to a load of 47.5% of its ultimate strength

Fig 3.6 Typical load-strain curves for Tensar SS20 tested in the machine direction

Fig 3.7 Typical load-strain curves for Tensar SS20 tested in the cross-machine direction

Fig 3.8 Cruciform shape of geogrid used for biaxial testing, Kupec (2004)

Fig 3.9 Index test curves for Tensar SS2, McGown (1984).

Fig 3.10 Comparison of uniaxial and biaxial load-strain behaviour of a geogrid with integral junctions, Kupec (2004)

Fig 3.11 Creep performance of Tensar SS20 MD at 10°C when subjected to a load of 30% of its ultimate strength

Fig 3.12 Creep performance of Tensar SS20 XMD at 10°C when subjected to a load of 30% of its ultimate strength

Fig 3.13 Comparison of Tensar SS20 MD & SS20 XMD creep performance

Fig 3.14 Uniaxial performance test results for a 40kN biaxial geogrid, with integral junctions, in the MD & XMD directions, Kupec (2004)

Fig 3.15 Uniaxial performance test results for a 30kN biaxial geogrid, with integral junctions, in the MD & XMD directions, Kupec (2004)

Fig 3.16 Uniaxial performance test results for a 20kN biaxial geogrid, with integral junctions, in the MD & XMD directions, Kupec (2004)

Fig 3.17 Biaxial performance test results for a 40kN biaxial geogrid, with integral junctions, in the MD & XMD directions, Kupec (2004)

Fig 3.18 Biaxial performance test results for a 30kN biaxial geogrid, with integral junctions, in the MD & XMD directions, Kupec (2004)

Fig 3.19 Biaxial performance test results for a 20kN biaxial geogrid, with integral junctions, in the MD & XMD directions, Kupec (2004)

Fig 3.20 Comparisons of uniaxial and biaxial performance test results for a 40kN biaxial geogrid with integral junctions tested at 30 and 50% of the ultimate strength, in the MD & XMD directions, Kupec (2004)

Fig 3.21 Comparisons of uniaxial and biaxial performance test results for a 30kN biaxial geogrid with integral junctions tested at 30 and 50% of the ultimate strength, in the MD & XMD directions, Kupec (2004)

Fig 3.22 Comparisons of uniaxial and biaxial performance test results for a 20kN biaxial geogrid with integral junctions tested at 30 and 50% of the ultimate strength, in the MD & XMD directions, Kupec (2004)

Fig 3.23 TriAx testing directions devised by Walsh (2003)

Fig 3.24 Triaxial testing directions as used in the EOTA TR41 document, EOTA (2012)

Fig 3.25 Typical wide width test data plot for a Tensar TX160 geogrid tested in the 0° direction in accordance to the ETA TR41 report

Fig 3.26 Typical wide width test data plot for a Tensar TX160 geogrid tested in the 30° direction in accordance to the ETA TR41 report

Fig 3.27 Typical wide width test data plot for a Tensar TX160 geogrid tested in the 60° direction in accordance to the ETA TR41 report

Fig 3.28 Typical wide width test data plot for a Tensar TX160 geogrid tested in the 90° direction in accordance to the ETA TR41 report

Fig 3.29 Trafficking test results, Jenner et al (2002), interpreted by Tensar International (2019), showing that pure tensile strength is not a good indicator of trafficking performance

Fig 3.30 Graph showing how different classes of geogrid affects the mechanically stabilised unbound layer and the effective thickness of that layer, CROW (2002)

Fig 4.1 Process Capability (Cp), showing the relationship between the width of the spread and the specification width, after Nielson (2020)

Fig 4.2 Process Capability Index (Cpk), showing the relationship with Cp and specification width. (If Cpk = Cp, the process sits in the middle of the specification limits), after Nielson (2020)

Fig 5.1 Q.C test data for TX160 (Batch Ref: 056218) tested at 0° (machine direction)

Fig 5.2 Q.C test data for TX160 (Batch Ref: 056218) tested at 30° (‘rib’ direction)

Fig 5.3 Q.C test data for TX160 (Batch Ref: 056218) tested at 60° (‘mid-rib’ direction)

Fig 5.4 Q.C test data for TX160 (Batch Ref: 056218) tested at 90° (cross machine direction)

Fig 5.5 Q.C test data for TX160 (Batch Ref: 059839) tested at 0° (machine direction)

Fig 5.6 Q.C test data for TX160 (Batch Ref: 059839) tested at 30° (‘rib’ direction)

Fig 5.7 Q.C test data for TX160 (Batch Ref: 059839) tested at 60° (‘mid-rib’ direction)

Fig 5.8 Q.C test data for TX160 (Batch Ref: 059839) tested at 90° (cross machine direction)

Fig 5.9 Index test data for TX160 (Batch Ref: 056218, TAP 1 Year) tested at 0° (machine direction)

Fig 5.10 Index test data for TX160 (Batch Ref: 056218, TAP 1 Year) tested at 30° (‘rib’ direction)

Fig 5.11 Index test data for TX160 (Batch Ref: 056218, TAP 1 Year) tested at 60° (‘mid-rib’ direction)

Fig 5.12 Index test data for TX160 (Batch Ref: 056218, TAP 1 Year) tested at 90° (cross machine direction)

Fig 5.13 Index test data for TX160 (Batch Ref: 059839, TAP 1 Week) tested at 0° (machine direction)

Fig 5.14 Index test data for TX160 (Batch Ref: 059839, TAP 1 Week) tested at 30° (‘rib’ direction)

Fig 5.15 Index test data for TX160 (Batch Ref: 059839, TAP 1 Week) tested a 60° (‘mid-rib’ direction)

Fig 5.16 Index test data for TX160 (Batch Ref: 059839, TAP 1 Week) tested at 90° (cross machine direction)

Fig 5.17 Polar plot showing 'Radial Secant Stiffness at 0.5% Strain' of TX160 (Batch Ref: 056218) tested for Q.C. purposes and TAP for 1 year

Fig 5.18 Polar plot showing 'Radial Secant Stiffness at 2% Strain' of TX160 (Batch Ref: 056218) tested for Q.C. purposes and TAP for 1 year

Fig 5.19 Polar plot showing 'Radial Secant Stiffness at 0.5% Strain' of TX160 (Batch Ref: 059839) tested straight off the production line and after 1 week

Fig 5.20 Polar plot showing 'Radial Secant Stiffness at 2% Strain' of TX160 (Batch Ref: 059839) tested straight off the production line and after 1 week

Fig 5.21 Polar plot showing 'Radial Secant Stiffness at 0.5% Strain' of TX160 (Batch Ref: 056218) tested by quality control straight off the production line and tested after 1 year, with Min, Mean & Max specifications

Fig 5.22 Polar plot showing 'Radial Secant Stiffness at 2% Strain' of TX160 (Batch Ref: 056218) tested by quality control straight off the production line and tested after 1 year, with Min, Mean & Max specifications

Fig 5.23 Polar plot showing 'Radial Secant Stiffness at 0.5% Strain' of TX160 (Batch Ref: 059839) tested by quality control straight off the production line and tested after 1 week, with Min, Mean & Max specifications

Fig 5.24 Polar plot showing 'Radial Secant Stiffness at 2% Strain' of TX160 (Batch Ref: 059839) tested by quality control straight off the production line and tested after 1 week, with Min, Mean & Max specifications

Fig 5.25 Graph showing Max. Load Vs 0.5% Secant Stiffness of Batch 056218 and 059839 – Straight after production and after curing for 1 year and 1 week respectively

Fig 5.26 Graph showing Max. Load Vs 2% Secant Stiffness of Batch 056218 and 059839 – Straight after production and after curing for 1 year and 1 week respectively

Fig 5.27 Graph showing Strain at Max. Load Vs 0.5% Secant Stiffness of Batch 056218 and 059839 – Straight after production and after curing for 1 year and 1 week respectively

Fig 5.28 Graph showing Strain at Max. Load Vs 2% Secant Stiffness of Batch 056218 and 059839 – Straight after production and after curing for 1 year and 1 week respectively

Fig 5.29 CRS, Load/m vs Strain plot of TX160 (Batch Ref: 056218) tested at 20% strain/min in all four directions

Fig 5.30 CRS, Load/m vs Strain plot of TX160 (Batch Ref: 056218) tested at 2% strain/min in all four directions

Fig 5.31 CRS, Load/m vs Strain plot of TX160 (Batch Ref: 056218) tested at 0.2% strain/min in all four directions

Fig 5.32 CRS, Load/m vs Strain plot of TX160 (Batch Ref: 056218) tested at 0.02% strain/min in all four directions

Fig 5.33 Polar plot showing 'Radial Secant Stiffness at 0.5% Strain' of TX160 (Batch Ref: 056218) tested by quality control straight off the production line and tested after 1 year at various testing speeds, with Min, Mean & Max specifications

Fig 5.34 Polar plot showing 'Radial Secant Stiffness at 2% Strain' of TX160 (Batch Ref: 056218) tested by quality control straight off the production line and tested after 1 year at various testing speeds, with Min, Mean & Max specifications

Fig 5.35 Graph showing secant stiffness at 0.5% strain versus time of TX160 (Batch Ref: 056218) tested at constant rates of strain of 20%, 2%, 0.2% and 0.02% of the gauge length

Fig 5.36 Graph showing secant stiffness at 2% strain versus time of TX160 (Batch Ref: 056218) tested at constant rates of strain of 20%, 2%, 0.2% and 0.02% of the gauge length

Fig 5.37 Presentation of creep test data, ASM (1988)

Fig 5.38 TX160 creep curves in four directions tested uniaxially at 40kg load

Fig 5.39 TX160 creep curves of the first 10 seconds, in four directions, tested uniaxially at 40kg load

Fig 5.40 TX160 creep curves in four directions tested uniaxially at 80kg load

Fig 5.41 TX160 creep curves of the first 10 seconds, in four directions, tested uniaxially at 80kg load

Fig 5.42 TX160 creep curves in four directions tested uniaxially at 120kg load

Fig 5.43 TX160 creep curves of the first 10 seconds, in four directions, tested uniaxially at 120kg load

Fig 5.44 TX160 creep curves in four directions tested uniaxially at 160kg load

Fig 5.45 TX160 creep curves of the first 10 seconds, in four directions, tested uniaxially at 160kg load

Fig 5.46 Derivation of isochronous load-strain curves from sustained loading test data, after Khan (1999)

Fig 5.47 Derivation of isochronous load-strain curves from CRS test data, after Kupec (2004)

Fig 5.48 Isochronous load-strain curves at 0.001 hours of TX160 creep data, tested in four directions

Fig 5.49 Isochronous load-strain curves at 0.01 hours of TX160 creep data, tested in four directions

Fig 5.50 Isochronous load-strain curves at 0.1 hours of TX160 creep data, tested in four directions

Fig 5.51 Isochronous load-strain curves at 1 hour of TX160 creep data, tested in four directions

Fig 5.52 Isochronous load-strain curves at 10 hours of TX160 creep data, tested in four directions

Fig 5.53 0.5% isochronous load versus time (best fit data) of TX160 (Batch Ref: 056218) creep data, tested in four directions

Fig 5.54 0.5% isochronous stiffness versus time (best fit data) of TX160 creep data, tested in four directions.

Fig 5.55 0.5% isochronous stiffness versus time (best fit data) of TX160 creep and CRS data tested in four directions

Fig 6.1 Quadrant radial creep testing apparatus

Fig 6.2 Birds-eye-view of quadrant radial creep testing apparatus and specimen (0° & 60° Direction)

Fig 6.3 Birds-eye-view of quadrant radial creep testing apparatus and specimen (30° & 90° Direction

Fig 6.4 Direction of load/strain in the ribs when tested in the 0° direction

Fig 6.5 Direction of load/strain in the ribs when tested in the 30° direction

Fig 6.6 Direction of load/strain in the ribs when tested in the 60° direction

Fig 6.7 Direction of load/strain in the ribs when tested in the 90° direction

Fig 6.8 Direction of load/strain in the ribs when tested radially in the 0° direction

Fig 6.9 Direction of load/strain in the ribs when tested radially in the 30° direction

Fig 6.10 Direction of load/strain in the ribs when tested radially in the 60° direction

Fig 6.11 Direction of load/strain in the ribs when tested radially in the 90° direction

Fig 6.12 0° Radial creep specimen

Fig 6.13 30° Radial creep specimen

Fig 6.14 60° Radial creep specimen

Fig 6.15 90° Radial creep specimen

Fig 6.16 Schematic of suggested shape and size of radial test specimen (0° & 60°)

Fig 6.17 Schematic of suggested shape and size of radial test specimen (30° & 90°)

Fig 6.18 Calculations of Applied Load/m at R560, Average Load/m Over Gauge Length and Radius at Average Load/m for 3x30kg loaded radial test specimen at 0° and 60° directions.

Fig 6.19 Calculations of Applied Load/m at R550, Average Load/m Over Gauge Length and Radius at Average Load/m for 3x30kg loaded radial test specimen at 30° and 90° directions

Fig 6.20 Plot showing Radius Vs Local Load/m and Radius Vs Local Strain for test Loaded at 30kg and tested in the 0° direction

Fig 6.21 Plot showing Radius Vs Local Load/m and Radius Vs Local Strain for test loaded at 30kg and tested in the 60° direction

Fig 6.22 Plot showing Radius Vs Local Load/m and Radius Vs Local Strain for test loaded at 30kg and tested in the 30° direction

Fig 6.23 Plot showing Radius Vs Local Load/m and Radius Vs Local Strain for test loaded at 30kg and tested in the 90° direction

Fig 6.24 Plot showing Radius Vs Local Load/m and Radius Vs Local Strain for test loaded at 40kg and tested in the 0° direction

Fig 6.25 Plot showing Radius Vs Local Load/m and Radius Vs Local Strain for test loaded at 40kg and tested in the 60° direction

Fig 6.26 Plot showing Radius Vs Local Load/m and Radius Vs Local Strain for test loaded at 40kg and tested in the 30° direction

Fig 6.27 Plot showing Radius Vs Local Load/m and Radius Vs Local Strain for test loaded at 40kg and rested in the 90° direction

Fig 6.28 Plot showing Radius Vs Local Load/m and Radius Vs Local Strain for test loaded at 50kg and tested in the 0° direction

Fig 6.29 Plot showing Radius Vs Local Load/m and Radius Vs Local Strain for test loaded at 50kg and tested in the 60° direction

Fig 6.30 Plot showing Radius Vs Local Load/m and Radius Vs Local Strain for test loaded at 50kg and tested in the 30° direction

Fig 6.31 Plot showing Radius Vs Local Load/m and Radius Vs Local Strain for test loaded at 50kg and Tested in the 90° direction

Fig 6.32 Plot showing Radius Vs Local Load/m and Radius Vs Local Strain for test loaded at 60kg and Tested in the 0° direction

Fig 6.33 Plot showing Radius Vs Local Load/m and Radius Vs Local Strain for test loaded at 60kg and Tested in the 60° direction

Fig 6.34 Plot showing Radius Vs Local Load/m and Radius Vs Local Strain for test loaded at 60kg and tested in the 30° direction

Fig 6.35 Plot showing Radius Vs Local Load/m and Radius Vs Local Strain for test loaded at 60kg and tested in the 90° direction

Fig 6.36 TX160 creep curves obtained from radial creep testing in the 0° direction

Fig 6.37 TX160 creep curves obtained from radial creep testing in the 30° direction

Fig 6.38 TX160 creep curves obtained from radial creep testing in the 60° direction

Fig 6.39 TX160 creep curves obtained from radial creep testing in the 90° direction

Fig 6.40 Radial Creep, Isochronous Load-Strain curves at 0.001 hours of TX160 creep data, tested in four directions

Fig 6.41 Radial Creep, Isochronous Load-Strain curves at 0.01 hours of TX160 creep data, tested in four directions

Fig 6.42 Radial Creep, Isochronous Load-Strain curves at 0.1 hours of TX160 creep data, tested in four directions

Fig 6.43 Radial Creep, Isochronous Load-Strain curves at 1 hour of TX160 creep data, tested in four directions

Fig 6.44 Radial Creep, Isochronous Load-Strain curves at 10 hours of TX160 creep data, tested in four directions

Fig 6.45 Radial Creep, Average load at 0.5% average strain versus time (upper and lower boundaries) of TX160, tested in four directions

Fig 6.46 Radial Creep, isochronous stiffness at 0.5% strain versus time (upper and lower boundaries) of TX160, tested in four directions

Fig 7.1 Comparison of Secant Stiffness at 0.5% Strain vs Log Time of Uniaxial CRS, Uniaxial Creep, and Radial Creep test data

Fig 7.2 Comparison of Secant Stiffness at 0.5% Strain vs Log Time Uniaxial Creep, and Radial Creep test data

Fig 7.3 Comparison of Secant Stiffness at 0.5% Strain vs Log Time Uniaxial CRS, and Uniaxial Creep test data

Fig 7.4 Comparison of Secant Stiffness at 0.5% Strain vs Log Time Uniaxial CRS, and Radial Creep test data

Fig 7.5 Comparison of Stiffness Ratios of Uniaxial Creep-to-Radial Creep and Uniaxial CRS-to-Radial Creep

Fig 7.6 CRS, Load/m vs Strain plot of TX160 tested at 20% strain/min in all four directions, with best fit upper and lower boundaries lines passing through locked-in stress of 1kN/m

Fig 7.7 CRS, Load/m vs Strain plot of TX160 tested at 2% strain/min in all four directions, with best fit upper and lower boundaries lines passing through locked-in stress of 1kN/m

Fig 7.8 CRS, Load/m vs Strain plot of TX160 tested at 0.2% strain/min in all four directions, with best fit upper and lower boundaries lines passing through locked-in stress of 1kN/m

Fig 7.9 CRS, Load/m vs Strain plot of TX160 tested at 0.02% strain/min in all four directions, with best fit upper and lower boundaries lines passing through locked-in stress of 1kN/m

Fig 7.10 Uniaxial creep, Isochronous Load-Strain curves at 0.001 hours of TX160 creep data, tested in four directions with best fit upper and lower boundaries passing through locked-in stress of 1kN/m

Fig 7.11 Uniaxial creep, Isochronous Load-Strain curves at 0.01 hours of TX160 creep data, tested in four directions with best fit upper and lower boundaries passing through locked-in stress of 1kN/m

Fig 7.12 Uniaxial creep, Isochronous Load-Strain curves at 0.1 hours of TX160 creep data, tested in four directions with best fit upper and lower boundaries passing through locked-in stress of 1kN/m

Fig 7.13 Uniaxial creep, Isochronous Load-Strain curves at 1 hour of TX160 creep data, tested in four directions with best fit upper and lower boundaries passing through locked-in stress of 1kN/m

Fig 7.14 Uniaxial creep, Isochronous Load-Strain curves at 10 hours of TX160 creep data, tested in four directions with best fit upper and lower boundaries passing through locked-in stress of 1kN/m

Fig 7.15 Radial creep, Isochronous Load-Strain curves at 0.001 hours of TX160 creep data, tested in four directions with best fit upper and lower boundaries passing through locked-in stress of 1kN/m

Fig 7.16 Radial creep, Isochronous Load-Strain curves at 0.01 hours of TX160 creep data, tested in four directions with best fit upper and lower boundaries passing through locked-in stress of 1kN/m

Fig 7.17 Radial creep, Isochronous Load-Strain curves at 0.1 hours of TX160 creep data, tested in four directions with best fit upper and lower boundaries passing through locked-in stress of 1kN/m

Fig 7.18 Radial creep, Isochronous Load-Strain curves at 1 hour of TX160 creep data, tested in four directions with best fit upper and lower boundaries passing through locked-in stress of 1kN/m

Fig 7.19 Radial creep, Isochronous Load-Strain curves at 10 hours of TX160 creep data, tested in four directions with best fit upper and lower boundaries passing through locked-in stress of 1kN/m

Fig 7.20 Comparison of Secant Stiffness at 0.5% Strain vs Log Time of Uniaxial CRS, Uniaxial Creep, and Radial Creep test data

Fig 7.21 Comparison of Stiffness Ratios of Uniaxial Creep-to-Radial Creep and Uniaxial CRS-to-Radial Creep when using a 1kN/m locked-in stress

Fig 7.22 Comparison of Stiffness Ratios of Uniaxial Creep-to-Radial Creep and Uniaxial CRS-to-Radial Creep with and without locked-in stress

List of Plates

Plate 2.1 Close up of screen printed regular orthogonal lines

Plate 2.2 A screen printed punched sheet

Plate 2.3 Stretched screen printed sample of Tensar SR2

Plate 2.4 Detail of the screen printing at the junction after stretching

Plate 6.1 Trial quadrant radial creep test, no load applied

Plate 6.2 Trial quadrant radial creep test, 40kg load applied. 30 second interval

Plate 6.3 Trial quadrant radial creep test, 40kg load applied. 1 minute interval

Plate 6.4 Trial quadrant radial creep test, 40kg load applied. 5 minute interval

Plate 6.5 Trial quadrant radial creep test, 40kg load applied. 1 hour interval

Plate 6.6 Trial quadrant radial creep test, 40kg load applied. 72 hour interval

TABLES

Woven	Non-Woven
Tensar	Terram
TenCate	TenCate
Wrekin	TMP
Don & Law	Wrekin
	NAUE
	Don & Law

Table 1.1 – Examples of geotextile manufacturers by category.

Extruded, Punched and Drawn	Coated Woven or Knit Yarns	Welded Straps or Bars
Tensar Tenax BOSTD TMP	Huesker TenCate	NAUE Colbond

Table 1.2 – Examples of geogrid manufacturers by category.

Product	**RE510**	**RE520**	**RE540**	**RE560**	**RE570**	**RE580**
Tensile Strength	44.0	57.0	68.0	93.0	123.0	142.0
Tolerance	-4	-4.2	-3.5	-4.3	-4.6	-4.7
Elongation At Maximum Load	11.0	11.0	11.0	11.0	11.0	11.0
Tolerance	±3	±3	±3	±3	±3	±3

Table 3.1. – Typical index properties for uniaxial (RE500 series) geogrids.

Long Term Strength	Units	Tensar RE500 Geogrids					
		RE510	RE520	RE540	RE560	RE570	RE580
Creep Ultimate Limit State (ULS) for 10°C	kN/m	20.71	27.34	33.40	45.93	61.31	71.09
Creep Ultimate Limit State (ULS) for 20°C	kN/m	19.01	25.10	30.66	42.16	56.28	65.27
Creep Ultimate Limit State (ULS) for 25°C	kN/m	18.11	23.90	29.20	40.15	53.59	62.15
Creep Ultimate Limit State (ULS) for 30°C	kN/m	17.24	22.76	27.80	38.23	51.03	59.17
ULS determined as a lower bound using standard extrapolation techniques to creep rupture data obtained following the test procedure in BS EN ISO 13431:1999 for 120 year design life.							

Table 3.2. – Typical performance properties for uniaxial (RE500 series) geogrids.

Testing Direction	Load at Max Load (kN)	Mean Strain at Max Load (%)	Mean Tensile Strength (kN/m)	Secant Stiffness at 0.5% strain (kN/m)	Secant Stiffness at 2% strain (kN/m)	Secant Stiffness at 5% strain (kN/m)	Secant Stiffness at 10% strain (kN/m)
0°	5.11	9.85	18.19	375	265.7	225.8	146.5
30°	3.77	7.36	15.44	377.8	287.2	243.4	~
60°	5.06	9.4	17.83	378.9	280.1	231.7	126.5
90°	5.11	10.5	20.44	430.2	344.8	278.1	198.2

Table 3.3. – Mean test data results for all four testing directions of a Tensar TX160 as plotted in Figs 3.25. to Fig 3.28.

Product	% Open Area
TX150	92.16
TX160	91.44
TX170	90.96
TX180	90.96

Table 4.1. – Theoretical percentage open area of TX geogrids.

Geometrical Feature	Longitudinal	Diagonal	Transverse	General
Rib Pitch (mm)	40	40	-	
Mid-Rib Depth (mm)	-	1.4	1.1	
Mid-Rib Width (mm)	-	1.0	1.2	
Nodal Thickness (mm)				3.0
Rib Shape				Rectangular

Table 4.2 – Basic dimensions of the TX150 geogrid.

Geometrical Feature	Longitudinal	Diagonal	Transverse	General
Rib Pitch (mm)	40	40	-	
Mid-Rib Depth (mm)	-	1.8	1.5	
Mid-Rib Width (mm)	-	1.1	1.3	
Nodal Thickness (mm)				3.1
Rib Shape				Rectangular

Table 4.3 - Basic dimensions of the TX160 geogrid.

Geometrical Feature	Longitudinal	Diagonal	Transverse	General
Rib Pitch (mm)	40	40	-	
Mid-Rib Depth (mm)	-	2.3	1.8	
Mid-Rib Width (mm)	-	1.2	1.3	
Nodal Thickness (mm)				4.1
Rib Shape				Rectangular

Table 4.4 - Basic dimensions of the TX170 geogrid.

Geometrical Feature	Longitudinal	Diagonal	Transverse	General
Rib Pitch (mm)	40	40	-	
Mid-Rib Depth (mm)	-	2.6	2.4	
Mid-Rib Width (mm)	-	1.2	1.3	
Nodal Thickness (mm)				6.0
Rib Shape				Rectangular

Table 4.5 - Basic dimensions of the TX180 geogrid.

Product Characteristic	Method of Testing	Unit of Characteristic	Declared Value	Tolerance
Radial Secant Stiffness at 0.5% Strain	TR041 B.1	kN/m	360	-75
Radial Secant Stiffness at 2% Strain	TR041 B.1	kN/m	250	-65
Radial Secant Stiffness Ratio	TR041 B.2	-	0.80	-0.15
Junction Efficiency	TR041 B.2	%	100	-10
Weight of the product	TR041 B.3	kg/m^2	0.205	-0.035
Hexagon Pitch	TR041 B.4	mm	80	±4

Table 4.6 – Characteristics and Properties of TX150 according to the EOTA TR41:2012.

Product Characteristic	Method of Testing	Unit of Characteristic	Declared Value	Tolerance
Radial Secant Stiffness at 0.5% Strain	TR041 B.1	kN/m	390	-75
Radial Secant Stiffness at 2% Strain	TR041 B.1	kN/m	290	-65
Radial Secant Stiffness Ratio	TR041 B.2	-	0.80	-0.15
Junction Efficiency	TR041 B.2	%	100	-10
Weight of the product	TR041 B.3	kg/m^2	0.220	-0.035
Hexagon Pitch	TR041 B.4	mm	80	±4

Table 4.7 – Characteristics and Properties of TX160 according to the EOTA TR41:2012.

Product Characteristic	Method of Testing	Unit of Characteristic	Declared Value	Tolerance
Radial Secant Stiffness at 0.5% Strain	TR041 B.1	kN/m	480	-90
Radial Secant Stiffness at 2% Strain	TR041 B.1	kN/m	360	-65
Radial Secant Stiffness Ratio	TR041 B.2	-	0.80	-0.15
Junction Efficiency	TR041 B.2	%	100	-10
Weight of the product	TR041 B.3	kg/m^2	0.270	-0.035
Hexagon Pitch	TR041 B.4	mm	80	±4

Table 4.8 – Characteristics and Properties of TX170 according to the EOTA TR41:2012.

Product Characteristic	Method of Testing	Unit of Characteristic	Declared Value	Tolerance
Radial Secant Stiffness at 0.5% Strain	TR041 B.1	kN/m	540	-90
Radial Secant Stiffness at 2% Strain	TR041 B.1	kN/m	420	-65
Radial Secant Stiffness Ratio	TR041 B.2	-	0.80	-0.15
Junction Efficiency	TR041 B.2	%	100	-10
Weight of the product	TR041 B.3	kg/m^2	0.315	-0.035
Hexagon Pitch	TR041 B.4	mm	80	±4

Table 4.9 – Characteristics and Properties of TX180 according to the EOTA TR41:2012.

TX150 CE Marking Properties	
Tensile strength (EN ISO 10319)	MD 20kN/m (-4kN/m) CMD 18kN/m (-3kN/m)
Elongation at maximum load (EN ISO 10319)	MD 11% (± 4%) CMD 11% (± 4%)

Table 4.10 – Properties of TX150 according to CE Marking for reinforcement specifications.

TX160 CE Marking Properties	
Tensile strength (EN ISO 10319)	MD 22kN/m (-4kN/m) CMD 20kN/m (-4kN/m)
Elongation at maximum load (EN ISO 10319)	MD 11% (± 4%) CMD 11% (± 4%)

Table 4.11 – Properties of TX160 according to CE Marking for reinforcement specifications.

TX170 CE Marking Properties	
Tensile strength (EN ISO 10319)	MD 28kN/m (-7kN/m) CMD 24kN/m (-4kN/m)
Elongation at maximum load (EN ISO 10319)	MD 11% (± 4%) CMD 11% (± 4%)

Table 4.12 – Properties of TX170 according to CE Marking for reinforcement specifications.

TX180 CE Marking Properties	
Tensile strength (EN ISO 10319)	MD 29kN/m (-5kN/m) CMD 27kN/m (-5kN/m)
Elongation at maximum load (EN ISO 10319)	MD 9% (± 4%) CMD 9% (± 3%)

Table 4.13 – Properties of TX180 according to CE Marking for reinforcement specifications.

	Load at 0.5% Strain (kN)	Load at 1% Strain (kN)	Load at 1.5% Strain (kN)	Load at 2% Strain (kN)	Load at Max Load (kN)	Mean Strain at Max Load (%)	Mean Tensile Strength (kN/m)	Secant Stiffness at 0.5% Strain (kN/m)	Secant Stiffness at 2% Strain (kN/m)
0°	0.62	1.06	1.43	1.76	5.35	9.39	19.33	447.78	318.21
30°	0.54	0.95	1.30	1.63	4.20	7.50	17.32	447.64	335.98
60°	0.61	1.06	1.44	1.79	5.50	10.30	19.34	426.54	314.45
90°	0.63	1.11	1.52	1.90	4.85	8.47	19.52	505.81	381.39
Mean	0.6	1.05	1.42	1.77	4.98	8.92	18.88	456.94	337.51

*** Note 0° is the machine direction.**

Table 5.1 – Mean properties of TX160 (Batch Ref: 056218, TAP 1 Year) as determined in the four directions and tested in accordance with the EOTA TR41:2012.

	Load at 0.5% Strain (kN)	Load at 1% Strain (kN)	Load at 1.5% Strain (kN)	Load at 2% Strain (kN)	Load at Max Load (kN)	Mean Strain at Max Load (%)	Mean Tensile Strength (kN/m)	Secant Stiffness at 0.5% Strain (kN/m)	Secant Stiffness at 2% Strain (kN/m)
0°	0.60	1.02	1.36	1.69	5.08	9.47	18.39	435.99	306.05
30°	0.52	0.89	1.22	1.54	3.99	7.49	16.65	431.52	321.67
60°	0.57	0.99	1.36	1.69	5.34	10.08	18.91	401.32	299.32
90°	0.61	1.08	1.48	1.85	5.14	11.00	20.82	493.92	374.33
Mean	0.58	1.00	1.36	1.69	4.89	9.51	18.69	440.69	325.34

*** Note 0° is the machine direction.**

Table 5.2 – Mean properties of TX160 (Batch Ref: 059839, TAP 1 Week) as determined in the four directions and tested in accordance with the EOTA TR41:2012.

Testing Direction	Load at Max (kN)	Mean Strain at Max Load (%)	Secant Stiffness at 0.5% Strain (kN/m)	Secant Stiffness at 2% Strain (kN/m)
0°	5.26	9.75	402.36 **(Range: 379.17 – 416.19)**	276.68 **(Range: 264.25 – 282.51)**
30°	3.78	7.21	401.87 **(Range: 388.69 – 413.80)**	292.91 **(Range: 284.04 – 299.75)**
60°	5.37	10.47	401.91 **(Range: 396.66 – 405.54)**	278.07 **(Range: 221.63 – 228.21)**
90°	4.87	9.87	454.45 **(Range: 401.80 – 481.61)**	336.26 **(Range: 317.04 – 346.92)**

Secant Stiffness Ratio = 0.88

Table 5.3 – Batch Ref: 056218 tested at a strain rate of 20% of gauge length straight off production tested by QC.

Testing Direction	Load at Max (kN)	Mean Strain at Max Load (%)	Secant Stiffness at 0.5% Strain (kN/m)	Secant Stiffness at 2% Strain (kN/m)
0°	5.35	9.39	447.78 **(Range: 438.21 – 457.42)**	318.21 **(Range: 312.96 – 322.69)**
30°	4.2	7.5	447.64 **(Range: 439.54 – 461.29**	335.98 **(Range: 331.18 – 346.05)**
60°	5.5	10.3	426.54 **(Range: 413.74 – 439.66)**	314.45 **(Range: 310.10 – 318.93)**
90°	4.85	8.47	505.81 **(Range: 495.37 – 514.39)**	381.39 **(Range: 374.14 – 387.37)**

Secant Stiffness Ratio = 0.84

Table 5.4 – Batch Ref: 056218 tested at a strain rate of 20% of gauge length TAP for 1 year.

Testing Direction	Q.C Data Taken Straight After Production (kN/m)	TAP = 1year (kN/m)	% Difference
0°	402.36	447.78	10.69
30°	401.87	447.64	10.78
60°	401.91	426.54	5.95
90°	454.45	505.81	10.70

Table 5.5 – Batch Ref: 056218 Secant Stiffness at 0.5%.

Testing Direction	Q.C Data Taken Straight After Production (kN/m)	TAP = 1year (kN/m)	% Difference
0°	276.68	318.21	13.96
30°	292.91	335.98	13.70
60°	278.07	314.45	12.28
90°	336.26	381.39	12.58

Table 5.6 – Batch Ref: 056218 Secant Stiffness at 2%.

Testing Direction	Load at Max (kN)	Mean Strain at Max Load (%)	Secant Stiffness at 0.5% Strain (kN/m)	Secant Stiffness at 2% Strain (kN/m)
0°	5.07	9.74	362.44 **(Range: 352.04 – 369.60)**	268.95 **(Range: 260.97 – 276.08)**
30°	3.94	8.21	379.58 **(Range: 372.98 – 384.03)**	292.24 **(Range: 289.03 – 295.40)**
60°	5.14	10.64	353.56 **(Range: 243.52 – 474.25)**	272.92 **(Range: 226.28 – 326.59)**
90°	5.07	11.96	410.24 **(Range: 344.19 – 446.51)**	331.31 **(Range: 309.16 – 343.99)**

Secant Stiffness Ratio = 0.86

Table 5.7 – Batch Ref: 059839 tested at a strain rate of 20% of gauge length straight after production.

Testing Direction	Load at Max (kN)	Mean Strain at Max Load (%)	Secant Stiffness at 0.5% Strain (kN/m)	Secant Stiffness at 2% Strain (kN/m)
0°	5.08	9.47	435.99 **(Range: 430.01 – 441.48)**	306.05 **(Range: 303.90 – 308.52)**
30°	3.99	7.49	431.52 **(Range: 424.06 – 434.37)**	321.67 **(Range: 319.84 – 323.91)**
60°	5.34	10.08	401.32 **(Range: 387.01 – 431.39)**	299.32 **(Range: 280.93 – 308.47)**
90°	5.14	11.00	493.92 **(Range: 448.13 – 513.74)**	374.33 **(Range: 358.12 – 382.77)**

Secant Stiffness Ratio = 0.81

Table 5.8 – Batch Ref: 059839 tested at a strain rate of 20% of gauge length TAP 1 week.

Testing Direction	Q.C Data Taken Straight After Production (kN/m)	TAP = 1 week (kN/m)	% Difference
0°	362.44	435.99	18.42
30°	379.58	431.52	12.81
60°	353.56	401.32	12.65
90°	410.24	493.92	18.51

Table 5.9 – Batch Ref: 059839 Secant Stiffness at 0.5%.

Testing Direction	Q.C Data Taken Straight After Production (kN/m)	TAP = 1 week (kN/m)	% Difference
0°	268.95	306.05	12.90
30°	292.24	321.67	9.59
60°	272.92	299.32	9.23
90°	331.31	374.33	12.19

Table 5.10 – Batch Ref: 059839 Secant Stiffness at 2%.

Testing Direction	Load at Max (kN)	Mean Strain at Max Load (%)	Secant Stiffness at 0.5% Strain (kN/m)	Secant Stiffness at 2% Strain (kN/m)
0°	5.04	9.73	391.62 **(Range: 383.52 – 398.06)**	282.22 **(Range: 280.53 – 285.90)**
30°	3.95	7.91	410.69 **(Range: 402.65 – 418.02**	309.38 **(Range: 304.75 – 312.26)**
60°	5.26	11.03	397.25 **(Range: 383.01 – 408.79)**	284.82 **(Range: 283.32 – 287.00)**
90°	4.61	10.29	459.54 **(Range: 455.44 – 463.11)**	340.02 **(Range: 335.62 – 346.02)**

Secant Stiffness Ratio = 0.85

Table 5.11 – Batch Ref: 056218 tested at a strain rate of 2% of gauge length TAP 1 year.

Testing Direction	Load at Max (kN)	Mean Strain at Max Load (%)	Secant Stiffness at 0.5% Strain (kN/m)	Secant Stiffness at 2% Strain (kN/m)
0°	4.67	10.87	364.61 **(Range: 352.68 – 376.19)**	245.62 **(Range: 241.87 – 252.06)**
30°	3.62	9.21	353.87 **(Range: 326.86 – 377.51)**	255.15 **(Range: 243.50 – 267.21)**
60°	4.74	12.14	388.89 **(Range: 378.83 – 404.94)**	256.33 **(Range: 249.24 – 265.37)**
90°	3.53	8.76	438.81 **(Range: 432.70 – 447.42)**	299.65 **(Range: 294.12 – 304.04)**

Secant Stiffness Ratio = 0.80

Table 5.12 – Batch Ref: 056218 tested at a strain rate of 0.2% of gauge length TAP 1 year.

Testing Direction	Load at Max (kN)	Mean Strain at Max Load (%)	Secant Stiffness at 0.5% Strain (kN/m)	Secant Stiffness at 2% Strain (kN/m)
0°	1.40	3.03	298.11 **(Range: 293.79 – 301.48)**	191.58 **(Range: 188.19 – 196.14)**
30°	1.36	3.36		
60°	1.64	3.48		
90°	1.61	3.12	383.59 **(Range: 366.17 – 413.87)**	241.33 **(Range: 233.94 – 254.43)**

Secant Stiffness Ratio = 0.78

*** Note CRS test at 0.02% of gauge length was not taken to failure. Test stopped at approximately 3% strain. Also, only one specimen tested in the 30° and 60° direction**

Table 5.13 – Batch Ref: 056218 tested at a strain rate of 0.02% of gauge length TAP for 1 year.

Load Direction	Applied Load/m at Each Outer Clamp	Average Load/m Over Gauge Length (kN/m)	Radius at Average Load/m (mm)
3x30kg - 0° & 60°	1.000	1.77	318
3x30kg - 30° & 90°	1.014	2.07	270
3x40kg - 0° & 60°	1.338	2.36	318
3x40kg - 30° & 90°	1.352	2.75	270
3x50kg - 0° & 60°	1.670	2.94	318
3x50kg - 30° & 90°	1.689	3.44	270
3x60kg - 0° & 60°	2.005	3.53	318
3x60kg - 30° & 90°	2.027	4.13	270

Table 6.1 – Calculations of Applied Load/m at Outer Clamps, Average Load/m Over Gauge Length and Radius at Average Load/m for all radial test specimens tested at 0°, 30°, 60° and 90° directions at four different loads.

Radii (mm)	Local Load/m @ 40mm (kN/m)	Local Strains (%) (0.001Hrs)	Local Strains (%) (0.01Hrs)	Local Strains (%) (0.1Hrs)	Local Strains (%) (1Hr)	Local Strains (%) (10Hr)
560						
520	1.080	0.145	0.158	0.179	0.218	0.282
480	1.171	0.157	0.171	0.194	0.236	0.305
440	1.277	0.171	0.186	0.211	0.256	0.331
400	1.405	0.187	0.203	0.231	0.281	0.363
360	1.561	0.207	0.225	0.255	0.311	0.401
320	1.756	0.232	0.252	0.285	0.347	0.449
280	2.007	0.263	0.285	0.324	0.394	0.509
240	2.341	0.304	0.330	0.374	0.455	0.588
200	2.809	0.360	0.391	0.443	0.539	0.697
160	3.512	0.442	0.480	0.544	0.662	0.855

Table 6.2 – Calculated local load/m and local strains for 30kg load tested in the 0° direction.

Radii (mm)	Local Load/m @ 40mm (kN/m)	Local Strains (%) (0.001Hrs)	Local Strains (%) (0.01Hrs)	Local Strains (%) (0.1Hrs)	Local Strains (%) (1Hr)	Local Strains (%) (10Hr)
560						
520	1.080	0.101	0.108	0.118	0.154	0.196
480	1.171	0.110	0.117	0.128	0.166	0.212
440	1.277	0.119	0.127	0.139	0.181	0.230
400	1.405	0.131	0.139	0.153	0.198	0.252
360	1.561	0.144	0.154	0.169	0.219	0.279
320	1.756	0.161	0.172	0.189	0.245	0.312
280	2.007	0.183	0.195	0.214	0.278	0.354
240	2.341	0.212	0.225	0.247	0.321	0.409
200	2.809	0.251	0.267	0.293	0.381	0.484
160	3.512	0.308	0.327	0.360	0.467	0.594

Table 6.3 – Calculated local load/m and local strains for 30kg load tested in the 60° direction.

Radii (mm)	Local Load/m @ 40mm (kN/m)	Local Strains (%) (0.001Hrs)	Local Strains (%) (0.01Hrs)	Local Strains (%) (0.1Hrs)	Local Strains (%) (1Hr)	Local Strains (%) (10Hr)
550						
510	1.093	0.152	0.163	0.176	0.202	0.243
470	1.186	0.165	0.177	0.192	0.220	0.265
430	1.297	0.180	0.193	0.209	0.240	0.288
390	1.430	0.198	0.212	0.230	0.263	0.317
350	1.593	0.219	0.235	0.255	0.292	0.351
310	1.798	0.246	0.263	0.286	0.327	0.394
270	2.065	0.280	0.300	0.325	0.373	0.449
230	2.424	0.326	0.349	0.378	0.433	0.521
190	2.934	0.389	0.416	0.451	0.517	0.622
150	3.717	0.483	0.517	0.560	0.642	0.773
115	4.848	0.622	0.665	0.721	0.827	0.995

Table 6.4 – Calculated local load/m and local strains for 30kg load tested in the 90° direction.

Radii (mm)	Local Load/m @ 40mm (kN/m)	Local Strains (%) (0.001Hrs)	Local Strains (%) (0.01Hrs)	Local Strains (%) (0.1Hrs)	Local Strains (%) (1Hr)	Local Strains (%) (10Hr)
550						
510	1.093	0.195	0.203	0.232	0.291	0.346
470	1.186	0.212	0.221	0.253	0.317	0.377
430	1.297	0.231	0.241	0.275	0.345	0.410
390	1.430	0.254	0.265	0.302	0.379	0.451
350	1.593	0.282	0.293	0.335	0.421	0.500
310	1.798	0.316	0.329	0.376	0.472	0.561
270	2.065	0.360	0.375	0.428	0.538	0.639
230	2.424	0.418	0.436	0.498	0.625	0.742
190	2.934	0.499	0.520	0.594	0.746	0.886
150	3.717	0.620	0.645	0.737	0.926	1.099
115	4.848	0.798	0.831	0.949	1.192	1.416

Table 6.5 – Calculated local load/m and local strains for 30kg load tested in the 30° direction.

Radii (mm)	Local Load/m @ 40mm (kN/m)	Local Strains (%) (0.001Hrs)	Local Strains (%) (0.01Hrs)	Local Strains (%) (0.1Hrs)	Local Strains (%) (1Hr)	Local Strains (%) (10Hr)
560						
520	1.441	0.183	0.205	0.234	0.289	0.356
480	1.561	0.218	0.244	0.278	0.344	0.423
440	1.703	0.235	0.263	0.300	0.371	0.457
400	1.873	0.256	0.286	0.327	0.404	0.497
360	2.081	0.281	0.313	0.358	0.442	0.545
320	2.341	0.310	0.347	0.396	0.489	0.602
280	2.675	0.347	0.388	0.443	0.547	0.674
240	3.121	0.394	0.440	0.502	0.620	0.764
200	3.746	0.455	0.508	0.580	0.717	0.883
160	4.682	0.539	0.602	0.688	0.849	1.046

Table 6.6 – Calculated local load/m and local strains for 40kg load tested in the 0° direction.

Radii (mm)	Local Load/m @ 40mm (kN/m)	Local Strains (%) (0.001Hrs)	Local Strains (%) (0.01Hrs)	Local Strains (%) (0.1Hrs)	Local Strains (%) (1Hr)	Local Strains (%) (10Hr)
560						
520	1.441	0.180	0.196	0.220	0.264	0.314
480	1.561	0.214	0.233	0.261	0.313	0.373
440	1.703	0.231	0.252	0.282	0.338	0.403
400	1.873	0.252	0.274	0.307	0.368	0.438
360	2.081	0.276	0.300	0.336	0.403	0.480
320	2.341	0.305	0.332	0.372	0.446	0.531
280	2.675	0.341	0.371	0.416	0.499	0.594
240	3.121	0.387	0.421	0.471	0.566	0.673
200	3.746	0.447	0.486	0.545	0.654	0.778
160	4.682	0.529	0.576	0.645	0.774	0.922

Table 6.7 – Calculated local load/m and local strains for 40kg load tested in the 60° direction.

Radii (mm)	Local Load/m @ 40mm (kN/m)	Local Strains (%) (0.001Hrs)	Local Strains (%) (0.01Hrs)	Local Strains (%) (0.1Hrs)	Local Strains (%) (1Hr)	Local Strains (%) (10Hr)
550						
510	1.458	0.233	0.249	0.275	0.324	0.380
470	1.582	0.270	0.289	0.319	0.376	0.440
430	1.729	0.294	0.314	0.347	0.408	0.479
390	1.906	0.322	0.344	0.380	0.447	0.525
350	2.124	0.356	0.381	0.420	0.495	0.580
310	2.398	0.398	0.426	0.470	0.553	0.649
270	2.753	0.452	0.483	0.533	0.628	0.736
230	3.232	0.522	0.558	0.616	0.725	0.850
190	3.912	0.618	0.661	0.730	0.859	1.007
150	4.956	0.759	0.811	0.896	1.055	1.236
115	6.464	0.984	1.052	1.162	1.367	1.603

Table 6.8 – Calculated local load/m and local strains for 40kg load tested in the 90° direction.

Radii (mm)	Local Load/m @ 40mm (kN/m)	Local Strains (%) (0.001Hrs)	Local Strains (%) (0.01Hrs)	Local Strains (%) (0.1Hrs)	Local Strains (%) (1Hr)	Local Strains (%) (10Hr)
550						
510	1.458	0.234	0.246	0.279	0.351	0.421
470	1.582	0.271	0.285	0.323	0.407	0.487
430	1.729	0.295	0.310	0.351	0.443	0.530
390	1.906	0.323	0.340	0.385	0.485	0.581
350	2.124	0.357	0.376	0.425	0.536	0.642
310	2.398	0.400	0.420	0.476	0.600	0.718
270	2.753	0.453	0.477	0.540	0.681	0.815
230	3.232	0.524	0.551	0.624	0.787	0.941
190	3.912	0.620	0.652	0.739	0.932	1.115
150	4.956	0.761	0.801	0.907	1.144	1.369
115	6.464	0.987	1.038	1.175	1.482	1.774

Table 6.9 – Calculated local load/m and local strains for 40kg load tested in the 30° direction.

Radii (mm)	Local Load/m @ 40mm (kN/m)	Local Strains (%) (0.001Hrs)	Local Strains (%) (0.01Hrs)	Local Strains (%) (0.1Hrs)	Local Strains (%) (1Hr)	Local Strains (%) (10Hr)
560						
520	1.799	0.276	0.305	0.357	0.452	0.542
480	1.949	0.370	0.408	0.478	0.605	0.726
440	2.126	0.402	0.443	0.520	0.658	0.790
400	2.339	0.440	0.486	0.569	0.721	0.865
360	2.598	0.487	0.537	0.630	0.797	0.957
320	2.923	0.545	0.601	0.704	0.892	1.070
280	3.341	0.618	0.682	0.799	1.012	1.214
240	3.898	0.714	0.788	0.923	1.169	1.403
200	4.677	0.846	0.933	1.093	1.385	1.662
160	5.847	1.038	1.145	1.342	1.700	2.040

Table 6.10 – Calculated local load/m and local strains for 50kg load tested in the 0° direction.

Radii (mm)	Local Load/m @ 40mm (kN/m)	Local Strains (%) (0.001Hrs)	Local Strains (%) (0.01Hrs)	Local Strains (%) (0.1Hrs)	Local Strains (%) (1Hr)	Local Strains (%) (10Hr)
560						
520	1.799	0.247	0.281	0.319	0.395	0.485
480	1.949	0.331	0.376	0.427	0.529	0.650
440	2.126	0.360	0.409	0.464	0.575	0.707
400	2.339	0.395	0.448	0.509	0.630	0.774
360	2.598	0.436	0.495	0.562	0.697	0.856
320	2.923	0.488	0.554	0.629	0.779	0.958
280	3.341	0.554	0.628	0.714	0.884	1.086
240	3.898	0.640	0.726	0.825	1.021	1.255
200	4.677	0.758	0.860	0.977	1.210	1.487
160	5.847	0.930	1.056	1.199	1.485	1.825

Table 6.11 – Calculated local load/m and local strains for 50kg load tested in the 60° direction.

Radii (mm)	Local Load/m @ 40mm (kN/m)	Local Strains (%) (0.001Hrs)	Local Strains (%) (0.01Hrs)	Local Strains (%) (0.1Hrs)	Local Strains (%) (1Hr)	Local Strains (%) (10Hr)
550						
510	1.822	0.258	0.283	0.320	0.389	0.467
470	1.977	0.348	0.381	0.430	0.524	0.629
430	2.161	0.379	0.415	0.469	0.571	0.685
390	2.383	0.416	0.455	0.515	0.627	0.752
350	2.655	0.461	0.505	0.571	0.695	0.834
310	2.997	0.517	0.566	0.640	0.780	0.936
270	3.441	0.589	0.645	0.729	0.888	1.066
230	4.040	0.684	0.750	0.847	1.032	1.238
190	4.890	0.817	0.895	1.011	1.232	1.478
150	6.195	1.014	1.111	1.256	1.529	1.835
115	8.080	1.306	1.430	1.617	1.969	2.363

Table 6.12 – Calculated local load/m and local strains for 50kg load tested in the 90° direction.

Radii (mm)	Local Load/m @ 40mm (kN/m)	Local Strains (%) (0.001Hrs)	Local Strains (%) (0.01Hrs)	Local Strains (%) (0.1Hrs)	Local Strains (%) (1Hr)	Local Strains (%) (10Hr)
550						
510	1.822	0.303	0.336	0.393	0.500	0.606
470	1.977	0.408	0.452	0.530	0.673	0.816
430	2.161	0.445	0.493	0.577	0.733	0.889
390	2.383	0.488	0.541	0.633	0.805	0.976
350	2.655	0.541	0.600	0.702	0.892	1.083
310	2.997	0.607	0.673	0.788	1.001	1.215
270	3.441	0.692	0.767	0.898	1.141	1.384
230	4.040	0.804	0.891	1.043	1.325	1.608
190	4.890	0.960	1.063	1.245	1.582	1.919
150	6.195	1.191	1.320	1.545	1.964	2.382
115	8.080	1.534	1.700	1.990	2.529	3.068

Table 6.13 – Calculated local load/m and local strains for 50kg load tested in the 30° direction.

Radii (mm)	Local Load/m @ 40mm (kN/m)	Local Strains (%) (0.001Hrs)	Local Strains (%) (0.01Hrs)	Local Strains (%) (0.1Hrs)	Local Strains (%) (1Hr)
560					
520	2.159	0.345	0.383	0.445	0.555
480	2.339	0.492	0.545	0.633	0.791
440	2.551	0.535	0.593	0.689	0.860
400	2.806	0.586	0.650	0.755	0.942
360	3.118	0.648	0.719	0.834	1.042
320	3.508	0.725	0.804	0.933	1.165
280	4.009	0.822	0.912	1.059	1.322
240	4.677	0.950	1.053	1.223	1.527
200	5.613	1.126	1.248	1.449	1.809
160	7.016	1.381	1.532	1.779	2.220

Table 6.14 – Calculated local load/m and local strains for 60kg load tested in the 0° direction.

Radii (mm)	Local Load/m @ 40mm (kN/m)	Local Strains (%) (0.001Hrs)	Local Strains (%) (0.01Hrs)	Local Strains (%) (0.1Hrs)	Local Strains (%) (1Hr)
560					
520	2.159	0.297	0.337	0.399	0.505
480	2.339	0.423	0.480	0.568	0.719
440	2.551	0.460	0.522	0.618	0.782
400	2.806	0.504	0.572	0.677	0.857
360	3.118	0.557	0.632	0.749	0.948
320	3.508	0.623	0.707	0.837	1.060
280	4.009	0.707	0.802	0.950	1.202
240	4.677	0.817	0.927	1.098	1.389
200	5.613	0.968	1.098	1.300	1.646
160	7.016	1.188	1.347	1.596	2.020

Table 6.15 – Calculated local load/m and local strains for 60kg load tested in the 60° direction.

Radii (mm)	Local Load/m @ 40mm (kN/m)	Local Strains (%) (0.001Hrs)	Local Strains (%) (0.01Hrs)	Local Strains (%) (0.1Hrs)	Local Strains (%) (1Hr)
550					
510	2.186	0.268	0.292	0.338	0.417
470	2.372	0.383	0.418	0.483	0.597
430	2.593	0.417	0.455	0.526	0.650
390	2.859	0.458	0.500	0.578	0.714
350	3.186	0.508	0.554	0.641	0.791
310	3.597	0.570	0.622	0.719	0.888
270	4.130	0.649	0.709	0.819	1.012
230	4.848	0.754	0.823	0.952	1.175
190	5.869	0.900	0.983	1.136	1.403
150	7.434	1.117	1.220	1.410	1.742
115	9.696	1.439	1.571	1.816	2.243

Table 6.16 – Calculated local load/m and local strains for 60kg load tested in the 90° direction.

Radii (mm)	Local Load/m @ 40mm (kN/m)	Local Strains (%) (0.001Hrs)	Local Strains (%) (0.01Hrs)	Local Strains (%) (0.1Hrs)	Local Strains (%) (1Hr)
550					
510	2.186	0.314	0.347	0.413	0.515
470	2.372	0.450	0.497	0.590	0.737
430	2.593	0.490	0.541	0.643	0.803
390	2.859	0.538	0.594	0.706	0.881
350	3.186	0.596	0.659	0.783	0.977
310	3.597	0.669	0.740	0.878	1.097
270	4.130	0.762	0.842	1.000	1.249
230	4.848	0.885	0.979	1.162	1.451
190	5.869	1.057	1.168	1.388	1.733
150	7.434	1.312	1.450	1.722	2.151
115	9.696	1.689	1.868	2.218	2.769

Table 6.17 – Calculated local load/m and local strains for 60kg load tested in the 30° direction.

Assuming a Locked-In Stress of 1 kN/m

	CRS	Radial Creep	Uniaxial Creep
Upper Gradient	37/1	34/1	94/1
Lower Gradient	40/1	50/1	108/1

Assuming No Locked-In Stress

	CRS	Radial Creep	Uniaxial Creep
Upper Gradient	55/1	20/1	124/1
Lower Gradient	45/1	42/1	126/1

Table 7.1 – Upper and lower gradients of CRS, Radial Creep, and Uniaxial Creep testing with and without an assumed locked-in stress

FIGURES



Fig 1.1 - Examples of geotextile fabrics. To the left are non-woven examples. To the right are woven geotextile fabrics, in which you can see the weave pattern, Study.com (2017)

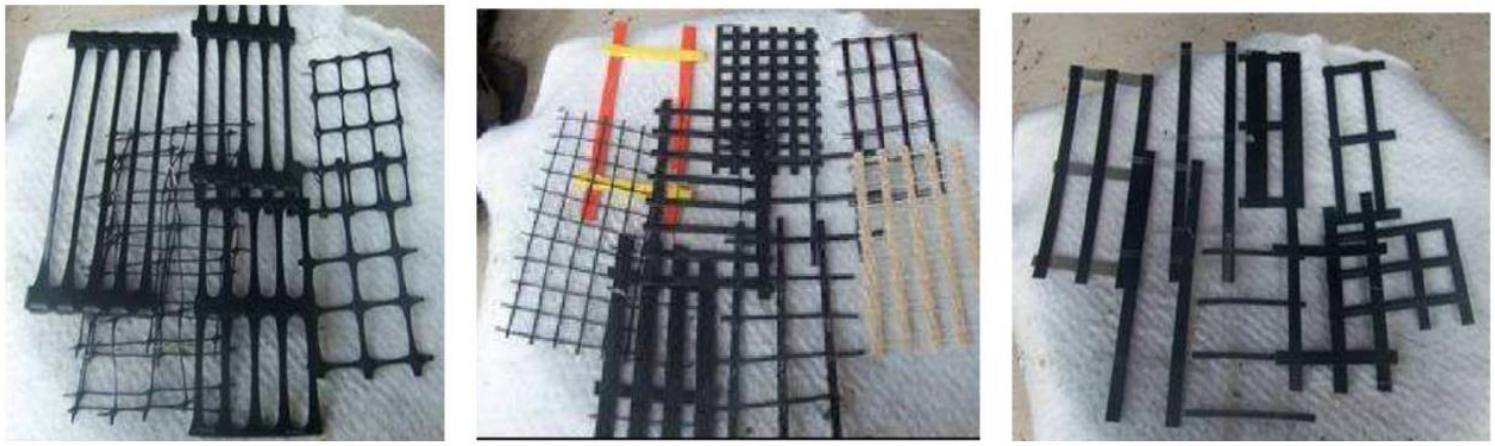


Fig 1.2 - Examples of the three major categories of geogrids, Koerner (2009)

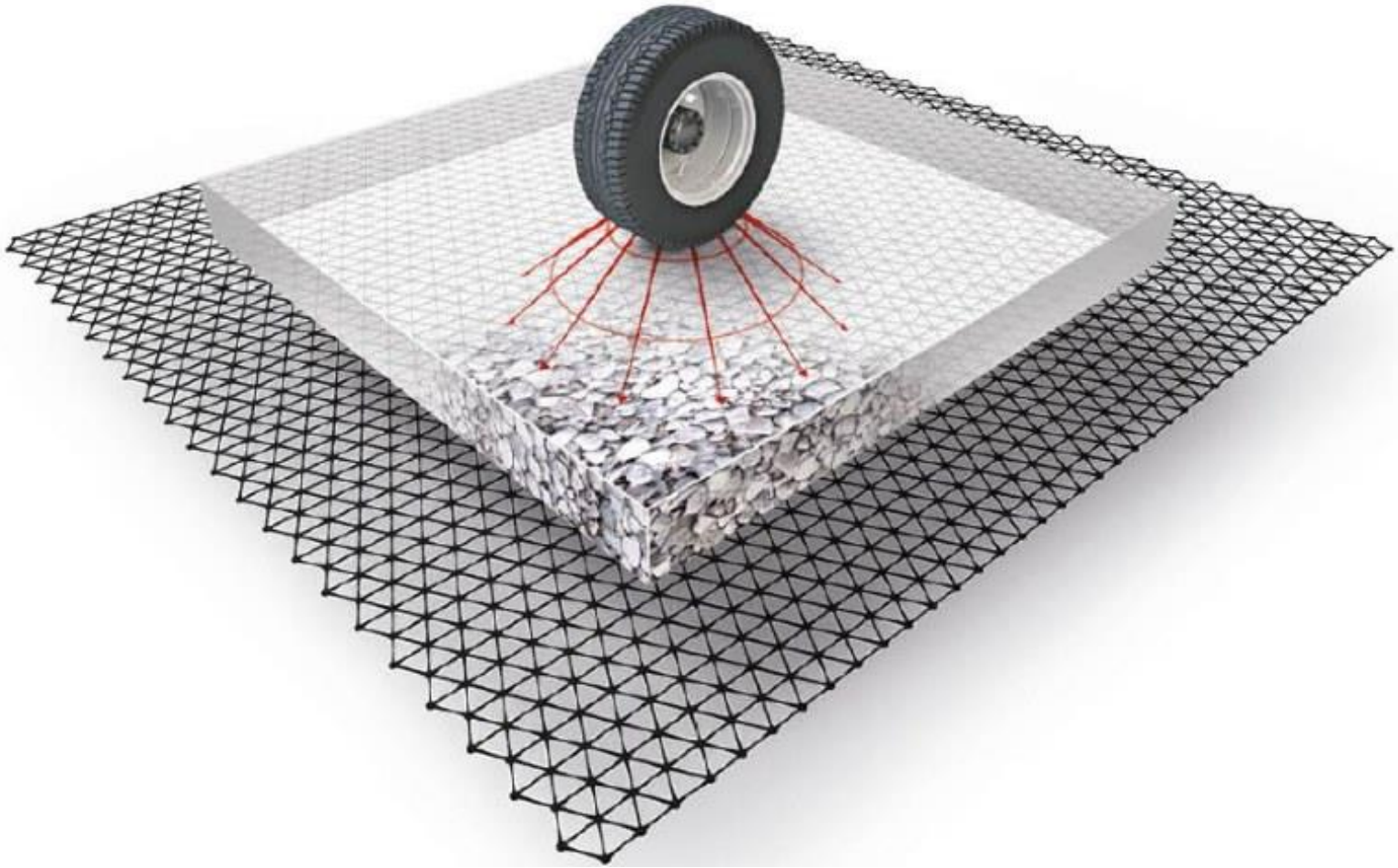


Fig 1.3 - Outward radial load distribution of triaxial geogrids, Tensar International Limited (2018).

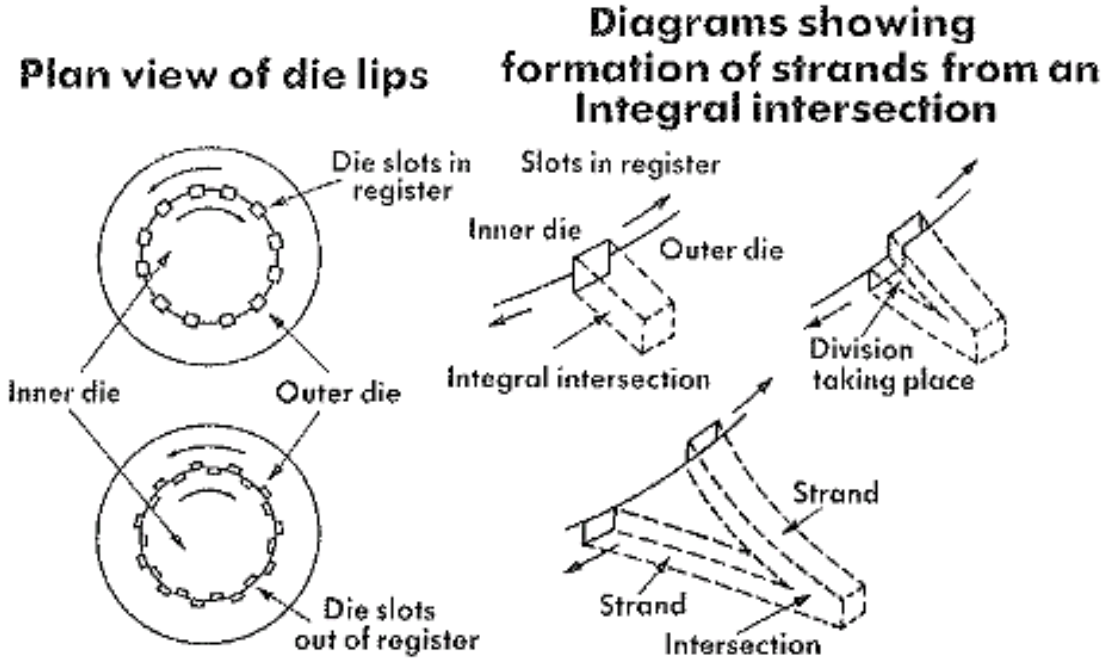


Fig 2.1 - Principal of the Netlon Process, after Mercer (1986).

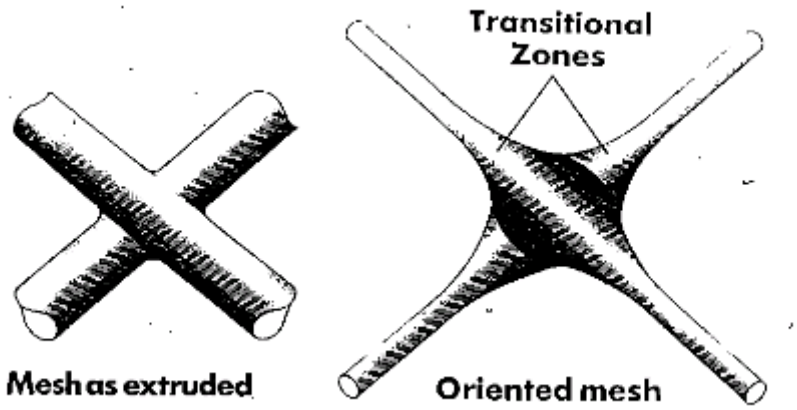


Fig 2.2 – Biplanar junctions produced by the Netlon Process, after Mercer (1986).

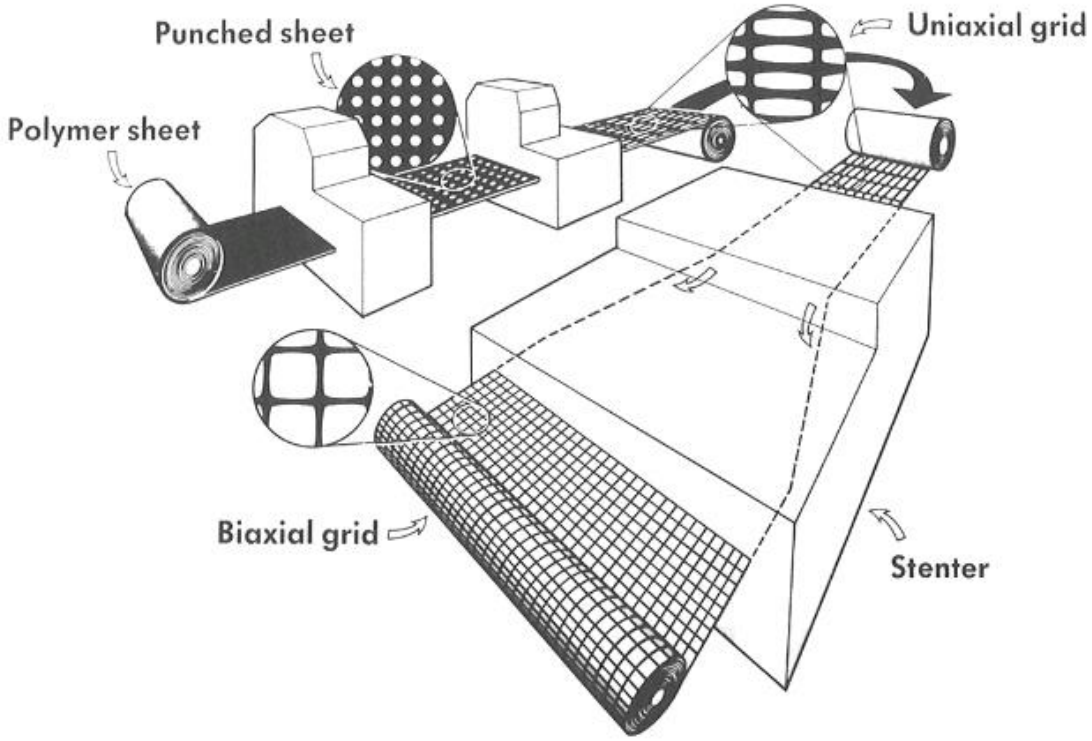
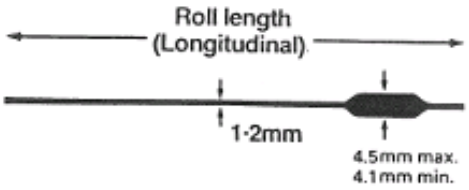
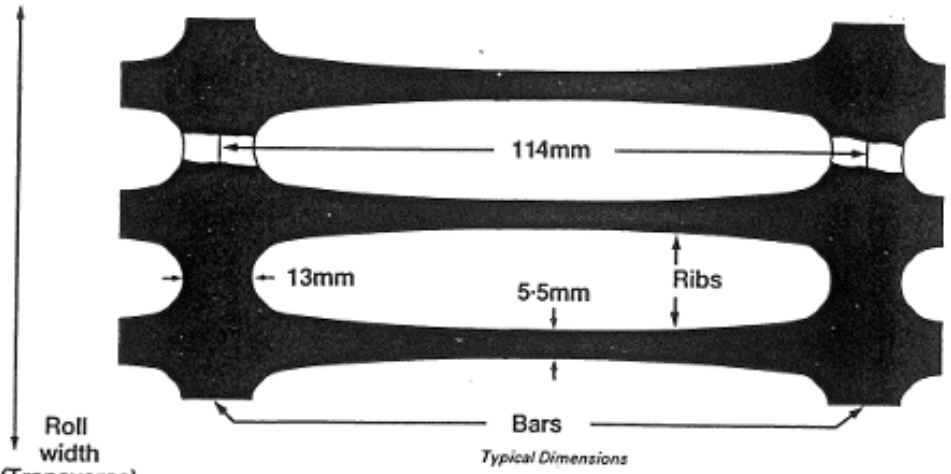


Fig 2.3 – The Tensar Process, after Mercer (1986).

Specification

'Tensar' SR2 Geogrids were developed for reinforcing soils.
e.g. in the construction of embankments and vertical walls.





Typical Dimensions

Roll dimensions

Length:	30m
Width:	1m
Approx diameter:	0·4m
Approx weight:	28 kg

Physical properties of the grids

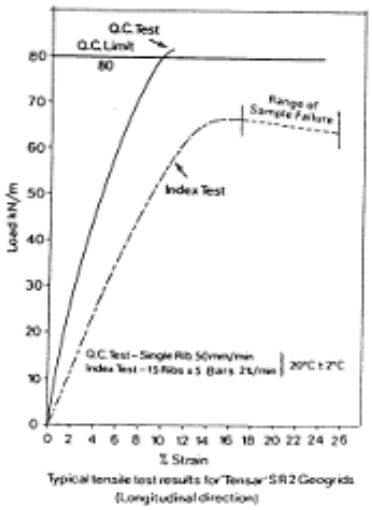
Weight: 0·85 kg/m²
Colour: Black

Quality Control Properties

	*Quality Control Strength (kN/m)	Approx Peak Strain (%)
Longitudinal	80·0	10·5

* Determined as a 95% lower confidence limit

To provide continuity of strength between successive rolls of 'Tensar' SR2, a 15mm diameter polyethylene bodkin should be used.



Typical tensile test results for Tensar SR2 Geogrids (Longitudinal direction)

Ref: 3/88

Fig 2.4 – Specification for Tensar SR2, after Paul (1994).

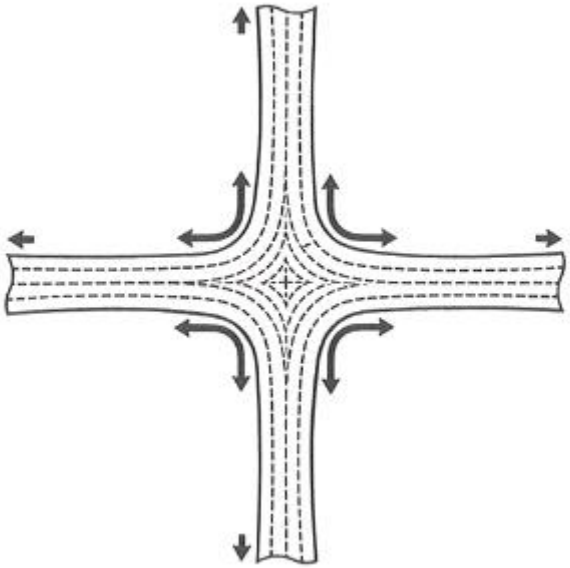


Fig 2.5 – Schematic alignment of molecular orientation in a biaxially stretched junction, after Mercer (1986).

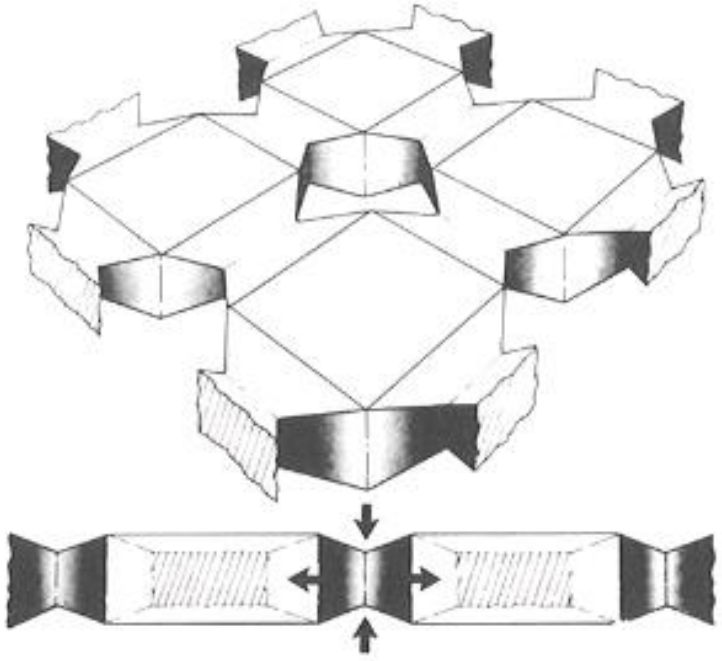


Fig 2.6 – A grooved polymer sheet prepared for biaxial orientation, after Paul (1994).

Specification

Tensar SS1 Geogrid was developed for stabilising weak, low load bearing soils e.g. for the construction of temporary and permanent roads.

Roll dimensions

Length:	50m
Width:	4m
Approx diameter:	0.4m
Approx weight:	44kg

Physical properties of the grid

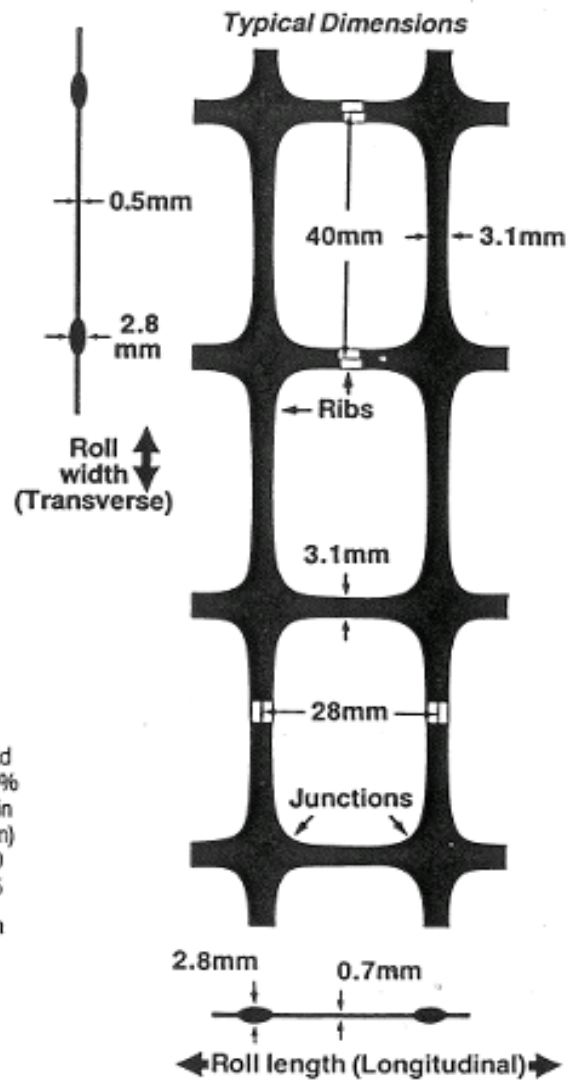
Weight:	0.2 kg/m²
Colour:	Black

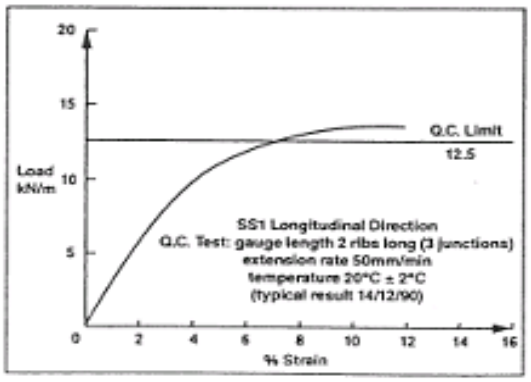
- **The typical strength of the nodes between the longitudinal and transverse ribs, as determined by the Geosynthetics Research Institute, Drexel University, USA, Test Method GG2-87, is ≥ 90% of the Quality Control Strength in both longitudinal and transverse directions.**

Quality Control Properties

	*Quality Control Strength (kN/m)	Approx Peak Strain (%)	Load at 2% Strain (kN/m)	Load at 5% Strain (kN/m)
Transverse	20.5	10.0	6.0	15.0
Longitudinal	12.5	12.0	4.5	9.5

*Determined as a lower 95% confidence limit in accordance with ISO 2602 1980 (BS 2846 Part 2 1981).





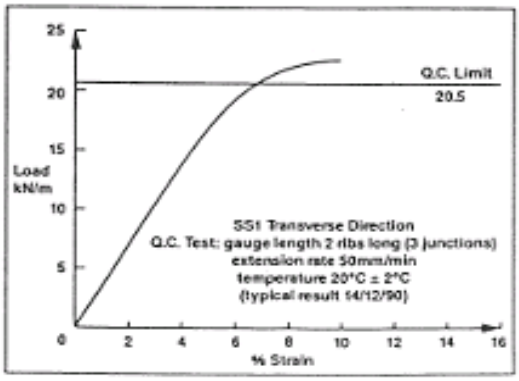


Fig 2.7 – Specification for Tensar SS1, after Paul (1994).

Specification

Tensar SS2 Geogrid was developed for stabilising weak, low load bearing soils e.g. for the construction of temporary and permanent roads.

Roll dimensions

Length:	50m
Width:	4m
Approx diameter:	0.5m
Approx weight:	68kg

Physical properties of the grid

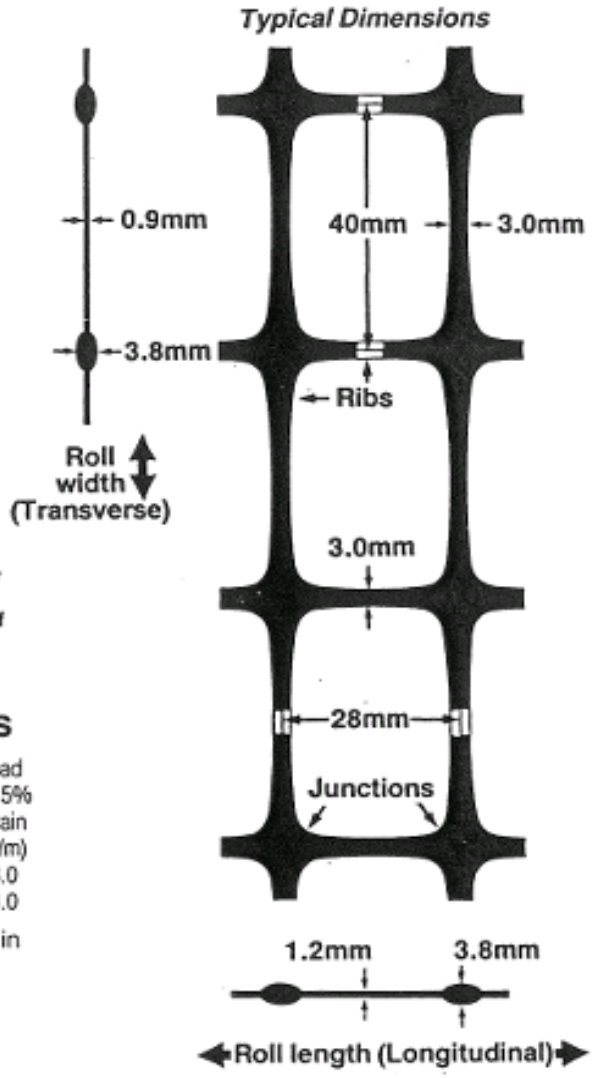
Weight	0.3 kg/m²
Colour:	Black

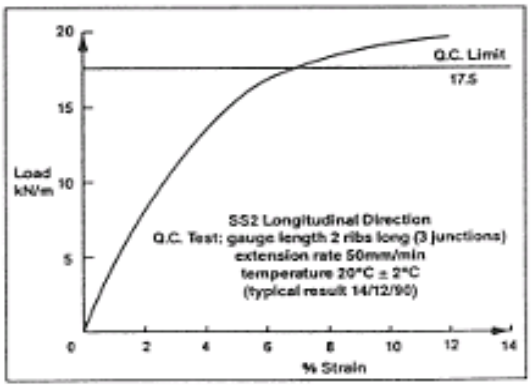
- **The typical strength of the nodes between the longitudinal and transverse ribs, as determined by the Geosynthetics Research Institute, Drexel University, USA, Test Method GG2-87, is ≥ 90% of the Quality Control Strength in both longitudinal and transverse directions.**

Quality Control Properties

	*Quality Control Strength (kN/m)	Approx Peak Strain (%)	Load at 2% Strain (kN/m)	Load at 5% Strain (kN/m)
Transverse	31.5	10.0	12.0	23.0
Longitudinal	17.5	12.0	7.0	14.0

*Determined as a lower 95% confidence limit in accordance with ISO 2602 1980 (BS 2846 Part 2 1981).





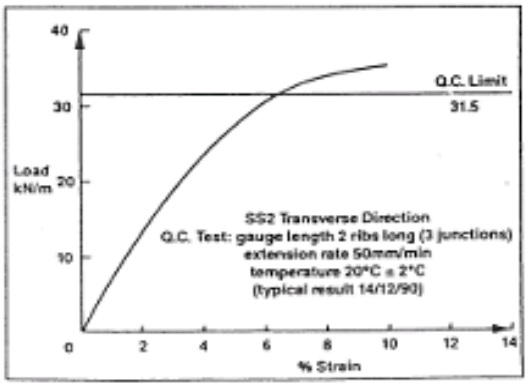


Fig 2.8 – Specification for Tensar SS2, after Paul (1994).

Specification

Tensar SS3 Geogrid was developed for stabilising weak, low load bearing soils e.g. for the construction of temporary and permanent roads.

Roll dimensions

Length	50m
Width:	4m
Approx diameter:	0.5m
Approx weight:	56kg

Physical properties of the grid

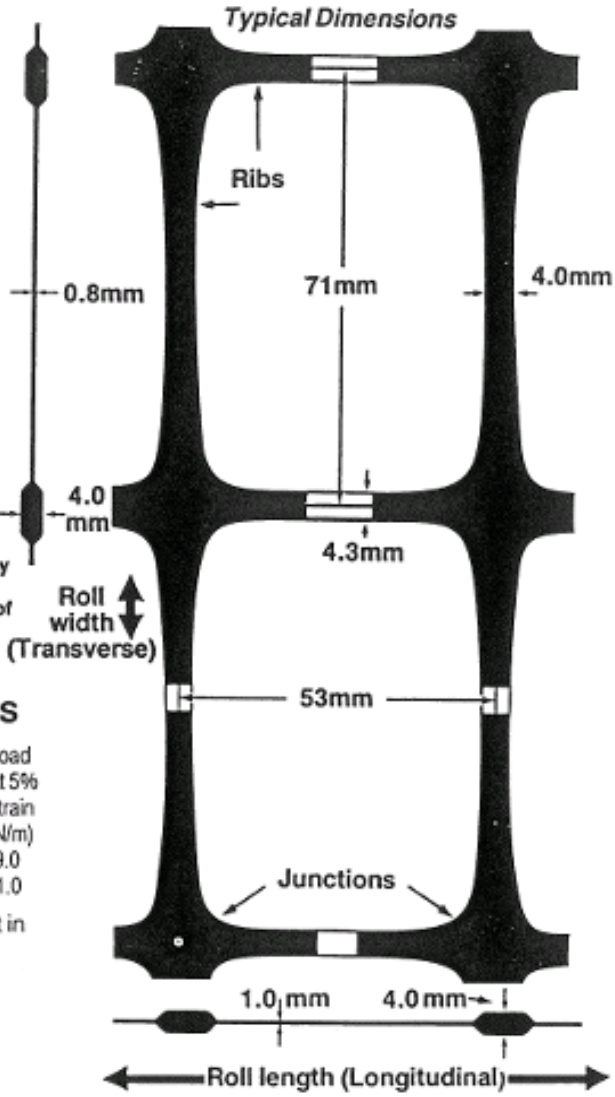
Weight:	0.24kg/m²
Colour:	Black

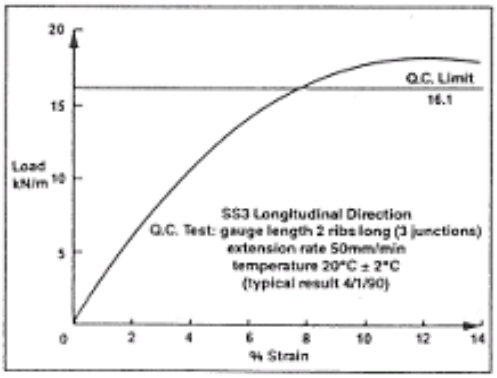
- **The typical strength of the nodes between the longitudinal and transverse ribs, as determined by the Geosynthetics Research Institute, Drexel University, USA, Test Method GG2-87, is ≥ 95% of the Quality Control Strength in both longitudinal and transverse directions.**

Quality Control Properties

	*Quality Control Strength (kN/m)	Approx Peak Strain (%)	Load at 2% Strain (kN/m)	Load at 5% Strain (kN/m)
Transverse	27.4	10.0	10.0	19.0
Longitudinal	16.1	12.0	5.5	11.0

*Determined as a lower 95% confidence limit in accordance with ISO 2602 1980 (BS 2846 Part 2 1981).





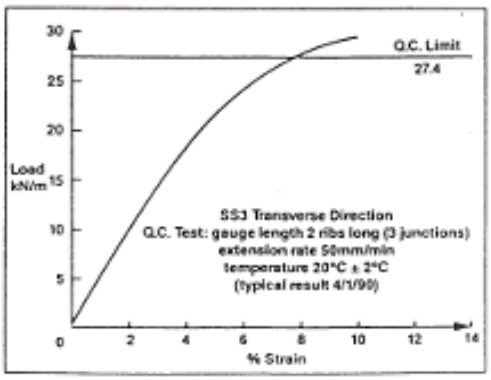


Fig 2.9 – Specification for Tensar SS3, after Paul (1994).



Fig 2.10 – Diabolo shaped punch, after Paul (1994).

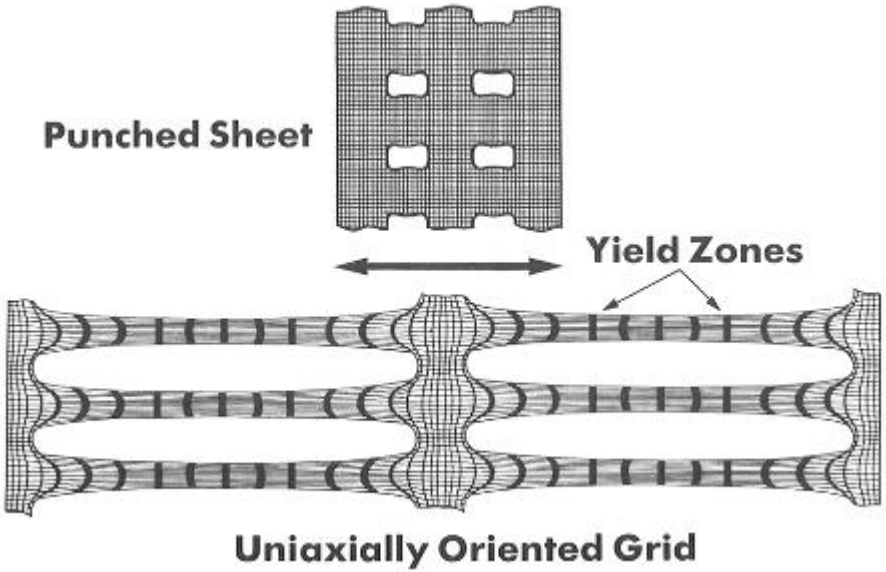
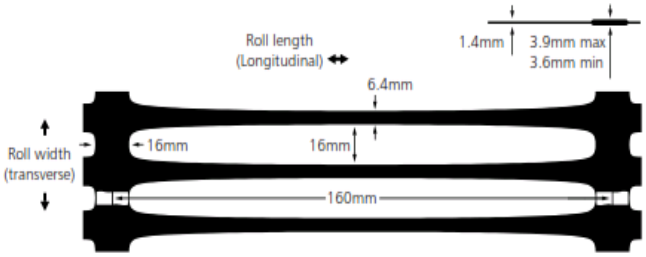


Fig 2.11 – Diabolo punched sheet showing two yield zones upon stretching, after Mercer (1986).

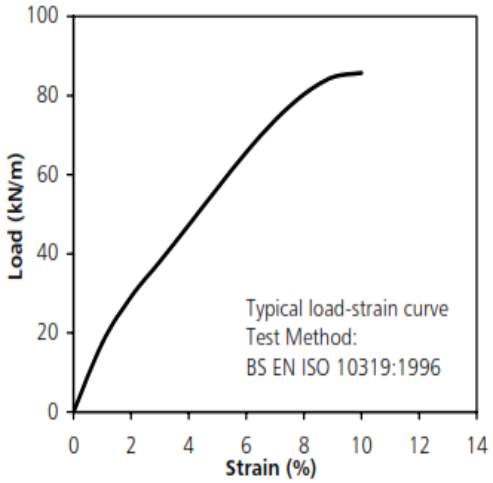
Tensar SR80 geogrid is used for reinforcement of soils in construction of structures such as retaining walls, bridge abutments, steep slopes, slip repairs and geocell mattresses in accordance with EN 13251:2000, EN 13254:2000, EN 13255:2000, EN 13257:2000 & EN 13265:2000.



BBA BRITISH BOARD OF AGRÉMENT ROADS & BRIDGES CERTIFICATE No 99/R108

Tested by BSI Z-20.1-102 Überwacht

Tensar SR80 Geogrid		
Polymer **(1)**		HDPE
Minimum carbon black **(2)**	%	2
Roll width	m	1.0
Roll length	m	30
Unit weight	Kg/m^2	0.74
Roll weight	kg	24
Tensile strength machine direction		
Tensile strength **(3)***	kN/m	86.0 (-3.8)
Load at 2% strain **(3)**	kN/m	26.0
Load at 5% strain **(3)**	kN/m	49.6
Elongation at max load **(3)***	%	10.0 (± 2.0)
Junction strength **(5)**	%	95
Long term creep rupture strength ULS (6)		
P_c or T_{CR} for 20° C **(7)**	kN/m	29.4



(1) HDPE denotes high density polyethylene.

(2) Carbon black inhibits attack by UV light. Determined in accordance with BS 2782:Part 4:Method 452B:1993. Any section of grid fully exposed to sunlight can be expected to retain 90% of its quality control strength for periods of approximately 50 years in temperate climates and 20 years in tropical climates.

(3) Determined in accordance with BS EN ISO 10319:1996.

(4) Parameters marked with an asterisk * are expressed as a mean value and a tolerance (..). The sum of the mean value and the negative tolerance represents the lower 95% confidence limit

(5) Determined in accordance with GRI Test Method GG2-87, and expressed as a % of the mean tensile strength.

(6) Determined as a lower bound using standard extrapolation techniques to creep rupture data obtained following the test procedure in BS EN ISO 13431:1999 for 120 year design life.

(7) In-soil temperature.

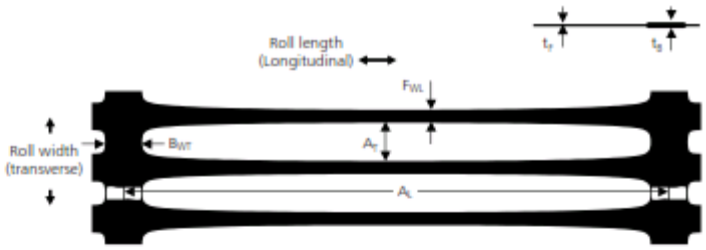
(8) **Tensar SR80** is inert to all chemicals naturally found in soils and has no solvents at ambient temperature. It is not susceptible to hydrolysis and is resistant to aqueous solutions of salts, acids and alkalis (pH 2.0 to 12.0) and is non-biodegradable.

(9) **Tensar SR80** is a stiff monolithic geogrid with integral junctions and is manufactured in accordance with a Quality Management System which complies with the requirements of BS EN ISO 9001:1994.

(10) All quoted dimensions and values are typical unless stated otherwise.

Fig 2.12 – Specification for Tensar SR80, after Paul (1994).

Tensar RE geogrids are used for the reinforcement of soils in construction of structures such as retaining walls, bridge abutments, steep slopes, slip repairs and geocell mattresses.



Properties	Units	Tensar RE geogrid				
		40RE	55RE	80RE	120RE	160RE
Polymer		High density polyethylene				
Minimum carbon black **(1)**	%	2	2	2	2	2
Roll width	m	1.0 & 1.3	1.0 & 1.3	1.0 & 1.3	1.0 & 1.3	1.0 & 1.3
Roll length	m	50	50	50	50	30
Unit weight	kg/m²	0.34	0.42	0.60	0.94	1.26
Roll weight	kg	19 & 24	23 & 29	32 & 41	49 & 63	40 & 51
Dimensions						
A_L	mm	235	235	235	235	230
A_r	mm	16	16	16	16	16
B_{WT}	mm	16	16	16	16	16
F_{WL}	mm	6	6	6	6	6
t_g	mm	1.8 - 2.0	2.5 - 2.7	3.4 - 3.7	5.5 - 5.9	7.1 - 7.7
t_r	mm	0.7	0.9	1.3	2.0	2.6
Quality control strength						
T_{ult} **(2)**	kN/m	52.5	64.5	88.0	136.0	173.0
Load at 2% strain **(2)**	kN/m	12.7	16.1	23.7	38.0	52.5
Load at 5% strain **(2)**	kN/m	24.7	30.9	45.2	75.5	103.0
Approx strain at T_{ult}	%	11.5	11.5	11.5	11.5	11.5
Junction strength (3)	%	100	100	100	100	100
Long term creep rupture strength ULS (4)						
P_c or T_{CR} for 20° C **(5)**	kN/m	20.7	25.5	34.0	48.7	61.7

(1) Carbon black inhibits attack by UV light. Determined in accordance with BS 2782:Part 4:Method 452B:1993. Any section of grid fully exposed to sunlight can be expected to retain 90% of its quality control strength for periods in excess of 40 years in temperature climates and 20 years in tropical climates.

(2) Determined in accordance with BS EN ISO 10319:1996 and as a lower 95% confidence limit in accordance with ISO 2602:1980 (BS 2846:Part 2:1981).

(3) Determined in accordance with GRI Test Method GG2-87, and expressed as a % of the quality control strength.

(4) Determined as a lower bound using standard extrapolation techniques to creep rupture data obtained following the test procedure in BS EN ISO 13431:1999 for 120 year design life.

(5) In-soil temperature.

(6) **Tensar RE geogrids** are inert to all chemicals naturally found in soils and have no solvents at ambient temperature. They are not susceptible to hydrolysis and are resistant to aqueous solutions of salts, acids and alkalis (pH 2.0 to 12.5) and are non-biodegradable.

(7) **Tensar RE geogrids** are stiff monolithic geogrids with integral junctions and are manufactured in accordance with a Quality Management System which complies with the requirements of BS EN ISO 9001:1994.

(8) All quoted dimensions and values are typical unless stated otherwise.

Tensar RE geogrids are stiff monolithic geogrids with integral junctions. They are manufactured from HDPE sheet, orientated in one direction so that the resulting ribs have a high degree of molecular orientation which is continued through the integral transverse bar.

Quality control testing is carried out following the wide width test method BS EN ISO 10319:1996. Typical load strain curves are shown on the adjacent graph.

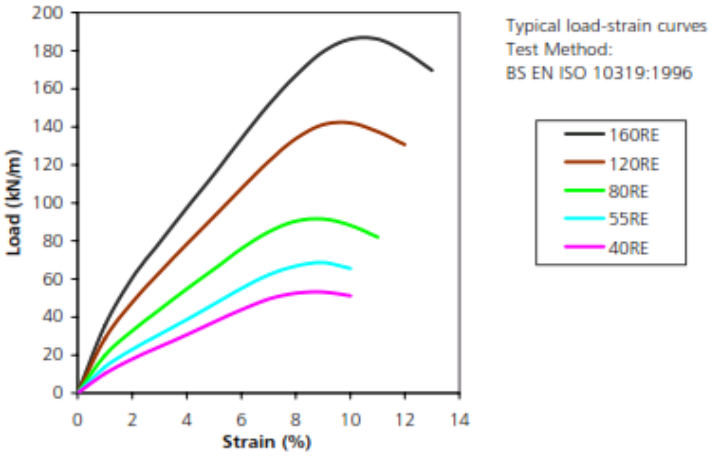
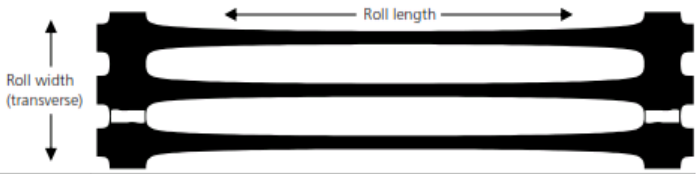


Fig 2.13 – Specifications for the Tensar RE series geogrids, Tensar International Limited (no date)

Tensar RE500 geogrids are used for the reinforcement of soils in the construction of structures such as retaining walls, bridge abutments, steep slopes, slip repairs and geocell mattresses.



Properties	Units	Tensar RE500 geogrids					
		RE510	RE520	RE540	RE560	RE570	RE580
Polymer		High density polyethylene					
Minimum carbon black **(1)**	%	2	2	2	2	2	2
Roll width	m	1.3	1.3	1.3	1.3	1.3	1.3
Roll length	m	75	75	50	50	50	50
Unit weight	kg/m^2	0.29	0.36	0.45	0.65	0.87	0.98
Roll weight	kg	30.0	37.0	31.0	45.0	58.8	67.0
Junction strength (2)	%	95	95	95	95	95	95
Long term strength (3)							
ULS P_c or T_{CR} for 20°C **(4)**	kN/m	19.01	25.10	30.66	42.16	56.28	65.27
Partial factors of safety to calculate safe ultimate limit state (ULS) design strength (P_{des}) (6)							
Manufacturing, extrapolation and database		$f_m=1.0$					
Installation damage max particle size 2mm		$f_d=1.01$	$f_d=1.00$	$f_d=1.00$	$f_d=1.00$	$f_d=1.00$	$f_d=1.00$
Installation damage max particle size 37.5mm		$f_d=1.18$	$f_d=1.07$	$f_d=1.07$	$f_d=1.07$	$f_d=1.07$	$f_d=1.00$
Installation damage max particle size 75mm		$f_d=1.30$	$f_d=1.25$	$f_d=1.20$	$f_d=1.15$	$f_d=1.12$	$f_d=1.06$
Installation damage max particle size 125mm		$f_d=1.60$	$f_d=1.48$	$f_d=1.36$	$f_d=1.25$	$f_d=1.19$	$f_d=1.12$
Environmental effects (pH = 2 to pH = 12.5)		$f_e=1.0$					

(1) Carbon black inhibits attack by UV light. Determined in accordance with BS 2782:Part 4:Method 452B:1993. Any section of grid fully exposed to sunlight can be expected to retain 90% of its quality control strength for periods in excess of 40 years in temperate climates and 20 years in tropical climates.

(2) Determined in accordance with GRI Test Method GG2-87, and expressed as a % of the quality control strength.

(3) ULS determined as a lower bound using standard extrapolation techniques to creep rupture data obtained following the test procedure in BS EN ISO 13431:1999 for 120 year design life.

(4) In-soil temperature.

(5) **Tensar RE500 geogrids** are inert to all chemicals naturally found in soils and have no solvents at ambient temperature. They are not susceptible to hydrolysis and are resistant to aqueous solutions of salts, acids and alkalis (pH 2.0 to 12.5) and are non-biodegradable.

(6) Partial factors are used to derive the ULS safe design strength which is given in the form: $P_{des} = P_c/(f_m \times f_d \times f_e \times LF)$

(7) **Tensar RE500 geogrids** are stiff monolithic geogrids with integral junctions and are manufactured in accordance with Quality and Environmental Management Systems which comply with the requirements of BS EN ISO 9001:2000 and BS EN ISO 14001:1996 respectively.

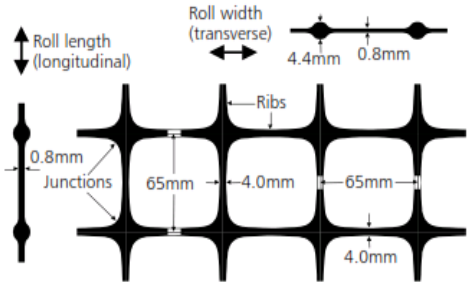
(8) All quoted dimensions and values are typical unless stated otherwise.

(9) **Tensar RE500 geogrids** accreditation includes:
- The British Board of Agrément (BBA) has awarded Roads and Bridges Certificates: No 99/R109 and No 99/R113.
- The Geotechnical Engineering Office of the Civil Engineering Department of the Government of Hong Kong SAR has awarded Certificate RF1/09

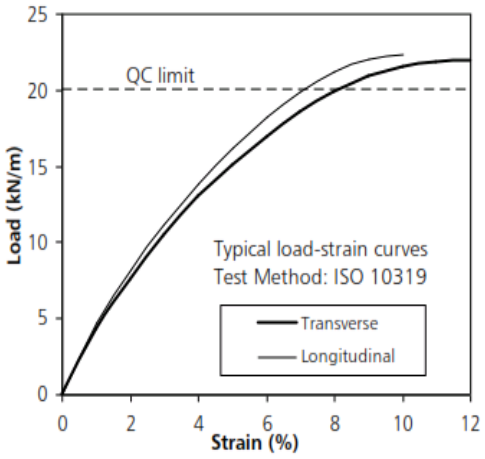
Fig 2.14 – Specification for the Tensar RE500 Series geogrids, Tensar International Limited (no date)

Tensar AR1 is used for both the reinforcement of asphalt layers in the construction of new pavements and of asphalt overlays in the rehabilitation of existing pavements.

Tensar AR1 is a stiff monolithic geogrid with integral junctions. It is orientated in two directions such that the resulting ribs have a high degree of molecular orientation which continues through the area of the integral node. The ribs have a rectangular cross section.



Tensar AR1 Geogrid		
Polymer **(1)**		PP
Minimum carbon black **(2)**	%	2
Roll width	m	3.8
Roll length	m	50
Unit weight	kg/m^2	0.22
Roll weight	kg	45
Quality control strength longitudinal		
Q.C. Strength **(3)**	kN/m	20.0
Load at 2% strain **(3)**	kN/m	7.0
Load at 5% strain **(3)**	kN/m	14.0
Approx peak strain	%	10.0
Junction strength *(4)*	%	95
Maximum shrinkage *(5)*	%	4.0
Quality control strength transverse		
Q.C. Strength **(3)**	kN/m	20.0
Load at 2% strain **(3)**	kN/m	8.0
Load at 5% strain **(3)**	kN/m	15.0
Approx peak strain	%	12.0
Junction strength *(4)*	%	95
Maximum shrinkage *(5)*	%	4.0

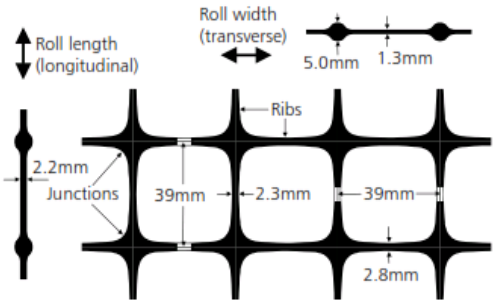


(1) PP denotes polypropylene.
(2) Carbon black inhibits attack by UV light.
Determined in accordance with BS 2782:Part 4:Method 452B:1993.
(3) Determined in accordance with BS EN ISO 10319:1996 and as a lower 95% confidence limit in accordance with ISO 2602:1980 (BS 2846:Part 2:1981).
(4) Determined in accordance with GRI Test Method GG2-87, and expressed as a % of the quality control strength.
(5) Determined as free relaxation in a forced circulation hot air oven at 140 °C for 30 minutes.
(6) **Tensar AR1** is inert to all chemicals naturally found in soils and has no solvents at ambient temperature. It is not susceptible to hydrolysis and is resistant to aqueous solutions of salts, acids and alkalis and is non-biodegradable.
(7) **Tensar AR1** is manufactured in accordance with a Quality Management System which complies with the requirements of BS EN ISO 9001:2000.
(8) All quoted dimensions and values are typical unless stated otherwise

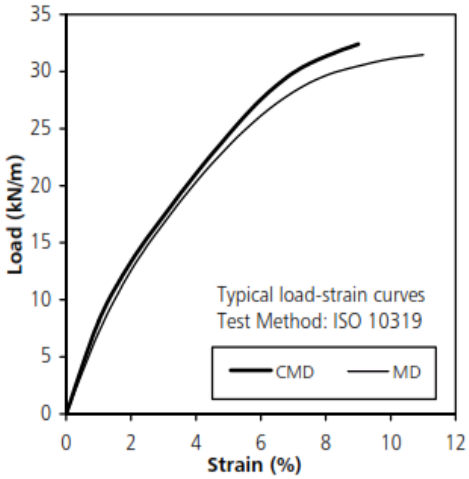
Fig 2.15 – Specification for Tensar AR1, after Paul (1994).

Tensar SS30 geogrid is used for the reinforcement of soils and aggregates in construction of structures such as road pavements, working platforms and reinforced foundations in accordance with with EN 13249:2000, 13250:2000, EN 13251:2000, EN 13253:2000, EN13254:2000, EN13255:2000, EN13257:2000 & EN 13265:2000.

Tensar SS30 is a stiff monolithic geogrid with integral junctions. It is orientated in two directions such that the resulting ribs have a high degree of molecular orientation which continues through the area of the integral node. The ribs have a rectangular cross section.



Tensar SS30 Geogrid		
Polymer **(1)**		PP
Minimum carbon black **(2)**	%	2
Roll width	m	4.0 & 3.8
Roll length	m	50
Unit weight	kg/m^2	0.33
Roll weight	kg	67 & 64
Tensile strength machine direction		
Tensile strength **(3)***	kN/m	31.6 (-0.9)
Load at 2% strain **(3)**	kN/m	10.5
Load at 5% strain **(3)**	kN/m	21.0
Elongation at max load **(3)***	%	15.0 (±3.7)
Junction strength **(5)**	%	90
Tensile strength cross machine direction		
Tensile strength **(3)***	kN/m	33.2 (-1.3)
Load at 2% strain **(3)**	kN/m	10.5
Load at 5% strain **(3)**	kN/m	21.0
Elongation at max load **(3)***	%	10.0 (±1.6)
Junction strength **(5)**	%	86

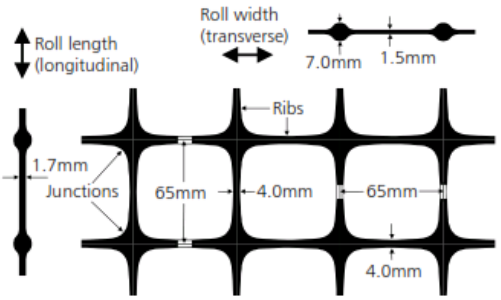


(1) PP denotes polypropylene.
(2) Carbon black inhibits attack by UV light. Determined in accordance with BS 2782:Part 4:Method 452B:1993.
(3) Determined in accordance with BS EN ISO 10319:1996.
(4) Parameters marked with an asterisk * are expressed as a mean value and a tolerance (..). The sum of the mean value and the negative tolerance represents the lower 95% confidence limit.
(5) Determined in accordance with GRI Test Method GG2-87, and expressed as a % of the mean tensile strength.
(6) **Tensar SS30** is inert to all chemicals naturally found in soils and has no solvents at ambient temperature. It is not susceptible to hydrolysis and is resistant to aqueous solutions of salts, acids and alkalis and is non-biodegradable.
(7) **Tensar SS30** is manufactured in accordance with a Quality Management System which complies with the requirements of BS EN ISO 9001:1994.
(8) All quoted dimensions and values are typical unless stated otherwise.

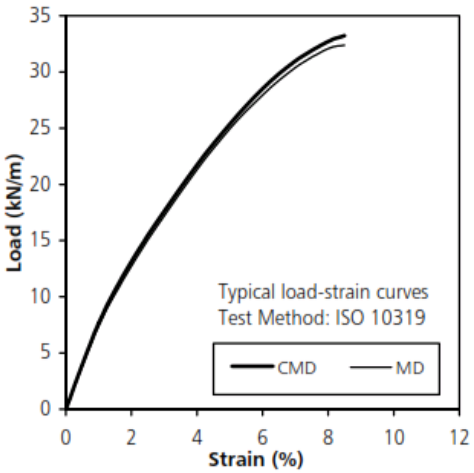
Fig 2.16 – Specification for Tensar SS30, Tensar International Limited (no date)

Tensar SSLA30 geogrid is used for the reinforcement of soils and aggregates in construction of structures such as road pavements, working platforms and reinforced foundations in accordance with EN 13249:2000, 13250:2000, EN 13251:2000, EN 13253:2000, EN13254:2000, EN13255:2000, EN13257:2000 & EN 13265:2000.

Tensar SSLA30 is a stiff monolithic geogrid with integral junctions. It is orientated in two directions such that the resulting ribs have a high degree of molecular orientation which continues through the area of the integral node. The ribs have a rectangular cross section.



Tensar SSLA20 Geogrid		
Polymer **(1)**		PP
Minimum carbon black **(2)**	%	2
Roll width	m	3.8
Roll length	m	50
Unit weight	kg/m^2	0.33
Roll weight	kg	65
Tensile strength machine direction		
Tensile strength **(3)***	kN/m	33.4 (-1.3)
Load at 2% strain **(3)**	kN/m	11.0
Load at 5% strain **(3)**	kN/m	22.0
Elongation at max load **(3)***	%	10.1 (±1.3)
Junction strength **(5)**	%	85
Tensile strength cross machine direction		
Tensile strength **(3)***	kN/m	35.5 (-1.9)
Load at 2% strain **(3)**	kN/m	12.0
Load at 5% strain **(3)**	kN/m	25.0
Elongation at max load **(3)***	%	9.5 (±1.4)
Junction strength **(5)**	%	80



(1) PP denotes polypropylene.
(2) Carbon black inhibits attack by UV light. Determined in accordance with BS 2782:Part 4:Method 452B:1993.
(3) Determined in accordance with BS EN ISO 10319:1996.
(4) Parameters marked with an asterisk * are expressed as a mean value and a tolerance (..). The sum of the mean value and the negative tolerance represents the lower 95% confidence limit.
(5) Determined in accordance with GRI Test Method GG2-87, and expressed as a % of the mean tensile strength.
(6) **Tensar SSLA30** is inert to all chemicals naturally found in soils and has no solvents at ambient temperature. It is not susceptible to hydrolysis and is resistant to aqueous solutions of salts, acids and alkalis and is non-biodegradable.
(7) **Tensar SSLA30** is manufactured in accordance with a Quality Management System which complies with the requirements of BS EN ISO 9001:1994.
(8) All quoted dimensions and values are typical unless stated otherwise.

Fig 2.17 – Specification for Tensar SSLA30, Tensar International Limited (no date)

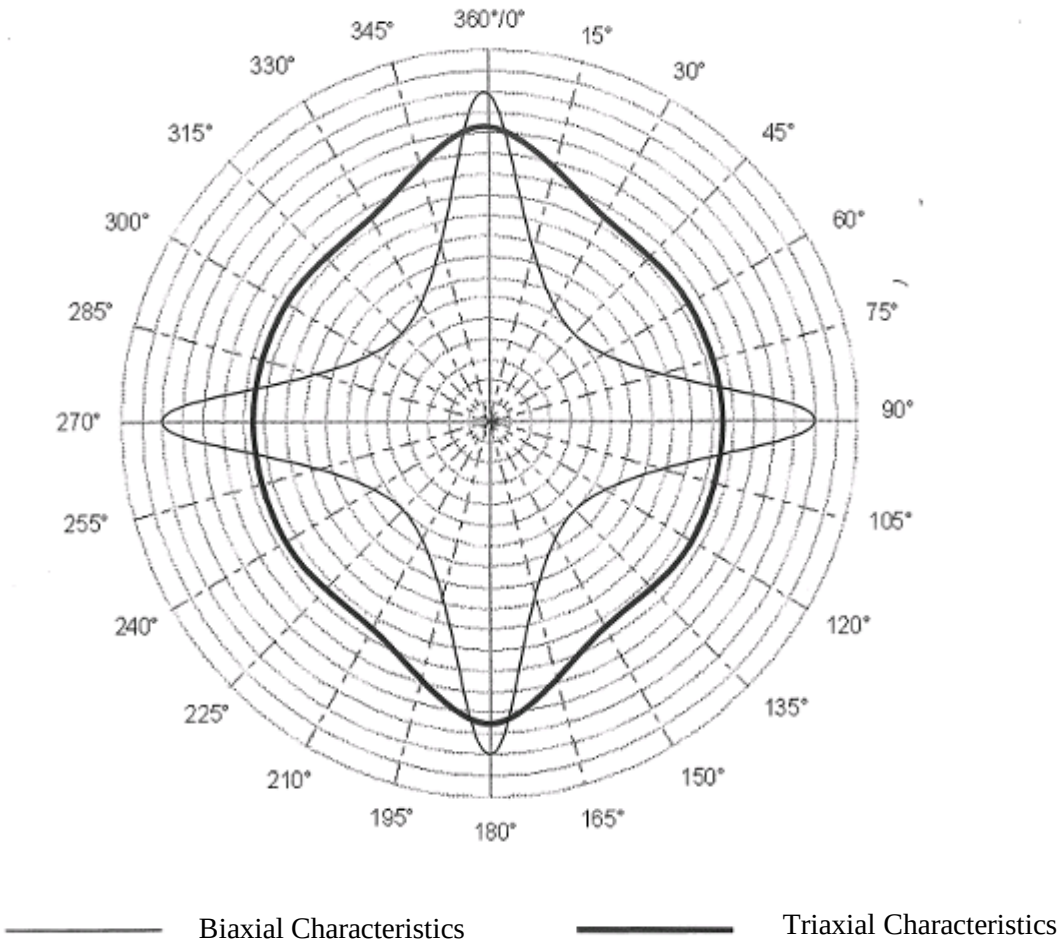


Fig 2.18 – Polar diagram of ultimate strength response, after Walsh (2006).
*Full scale deflection = 36kN/m

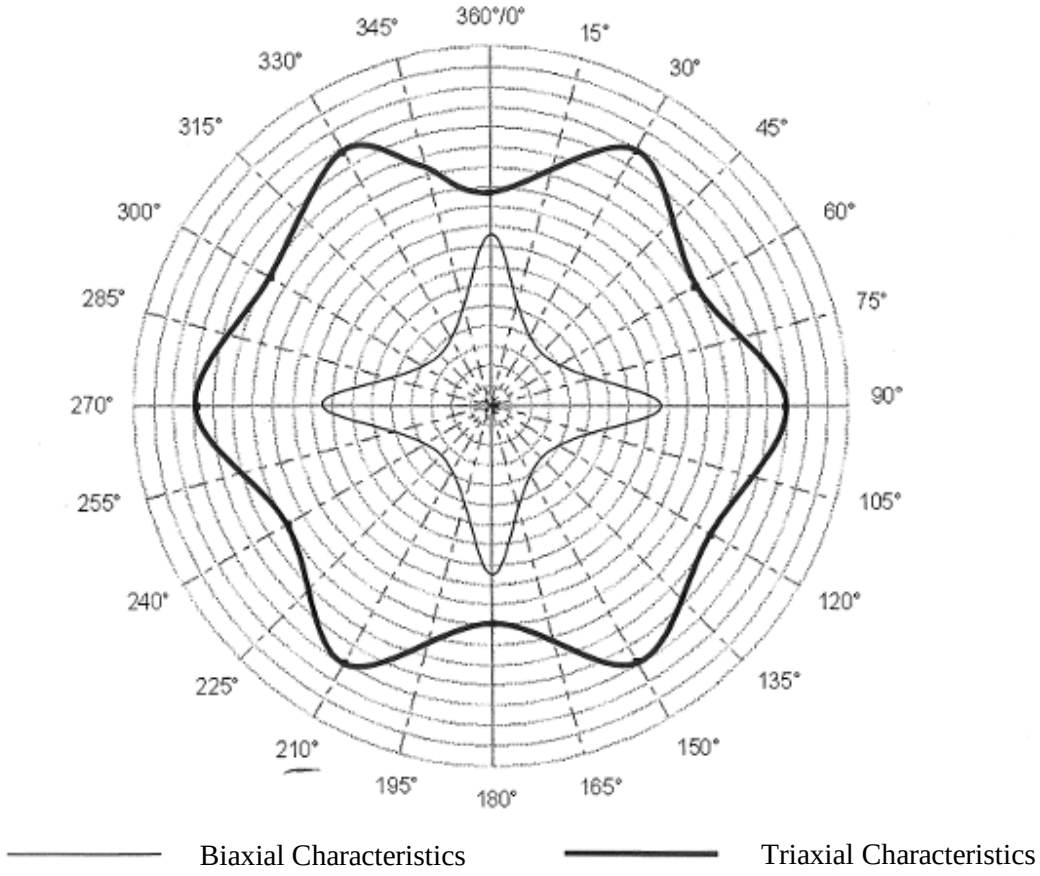


Fig 2.19 – Polar diagram of secant modulus response calculated at maximum load, after Walsh (2006).
*Full scale deflection = 6kN/m

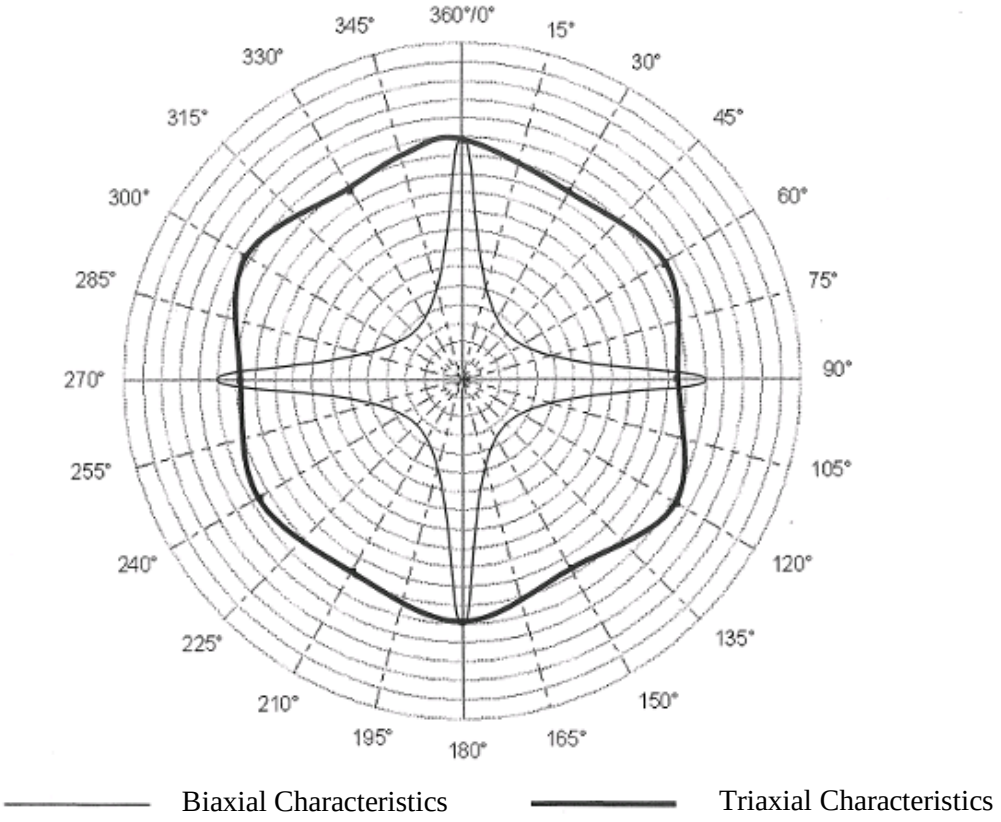


Fig 2.20 – Polar diagram of grid strength at 2% strain response, after Walsh (2006).
*Full scale deflection = 18kN/m

Fig 2.21 – TriAx punch geometry, Walsh (2006).

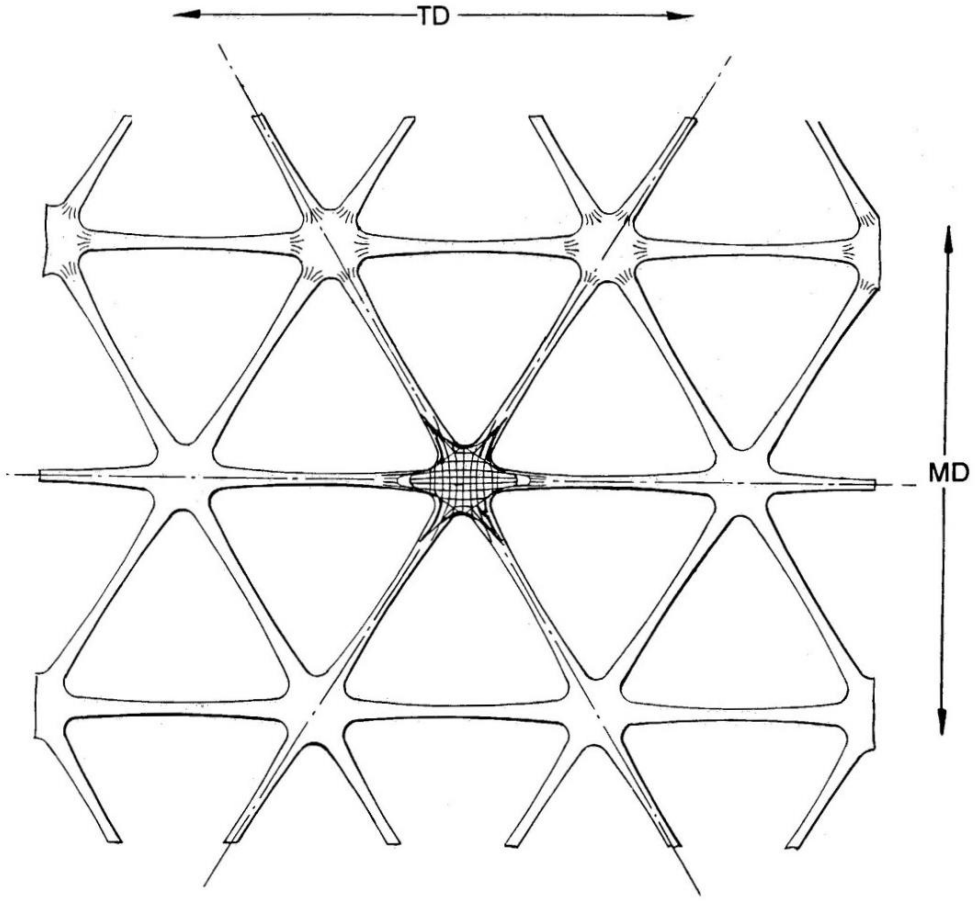


Fig 2.22 – Typical TriAx geometry upon stretching the repeat cluster in Fig 2.21, Tensar Technologies Limited (2004).

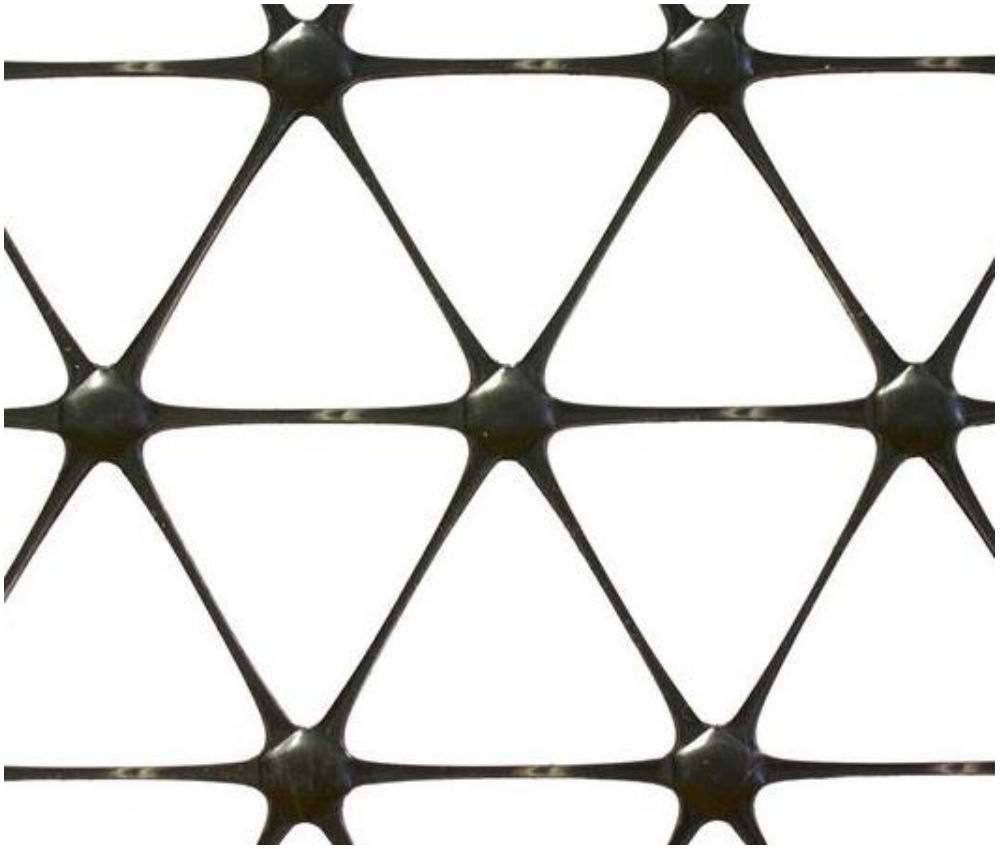


Fig 2.23 – “Across the flats” (AF) dimension of the initial TriAx, Walsh (2006).

Tensar TriAx® Stabilisation Geogrid

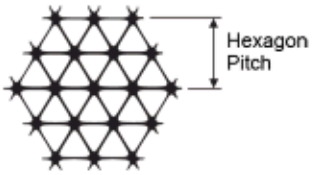
Technical Data – TX160

This Tensar Technical Note provides parameters appropriate for the named Tensar TriAx geogrid for product identification purposes only. The parameters included relate to the stabilisation function of the Tensar TriAx product.

Model Specification documents are available from Tensar International. These include recommended clauses to assist Designers in the preparation of specification documents.

Technical Data

1. The primary geogrid function is stabilisation as defined by European Organisation for Technical Approvals (EOTA) Technical report TR41.
2. The geogrid has European Technical Approval (ETA) certification for the stabilisation of unbound layers by way of interlock with the aggregate.
3. The geogrid is manufactured in accordance with a management system which complies with the requirements of BS EN ISO 9001:2008.
4. The geogrid is a hexagonal structure with triangular apertures manufactured from a punched and stretched polypropylene sheet which is then oriented in three directions so that the resulting ribs of rectangular cross-section have a high degree of molecular orientation which continues through the mass of the integral node.
5. The geogrid has a minimum of 2% finely divided carbon black content.
6. The properties contributing to the performance of a mechanically stabilised layer are:



Required certification for stabilisation function	European Technical Approval (ETA) Certificate		ETA 12/0530	
Performance related physical properties of the product	**Product Characteristic**	**Unit**	**Declared Value**	**Tolerance**
	Radial Secant Stiffness at 0.5% strain[1]	kN/m	390	-75
	Radial Secant Stiffness Ratio[1]	-	0.80	-0.15
	Junction Efficiency[2]	%	100	-10
	Hexagon Pitch[3]	mm	80	±4
Durability Statement [5,6,7]	The minimum working life of the geogrid in natural soils with a pH value between 4 and 9 is assumed to be 100 years in soil temperatures less than 15°C and expected to be 50 years in soil temperatures less than 25°C, when covered within 30 days.			
Properties for identification of the product	Radial Secant Stiffness at 2% strain[1]	kN/m	290	-65
	Hexagon Pitch[3]	mm	80	±4
	Weight of the product[4]	kg/m²	0.220	-0.035

Notes

1. Measured in accordance with EOTA Technical report TR41 B.1.
2. Measured in accordance with EOTA Technical report TR41 B.2.
3. Measured in accordance with EOTA Technical report TR41 B.4.
4. Measured in accordance with EOTA Technical report TR41 B.3.
5. Resistance to weathering of geogrid assessed in accordance with EN 12224. The retained strength is greater than 80% giving a maximum time for exposure after installation of 1 month.
6. Resistance to Oxidation is determined in accordance with EN ISO 13438. For the assumed working life of 50 years, the principle of Method A2 of EN ISO 12438 is followed, with the deviation that the exposure temperature is 120°C and the exposure time 28 days. Justification for this is provided in ETA Certificate 12/0530.
7. Resistance to acid and alkali liquids is determined in accordance with EN 14030.

Fig 2.24. – TX160 technical data, Tensar International Limited (no date)

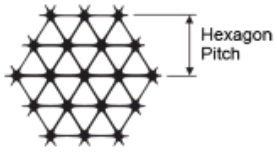
Tensar TriAx® Stabilisation Geocomposite
Technical Data – TX170-GD

This Tensar Technical Note provides parameters appropriate for the named Tensar TriAx geogrid for product identification purposes only. The parameters included relate to the stabilisation function of the Tensar TriAx product.

Model Specification documents are available from Tensar International. These include recommended clauses to assist Designers in the preparation of specification documents.

Technical Data

1. The product is a geogrid/geotextile composite manufactured in accordance with a management system which complies with the requirements of BS EN ISO 9001:2008.
2. The primary geocomposite function is stabilisation as defined by European Organisation for Technical Approvals (EOTA) Technical report TR41. A secondary application is separation
3. The geocomposite has European Technical Approval (ETA) certification for the stabilisation of unbound layers by way of interlock with the aggregate.
4. The geogrid component is manufactured from a punched and stretched polypropylene sheet. It shall have a hexagonal structure with ribs oriented in three directions. The resulting triangular-shaped apertures are defined by ribs of rectangular cross section having a high degree of molecular orientation which is continuous through the node.
5. The geogrid has a minimum of 2% finely divided carbon black content.
6. The properties contributing to the performance of a mechanically stabilised layer are:



Required certification for stabilisation function	European Technical Approval (ETA) Certificate		ETA 12/0531	
Performance related physical properties of the product	**Product Characteristic**	**Unit**	**Declared Value**	**Tolerance**
	Radial Secant Stiffness at 0.5% strain[1]	kN/m	480	-90
	Radial Secant Stiffness Ratio[1]	-	0.80	-0.15
	Junction Efficiency[2]	%	100	-10
	Hexagon Pitch[3]	mm	80	±4
	Static Puncture Resistance (CBR test)[9]	kN	1.64	-0.14
	Dynamic Perforation Resistance[10]	mm	26	+5
	Characteristic Opening Size[11]	µm	110	±40
	Water Permeability Normal to the Plane (Velocity Index)[12]	(VI_{H50}) ms^{-1}	0.135	-0.035

Durability Statement [5,6 7,8]	The minimum working life of the geogrid in natural soils with a pH value between 4 and 9 is assumed to be 100 years in soil temperatures less than 15°C and expected to be 50 years in soil temperatures less than 25°C, when covered within 30 days. The minimum working life of the geotextile component in natural soils with a pH value between 4 and 9 is assumed to be 50 years in soil temperatures less than 15°C and expected to be 25 years in soil temperatures less than 25°C, when covered within 14 days.			
Properties for identification of the product	Radial Secant Stiffness at 2% strain[1]	kN/m	360	-65
	Hexagon Pitch[3]	mm	80	±4
	Weight of the product[4]	kg/m^2	0.440	-0.035

Notes

1. Measured in accordance with EOTA Technical report TR41 B.1.
2. Measured in accordance with EOTA Technical report TR41 B.2.
3. Measured in accordance with EOTA Technical report TR41 B.4.
4. Measured in accordance with EOTA Technical report TR41 B.3.
5. Resistance to weathering of geogrid assessed in accordance with EN 12224. The retained strength is greater than 80% giving a maximum time for exposure after installation of 1 month.
6. Resistance to Oxidation is determined in accordance with EN ISO 13438. For the assumed working life of 50 years, the principle of Method A2 of EN ISO 12438 is followed, with the deviation that the exposure temperature is 120°C and the exposure time 28 days. Justification for this is provided in ETA Certificate 12/0531.
7. Resistance to acid and alkali liquids is determined in accordance with EN 14030.
8. Durability of the geotextile component is assessed in accordance with Annex B of EN 13249.
9. Measured in accordance with EN ISO 12236.
10. Measured in accordance with EN ISO 13433.
11. Measured in accordance with EN ISO 12956.
12. Measured in accordance with EN ISO 11058.

Fig 2.25. – TX170-G technical data, Tensar International Limited (no date)

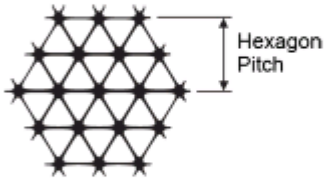
Tensar TriAx® Stabilisation Geogrid
Technical Data – TX190L

This Tensar Technical Note provides parameters appropriate for the named Tensar TriAx geogrid for product identification purposes only. The parameters included relate to the stabilisation function of the Tensar TriAx product.

Model Specification documents are available from Tensar International. These include recommended clauses to assist Designers in the preparation of specification documents.

Technical Data

1. The primary geogrid function is stabilisation as defined by European Organisation for Technical Approvals (EOTA) Technical report TR41.
2. The geogrid has European Technical Approval (ETA) certification for the stabilisation of unbound layers by way of interlock with the aggregate.
3. The geogrid is manufactured in accordance with a management system which complies with the requirements of BS EN ISO 9001:2008.
4. The geogrid is manufactured from a punched and stretched polypropylene sheet. It shall have a hexagonal structure with ribs oriented in three directions. The resulting triangular-shaped apertures are defined by ribs of rectangular cross section having a high degree of molecular orientation which is continuous through the node.
5. The geogrid has a minimum of 2% finely divided carbon black content.
6. The properties contributing to the performance of a mechanically stabilised layer are:



Required certification for stabilisation function	European Technical Approval (ETA) Certificate		ETA 12/0530	
Performance related physical properties of the product	**Product Characteristic**	**Unit**	**Declared Value**	**Tolerance**
	Radial Secant Stiffness at 0.5% strain[1]	kN/m	540	-90
	Radial Secant Stiffness Ratio[1]	-	0.75	-0.15
	Junction Efficiency[2]	%	100	-10
	Hexagon Pitch[3]	mm	120	±6
Durability Statement [5,6,7]	The minimum working life of the geogrid in natural soils with a pH value between 4 and 9 is assumed to be 100 years in soil temperatures less than 15°C and expected to be 50 years in soil temperatures less than 25°C, when covered within 30 days.			
Properties for identification of the product	Radial Secant Stiffness at 2% strain[1]	kN/m	400	-100
	Hexagon Pitch[3]	mm	120	±6
	Weight of the product[4]	kg/m²	0.300	-0.035

Notes

1. Measured in accordance with EOTA Technical report TR41 B.1.
2. Measured in accordance with EOTA Technical report TR41 B.2.
3. Measured in accordance with EOTA Technical report TR41 B.4.
4. Measured in accordance with EOTA Technical report TR41 B.3.
5. Resistance to weathering of geogrid assessed in accordance with EN 12224. The retained strength is greater than 80% giving a maximum time for exposure after installation of 1 month.
6. Resistance to Oxidation is determined in accordance with EN ISO 13438. For the assumed working life of 50 years, the principle of Method A2 of EN ISO 12438 is followed, with the deviation that the exposure temperature is 120°C and the exposure time 28 days. Justification for this is provided in ETA Certificate 12/0530.
7. Resistance to acid and alkali liquids is determined in accordance with EN 14030.

Fig 2.26. – TX190L technical data, Tensar International Limited (no date)

Tensar TriAx® Stabilisation Geogrid

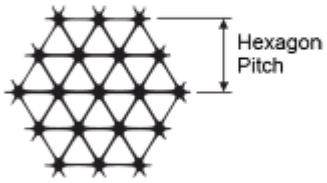
Technical Data – TX130S

This Tensar Technical Note provides parameters appropriate for the named Tensar TriAx geogrid for product identification purposes only. The parameters included relate to the stabilisation function of the Tensar TriAx product.

Model Specification documents are available from Tensar International. These include recommended clauses to assist Designers in the preparation of specification documents.

Technical Data

1. The primary geogrid function is stabilisation as defined by European Organisation for Technical Approvals (EOTA) Technical report TR41.
2. The geogrid has European Technical Approval (ETA) certification for the stabilisation of unbound layers by way of interlock with the aggregate.
3. The geogrid is manufactured in accordance with a management system which complies with the requirements of BS EN ISO 9001:2008.
4. The geogrid is manufactured from a punched and stretched polypropylene sheet. It shall have a hexagonal structure with ribs oriented in three directions. The resulting triangular-shaped apertures are defined by ribs of rectangular cross section having a high degree of molecular orientation which is continuous through the node.
5. The geogrid has a minimum of 2% finely divided carbon black content.
6. The properties contributing to the performance of a mechanically stabilised layer are:



Required certification for stabilisation function	European Technical Approval (ETA) Certificate		ETA 12/0530	
Performance related physical properties of the product	**Product Characteristic**	**Unit**	**Declared Value**	**Tolerance**
	Radial Secant Stiffness at 0.5% strain[1]	kN/m	275	-75
	Radial Secant Stiffness Ratio[1]	-	0.75	-0.15
	Junction Efficiency[2]	%	100	-10
	Hexagon Pitch[3]	mm	66	±4
Durability Statement [5,6,7]	The minimum working life of the geogrid in natural soils with a pH value between 4 and 9 is assumed to be 100 years in soil temperatures less than 15°C and expected to be 50 years in soil temperatures less than 25°C, when covered within 30 days.			
Properties for identification of the product	Radial Secant Stiffness at 2% strain[1]	kN/m	205	-65
	Hexagon Pitch[3]	mm	66	±4
	Weight of the product[4]	kg/m²	0.180	-0.030

Notes

1. Measured in accordance with EOTA Technical report TR41 B.1.
2. Measured in accordance with EOTA Technical report TR41 B.2.
3. Measured in accordance with EOTA Technical report TR41 B.4.
4. Measured in accordance with EOTA Technical report TR41 B.3.
5. Resistance to weathering of geogrid assessed in accordance with EN 12224. The retained strength is greater than 80% giving a maximum time for exposure after installation of 1 month.
6. Resistance to Oxidation is determined in accordance with EN ISO 13438. For the assumed working life of 50 years, the principle of Method A2 of EN ISO 12438 is followed, with the deviation that the exposure temperature is 120°C and the exposure time 28 days. Justification for this is provided in ETA Certificate 12/0530.
7. Resistance to acid and alkali liquids is determined in accordance with EN 14030.

Fig 2.27. – TX130S technical data, Tensar International Limited (no date)

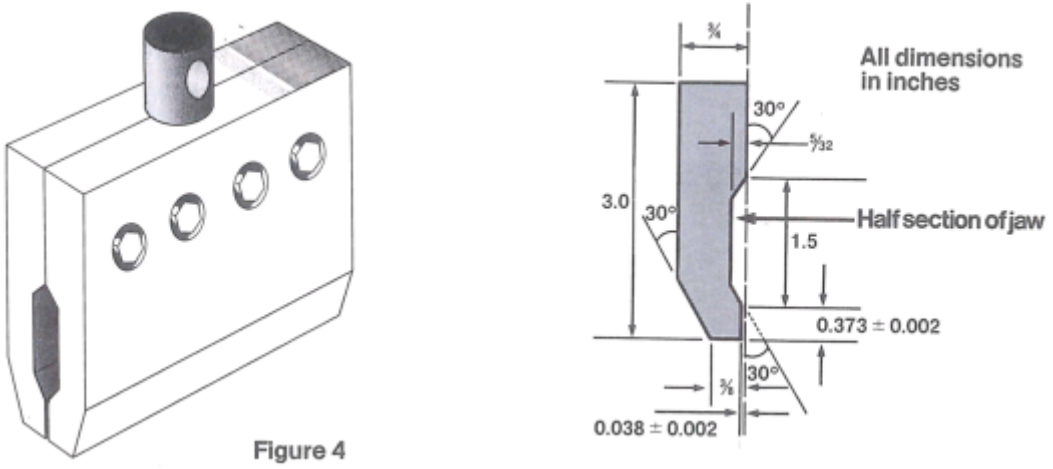


Fig 3.1 – Isometric view and half section of the clamps used to determine the load-strain properties, McGown (1984).

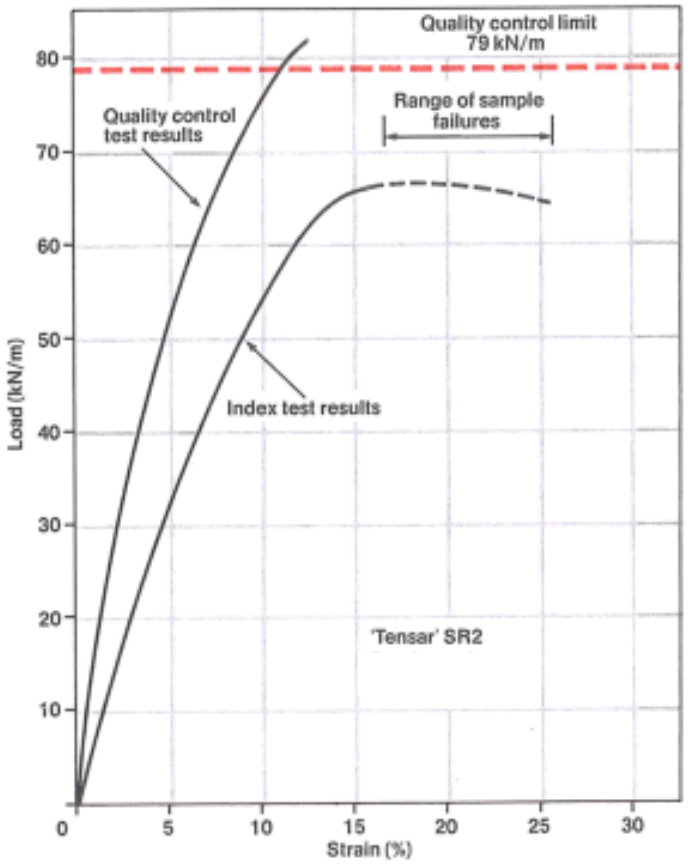
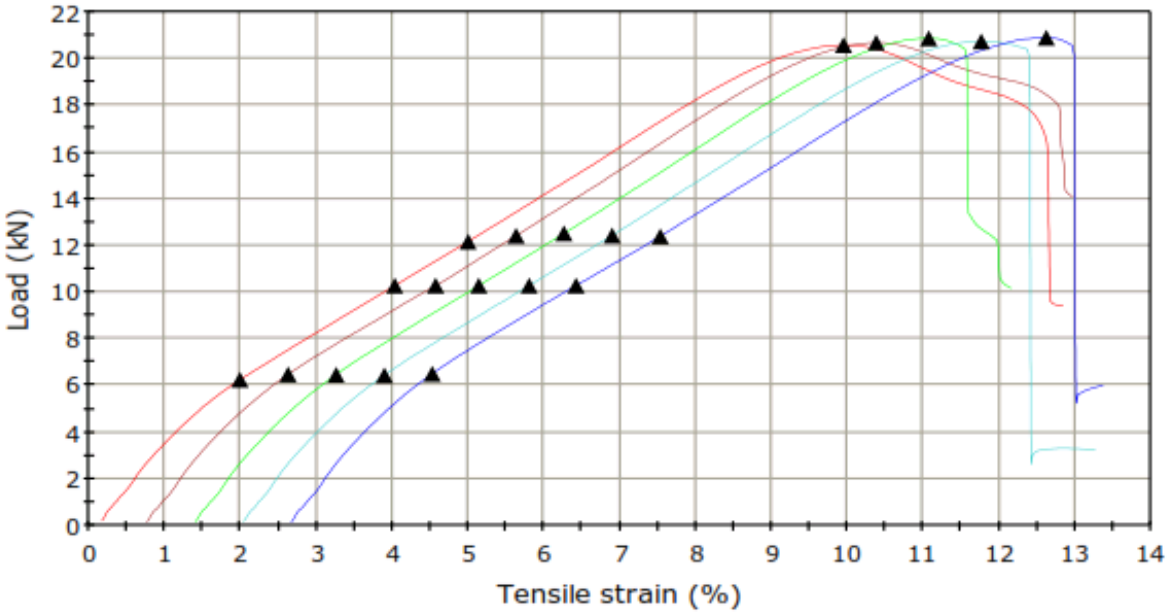


Fig 3.2 – Typical load-strain curve for a Tensar SR2 geogrid, after McGown (1984)



***All data starts at zero but for visualisation purposes the plots are offset.**

	Displacement at Maximum Load (mm)	Maximum Load (kN)	Strain at Maximum Load (%)	Mean Strength (kN/m)	Load at 2% (kN/m)	Load at 5% (kN/m)
1	45.95	20.57	9.94	92.54	28.18	54.77
2	45.15	20.66	9.74	92.99	29.20	55.91
3	45.30	20.85	9.80	93.83	29.19	56.33
4	45.47	20.72	9.86	93.23	29.03	55.95
5	46.40	20.88	10.08	93.94	29.35	55.79
Mean	45.66	20.73	9.88	93.31	28.99	55.75

Fig 3.3 – Typical load-strain curves for a Tensar RE560 geogrid.

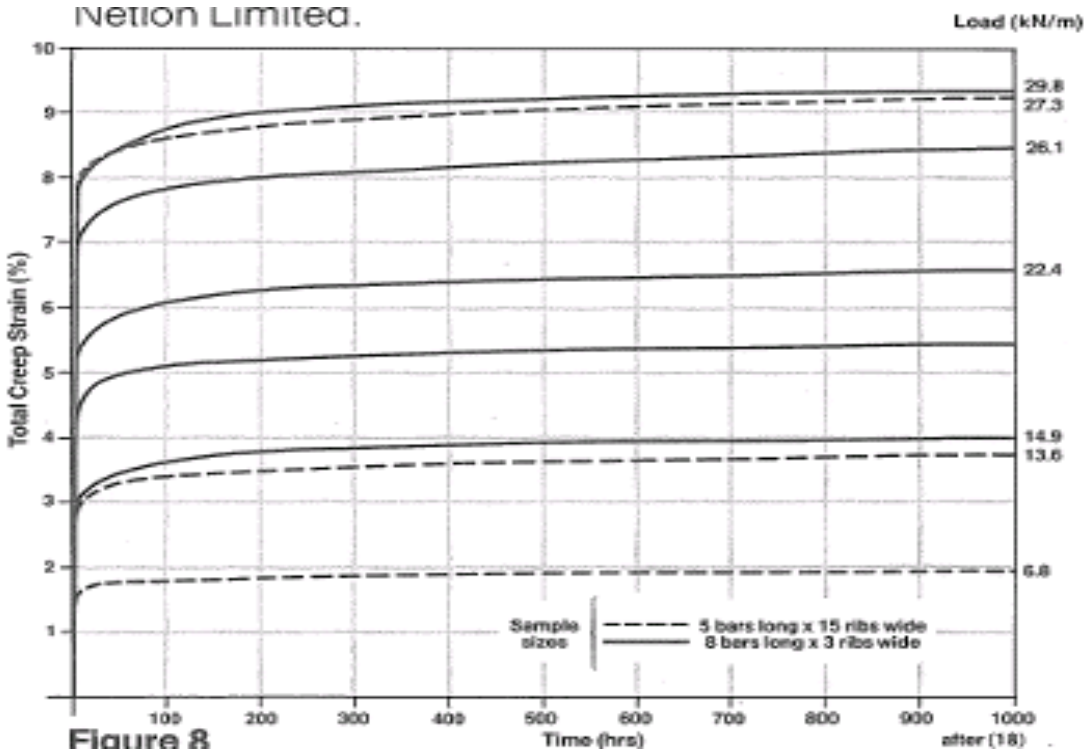


Fig 3.4. – Creep performance of Tensar SR2 geogrids at 20°C when subjected to a range of loads, after McGown (1984)

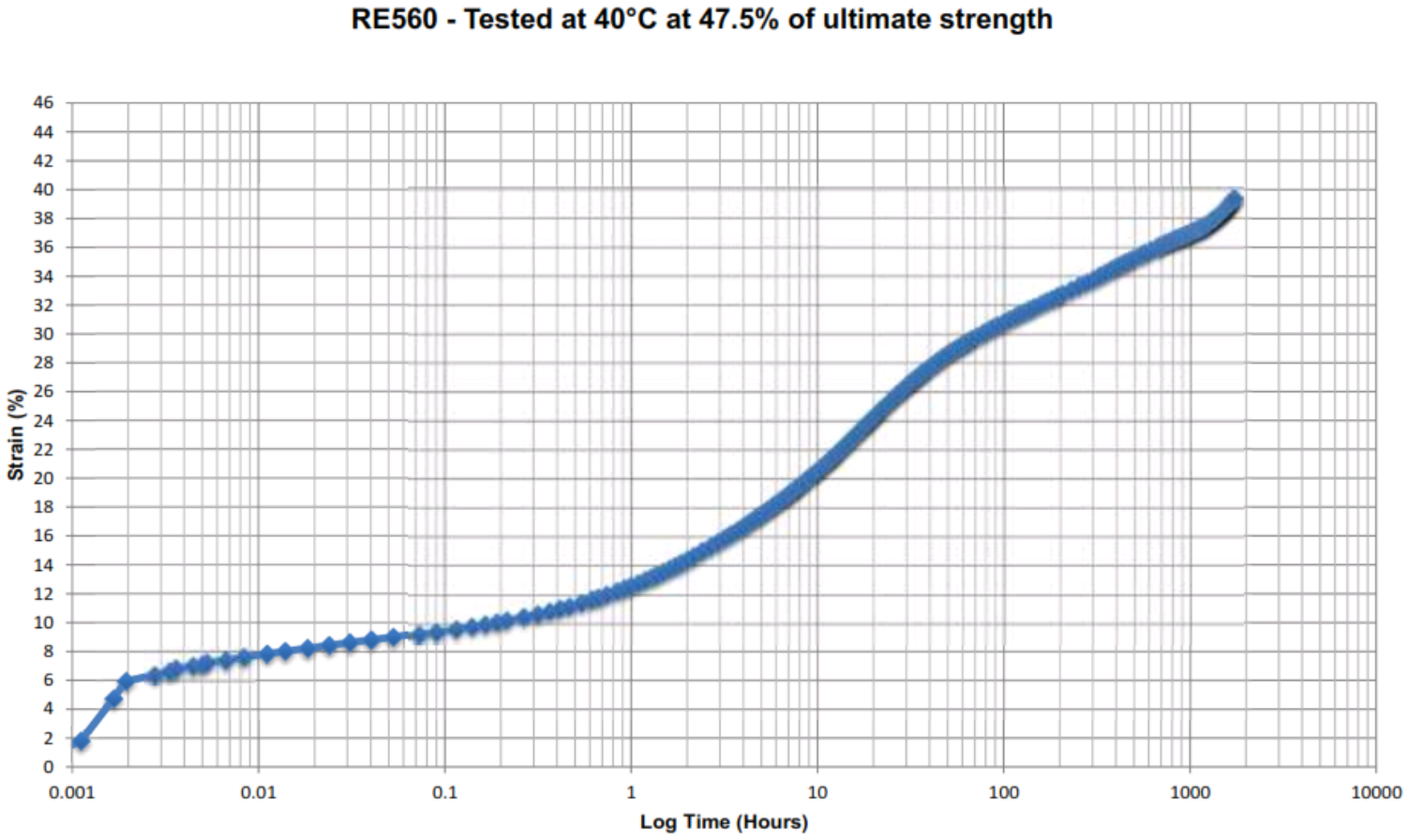
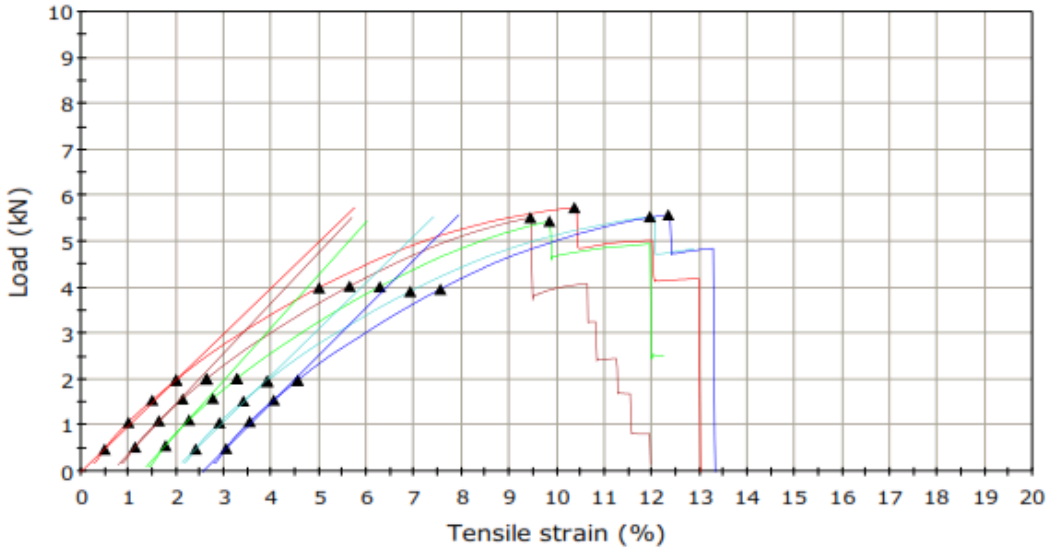


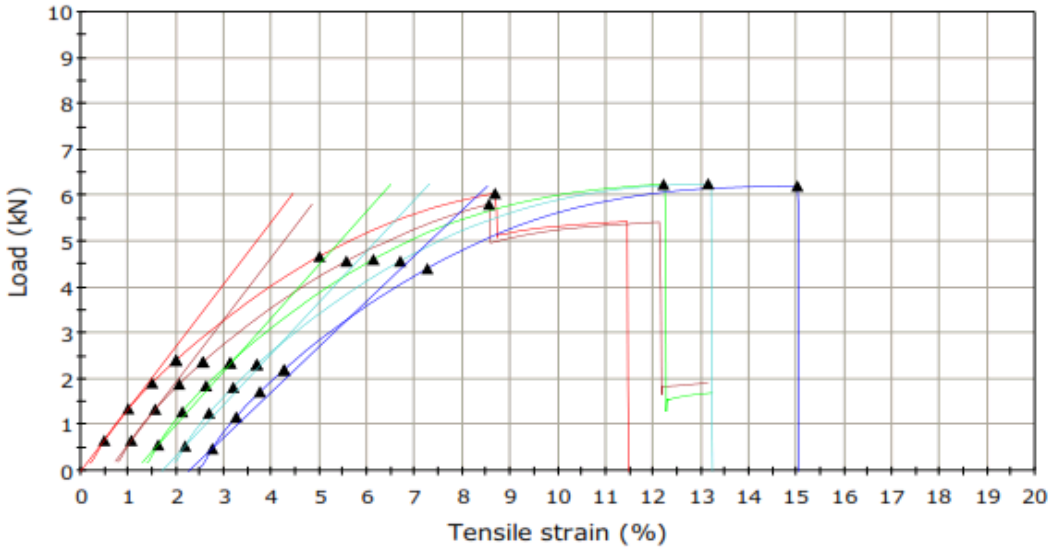
Fig 3.5. – Creep performance of Tensar RE560 at 40°C when subjected to a load of 47.5% of its ultimate strength.



***All data starts at zero but for visualisation purposes the plots are offset.**

	Displacement at Maximum Load (mm)	Maximum Load (kN)	Strain at Maximum Load (%)	Mean Strength (kN/m)	Load at 2% (kN/m)	Load at 5% (kN/m)	Strain at 20kN/m (%)
1	23.37	5.75	10.36	21.10	7.36	14.70	8.33
2	19.77	5.53	8.80	20.30	7.44	14.81	8.14
3	19.24	5.45	8.56	20.02	7.47	14.78	8.23
4	22.54	5.55	10.03	20.37	7.27	14.40	9.02
5	22.08	5.59	9.78	20.53	7.33	14.59	8.62
Mean	21.40	5.57	9.50	20.46	7.37	14.66	8.47
Standard Deviation	1.80	0.11	0.79	0.40	0.08	0.17	0.36
Mean - 1 SD	19.60	5.46	8.72	20.06	7.29	14.49	8.11

Fig 3.6. – Typical load-strain curves for Tensar SS20 tested in the machine direction.



***All data starts at zero but for visualisation purposes the plots are offset.**

	Displacement at Maximum Load (mm)	Maximum Load (kN)	Strain at Maximum Load (%)	Mean Strength (kN/m)	Load at 2% (kN/m)	Load at 5% (kN/m)	Strain at 20kN/m (%)
1	20.54	6.05	8.67	22.91	9.18	17.72	6.74
2	18.60	5.82	7.99	22.03	9.03	17.33	7.02
3	27.52	6.25	11.07	23.67	8.98	17.47	6.94
4	26.60	6.26	11.44	23.70	8.83	17.33	6.98
5	29.00	6.22	12.75	23.54	8.37	16.71	7.35
Mean	24.45	6.12	10.38	23.17	8.88	17.31	7.01
Standard Deviation	4.59	0.19	1.99	0.72	0.31	0.37	0.22
Mean - 1 SD	19.86	5.93	8.39	22.46	8.57	16.94	6.78

Fig 3.7. – Typical load-strain curves for Tensar SS20 tested in the cross-machine direction.

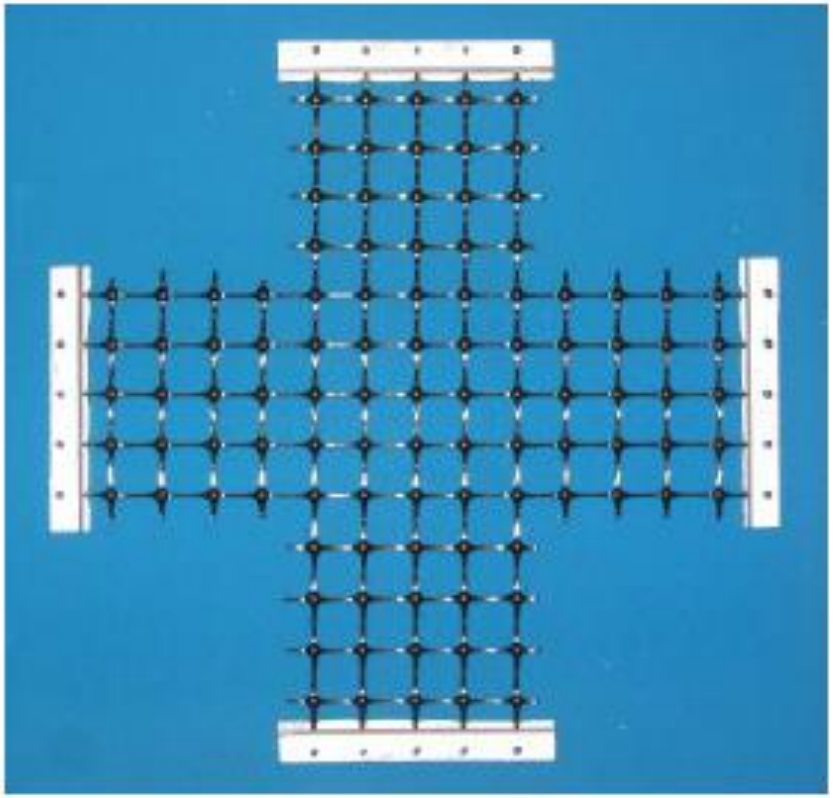


Fig 3.8. – Cruciform shape of geogrid used for biaxial testing, Kupec (2004).

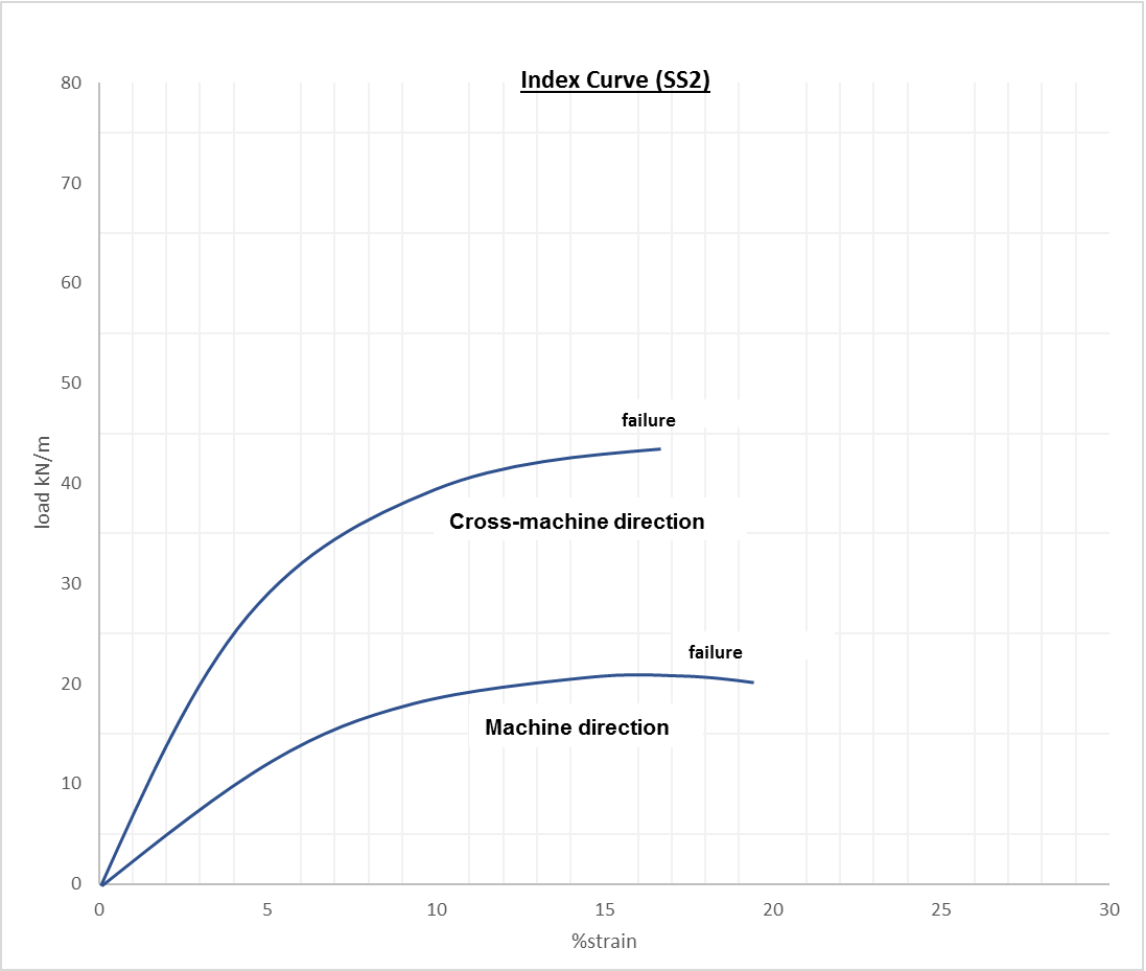
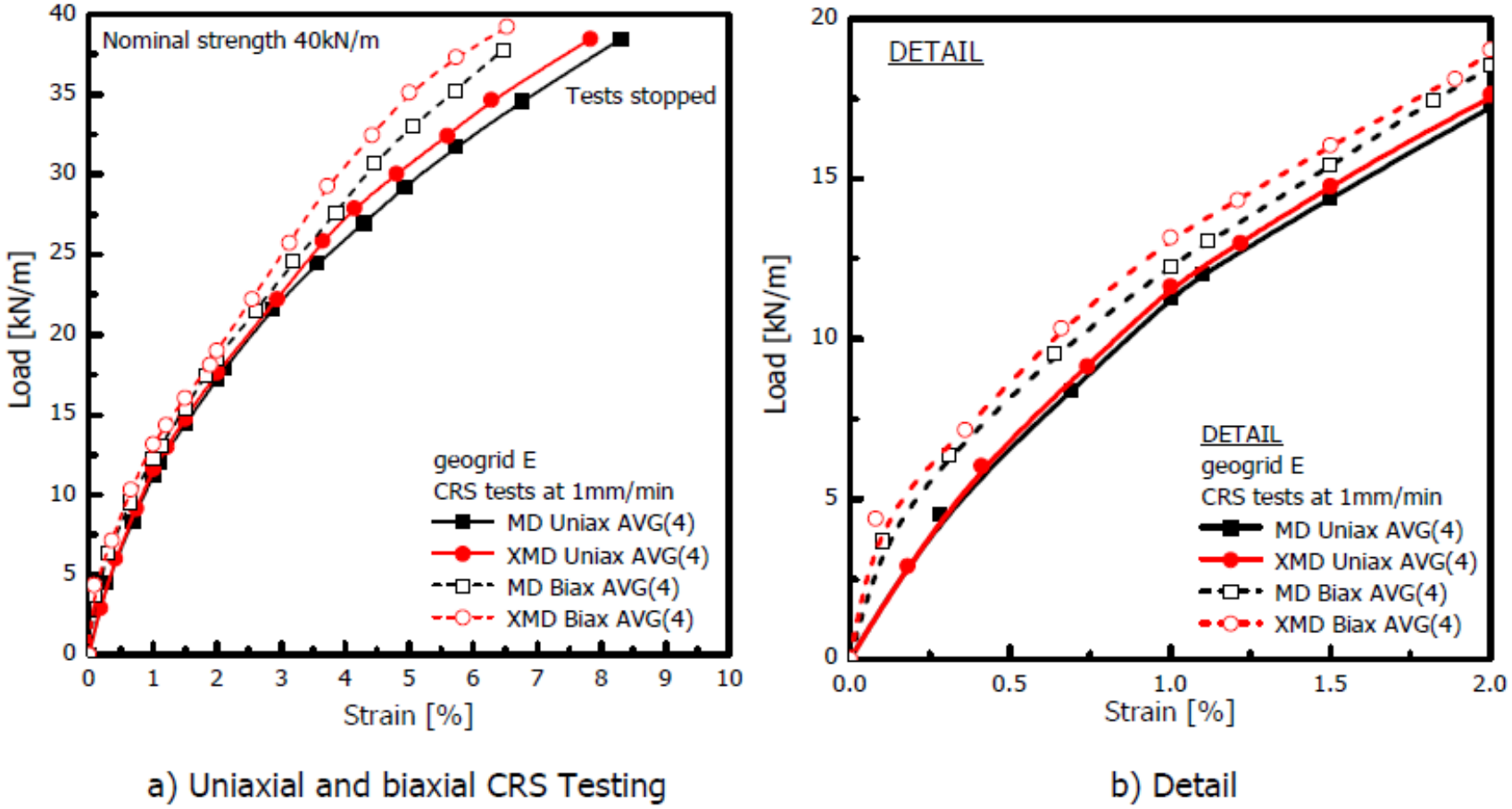


Fig 3.9. – Index test curves for Tensar SS2, McGown (1984).



a) Uniaxial and biaxial CRS Testing

b) Detail

Fig 3.10. – Comparison of uniaxial and biaxial load-strain behaviour of a geogrid with integral junctions, Kupec (2004).

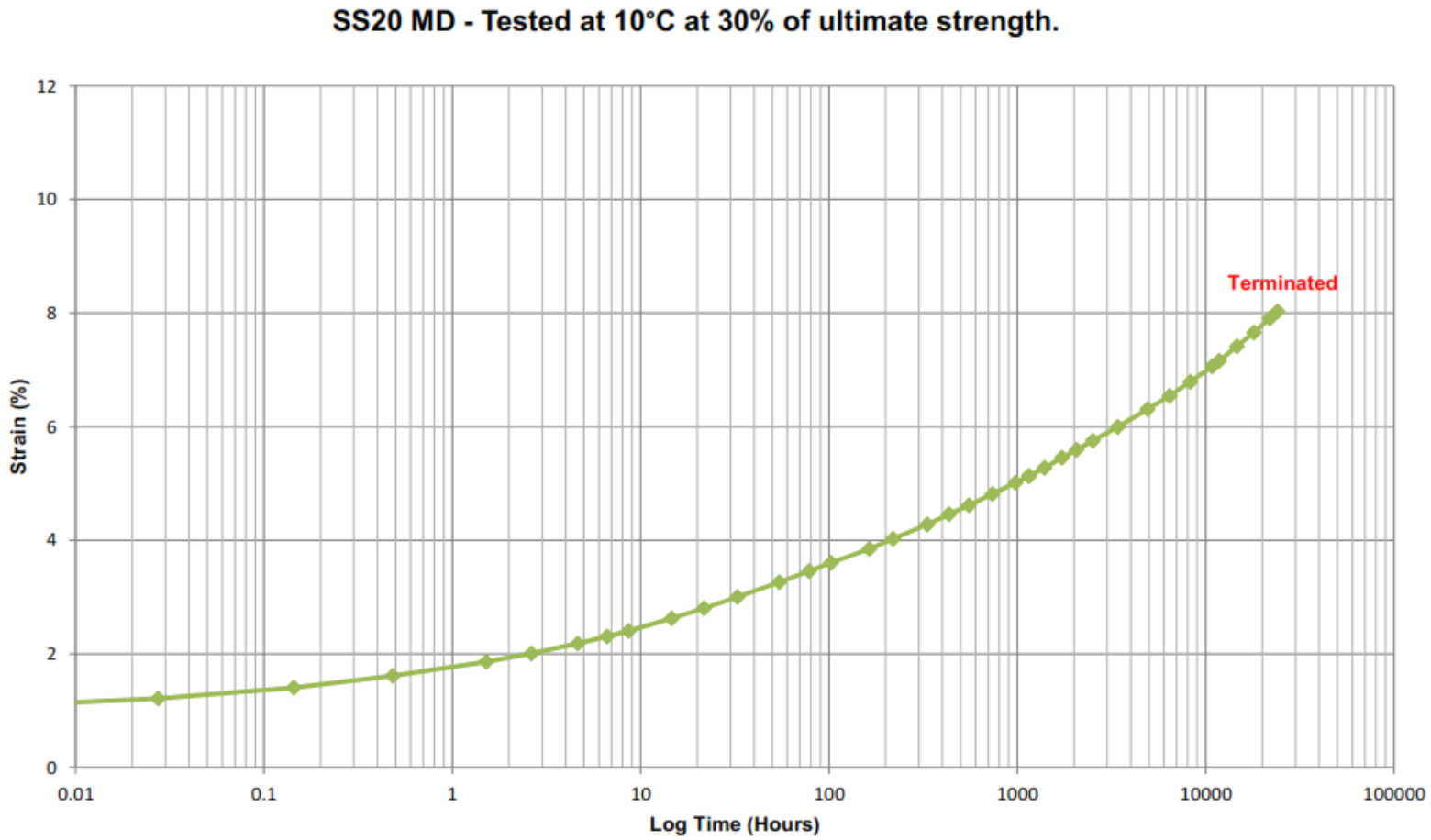


Fig 3.11 – Creep performance of Tensar SS20 MD at 10°C when subjected to a load of 30% of its ultimate strength.

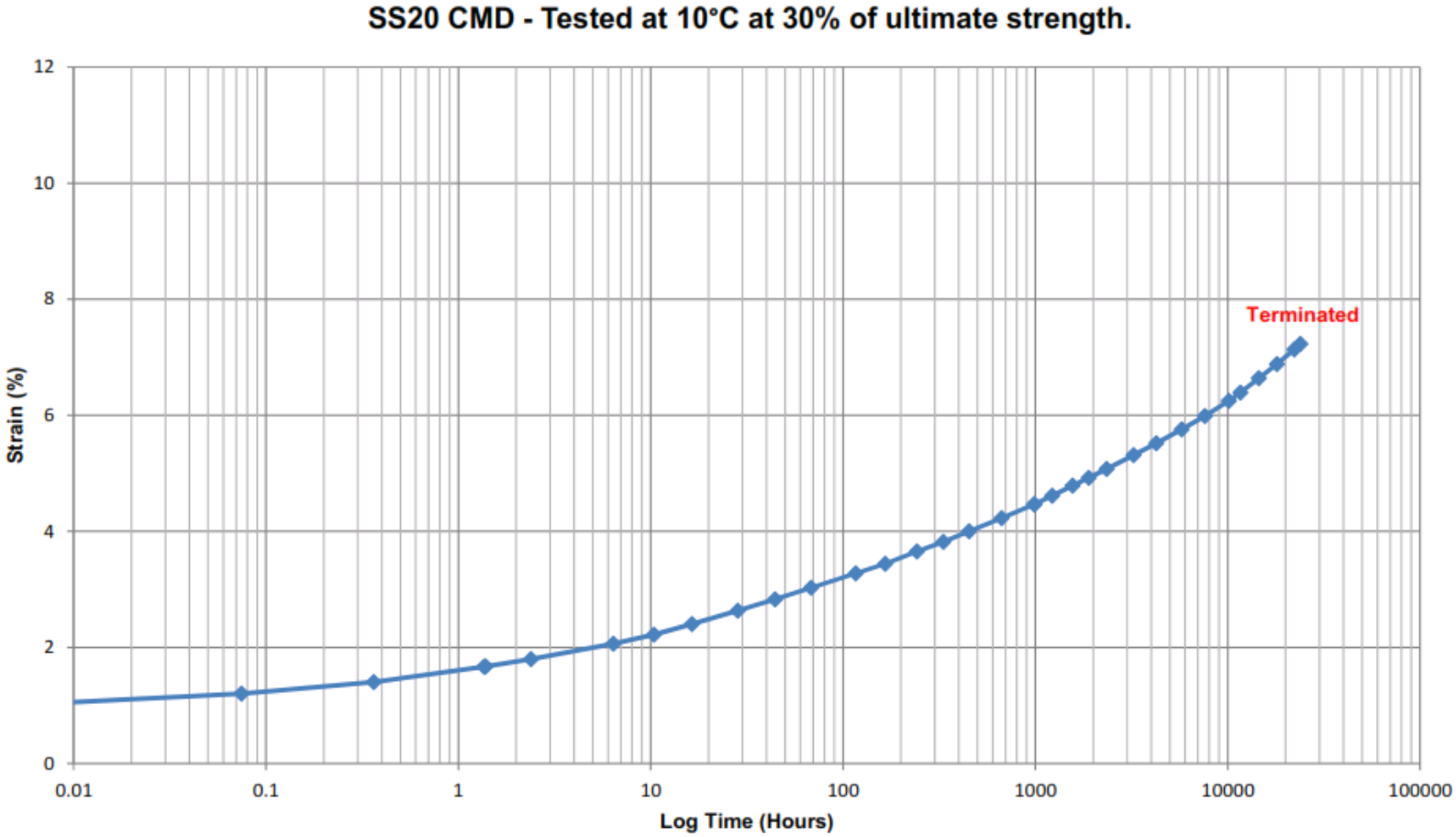


Fig 3.12 – Creep performance of Tensar SS20 XMD at 10°C when subjected to a load of 30% of its ultimate strength.

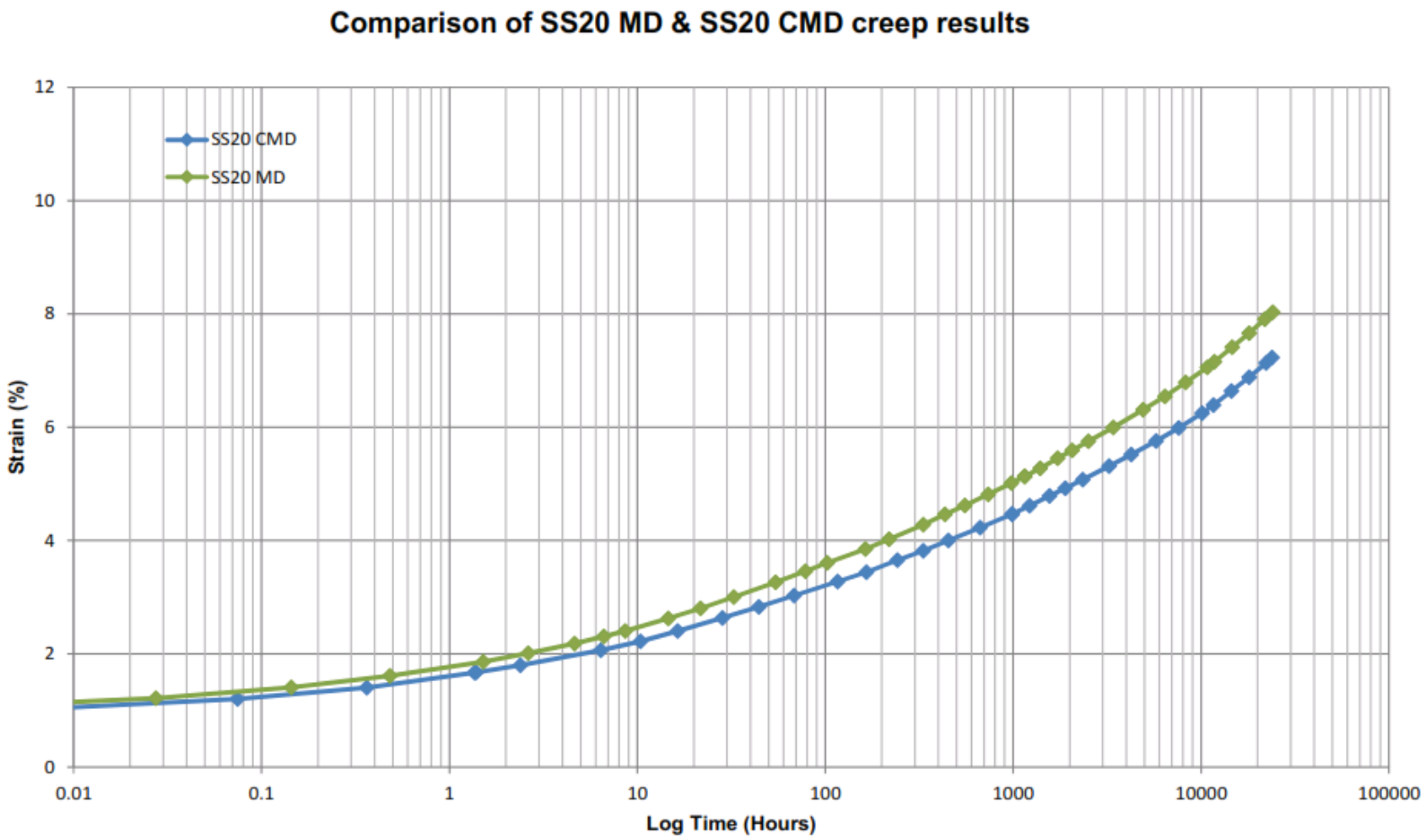


Fig 3.13 – Comparison of Tensar SS20 MD & SS20 XMD creep performance.

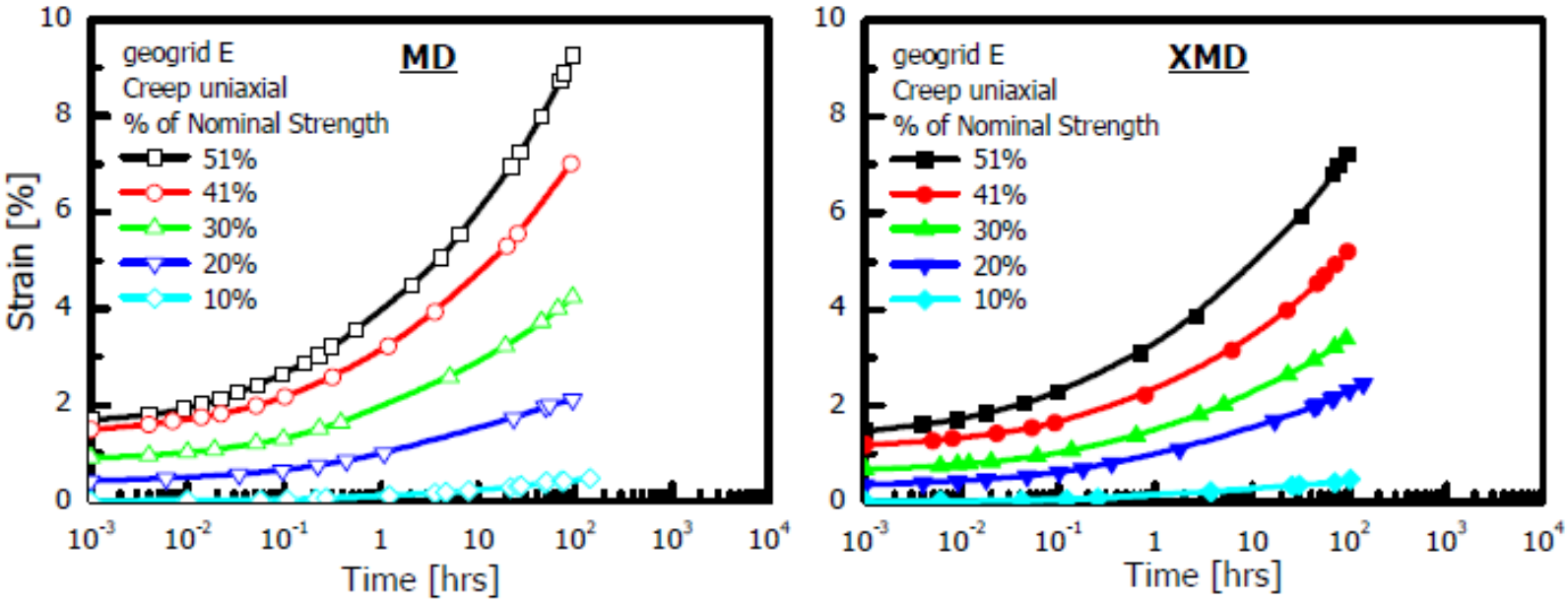


Fig 3.14 – Uniaxial performance test results for a 40kN biaxial geogrid, with integral junctions, in the MD & XMD directions, Kupec (2004).

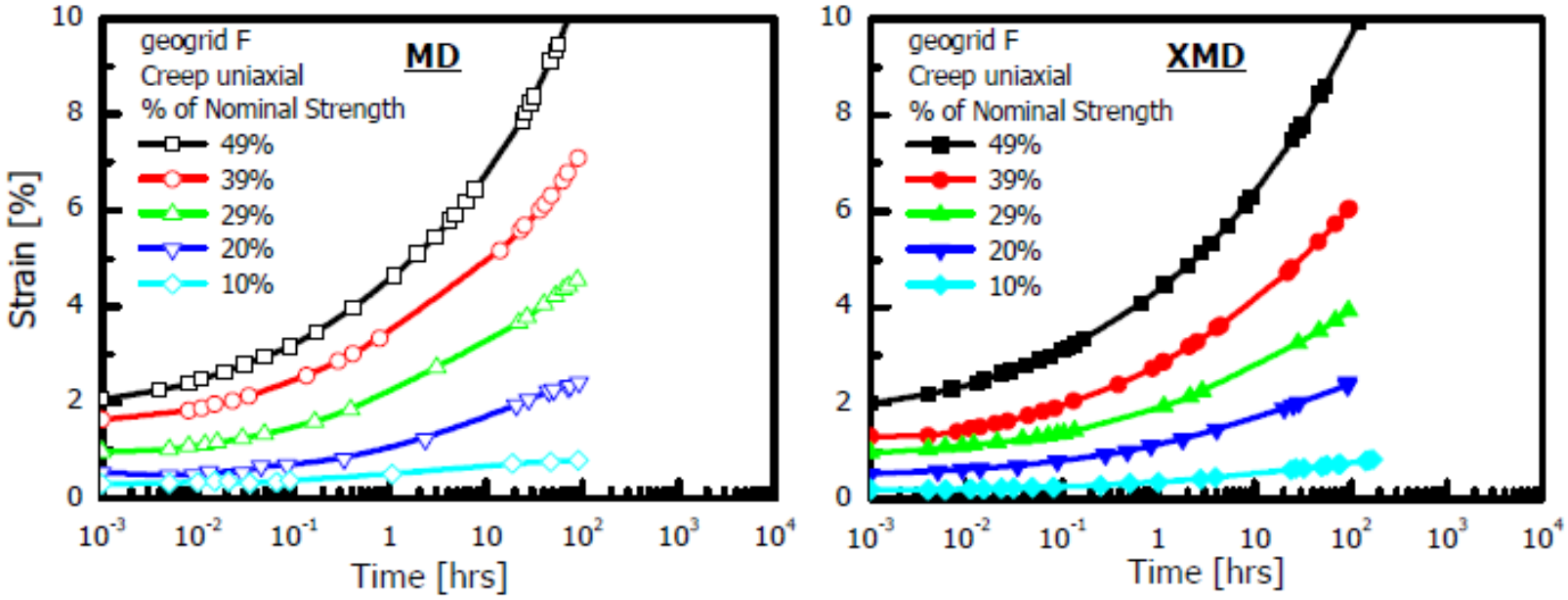


Fig 3.15 – Uniaxial performance test results for a 30kN biaxial geogrid, with integral junctions, in the MD & XMD directions, Kupec (2004).

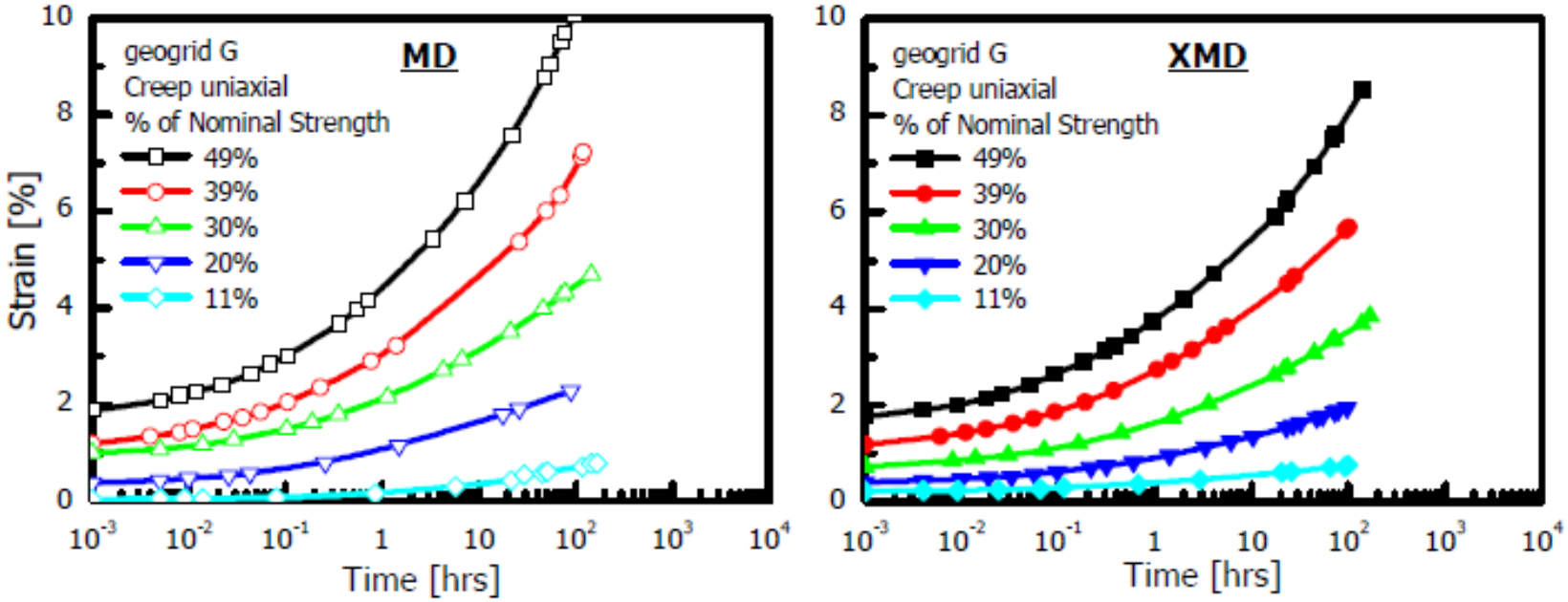


Fig 3.16 – Uniaxial performance test results for a 20kN biaxial geogrid, with integral junctions, in the MD & XMD directions, Kupec (2004).

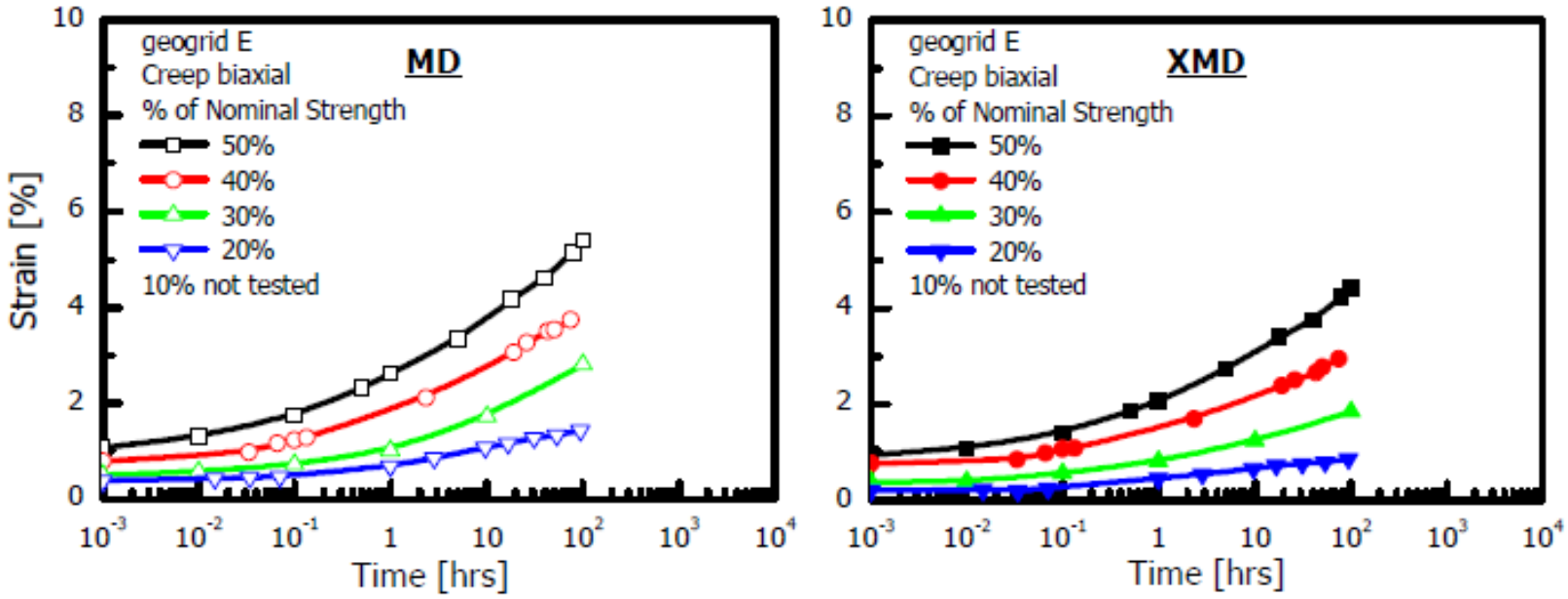


Fig 3.17. – Biaxial performance test results for a 40kN biaxial geogrid, with integral junctions, in the MD & XMD directions, Kupec (2004).

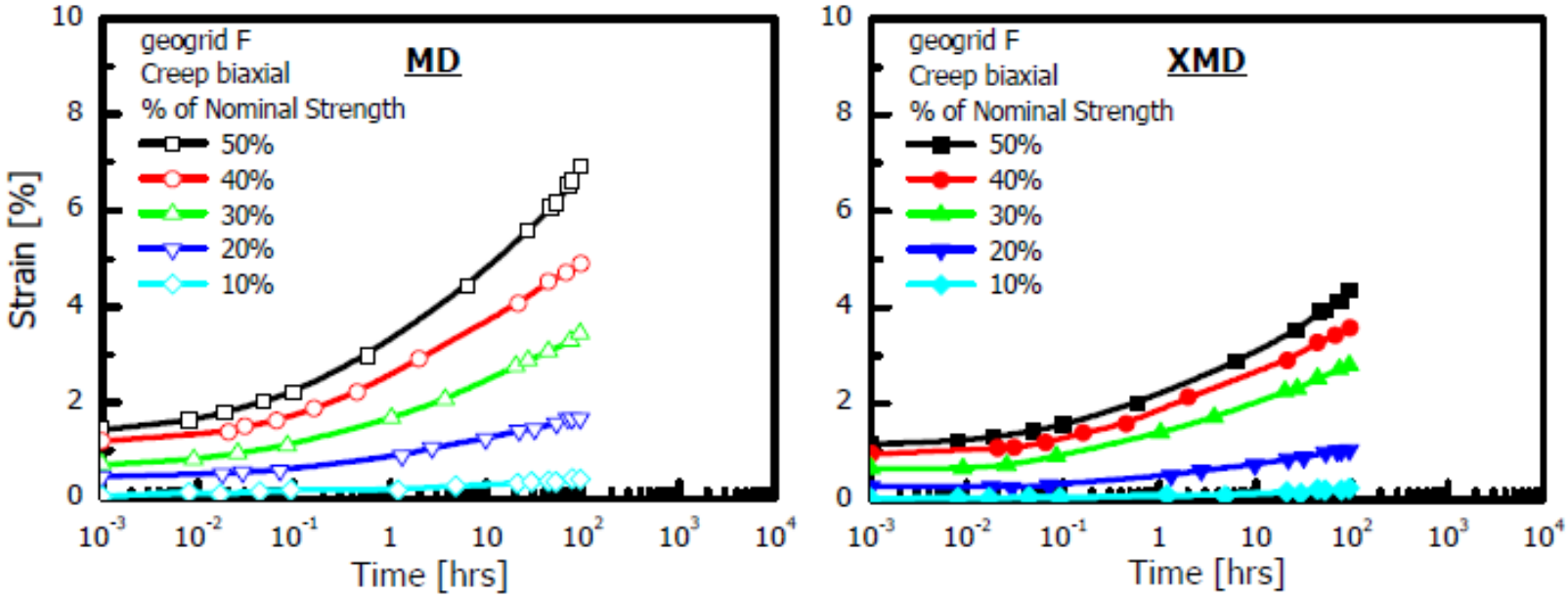


Fig 3.18. – Biaxial performance test results for a 30kN biaxial geogrid, with integral junctions, in the MD & XMD directions, Kupec (2004).

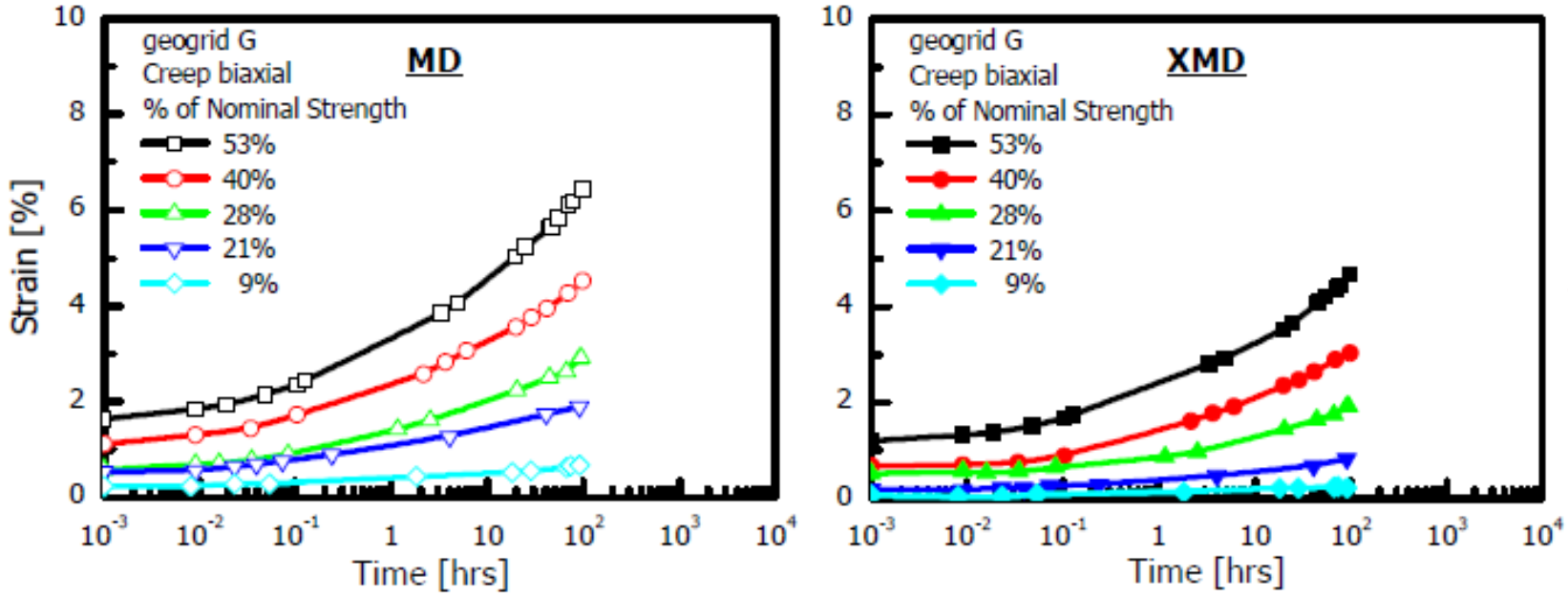


Fig 3.19. – Biaxial performance test results for a 20kN biaxial geogrid, with integral junctions, in the MD & XMD directions, Kupec (2004).

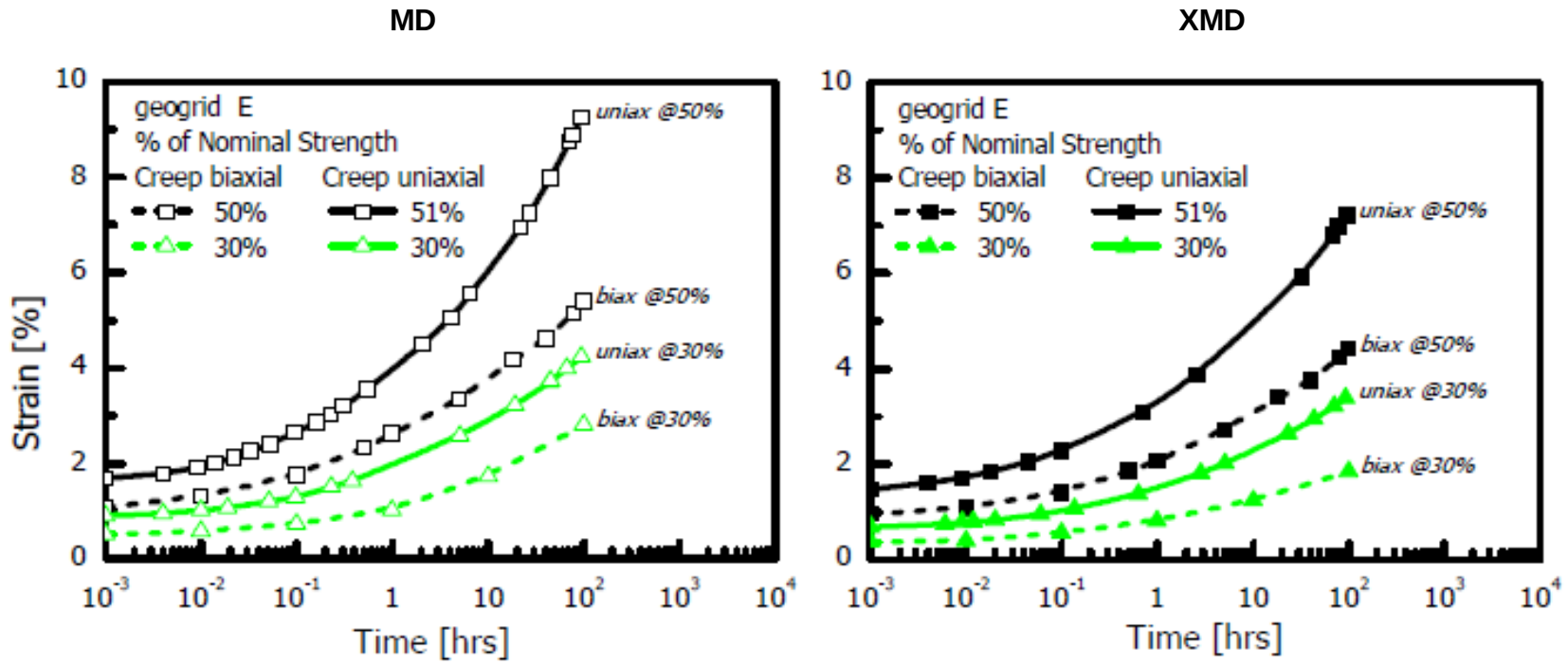


Fig 3.20. – Comparisons of uniaxial and biaxial performance test results for a 40kN biaxial geogrid with integral junctions tested at 30 and 50% of the ultimate strength, in the MD & XMD directions, Kupec (2004).

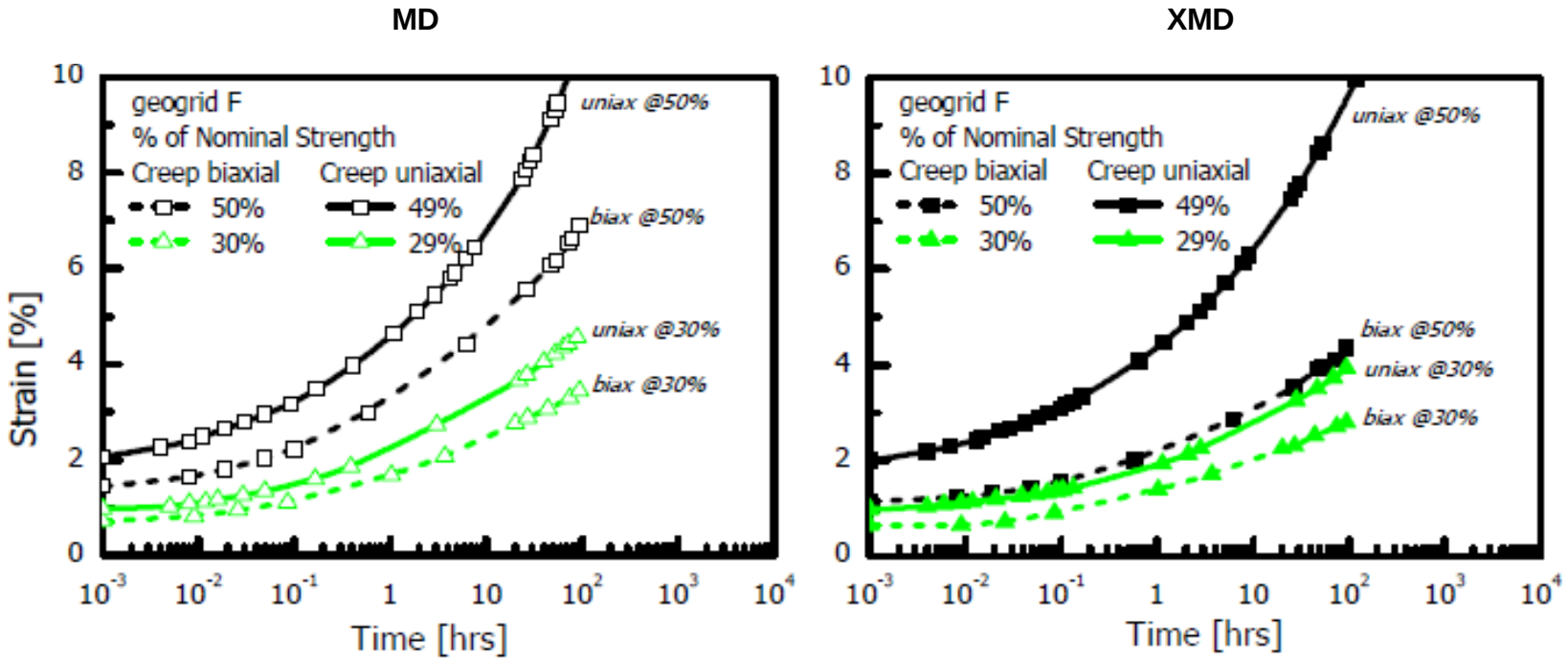


Fig 3.21. – Comparisons of uniaxial and biaxial performance test results for a 30kN biaxial geogrid with integral junctions tested at 30 and 50% of the ultimate strength, in the MD & XMD directions, Kupec (2004).

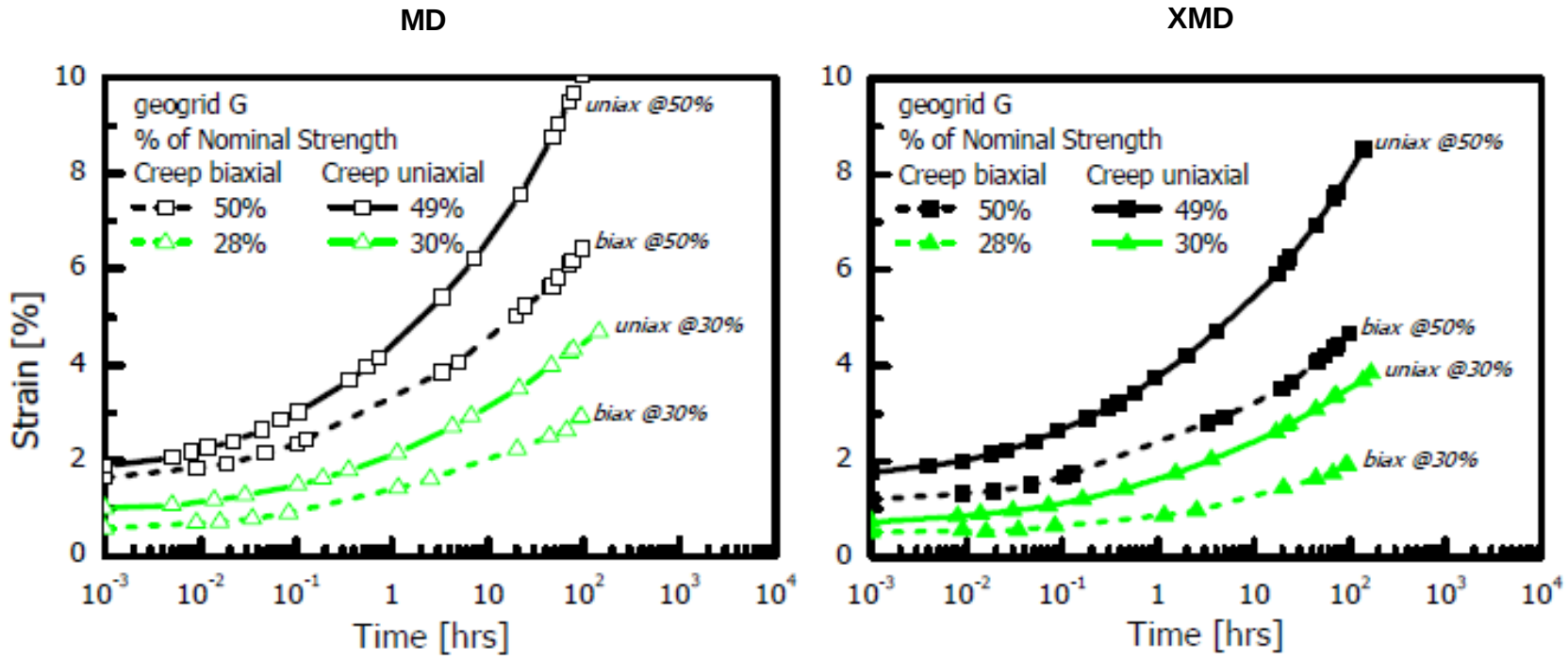


Fig 3.22. – Comparisons of uniaxial and biaxial performance test results for a 20kN biaxial geogrid with integral junctions tested at 30 and 50% of the ultimate strength, in the MD & XMD directions, Kupec (2004).

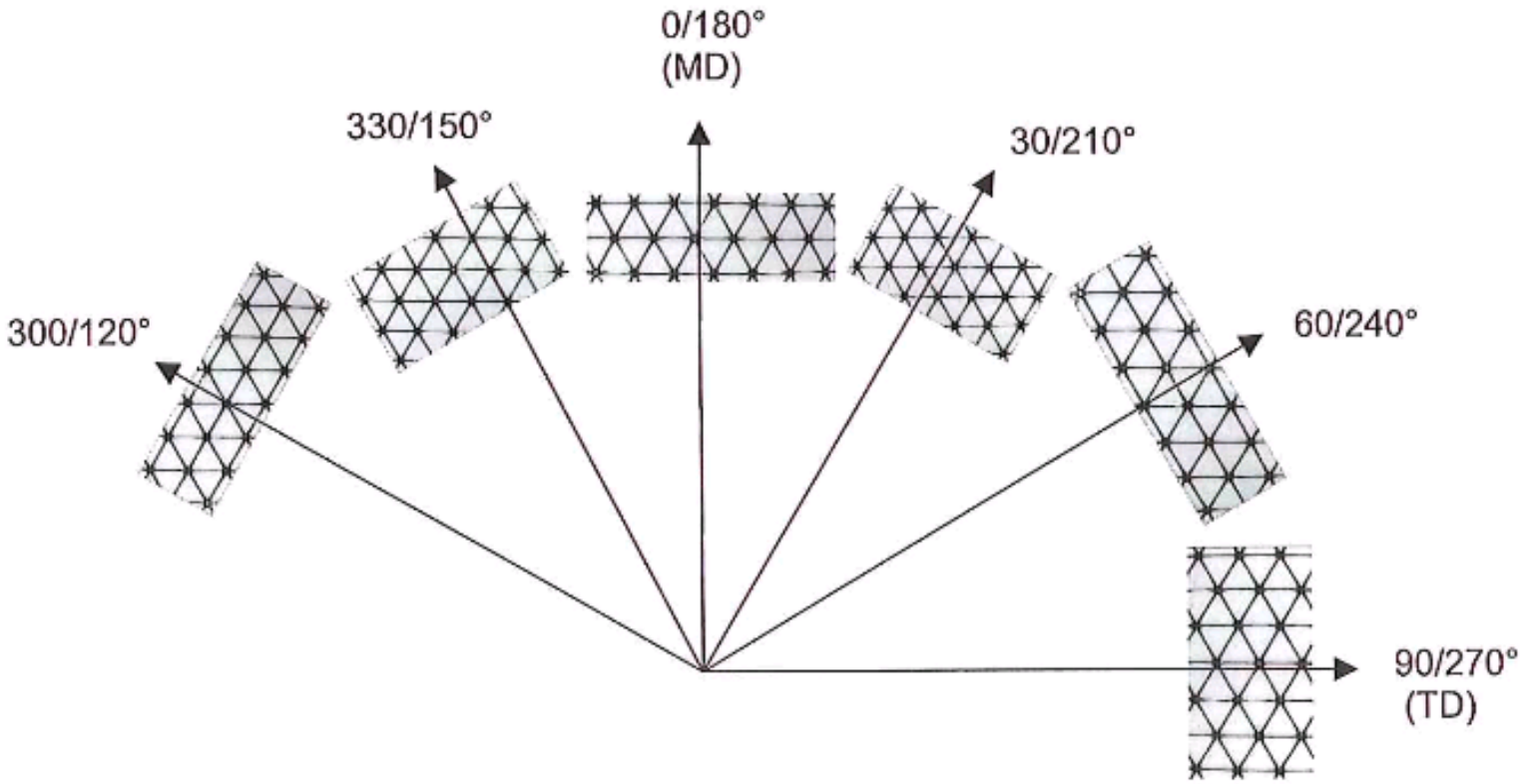


Fig 3.23 – TriAx testing directions devised by Walsh (2003).

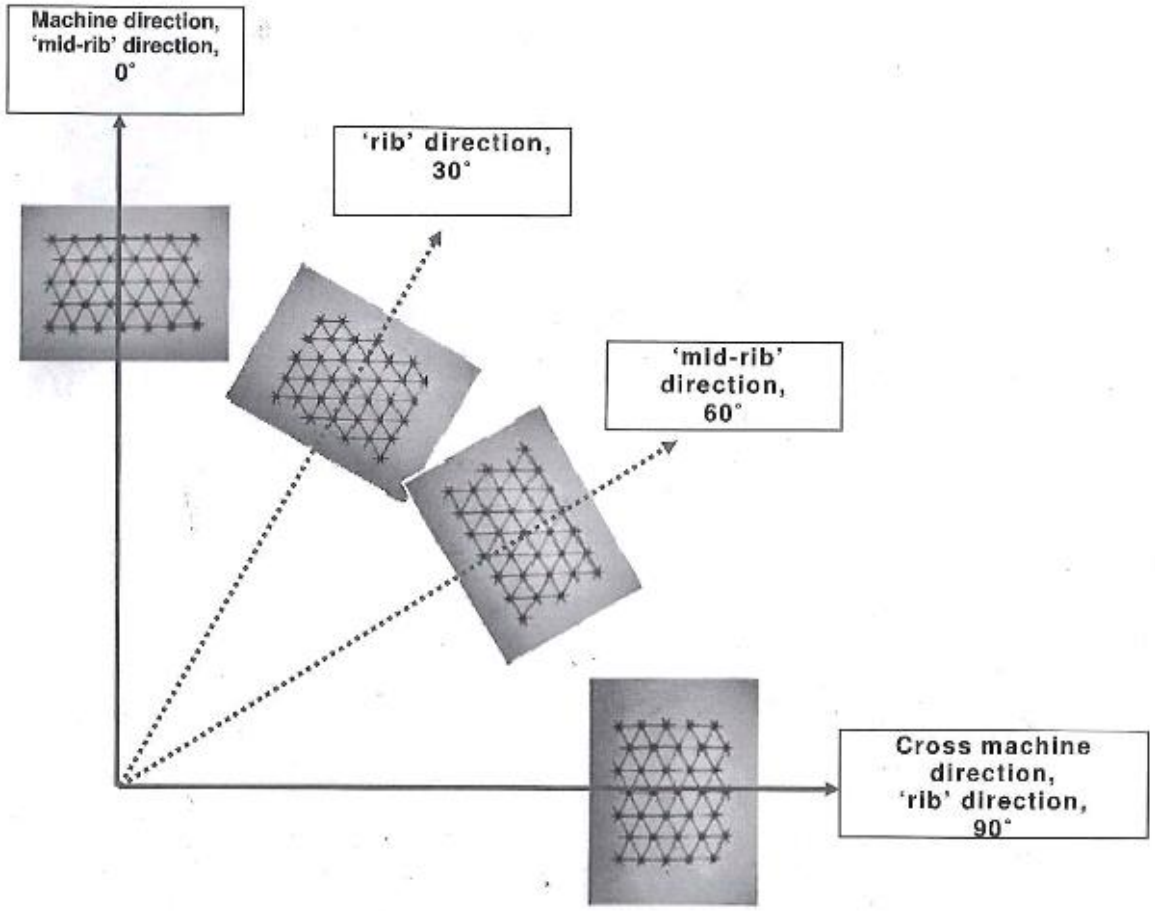
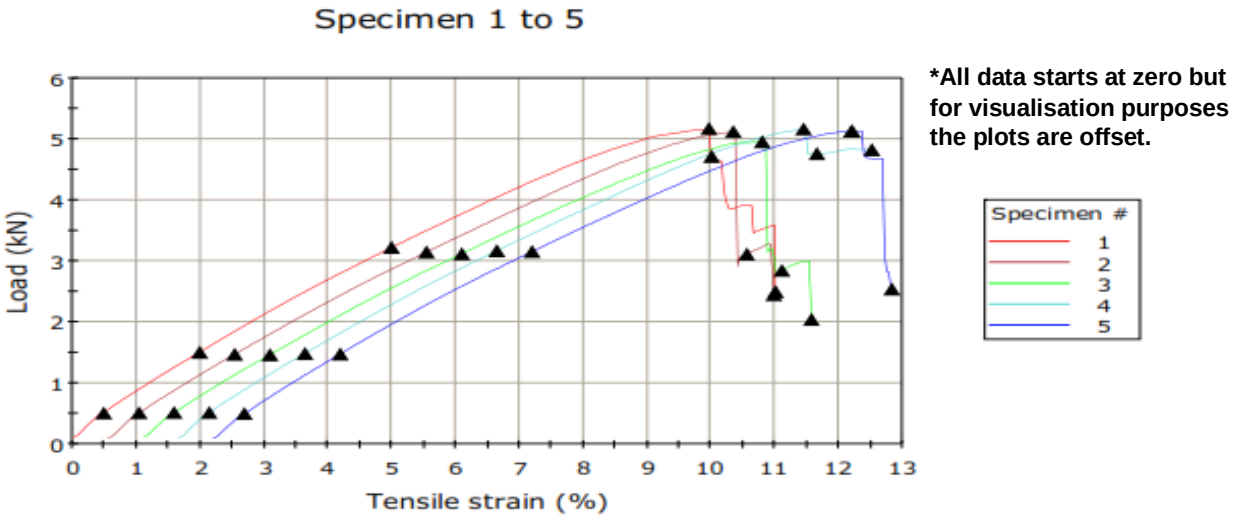


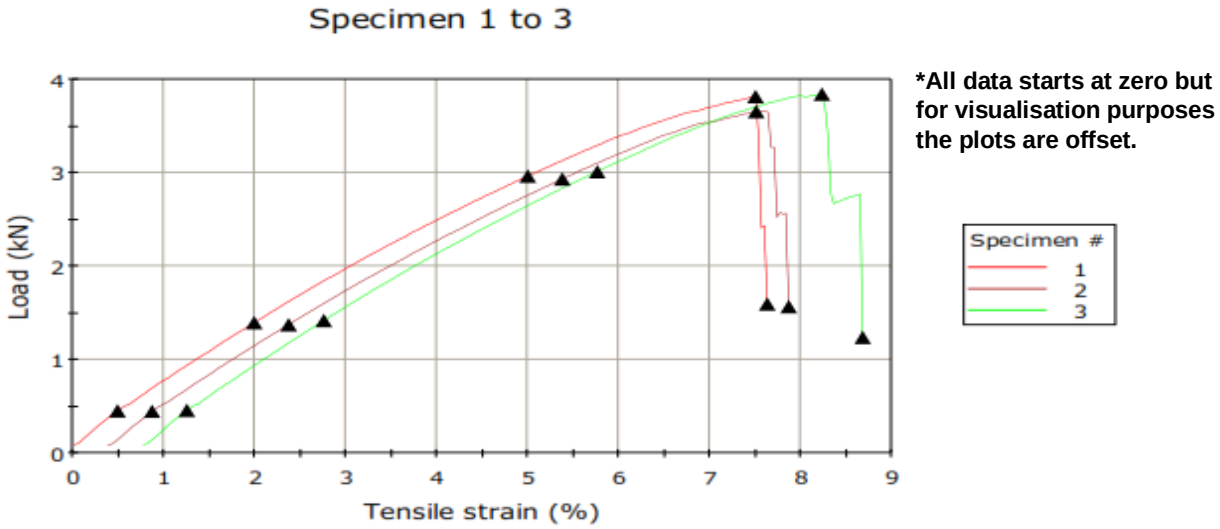
Fig 3.24 – Triaxial testing directions as used in the EOTA TR41 document, EOTA (2012).



***All data starts at zero but for visualisation purposes the plots are offset.**

	Load @ Max Load (kN)	Mean Strain @ Max Load (%)	Mean Tensile Strength (kN/m)	Secant Stiffness @ 0.5% Strain (kN/m)	Secant Stiffness @ 2% Strain (kN/m)	Secant Stiffness @ 5% Strain (kN/m)	Secant Stiffness @ 10% Strain (kN/m)
1	5.17	9.96	18.82	381.6	276.0	235.0	171.5
2	5.12	9.79	18.42	381.0	267.0	227.2	112.4
3	4.96	9.70	17.52	375.5	260.7	221.0	100.9
4	5.17	9.79	18.32	378.8	265.6	225.4	168.9
5	5.13	9.99	17.89	358.0	259.0	220.5	178.7
Mean	5.11	9.85	18.19	375.0	265.7	225.8	146.5
Standard Deviation	0.09	0.12	0.50	9.8	6.6	5.9	36.8
Coefficient of Variation	1.74	1.27	2.76	2.6	2.5	2.6	25.1

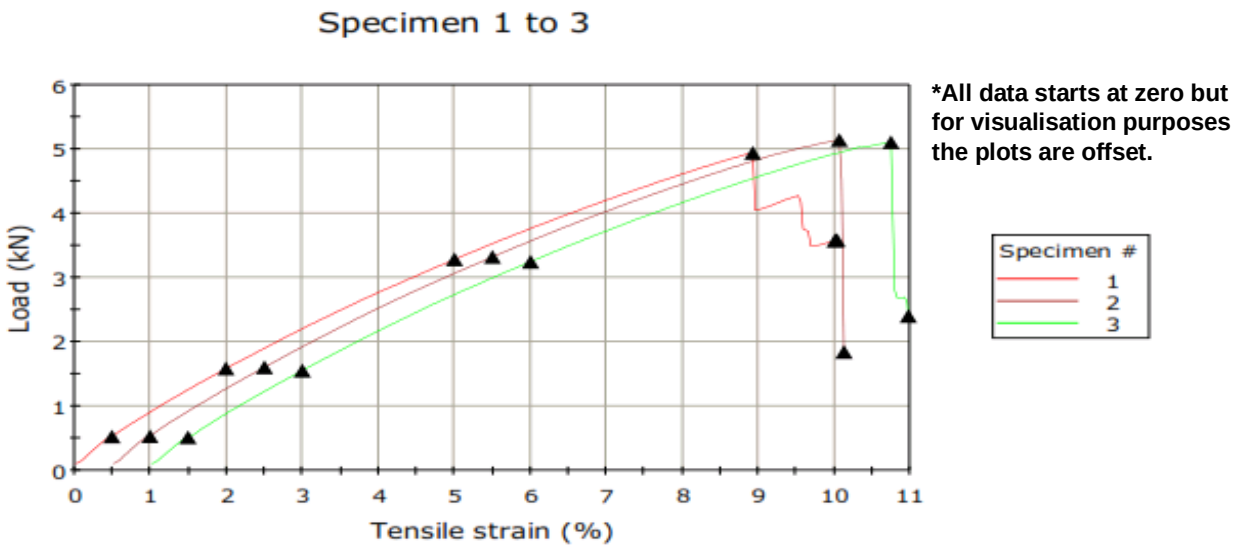
Fig 3.25. – Typical wide width test data plot for a Tensar TX160 geogrid tested in the 0° direction in accordance to the ETA TR41 report.



***All data starts at zero but for visualisation purposes the plots are offset.**

	Load @ Max Load (kN)	Mean Strain @ Max Load (%)	Mean Tensile Strength (kN/m)	Secant Stiffness @ 0.5% Strain (kN/m)	Secant Stiffness @ 2% Strain (kN/m)	Secant Stiffness @ 5% Strain (kN/m)	Secant Stiffness @ 10% Strain (kN/m)
1	3.81	7.50	15.44	372.8	283.7	239.9	-----
2	3.65	7.13	14.91	371.1	281.5	239.3	-----
3	3.84	7.46	15.99	389.6	296.4	251.0	-----
Mean	3.77	7.36	15.44	377.8	287.2	243.4	-----
Standard Deviation	0.10	0.21	0.54	10.2	8.0	6.6	-----
Coefficient of Variation	2.67	2.79	3.50	2.7	2.8	2.7	-----

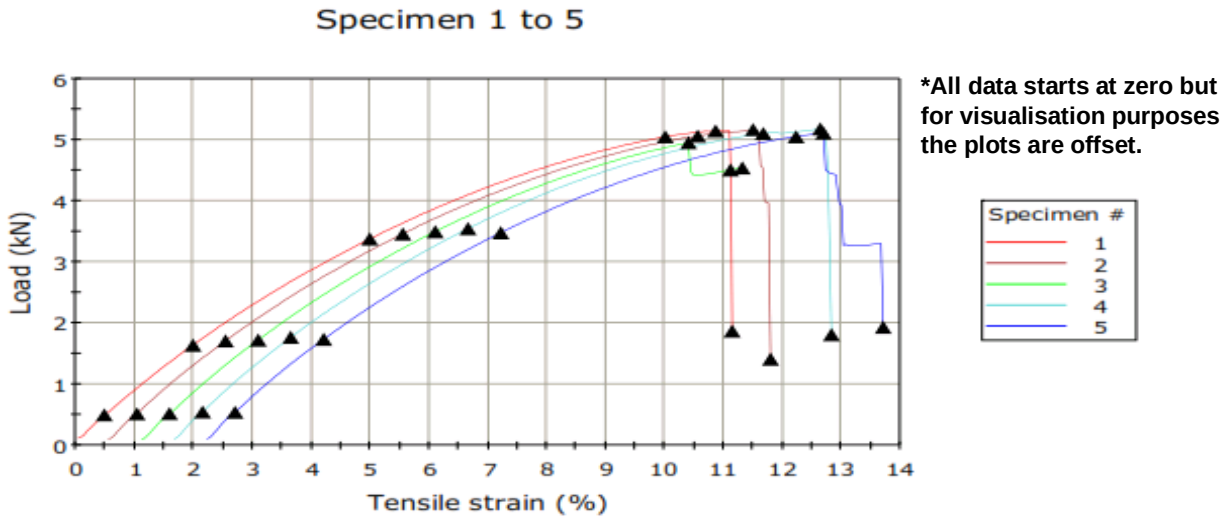
Fig 3.26. – Typical wide width test data plot for a Tensar TX160 geogrid tested in the 30° direction in accordance to the ETA TR41 report.



***All data starts at zero but for visualisation purposes the plots are offset.**

	Load @ Max Load (kN)	Mean Strain @ Max Load (%)	Mean Tensile Strength (kN/m)	Secant Stiffness @ 0.5% Strain (kN/m)	Secant Stiffness @ 2% Strain (kN/m)	Secant Stiffness @ 5% Strain (kN/m)	Secant Stiffness @ 10% Strain (kN/m)
1	4.94	8.92	17.46	381.5	281.9	232.5	126.5
2	5.14	9.56	18.11	384.6	283.9	234.3	-----
3	5.11	9.74	17.92	370.5	274.4	228.4	-----
Mean	5.06	9.40	17.83	378.9	280.1	231.7	126.5
Standard Deviation	0.11	0.43	0.33	7.4	5.0	3.0	-----
Coefficient of Variation	2.12	4.57	1.87	2.0	1.8	1.3	-----

Fig 3.27. – Typical wide width test data plot for a Tensar TX160 geogrid tested in the 60° direction in accordance to the ETA TR41 report.



	Load @ Max Load (kN)	Mean Strain @ Max Load (%)	Mean Tensile Strength (kN/m)	Secant Stiffness @ 0.5% Strain (kN/m)	Secant Stiffness @ 2% Strain (kN/m)	Secant Stiffness @ 5% Strain (kN/m)	Secant Stiffness @ 10% Strain (kN/m)
1	5.15	10.86	20.58	409.5	329.6	270.6	202.0
2	5.17	10.94	20.67	422.4	344.1	277.2	202.4
3	4.95	9.29	19.73	425.7	345.0	279.0	179.6
4	5.18	10.96	20.71	447.6	355.1	284.0	204.1
5	5.11	10.47	20.51	445.7	350.0	279.9	202.8
Mean	5.11	10.50	20.44	430.2	344.8	278.1	198.2
Standard Deviation	0.09	0.71	0.40	16.2	9.6	4.9	10.4
Coefficient of Variation	1.80	6.73	1.97	3.8	2.8	1.8	5.3

Fig 3.28. – Typical wide width test data plot for a Tensar TX160 geogrid tested in the 90° direction in accordance to the ETA TR41 report.

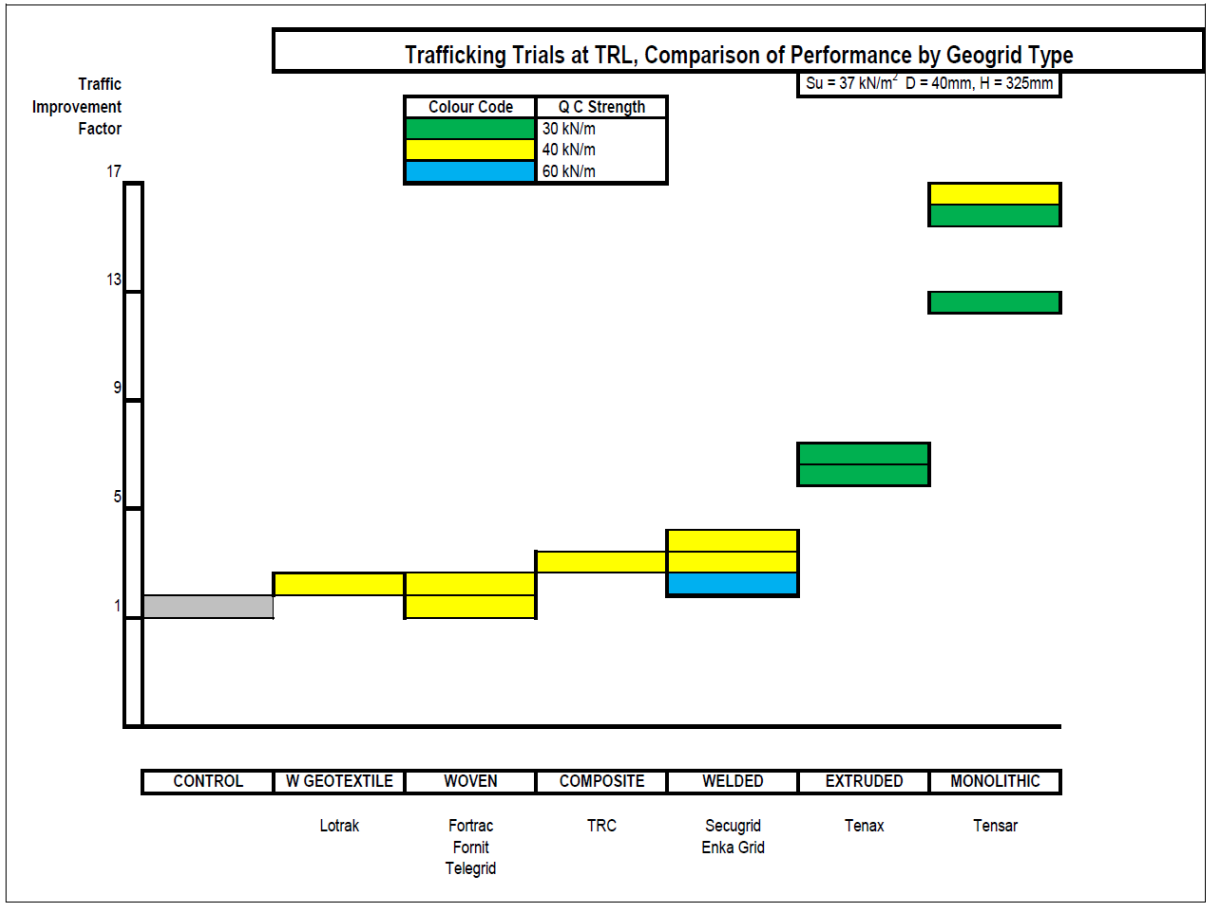


Fig 3.29. – Trafficking test results, Jenner et al (2002), interpreted by Tensar International (2019), showing that pure tensile strength is not a good indicator of trafficking performance.

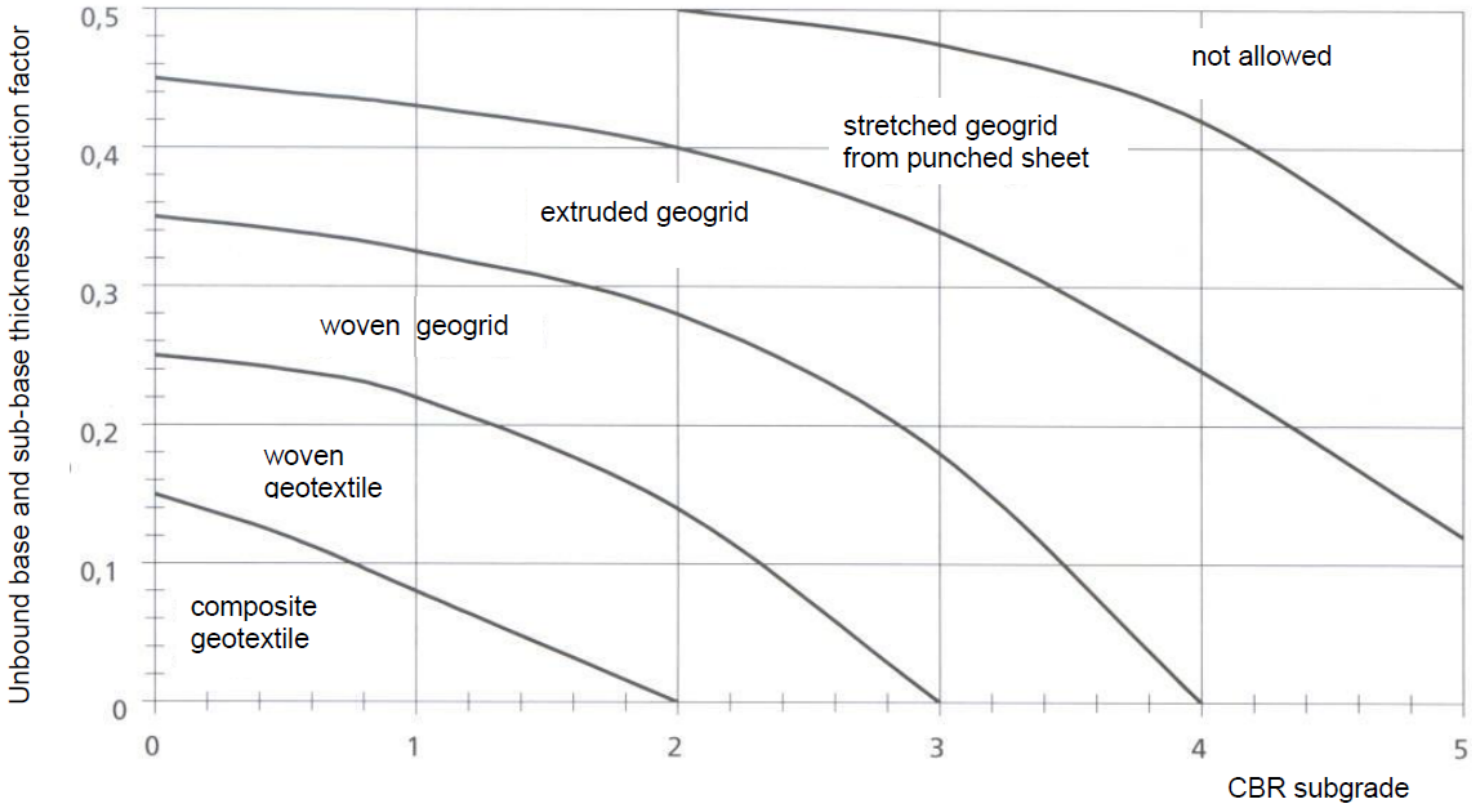


Fig 3.30. – Graph showing how different classes of geogrid affects the mechanically stabilised unbound layer and the effective thickness of that layer, CROW (2002)

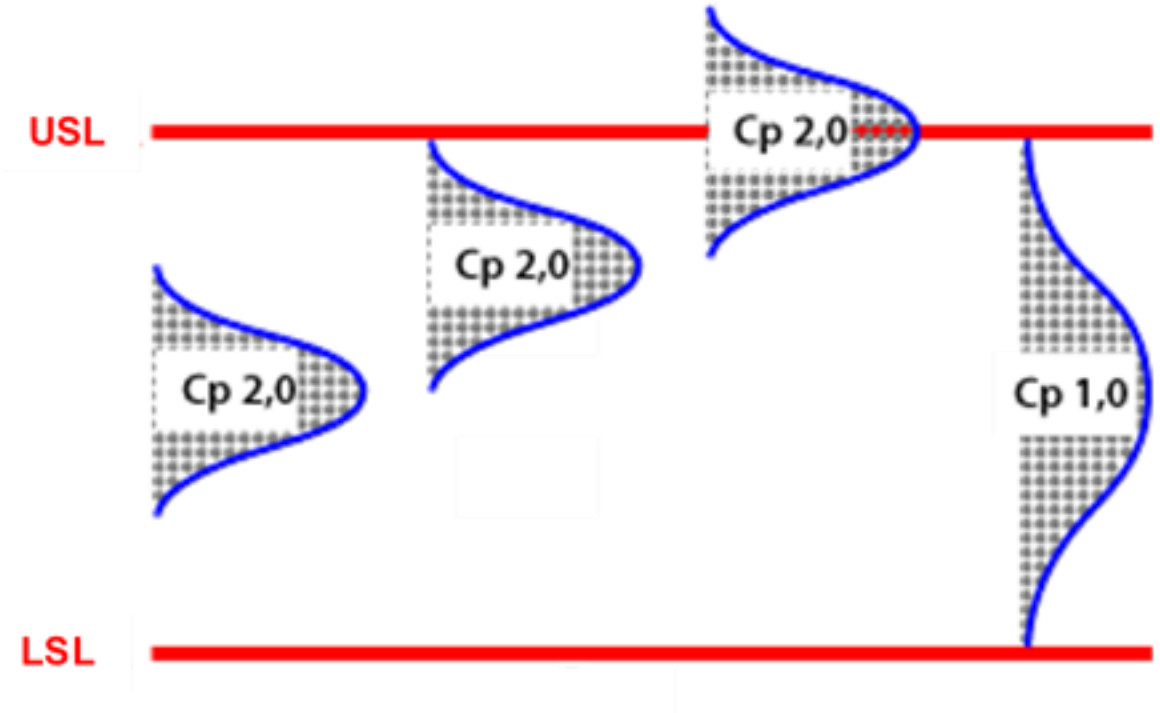


Fig 4.1. – Process Capability (Cp), showing the relationship between the width of the spread and the specification width, after Nielson (2020)

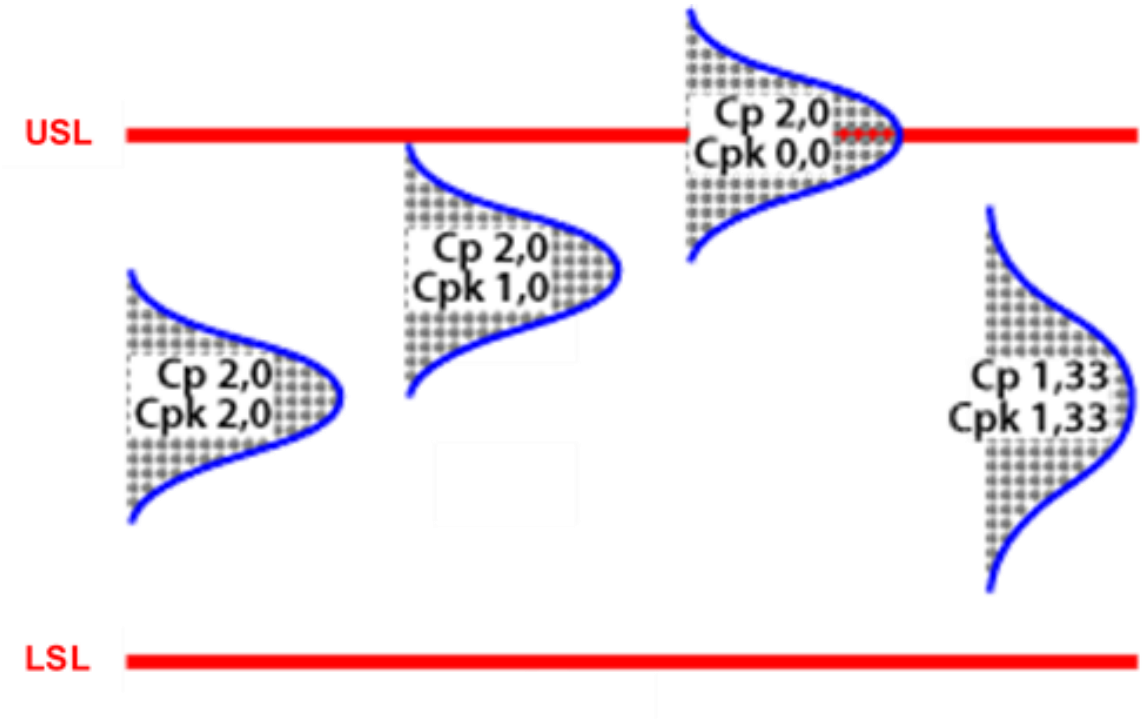
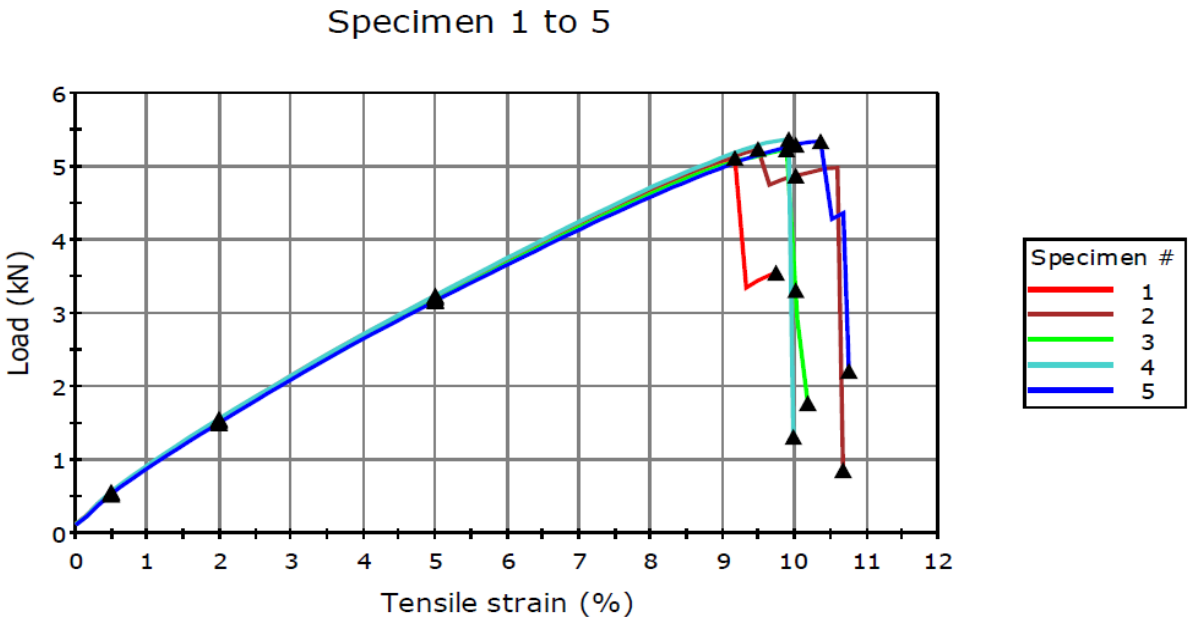
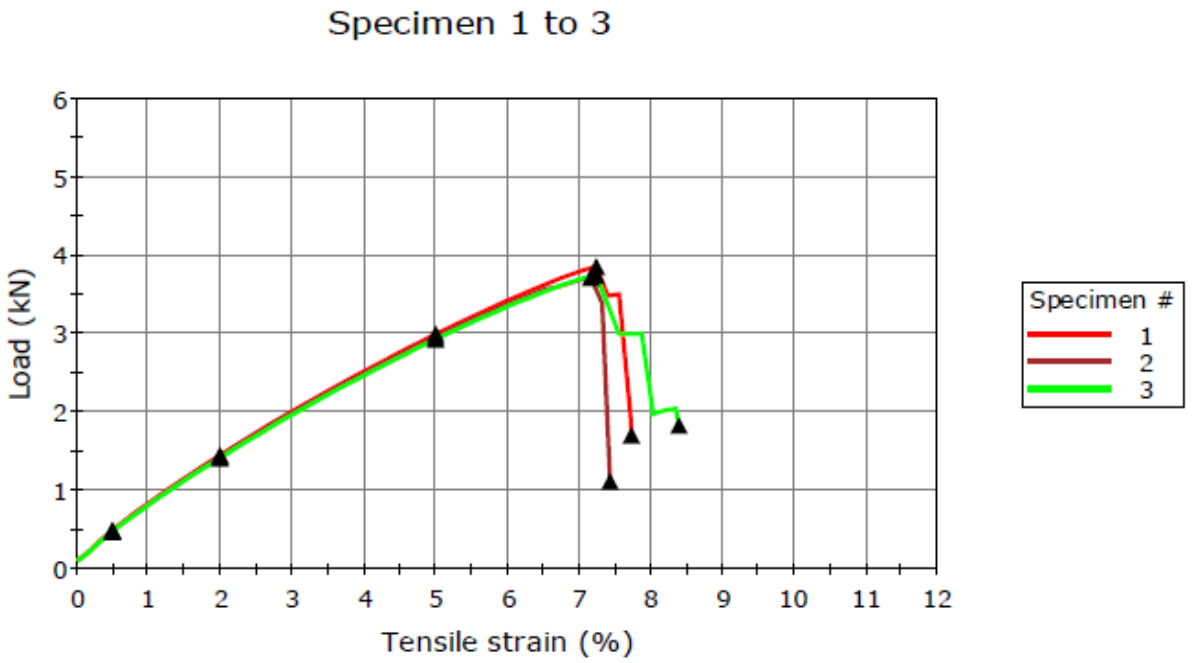


Fig 4.2. – Process Capability Index (Cpk), showing the relationship with Cp and specification width. (If Cpk = Cp, the process sits in the middle of the specification limits), after Nielson (2020)



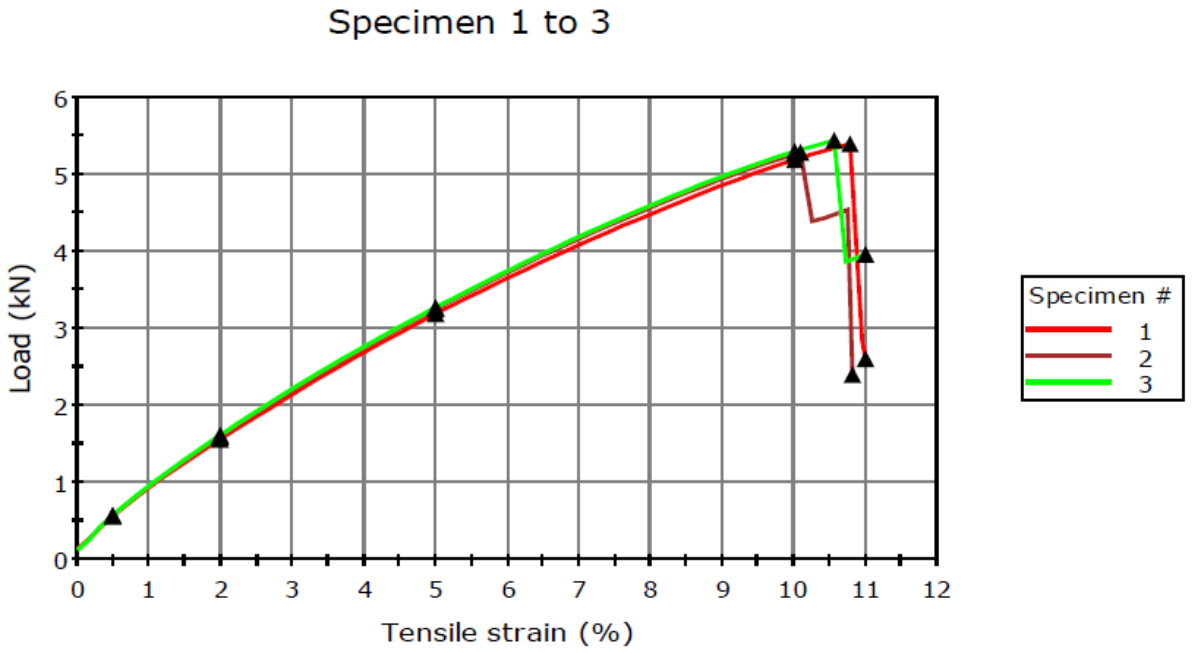
	Maximum Load (kN)	Strain at Maximum Load (%)	Maximum Strength (kN/m)	Secant Stiffness @ 0.5% Strain (kN/m)	Secant Stiffness @ 2% Strain (kN/m)	Secant Stiffness @ 5% Strain (kN/m)	Secant Stiffness @ 10% Strain (kN/m)
1	5.12	9.15	18.41	401.95	279.98	232.92	-----
2	5.24	9.47	19.05	412.22	281.61	233.95	177.52
3	5.23	9.87	18.76	402.29	275.03	228.35	119.00
4	5.38	9.90	19.34	416.19	282.51	233.78	-----
5	5.35	10.35	18.70	379.17	264.25	221.87	185.29
Mean	5.26	9.75	18.85	402.36	276.68	230.17	160.60
Standard Deviation	0.10	0.45	0.35	14.37	7.52	5.18	36.24
Coefficient of Variation	1.95	4.65	1.88	3.57	2.72	2.25	22.57

Fig 5.1. – Q.C test data for TX160 (Batch Ref: 056218) tested at 0° (machine direction)



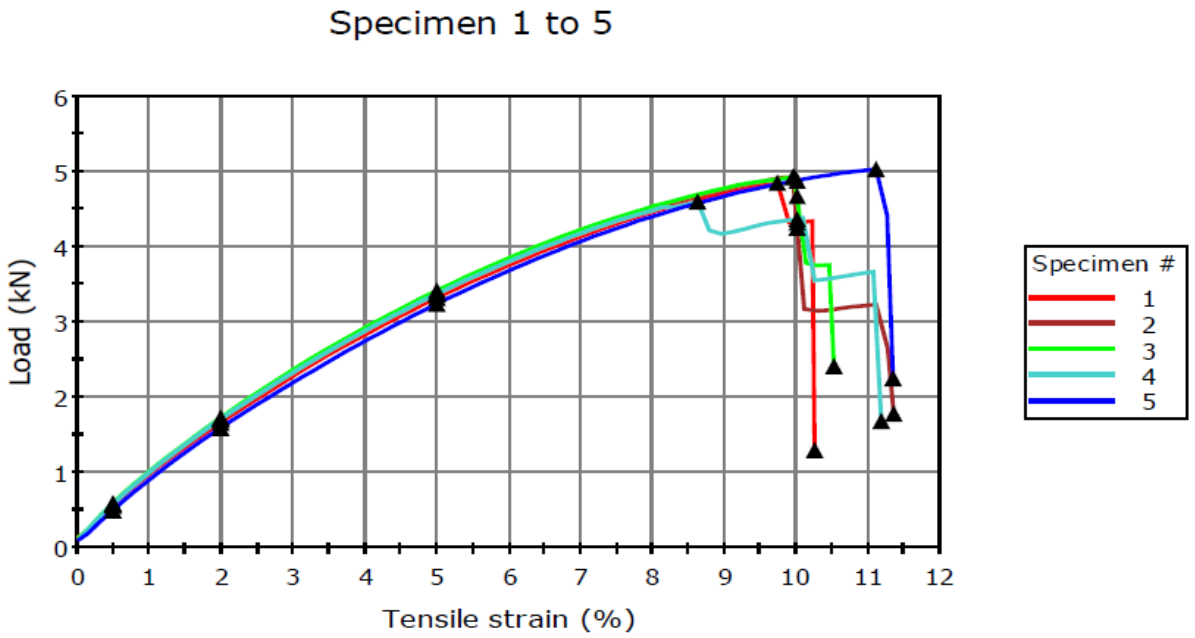
	Maximum Load (kN)	Strain at Maximum Load (%)	Maximum Strength (kN/m)	Secant Stiffness @ 0.5% Strain (kN/m)	Secant Stiffness @ 2% Strain (kN/m)	Secant Stiffness @ 5% Strain (kN/m)	Secant Stiffness @ 10% Strain (kN/m)
1	3.86	7.23	15.89	413.80	299.75	247.09	-----
2	3.72	7.15	15.19	403.13	294.94	241.66	-----
3	3.75	7.23	15.01	388.69	284.04	234.66	-----
Mean	3.78	7.21	< 15.36	401.87	292.91	241.14	-----
Standard Deviation	0.07	0.04	0.47	12.60	8.05	6.23	-----
Coefficient of Variation	1.95	0.61	3.03	3.14	2.75	2.58	-----

Fig 5.2. – Q.C test data for TX160 (Batch Ref: 056218) tested at 30° (‘rib’ direction)



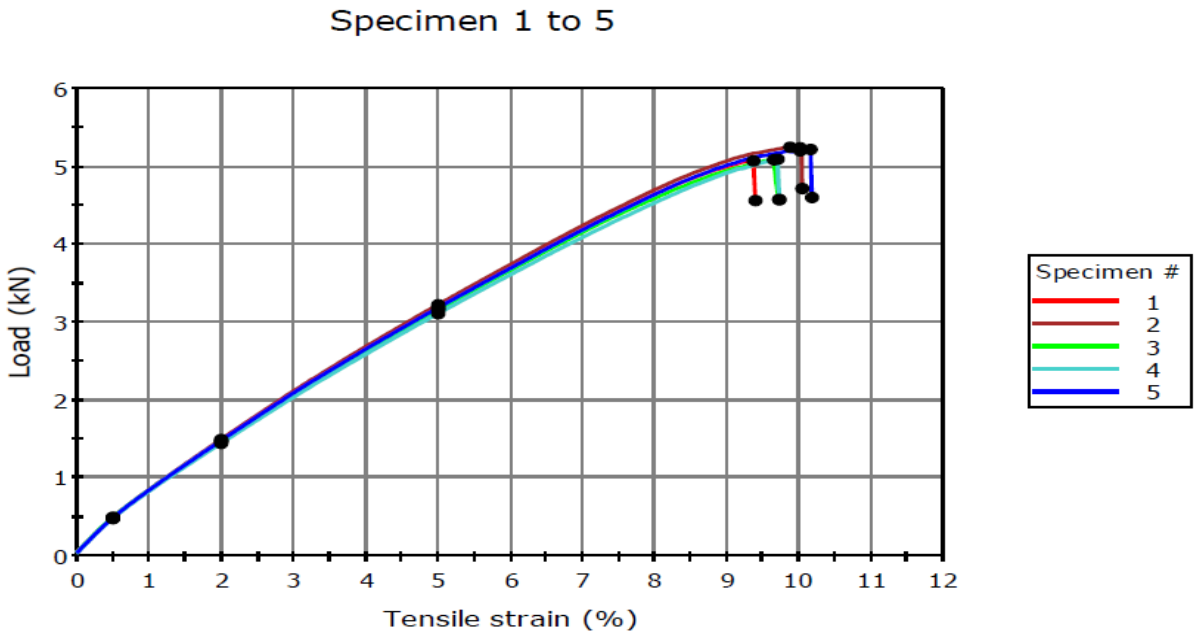
	Maximum Load (kN)	Strain at Maximum Load (%)	Maximum Strength (kN/m)	Secant Stiffness @ 0.5% Strain (kN/m)	Secant Stiffness @ 2% Strain (kN/m)	Secant Stiffness @ 5% Strain (kN/m)	Secant Stiffness @ 10% Strain (kN/m)
1	5.39	10.77	18.72	396.66	272.06	221.63	180.14
2	5.28	10.08	18.47	403.53	279.73	227.69	183.88
3	5.44	10.55	18.94	405.54	282.42	228.21	184.45
Mean	5.37	10.47	18.71	401.91	278.07	225.84	182.82
Standard Deviation	0.08	0.35	0.23	4.66	5.38	3.66	2.34
Coefficient of Variation	1.47	3.36	1.25	1.16	1.93	1.62	1.28

Fig 5.3. – Q.C test data for TX160 (Batch Ref: 056218) tested at 60° (‘mid-rib’ direction)



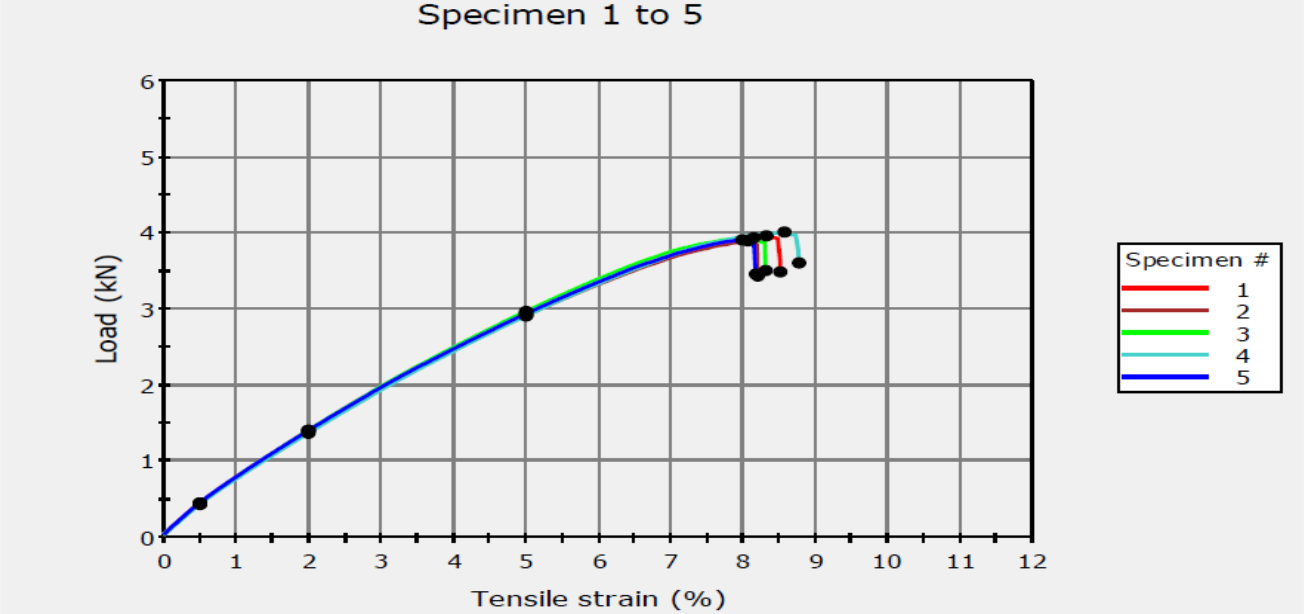
	Maximum Load (kN)	Strain at Maximum Load (%)	Maximum Strength (kN/m)	Secant Stiffness @ 0.5% Strain (kN/m)	Secant Stiffness @ 2% Strain (kN/m)	Secant Stiffness @ 5% Strain (kN/m)	Secant Stiffness @ 10% Strain (kN/m)
1	4.85	9.72	19.41	455.51	333.21	265.93	172.83
2	4.92	9.94	19.70	464.44	341.12	270.52	170.26
3	4.93	9.96	19.71	481.61	346.92	273.64	186.97
4	4.60	8.62	18.41	468.90	343.01	269.87	174.76
5	5.03	11.09	19.96	401.80	317.04	257.52	193.68
Mean	4.87	9.87	19.44	454.45	336.26	267.50	179.70
Standard Deviation	0.16	0.88	0.61	30.90	11.85	6.22	10.11
Coefficient of Variation	3.31	8.92	3.12	6.80	3.52	2.32	5.63

Fig 5.4. – Q.C test data for TX160 (Batch Ref: 056218) tested at 90° (cross machine direction)



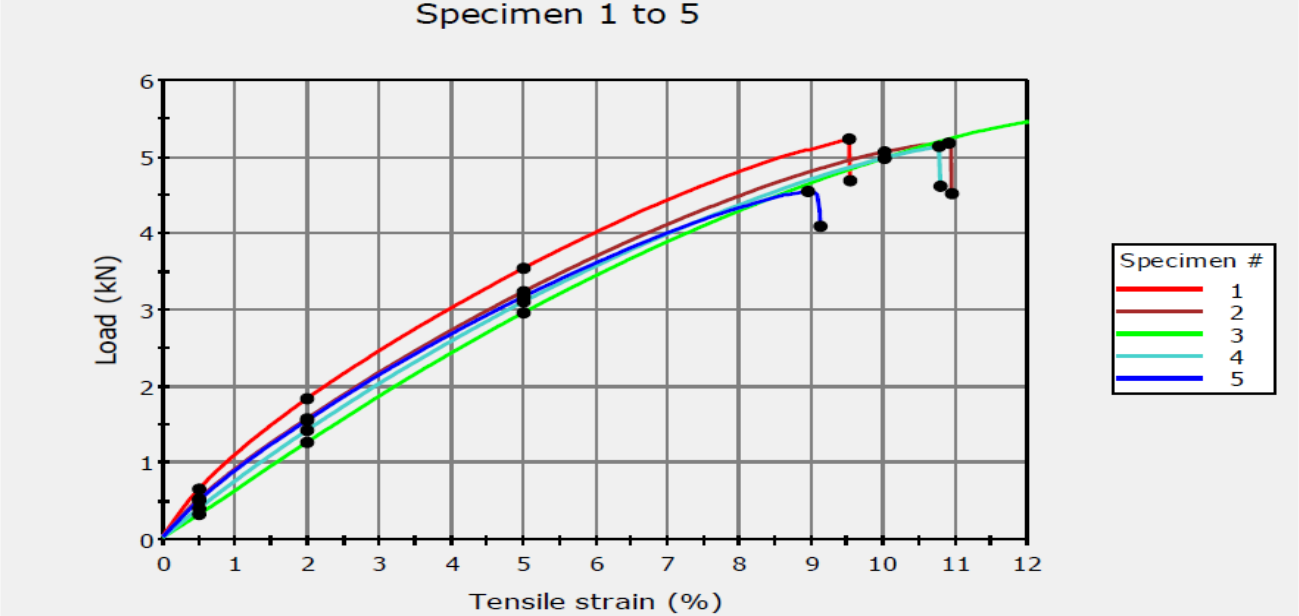
	Maximum Load (kN)	Strain at Maximum Load (%)	Maximum Strength (kN/m)	Secant Stiffness @ 0.5% Strain (kN/m)	Secant Stiffness @ 2% Strain (kN/m)	Secant Stiffness @ 5% Strain (kN/m)	Secant Stiffness @ 10% Strain (kN/m)
1	5.07	9.35	18.51	364.96	269.78	232.29	-----
2	5.25	9.86	19.29	369.60	276.08	237.32	192.66
3	5.09	9.64	18.36	363.25	265.92	228.08	-----
4	5.09	9.69	18.32	352.04	260.97	223.92	-----
5	5.22	10.15	19.11	362.38	271.99	233.48	190.47
Mean	5.14	9.74	18.72	362.44	268.95	> 231.02	> 191.57
Standard Deviation	0.08	0.29	0.45	6.45	5.78	5.16	1.55
Coefficient of Variation	1.58	3.00	2.39	1.78	2.15	2.23	0.81

Fig 5.5. – Q.C test data for TX160 (Batch Ref: 059839) tested at 0° (machine direction)



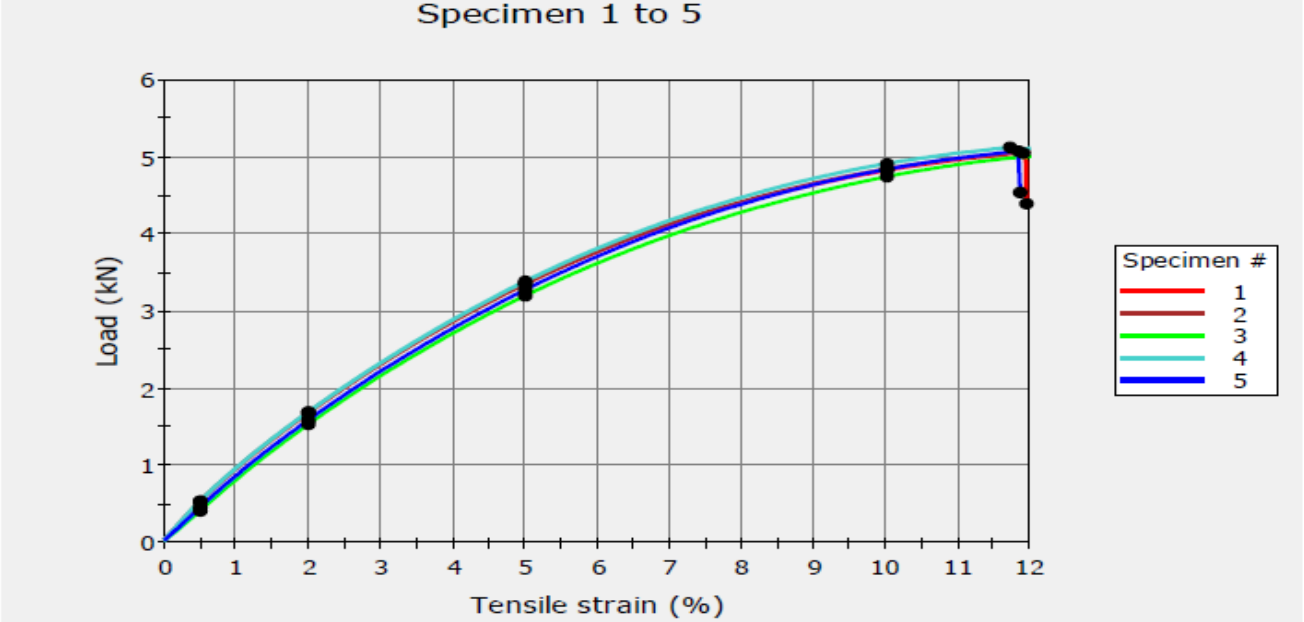
	Maximum Load (kN)	Strain at Maximum Load (%)	Maximum Strength (kN/m)	Secant Stiffness @ 0.5% Strain (kN/m)	Secant Stiffness @ 2% Strain (kN/m)	Secant Stiffness @ 5% Strain (kN/m)	Secant Stiffness @ 10% Strain (kN/m)
1	3.96	8.31	16.51	383.59	294.45	246.92	-----
2	3.90	8.06	16.11	378.45	289.87	241.24	-----
3	3.94	8.14	16.48	378.86	295.40	248.81	-----
4	4.01	8.56	16.85	372.98	289.03	244.99	-----
5	3.91	7.98	16.22	384.03	292.43	244.14	-----
Mean	3.94	8.21	< 16.43	379.58	292.24	245.22	-----
Standard Deviation	0.05	0.23	0.29	4.51	2.78	2.87	-----
Coefficient of Variation	1.15	2.82	1.77	1.19	0.95	1.17	-----

Fig 5.6. – Q.C test data for TX160 (Batch Ref: 059839) tested at 30° (‘rib’ direction)



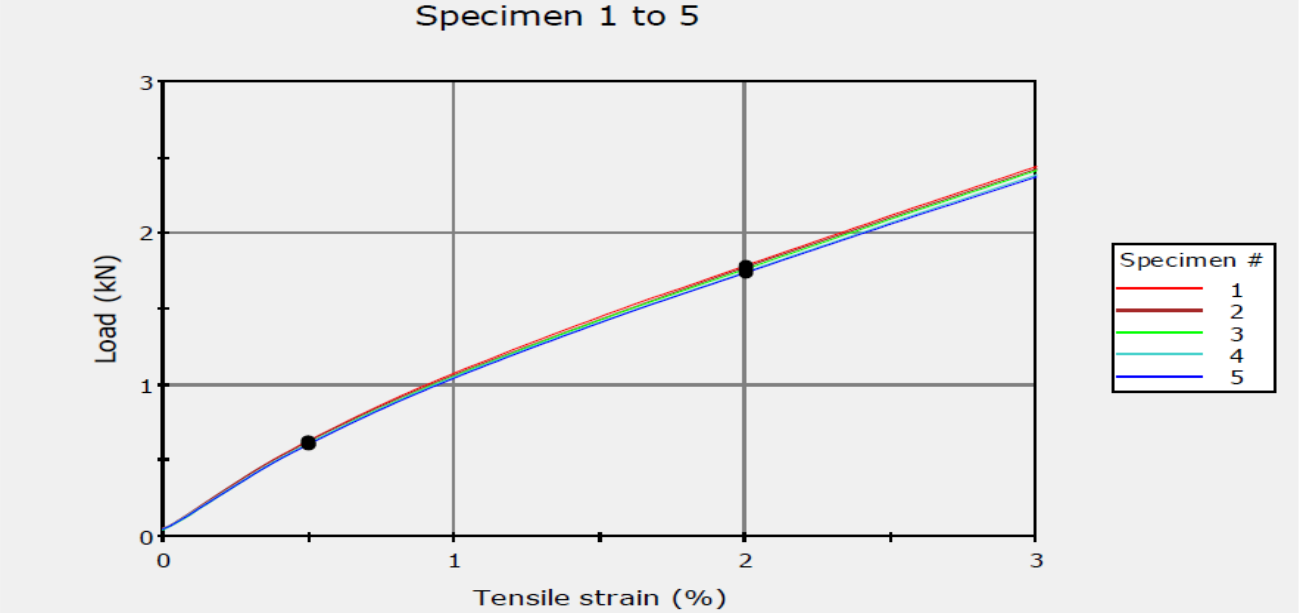
	Maximum Load (kN)	Strain at Maximum Load (%)	Maximum Strength (kN/m)	Secant Stiffness @ 0.5% Strain (kN/m)	Secant Stiffness @ 2% Strain (kN/m)	Secant Stiffness @ 5% Strain (kN/m)	Secant Stiffness @ 10% Strain (kN/m)
1	5.23	9.51	18.50	474.25	326.59	250.77	-----
2	5.18	10.89	18.25	382.25	279.62	228.52	178.49
3	5.57	13.08	19.69	243.52	226.28	209.95	176.14
4	5.14	10.76	18.22	296.80	254.74	220.71	176.83
5	4.55	8.94	16.15	370.97	277.40	225.42	-----
Mean	5.14	10.64	18.16	353.56	272.92	227.07	177.15
Standard Deviation	0.37	1.60	1.28	88.07	36.92	15.00	1.21
Coefficient of Variation	7.16	15.00	7.02	24.91	13.53	6.61	0.68

Fig 5.7. – Q.C test data for TX160 (Batch Ref: 059839) tested at 60° (‘mid-rib’ direction)



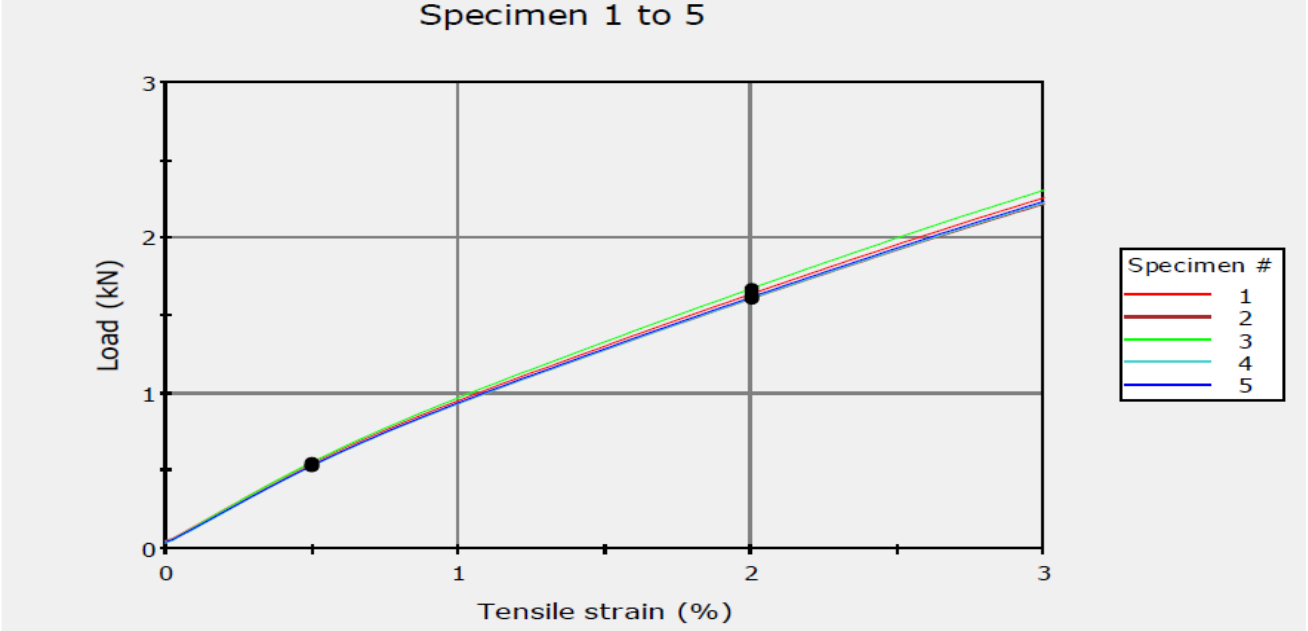
	Maximum Load (kN)	Strain at Maximum Load (%)	Maximum Strength (kN/m)	Secant Stiffness @ 0.5% Strain (kN/m)	Secant Stiffness @ 2% Strain (kN/m)	Secant Stiffness @ 5% Strain (kN/m)	Secant Stiffness @ 10% Strain (kN/m)
1	5.05	11.89	20.38	438.37	341.23	270.88	194.67
2	5.07	12.12	20.45	443.47	342.01	271.38	195.51
3	5.02	12.27	20.09	344.19	309.16	256.71	189.92
4	5.13	11.70	20.68	446.51	343.99	273.71	198.18
5	5.08	11.82	20.31	378.66	320.16	262.76	193.71
Mean	5.07	11.96	20.38	410.24	331.31	267.09	194.40
Standard Deviation	0.04	0.23	0.21	46.29	15.72	7.13	3.00
Coefficient of Variation	0.76	1.92	1.05	11.28	4.74	2.67	1.54

Fig 5.8. – Q.C test data for TX160 (Batch Ref: 059839) tested at 90° (cross machine direction)



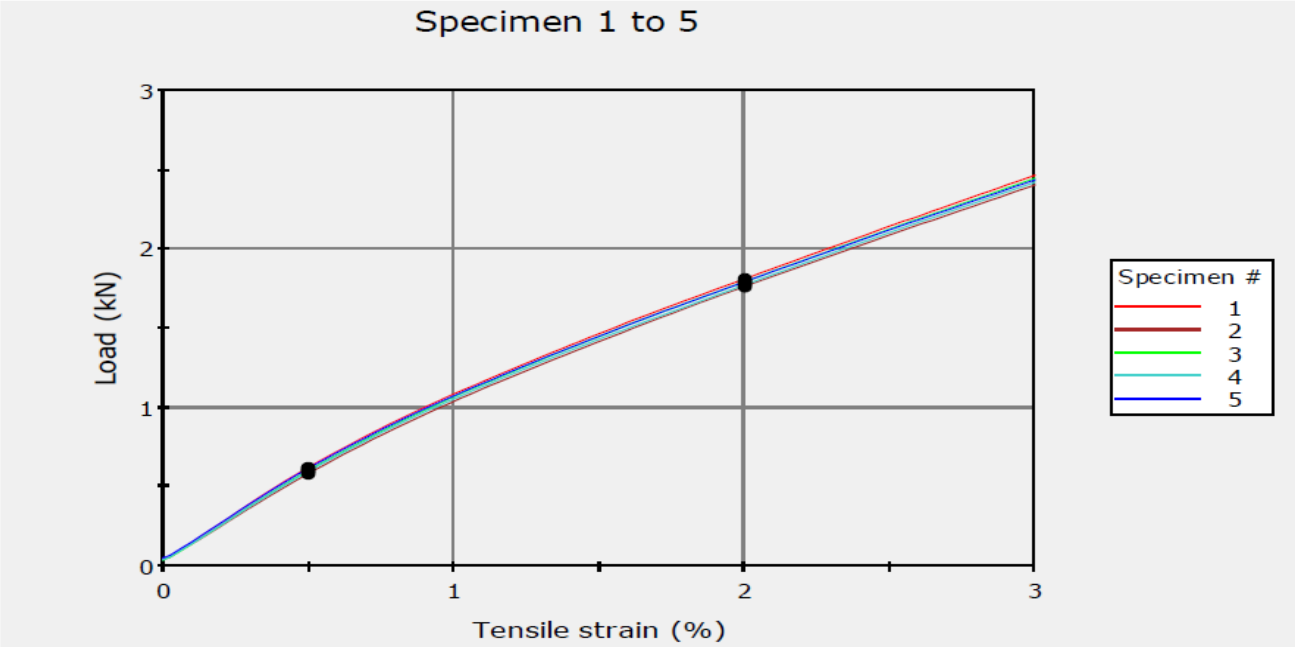
	Maximum Load (kN)	Strain at Maximum Load (%)	Maximum Strength (kN/m)	Secant Stiffness @ 0.5% Strain (kN/m)	Secant Stiffness @ 2% Strain (kN/m)	Secant Stiffness @ 5% Strain (kN/m)	Secant Stiffness @ 10% Strain (kN/m)
1	5.56	9.30	20.08	457.42	322.69	261.16	-----
2	5.17	8.36	18.68	454.25	320.72	258.84	-----
3	5.49	9.80	19.95	447.18	320.84	258.95	-----
4	5.26	9.27	18.93	441.82	313.84	252.71	-----
5	5.28	10.21	19.00	438.21	312.96	249.45	189.76
Mean	5.35	9.39	19.33	447.78	318.21	256.22	189.76
Standard Deviation	0.16	0.69	0.64	8.10	4.47	4.92	-----
Coefficient of Variation	3.05	7.40	3.31	1.81	1.40	1.92	-----

Fig 5.9. – Index test data for TX160 (Batch Ref: 056218, TAP 1 Year) tested at 0° (machine direction)



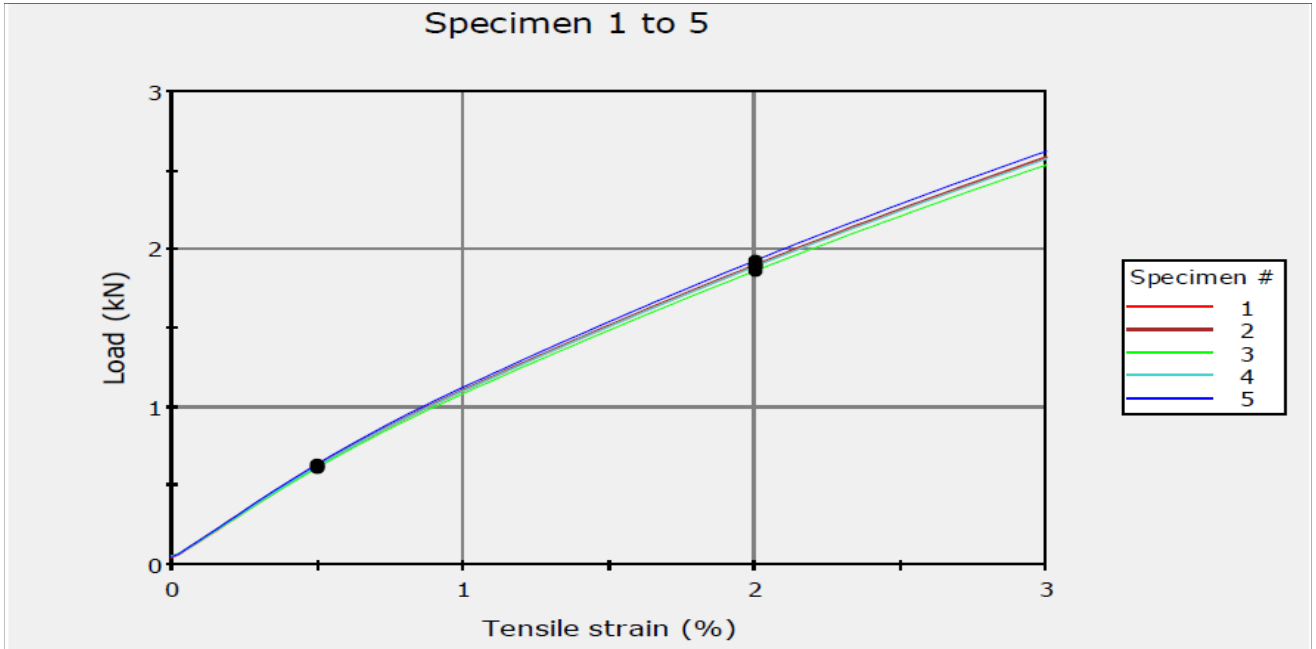
	Maximum Load (kN)	Strain at Maximum Load (%)	Maximum Strength (kN/m)	Secant Stiffness @ 0.5% Strain (kN/m)	Secant Stiffness @ 2% Strain (kN/m)	Secant Stiffness @ 5% Strain (kN/m)	Secant Stiffness @ 10% Strain (kN/m)
1	4.22	7.47	17.31	451.73	336.09	270.30	-----
2	4.12	7.52	16.97	441.83	331.18	266.86	-----
3	4.25	7.33	17.55	461.29	346.05	277.98	-----
4	4.17	7.46	17.16	439.54	331.82	268.40	-----
5	4.26	7.71	17.60	443.83	334.76	270.24	-----
Mean	4.20	7.50	< 17.32	447.64	335.98	270.76	-----
Standard Deviation	0.06	0.14	0.27	8.90	5.99	4.28	-----
Coefficient of Variation	1.37	1.86	1.54	1.99	1.78	1.58	-----

Fig 5.10. – Index test data for TX160 (Batch Ref: 056218, TAP 1 Year) tested at 30° (‘rib’ direction)



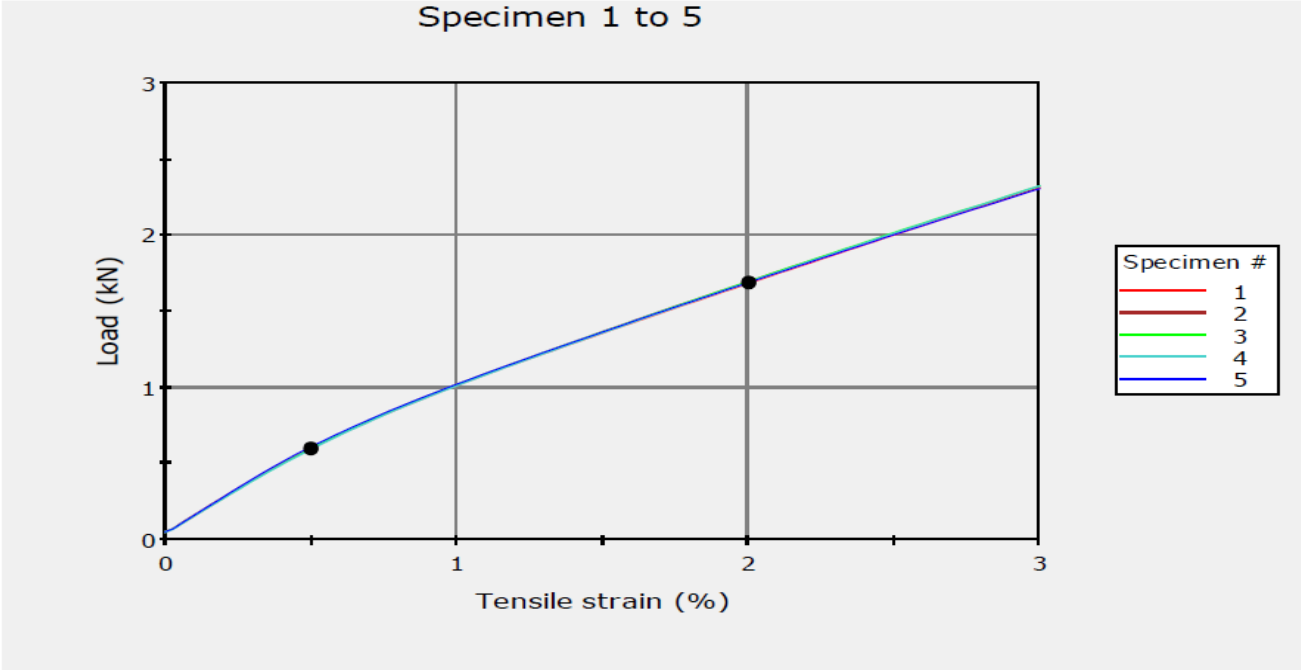
	Maximum Load (kN)	Strain at Maximum Load (%)	Maximum Strength (kN/m)	Secant Stiffness @ 0.5% Strain (kN/m)	Secant Stiffness @ 2% Strain (kN/m)	Secant Stiffness @ 5% Strain (kN/m)	Secant Stiffness @ 10% Strain (kN/m)
1	5.68	10.59	20.00	439.66	318.93	253.94	195.90
2	5.55	10.29	19.60	413.74	311.67	249.34	193.62
3	5.62	10.59	19.77	426.12	315.81	252.24	194.03
4	5.26	9.79	18.41	418.19	310.10	247.46	----
5	5.38	10.26	18.94	435.01	315.76	249.51	188.48
Mean	5.50	10.30	19.34	426.54	314.45	250.50	193.01
Standard Deviation	0.17	0.33	0.66	10.93	3.55	2.57	3.18
Coefficient of Variation	3.13	3.17	3.40	2.56	1.13	1.03	1.65

Fig 5.11. – Index test data for TX160 (Batch Ref: 056218, TAP 1 Year) tested at 60° (‘mid-rib’ direction)



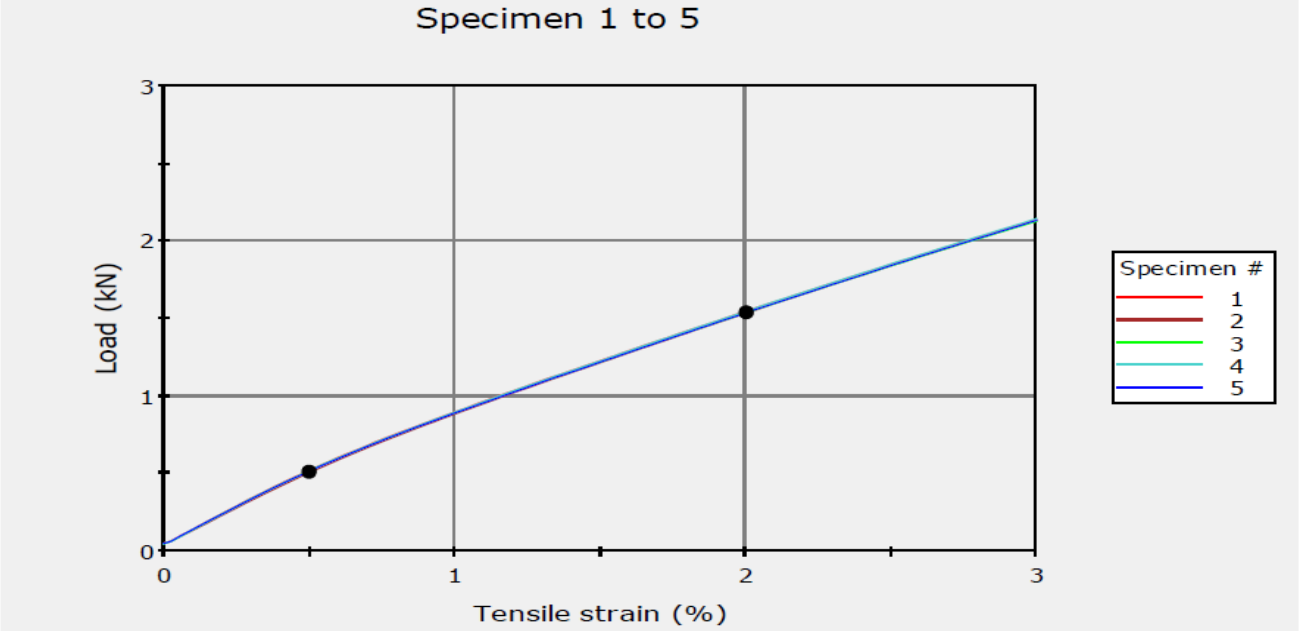
	Maximum Load (kN)	Strain at Maximum Load (%)	Maximum Strength (kN/m)	Secant Stiffness @ 0.5% Strain (kN/m)	Secant Stiffness @ 2% Strain (kN/m)	Secant Stiffness @ 5% Strain (kN/m)	Secant Stiffness @ 10% Strain (kN/m)
1	4.84	8.21	19.66	506.02	384.85	300.28	-----
2	4.85	8.19	19.34	506.47	379.15	294.65	-----
3	4.87	8.94	19.57	495.37	374.14	290.18	-----
4	4.73	8.19	19.09	506.79	381.45	295.48	-----
5	4.97	8.81	19.96	514.39	387.37	299.47	-----
Mean	4.85	8.47	19.52	505.81	381.39	296.01	-----
Standard Deviation	0.08	0.37	0.33	6.78	5.13	4.07	-----
Coefficient of Variation	1.74	4.40	1.69	1.34	1.35	1.38	-----

Fig 5.12. – Index test data for TX160 (Batch Ref: 056218, TAP 1 Year) tested at 90° (cross machine direction)



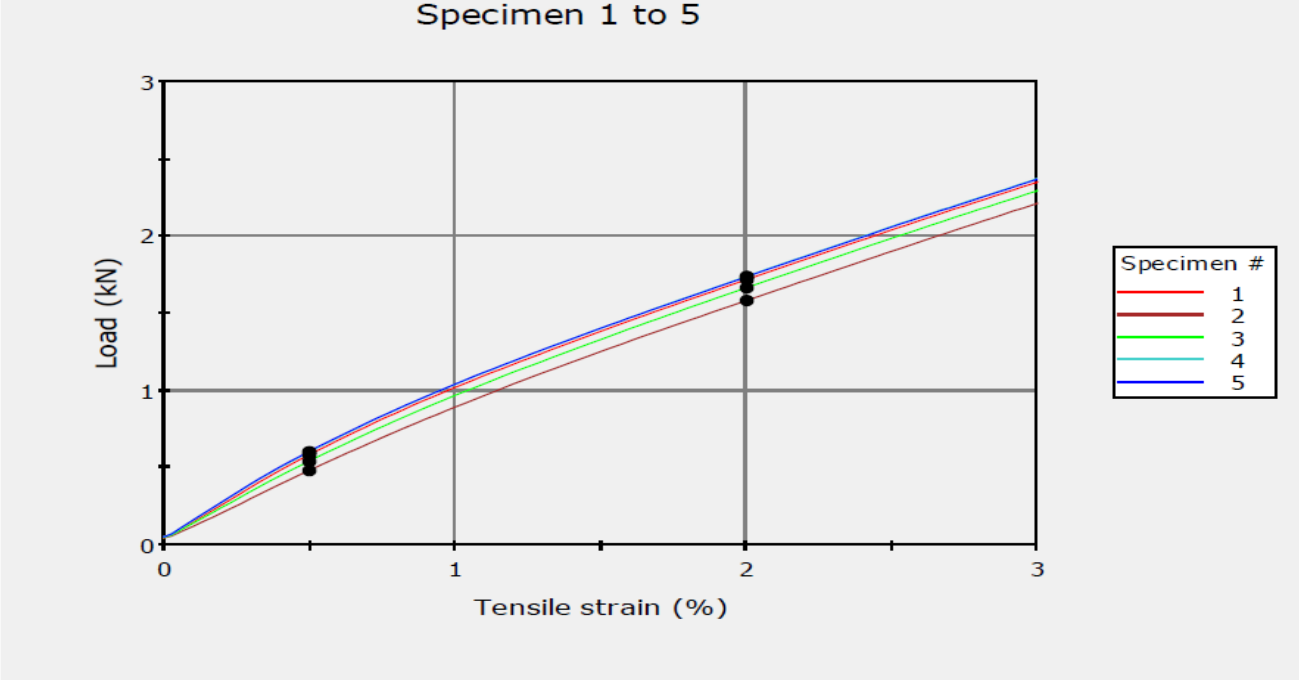
	Maximum Load (kN)	Strain at Maximum Load (%)	Maximum Strength (kN/m)	Secant Stiffness @ 0.5% Strain (kN/m)	Secant Stiffness @ 2% Strain (kN/m)	Secant Stiffness @ 5% Strain (kN/m)	Secant Stiffness @ 10% Strain (kN/m)
1	5.10	9.30	18.41	433.52	303.90	246.90	-----
2	4.87	9.24	17.72	441.13	308.61	244.14	-----
3	5.21	9.69	18.68	430.01	304.23	244.81	-----
4	5.24	9.66	19.12	433.81	308.52	252.03	-----
5	4.98	9.47	18.00	441.48	305.01	243.53	172.60
Mean	5.08	9.47	18.39	435.99	306.05	246.28	172.60
Standard Deviation	0.15	0.20	0.55	5.08	2.33	3.45	-----
Coefficient of Variation	3.03	2.14	3.00	1.16	0.76	1.40	-----

Fig 5.13. – Index test data for TX160 (Batch Ref: 059839, TAP 1 Week) tested at 0° (machine direction)



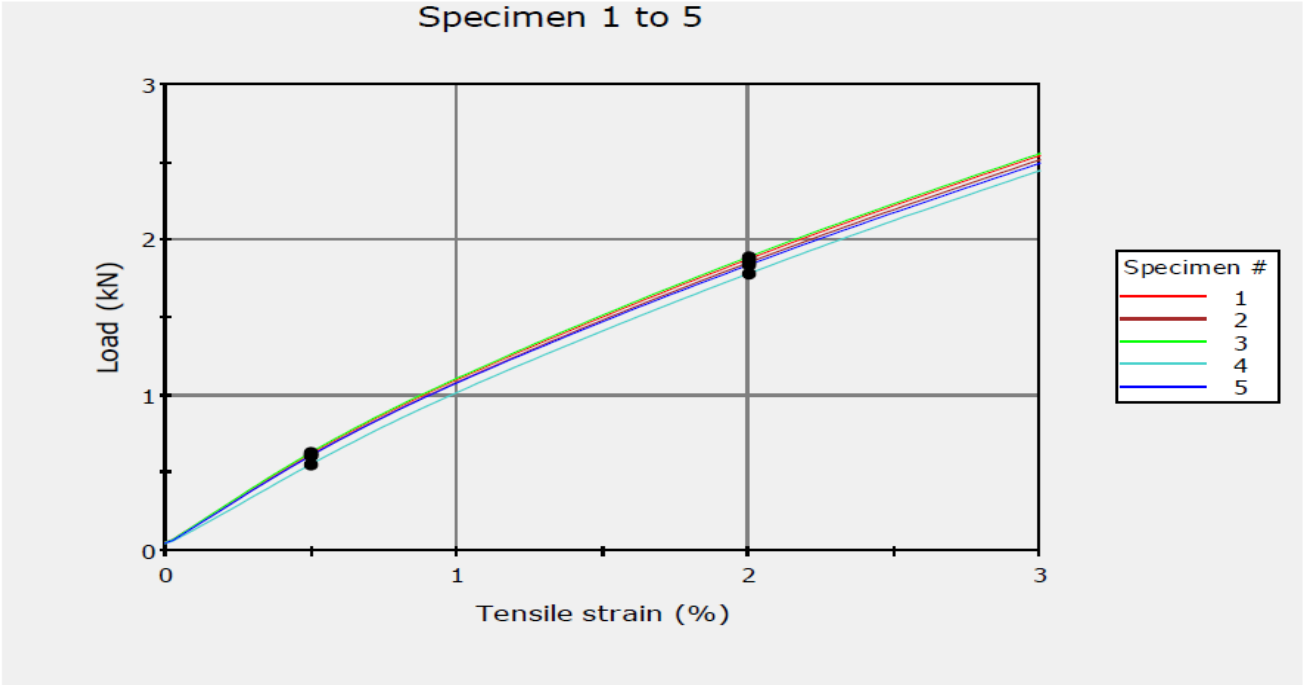
	Maximum Load (kN)	Strain at Maximum Load (%)	Maximum Strength (kN/m)	Secant Stiffness @ 0.5% Strain (kN/m)	Secant Stiffness @ 2% Strain (kN/m)	Secant Stiffness @ 5% Strain (kN/m)	Secant Stiffness @ 10% Strain (kN/m)
1	3.86	7.04	15.94	432.17	319.84	259.41	-----
2	3.99	7.29	16.68	424.06	321.10	263.37	-----
3	4.00	7.64	16.66	432.62	320.38	260.94	-----
4	4.01	7.74	16.77	434.37	323.91	264.39	-----
5	4.09	7.72	17.19	434.36	323.10	264.63	-----
Mean	3.99	7.49	< 16.65	431.52	321.67	262.55	-----
Standard Deviation	0.08	0.31	0.45	4.28	1.76	2.28	-----
Coefficient of Variation	2.11	4.11	2.70	0.99	0.55	0.87	-----

Fig 5.14. – Index test data for TX160 (Batch Ref: 059839, TAP 1 Week) tested at 30° (‘rib’ direction)



	Maximum Load (kN)	Strain at Maximum Load (%)	Maximum Strength (kN/m)	Secant Stiffness @ 0.5% Strain (kN/m)	Secant Stiffness @ 2% Strain (kN/m)	Secant Stiffness @ 5% Strain (kN/m)	Secant Stiffness @ 10% Strain (kN/m)
1	5.45	10.23	19.25	414.56	303.74	244.66	190.60
2	5.23	9.69	18.53	344.81	280.93	236.12	-----
3	5.35	10.70	18.99	387.01	295.50	240.42	185.74
4	5.35	9.96	18.96	428.72	308.47	246.78	-----
5	5.31	9.80	18.85	431.49	307.95	246.69	-----
Mean	5.34	10.08	18.91	401.32	299.32	242.93	188.17
Standard Deviation	0.08	0.40	0.26	36.17	11.52	4.60	3.43
Coefficient of Variation	1.50	4.00	1.38	9.01	3.85	1.89	1.82

Fig 5.15. – Index test data for TX160 (Batch Ref: 059839, TAP 1 Week) tested at 60° (‘mid-rib’ direction)



	Maximum Load (kN)	Strain at Maximum Load (%)	Maximum Strength (kN/m)	Secant Stiffness @ 0.5% Strain (kN/m)	Secant Stiffness @ 2% Strain (kN/m)	Secant Stiffness @ 5% Strain (kN/m)	Secant Stiffness @ 10% Strain (kN/m)
1	5.17	11.19	20.93	507.87	380.08	293.23	205.61
2	5.24	11.39	21.28	500.45	376.91	291.90	206.25
3	5.24	11.51	21.22	513.74	382.77	293.88	205.93
4	4.86	9.46	19.52	448.13	358.12	283.62	-----
5	5.20	11.46	21.14	499.40	373.76	289.84	205.04
Mean	5.14	11.00	20.82	493.92	374.33	290.50	205.71
Standard Deviation	0.16	0.87	0.74	26.25	9.67	4.14	0.52
Coefficient of Variation	3.11	7.92	3.55	5.32	2.58	1.43	0.25

Fig 5.16. – Index test data for TX160 (Batch Ref: 059839, TAP 1 Week) tested at 90° (cross machine direction)

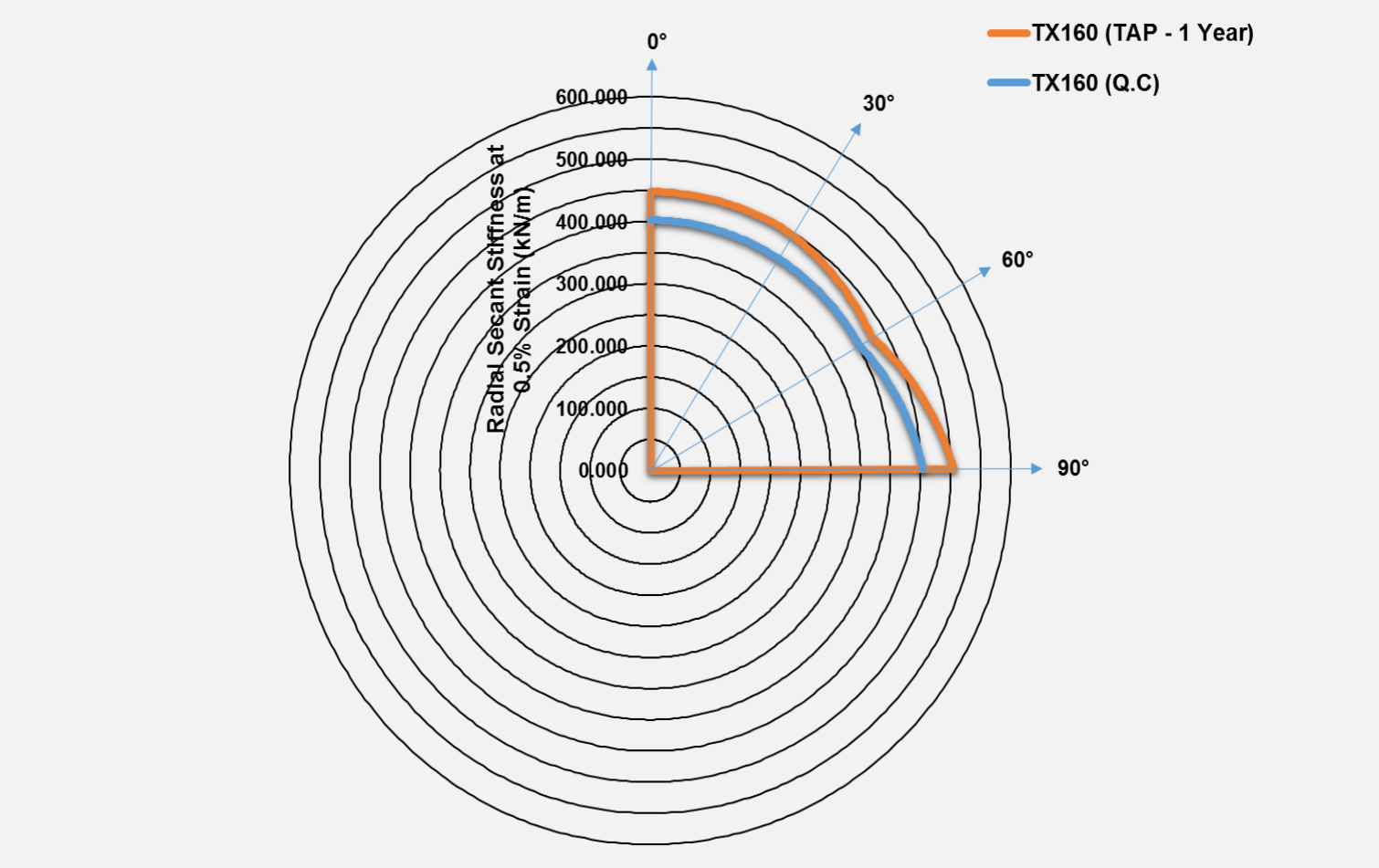


Fig 5.17. - Polar plot showing 'Radial Secant Stiffness at 0.5% Strain' of TX160 (Batch Ref: 056218) tested for Q.C. purposes and TAP for 1 year.

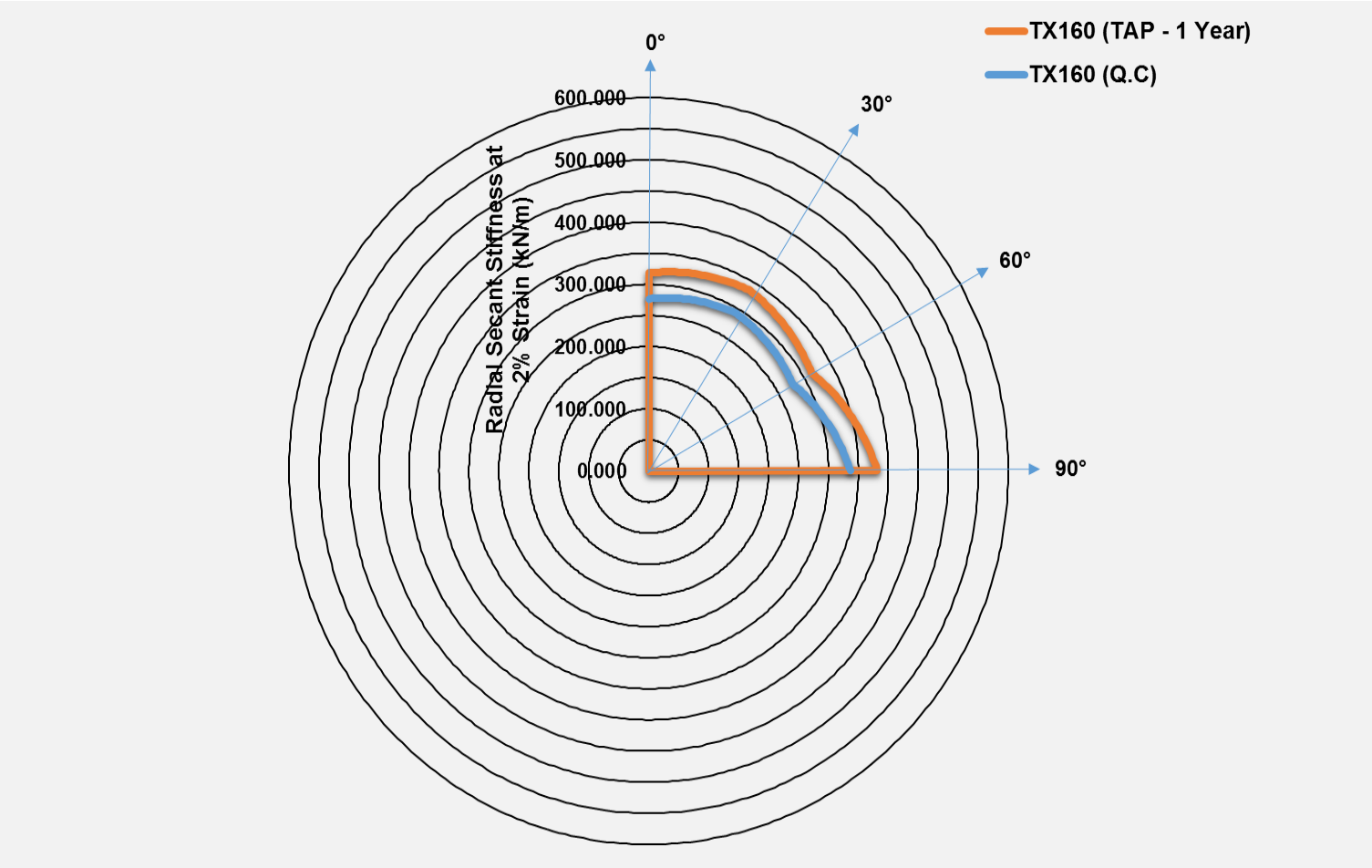


Fig 5.18. - Polar plot showing 'Radial Secant Stiffness at 2% Strain' of TX160 (Batch Ref: 056218) tested for Q.C. purposes and TAP for 1 year.

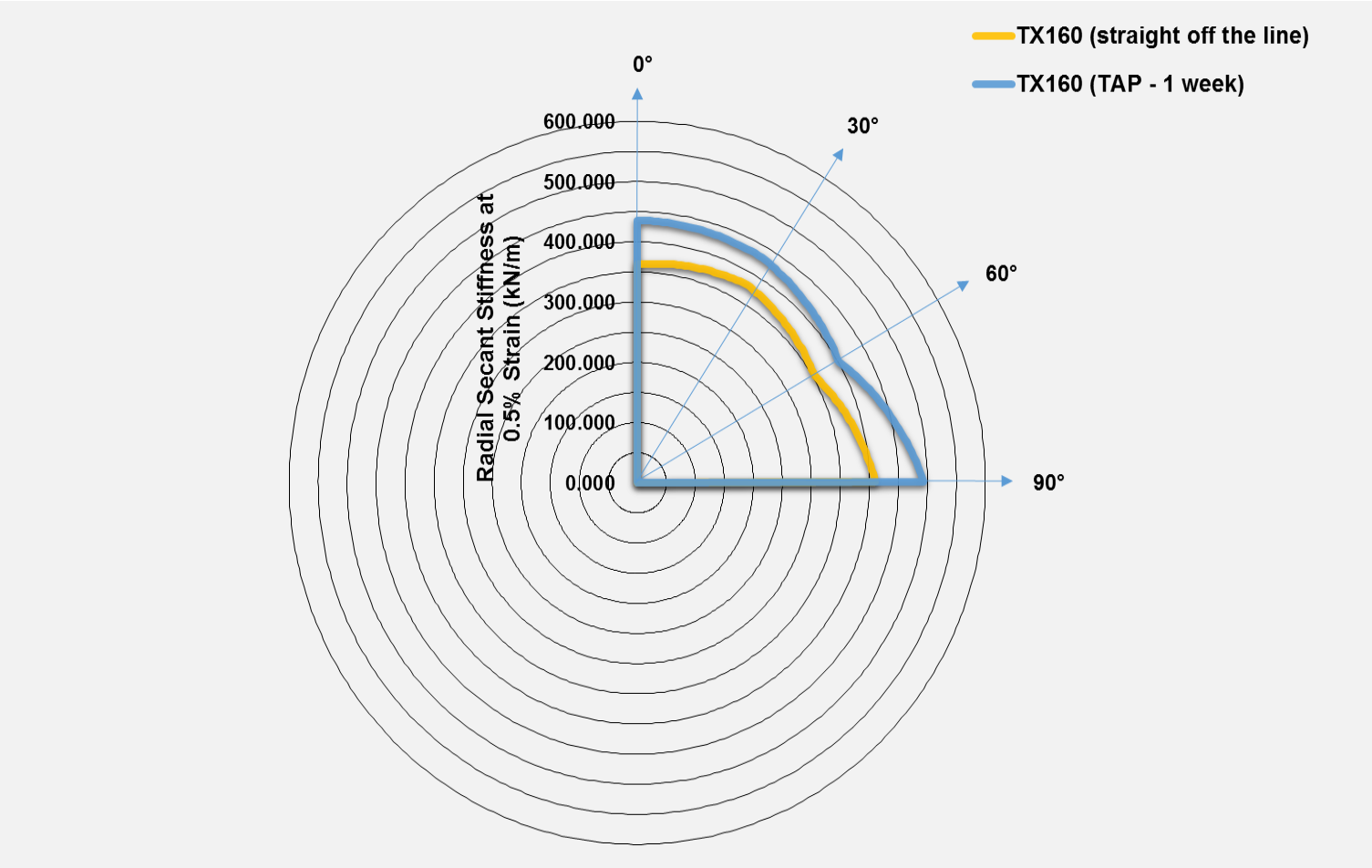


Fig 5.19 - Polar plot showing 'Radial Secant Stiffness at 0.5% Strain' of TX160 (Batch Ref: 059839) tested straight off the production line and after 1 week.

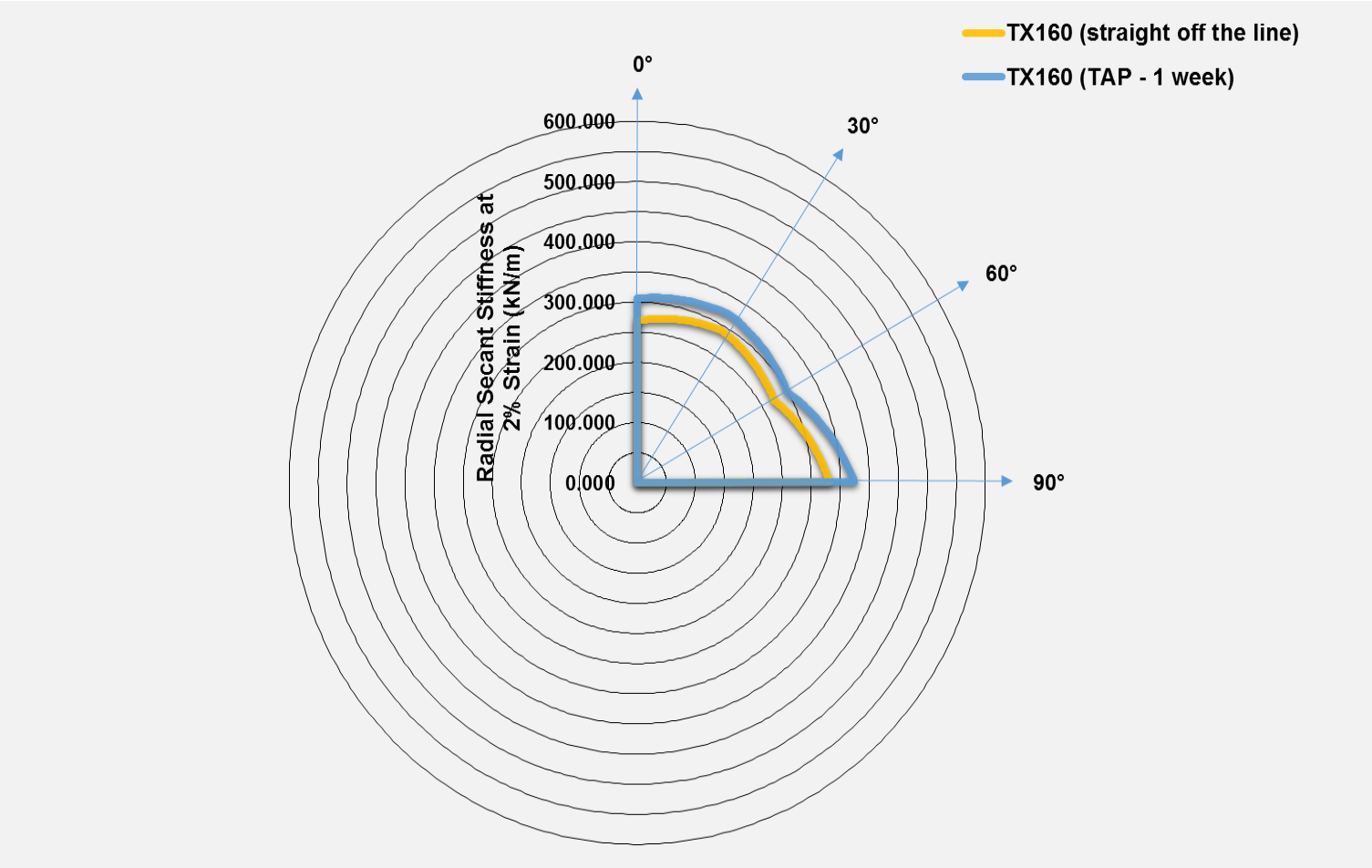


Fig 5.20 - Polar plot showing 'Radial Secant Stiffness at 2% Strain' of TX160 (Batch Ref: 059839) tested straight off the production line and after 1 week.

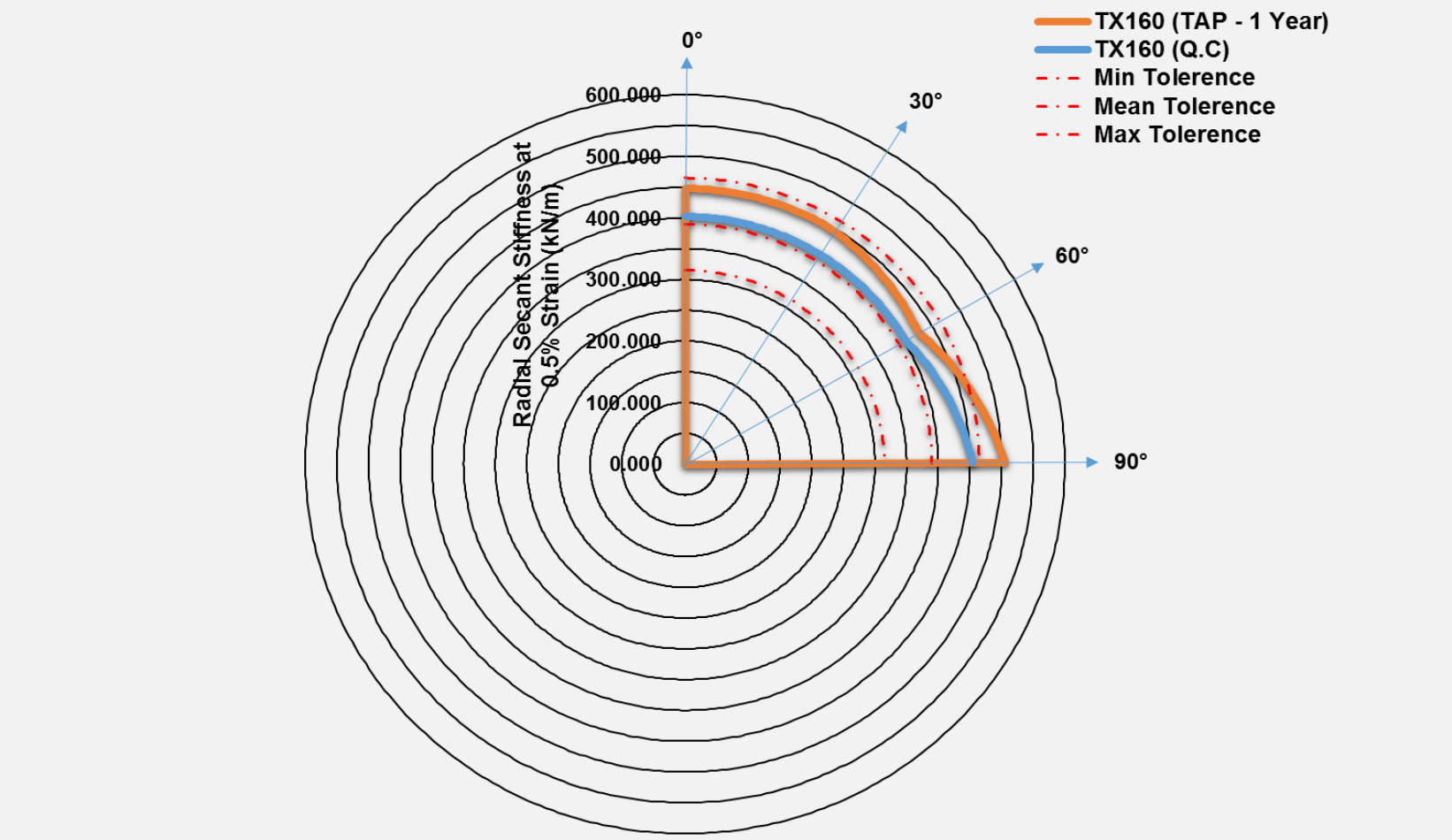


Fig 5.21 - Polar plot showing 'Radial Secant Stiffness at 0.5% Strain' of TX160 (Batch Ref: 056218) tested by quality control straight off the production line and tested after 1 year, with Min, Mean & Max specifications.

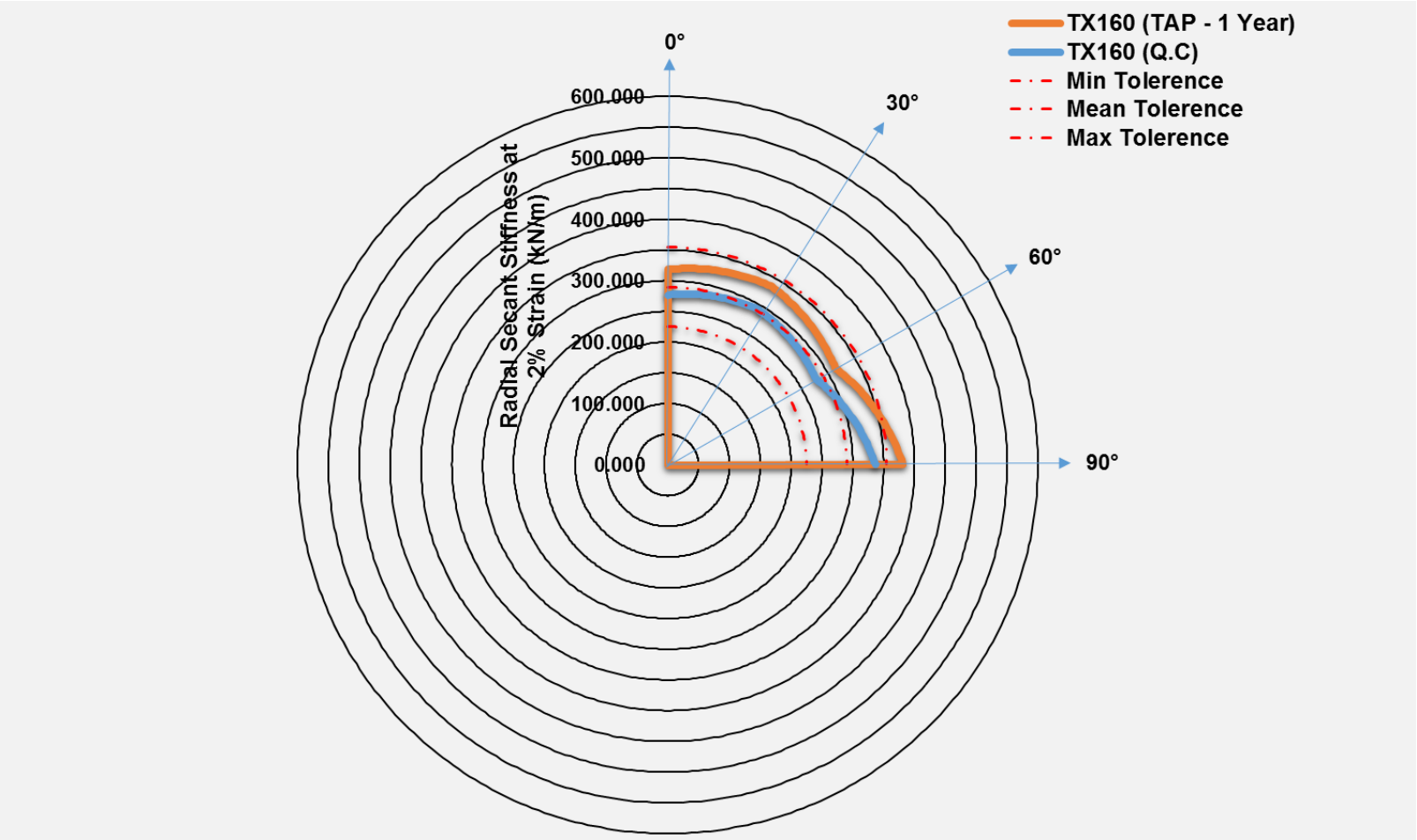


Fig 5.22 - Polar plot showing 'Radial Secant Stiffness at 2% Strain' of TX160 (Batch Ref: 056218) tested by quality control straight off the production line and tested after 1 year, with Min, Mean & Max specifications.

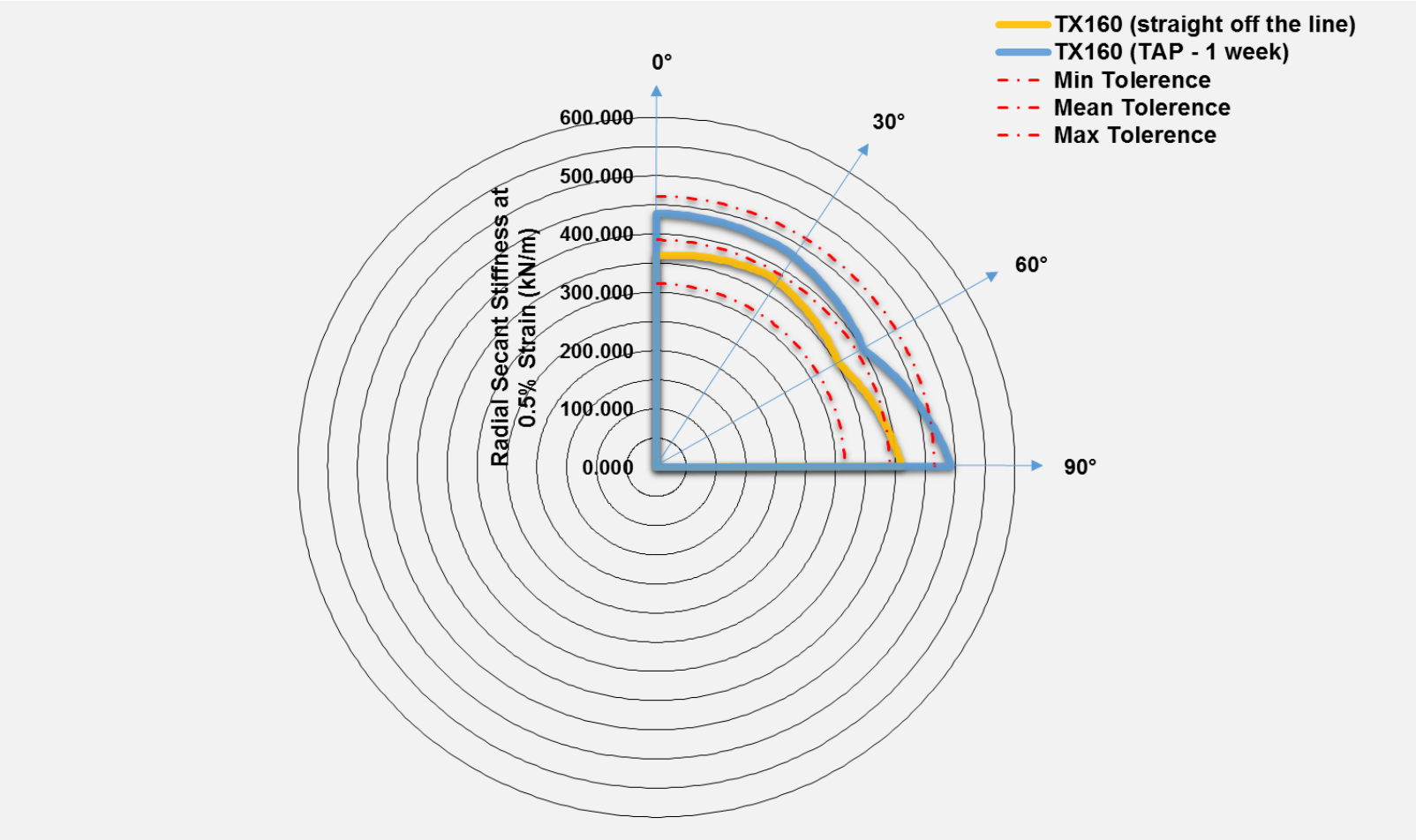


Fig 5.23 - Polar plot showing 'Radial Secant Stiffness at 0.5% Strain' of TX160 (Batch Ref: 059839) tested by quality control straight off the production line and tested after 1 week, with Min, Mean & Max specifications.

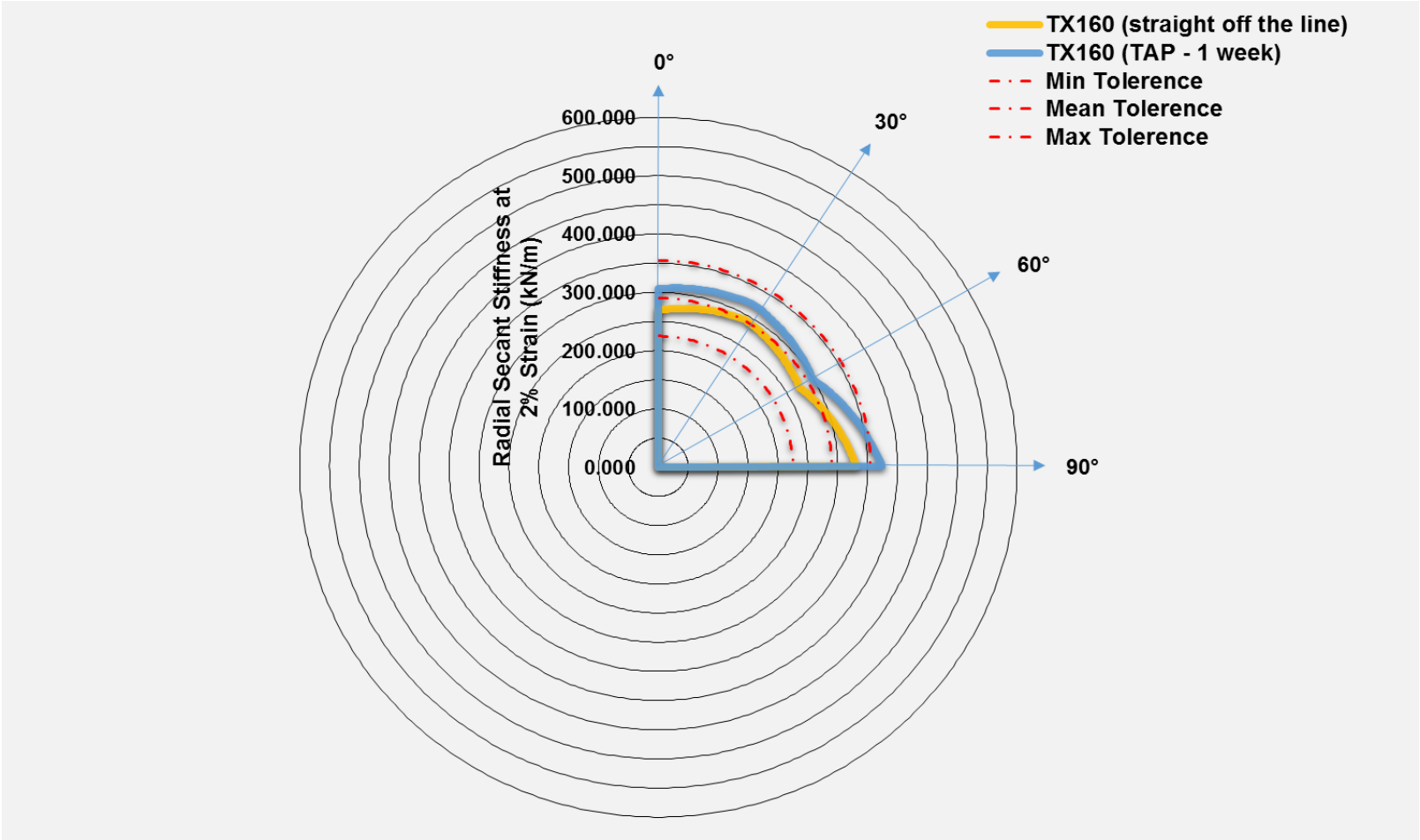


Fig 5.24 - Polar plot showing 'Radial Secant Stiffness at 2% Strain' of TX160 (Batch Ref: 059839) tested by quality control straight off the production line and tested after 1 week, with Min, Mean & Max specifications.

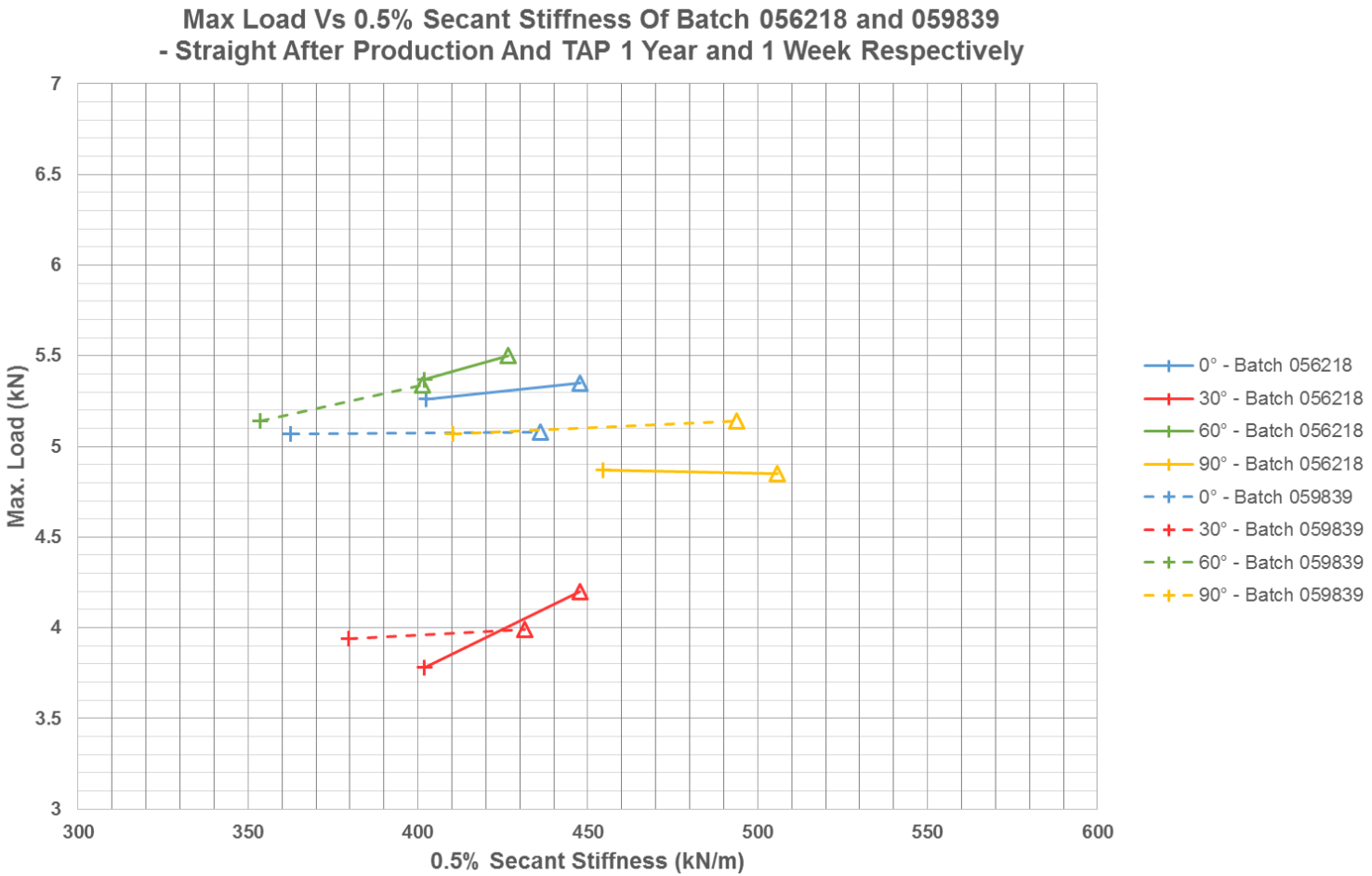


Fig 5.25 – Graph showing Max. Load Vs 0.5% Secant Stiffness of Batch 056218 and 059839 – Straight after production and after curing for 1 year and 1 week respectively.

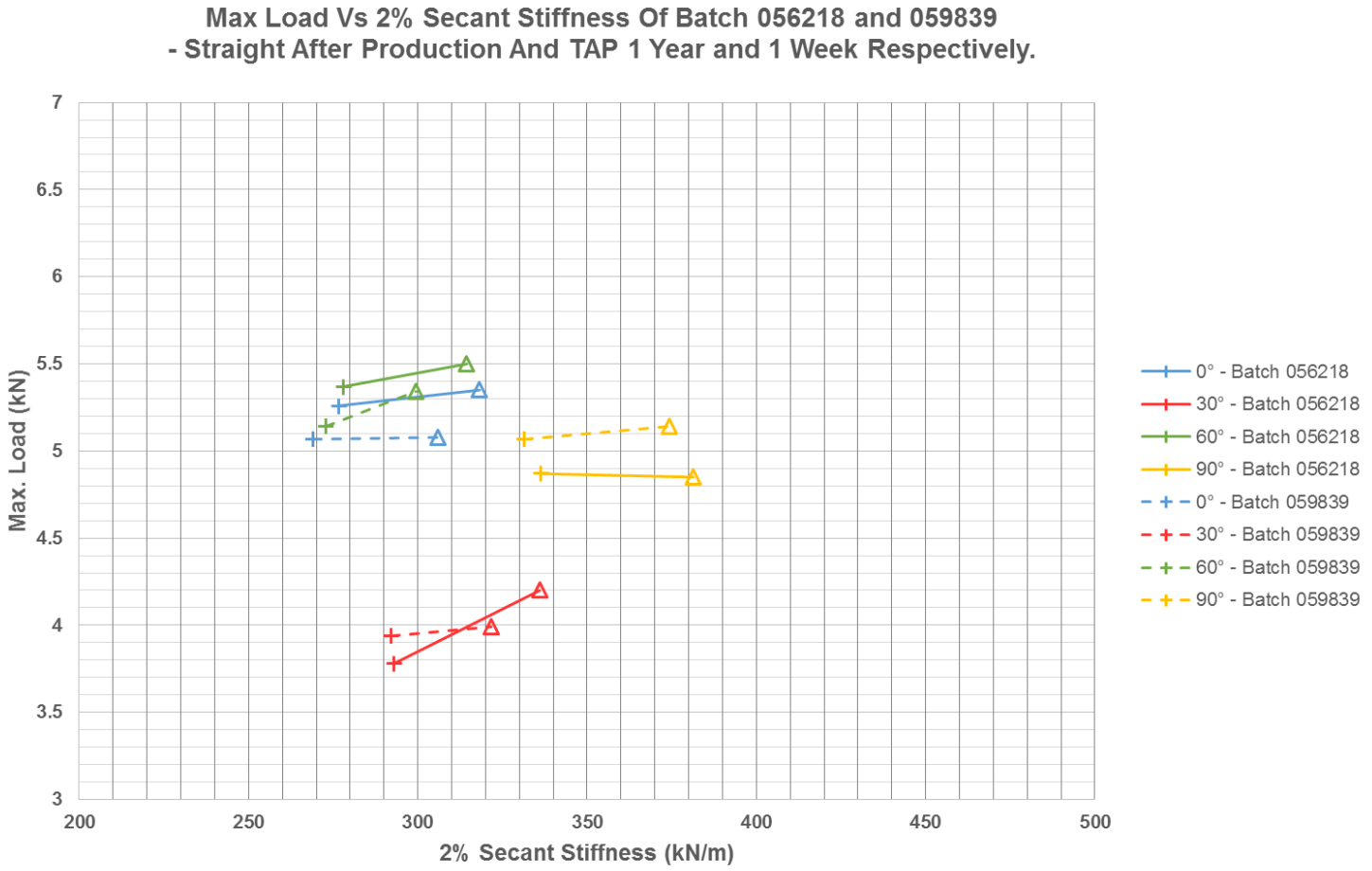


Fig 5.26 – Graph showing Max. Load Vs 2% Secant Stiffness of Batch 056218 and 059839 – Straight after production and after curing for 1 year and 1 week respectively.

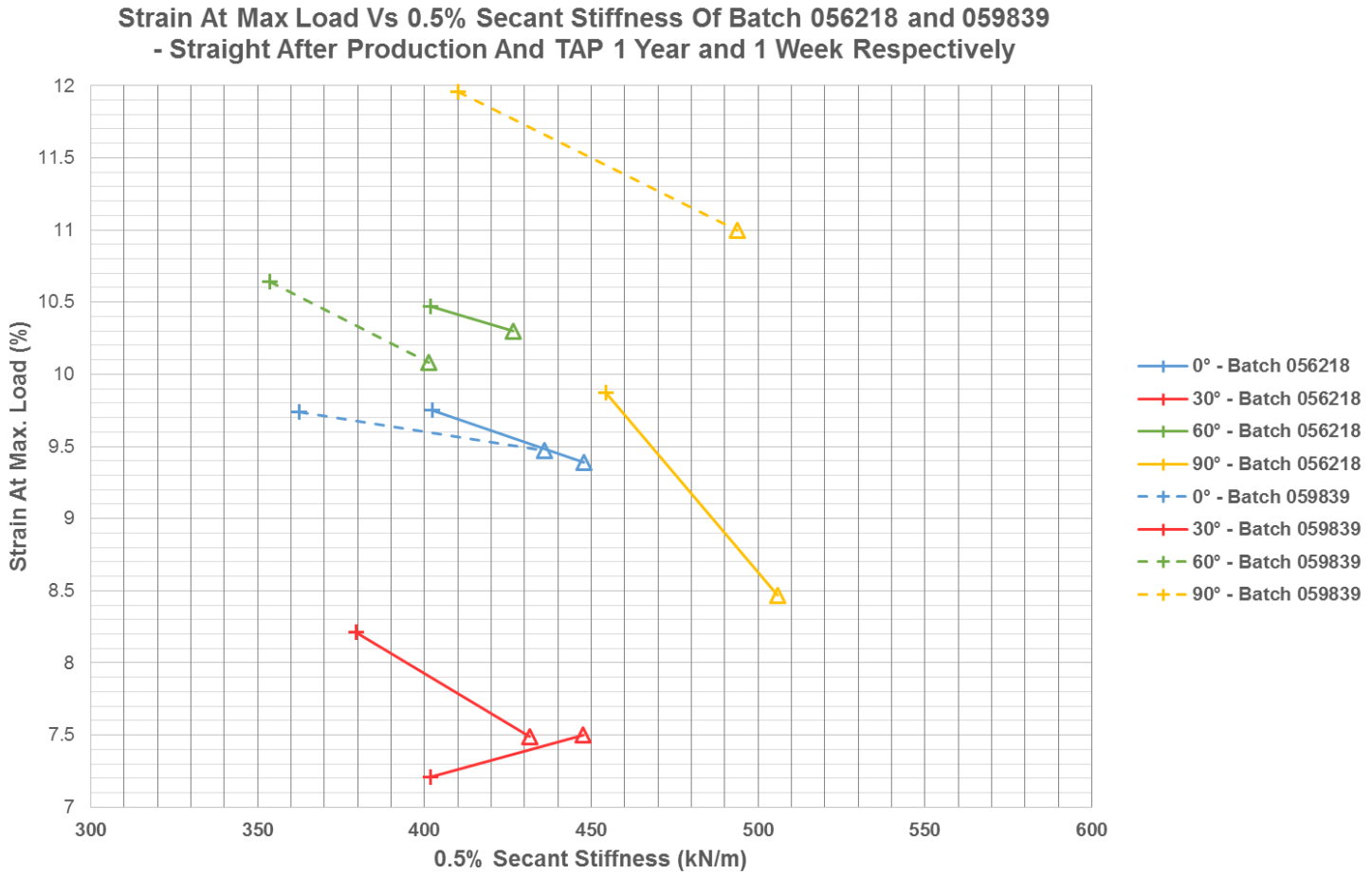


Fig 5.27 – Graph showing Strain at Max. Load Vs 0.5% Secant Stiffness of Batch 056218 and 059839 – Straight after production and after curing for 1 year and 1 week respectively.

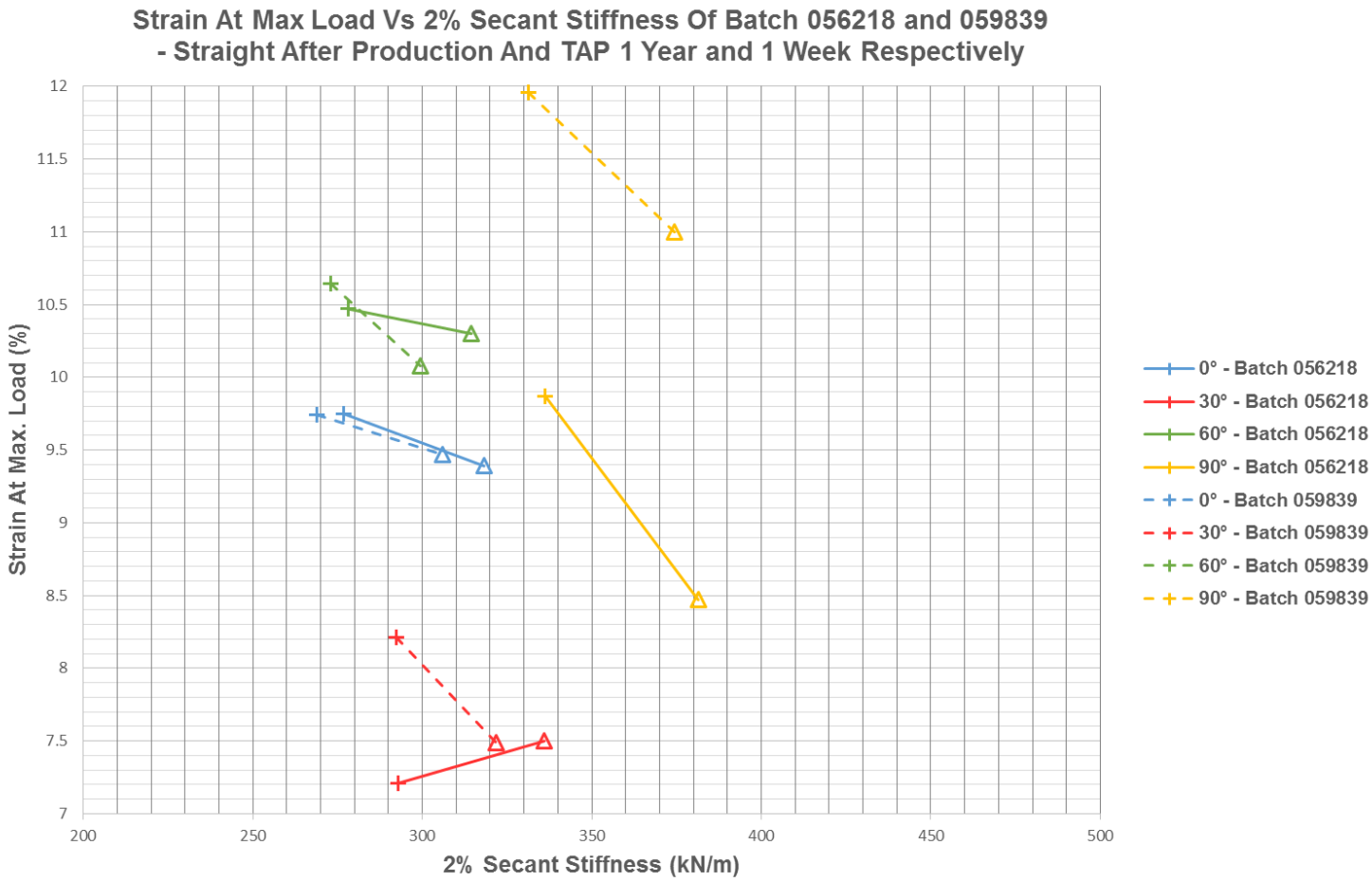


Fig 5.28 – Graph showing Strain at Max. Load Vs 2% Secant Stiffness of Batch 056218 and 059839 – Straight after production and after curing for 1 year and 1 week respectively.

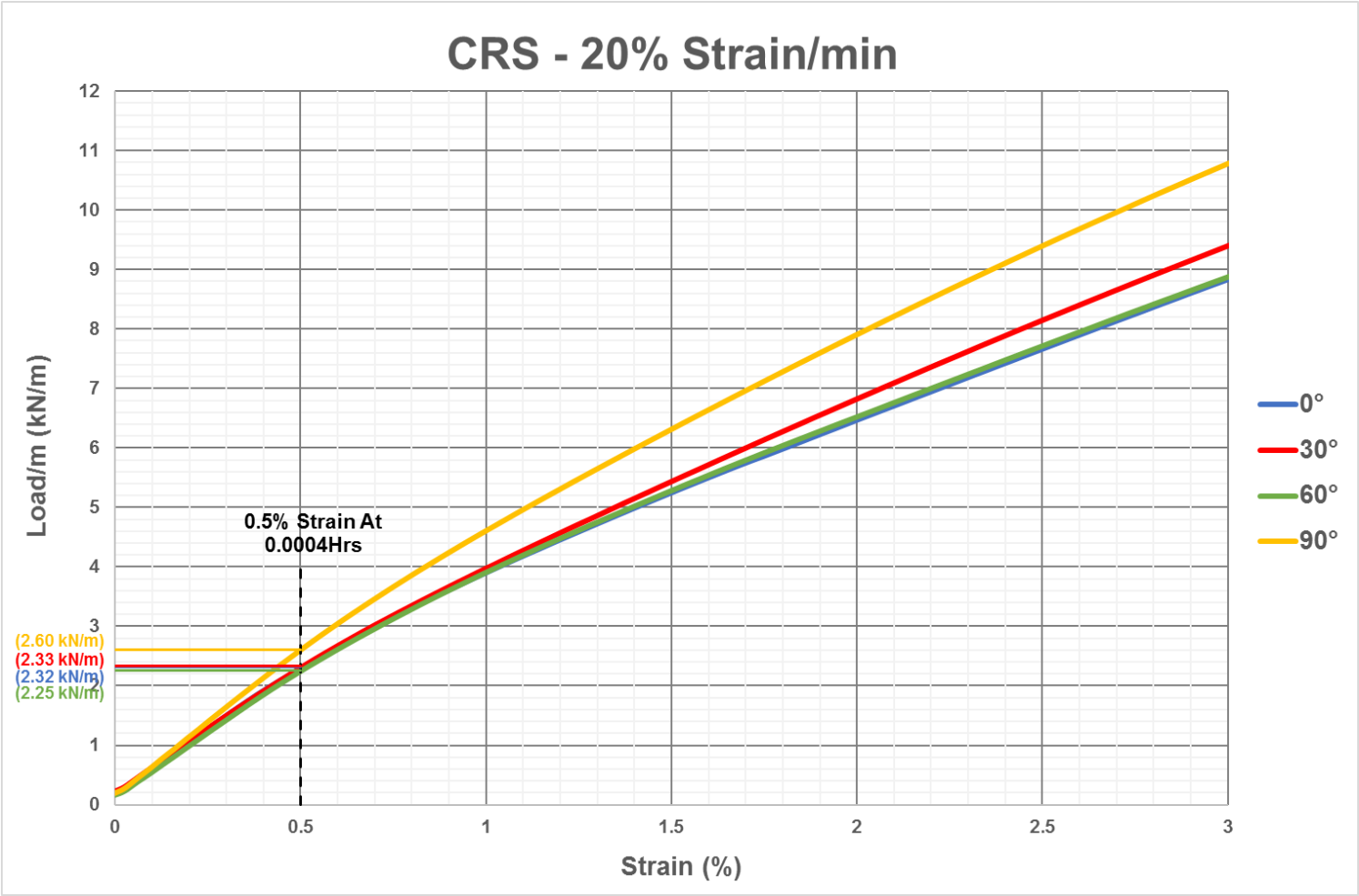


Fig 5.29 – CRS, Load/m vs Strain plot of TX160 (Batch Ref: 056218) tested at 20% strain/min in all four directions.

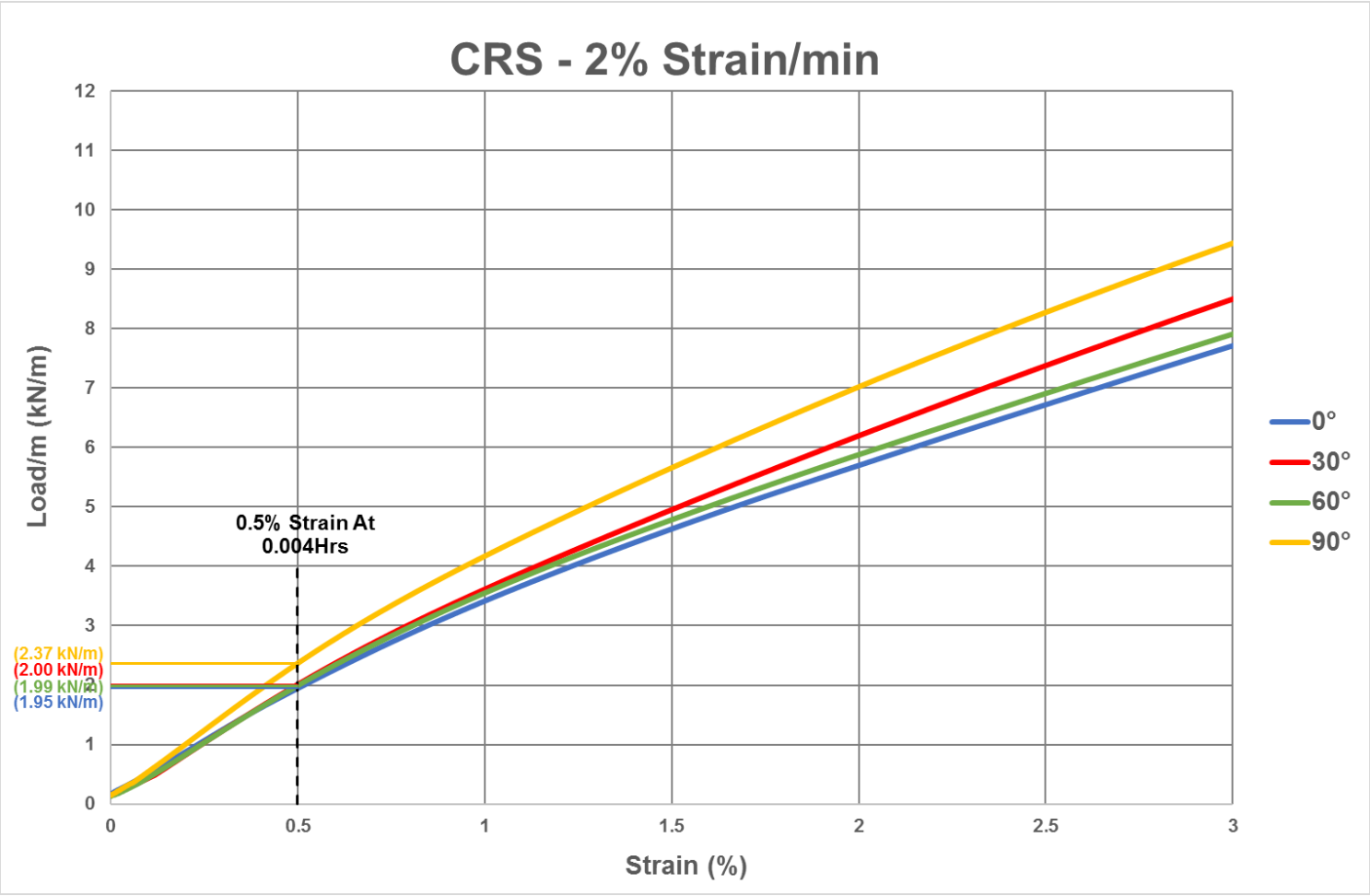


Fig 5.30 – CRS, Load/m vs Strain plot of TX160 (Batch Ref: 056218) tested at 2% strain/min in all four directions.

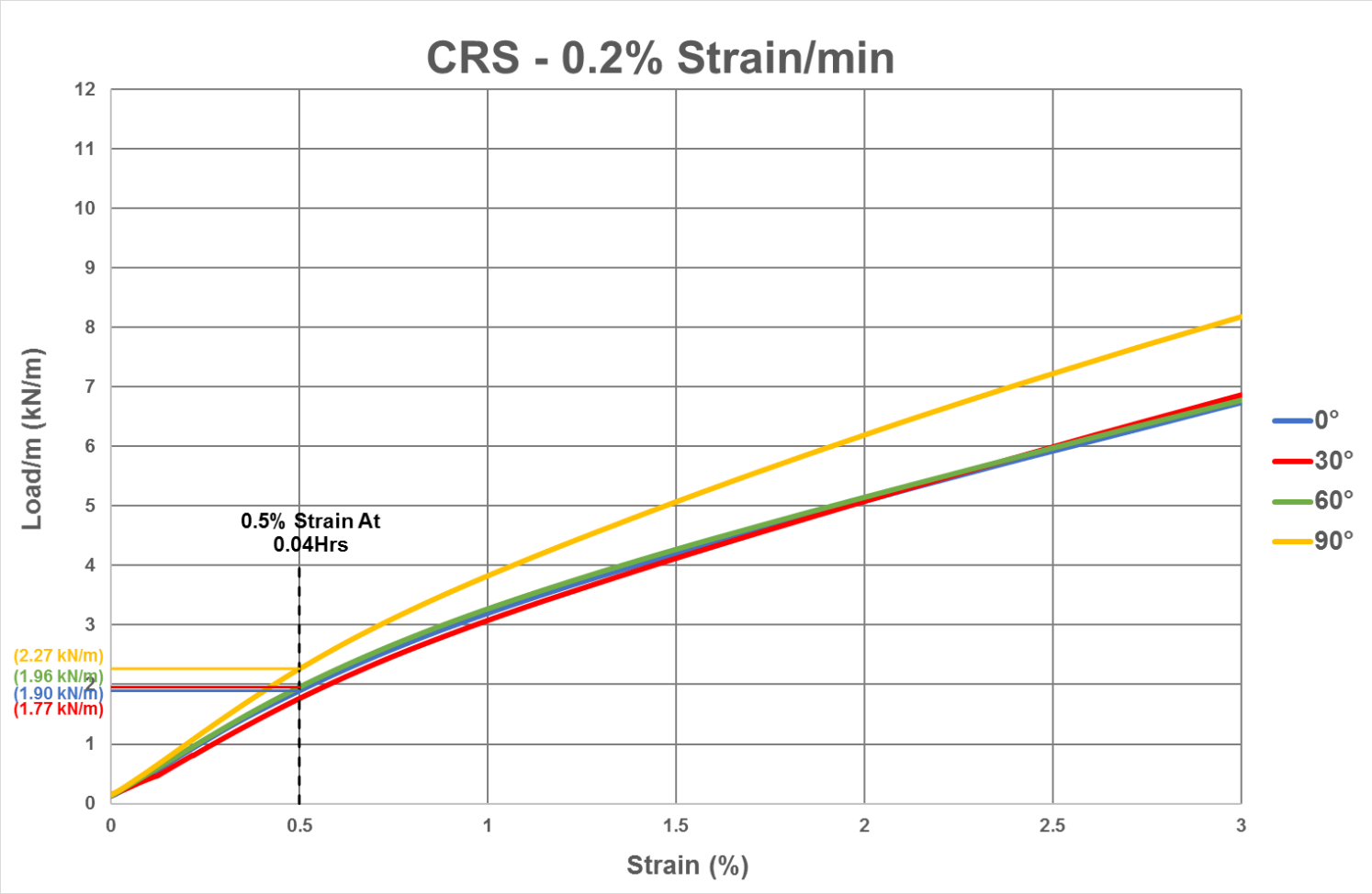


Fig 5.31 – CRS, Load/m vs Strain plot of TX160 (Batch Ref: 056218) tested at 0.2% strain/min in all four directions.

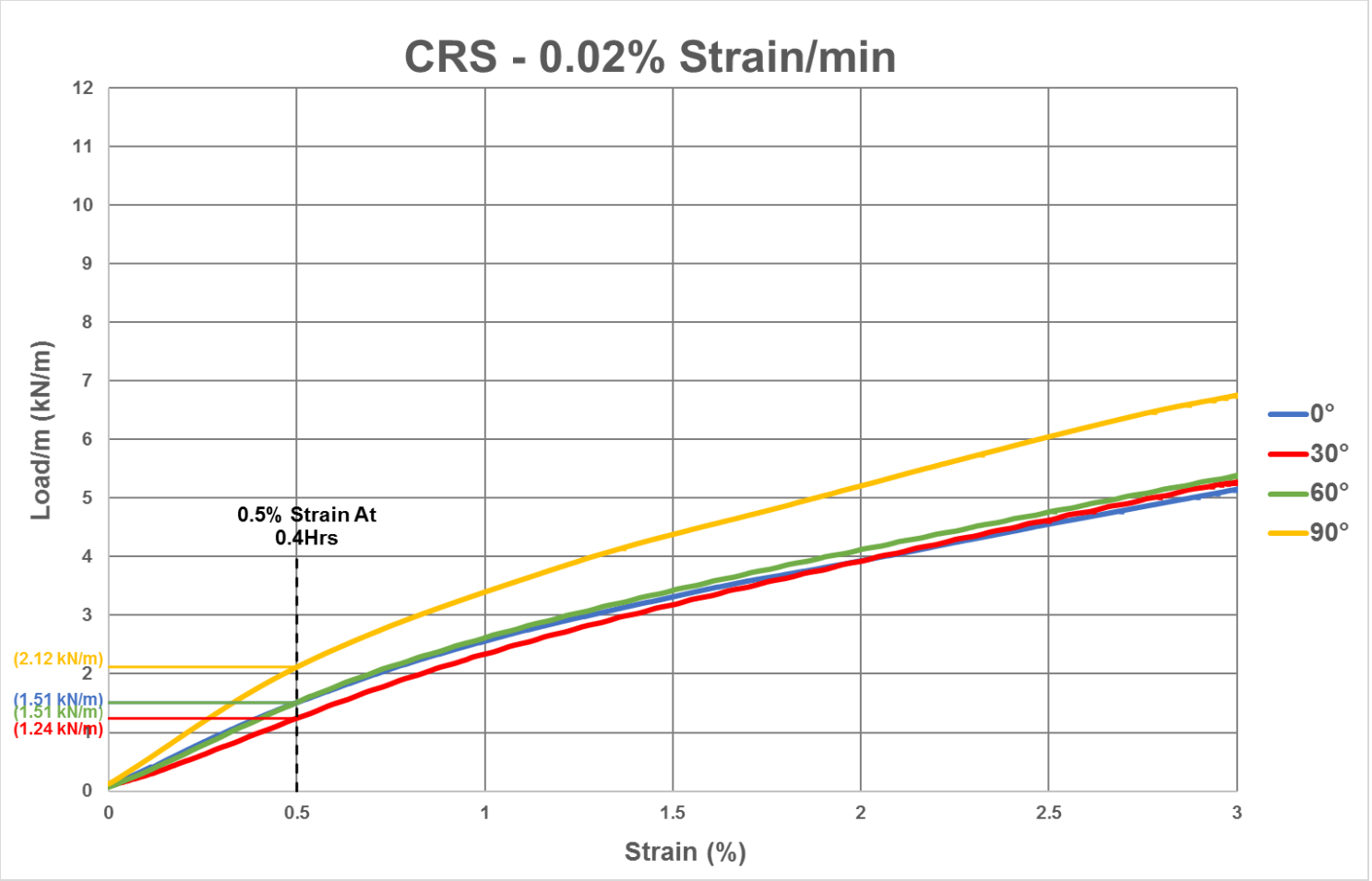


Fig 5.32 – CRS, Load/m vs Strain plot of TX160 (Batch Ref: 056218) tested at 0.02% strain/min in all four directions.

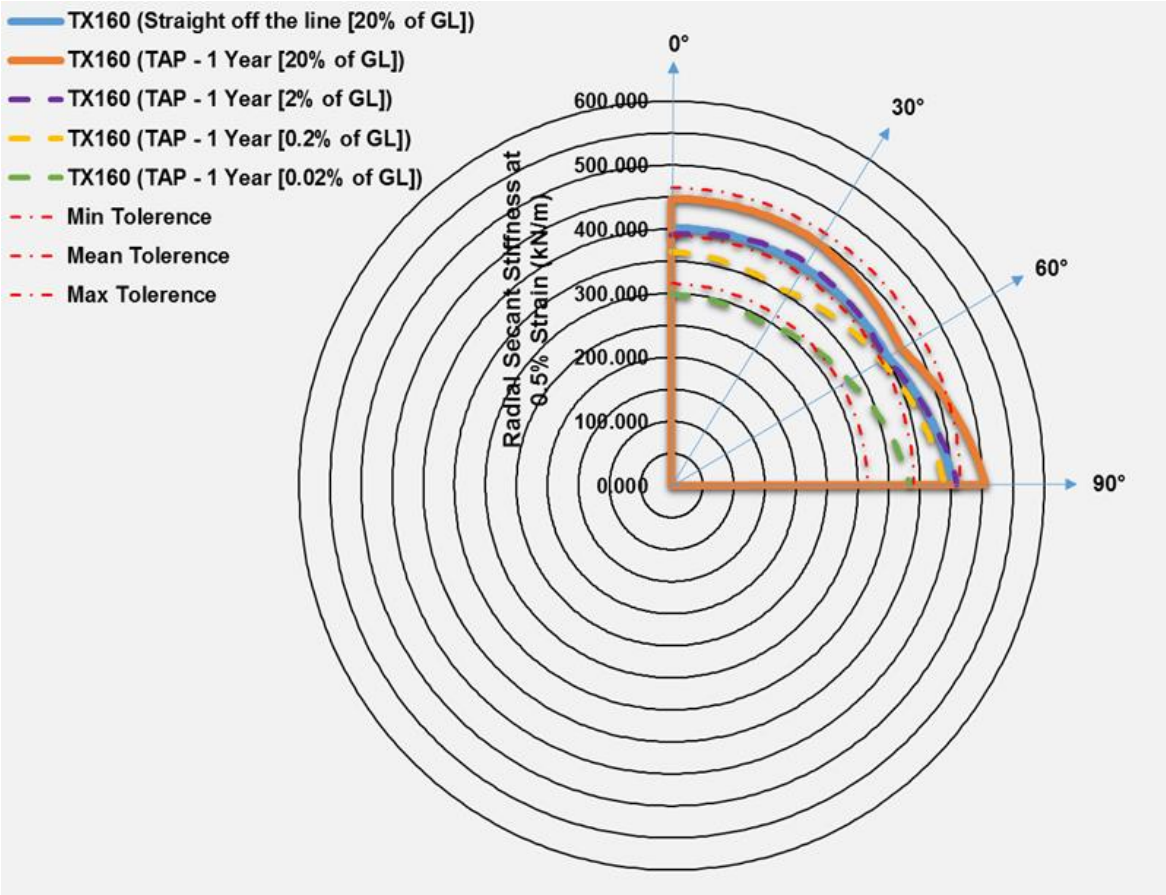


Fig 5.33 – Polar plot showing 'Radial Secant Stiffness at 0.5% Strain' of TX160 (Batch Ref: 056218) tested by quality control straight off the production line and tested after 1 year at various testing speeds, with Min, Mean & Max specifications.

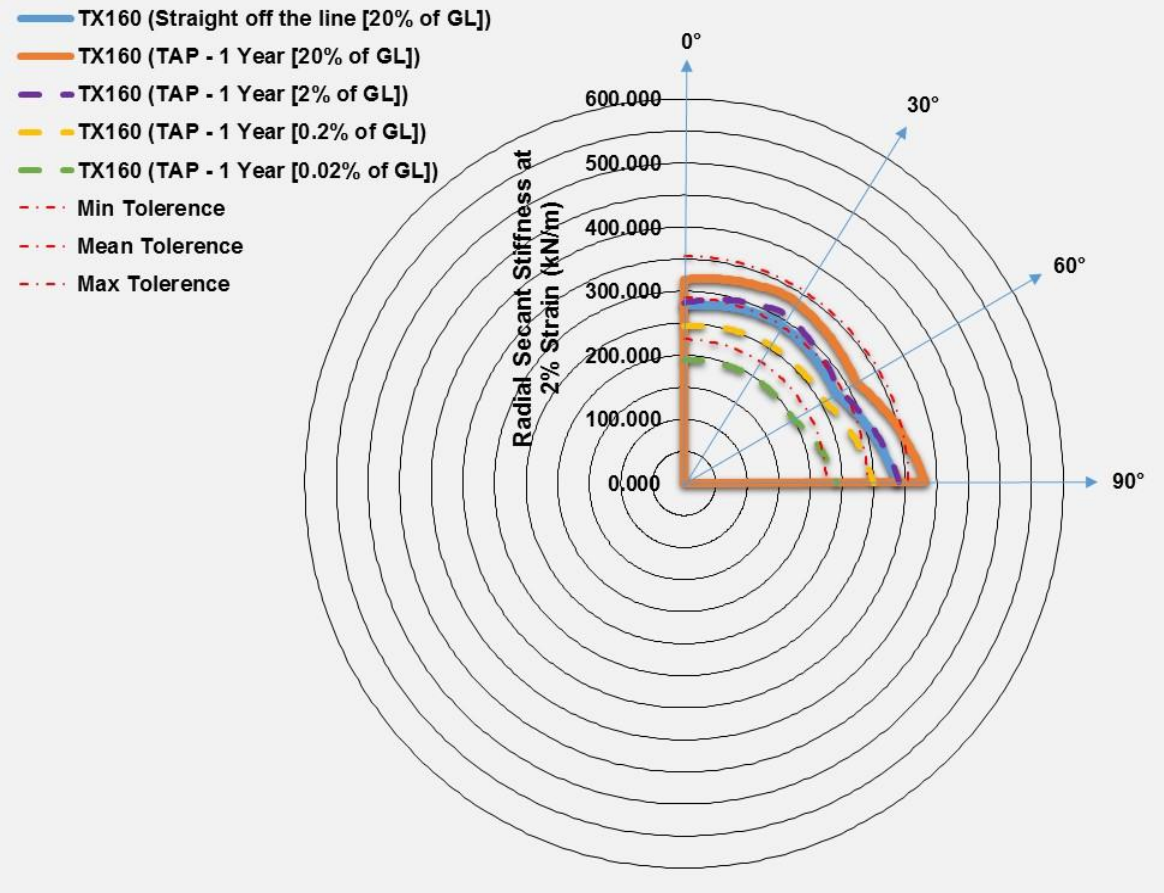


Fig 5.34 – Polar plot showing 'Radial Secant Stiffness at 2% Strain' of TX160 (Batch Ref: 056218) tested by quality control straight off the production line and tested after 1 year at various testing speeds, with Min, Mean & Max specifications.

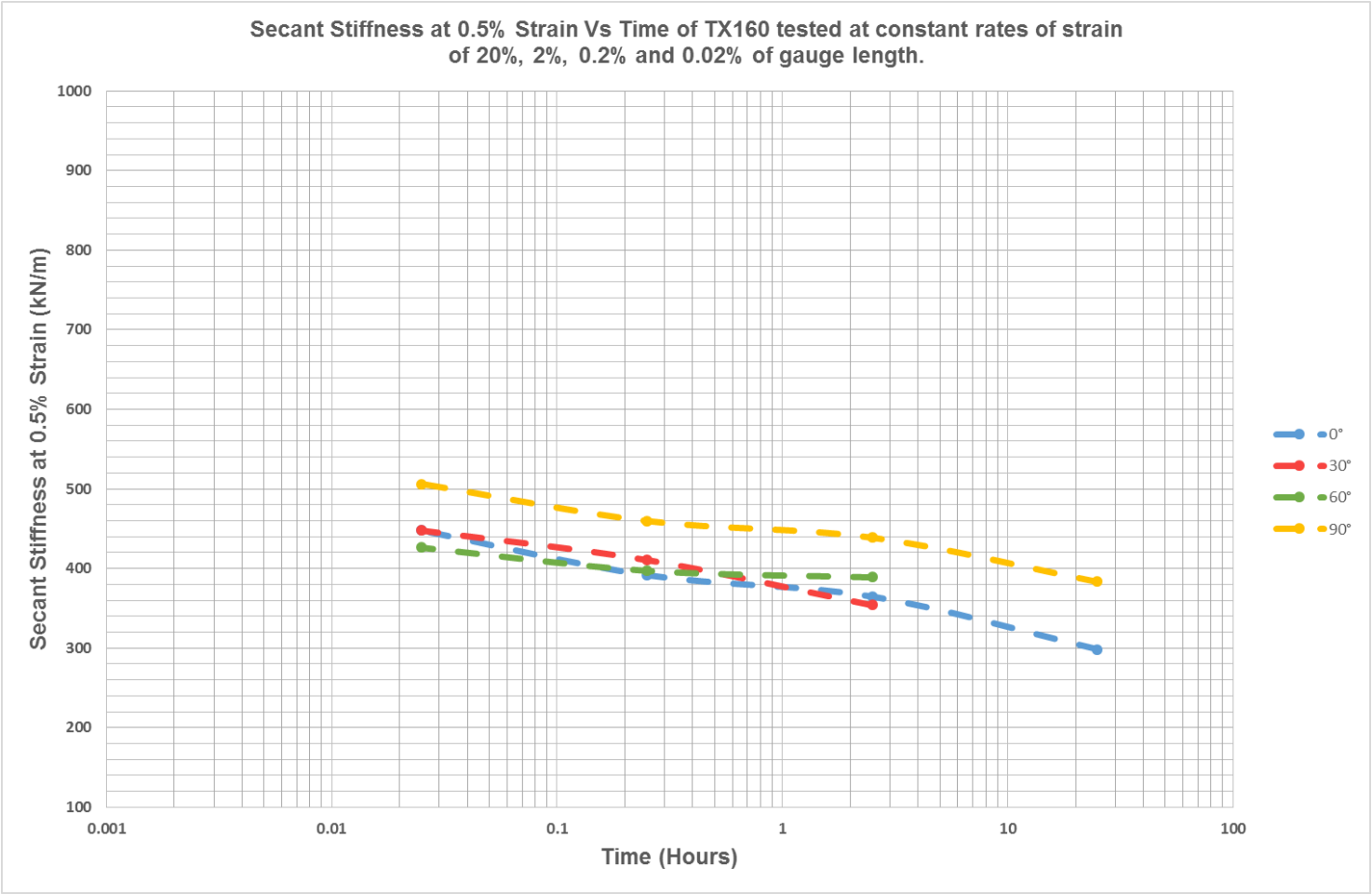


Fig 5.35 – Graph showing secant stiffness at 0.5% strain versus time of TX160 (Batch Ref: 056218) tested at constant rates of strain of 20%, 2%, 0.2% and 0.02% of the gauge length.

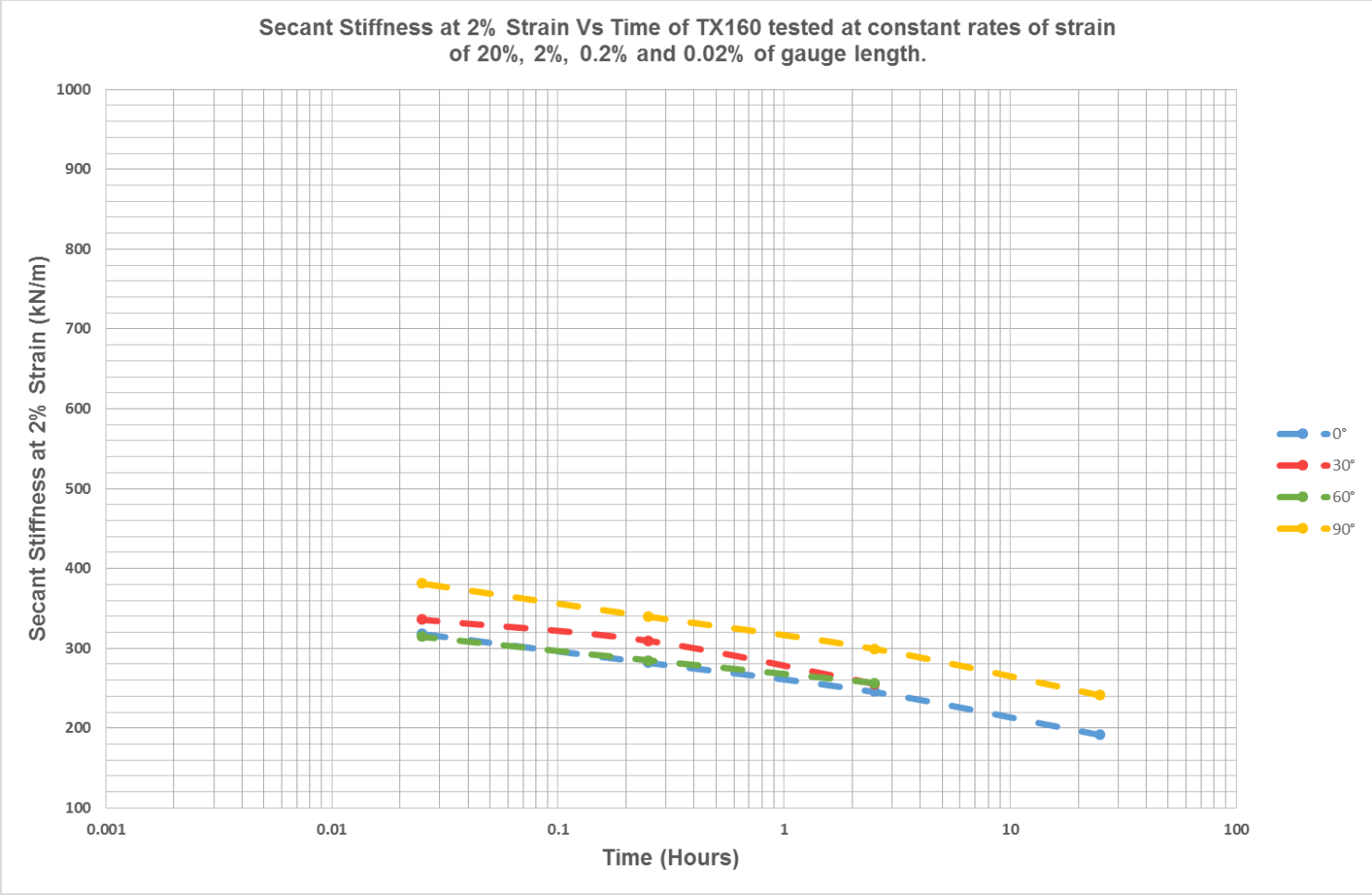


Fig 5.36 – Graph showing secant stiffness at 2% strain versus time of TX160 (Batch Ref: 056218) tested at constant rates of strain of 20%, 2%, 0.2% and 0.02% of the gauge length.

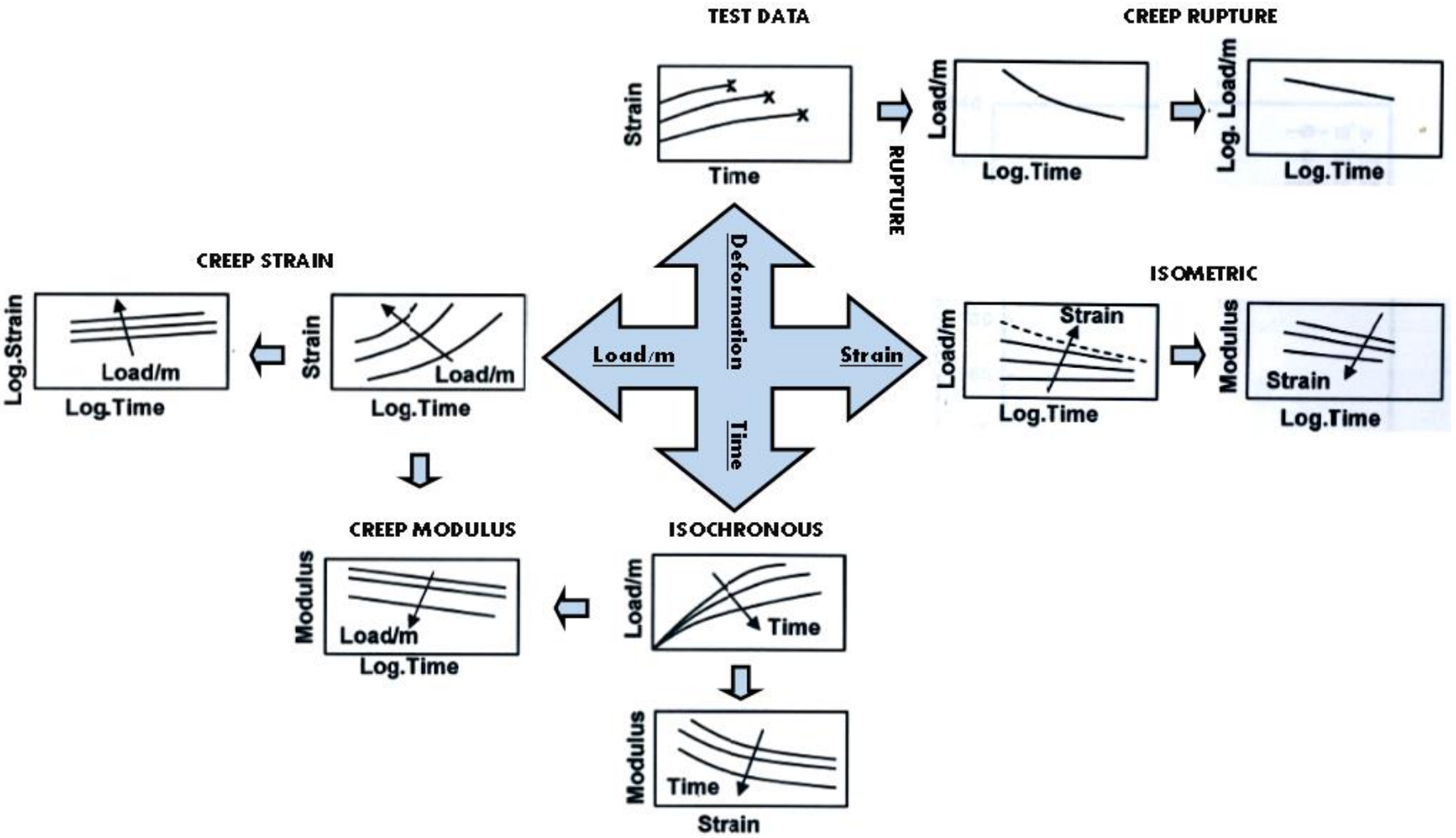


Fig 5.37 – Presentation of creep test data, ASM (1988).

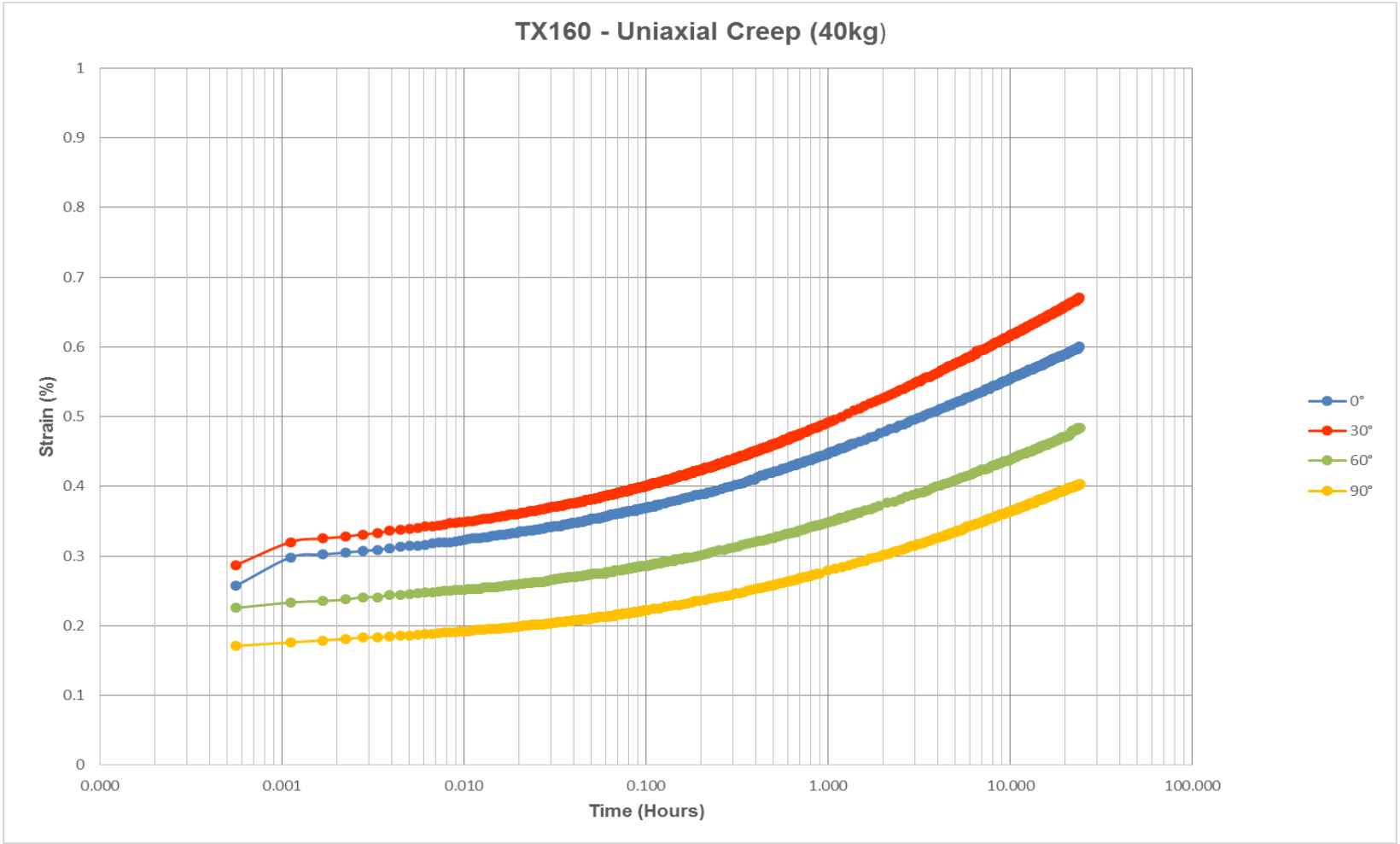


Fig 5.38 – TX160 creep curves in four directions tested uniaxially at 40kg load.

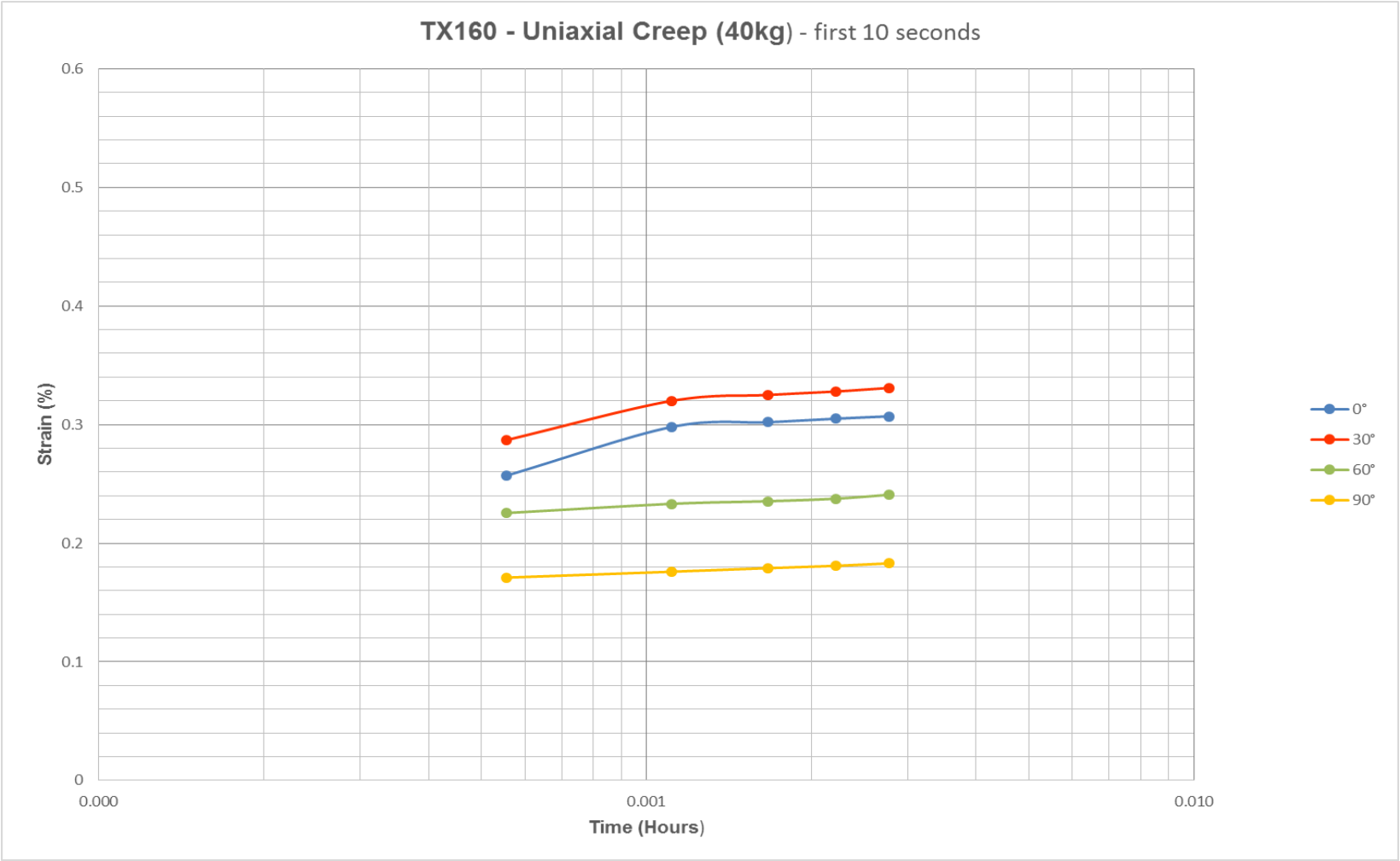


Fig 5.39 – TX160 creep curves of the first 10 seconds, in four directions, tested uniaxially at 40kg load.

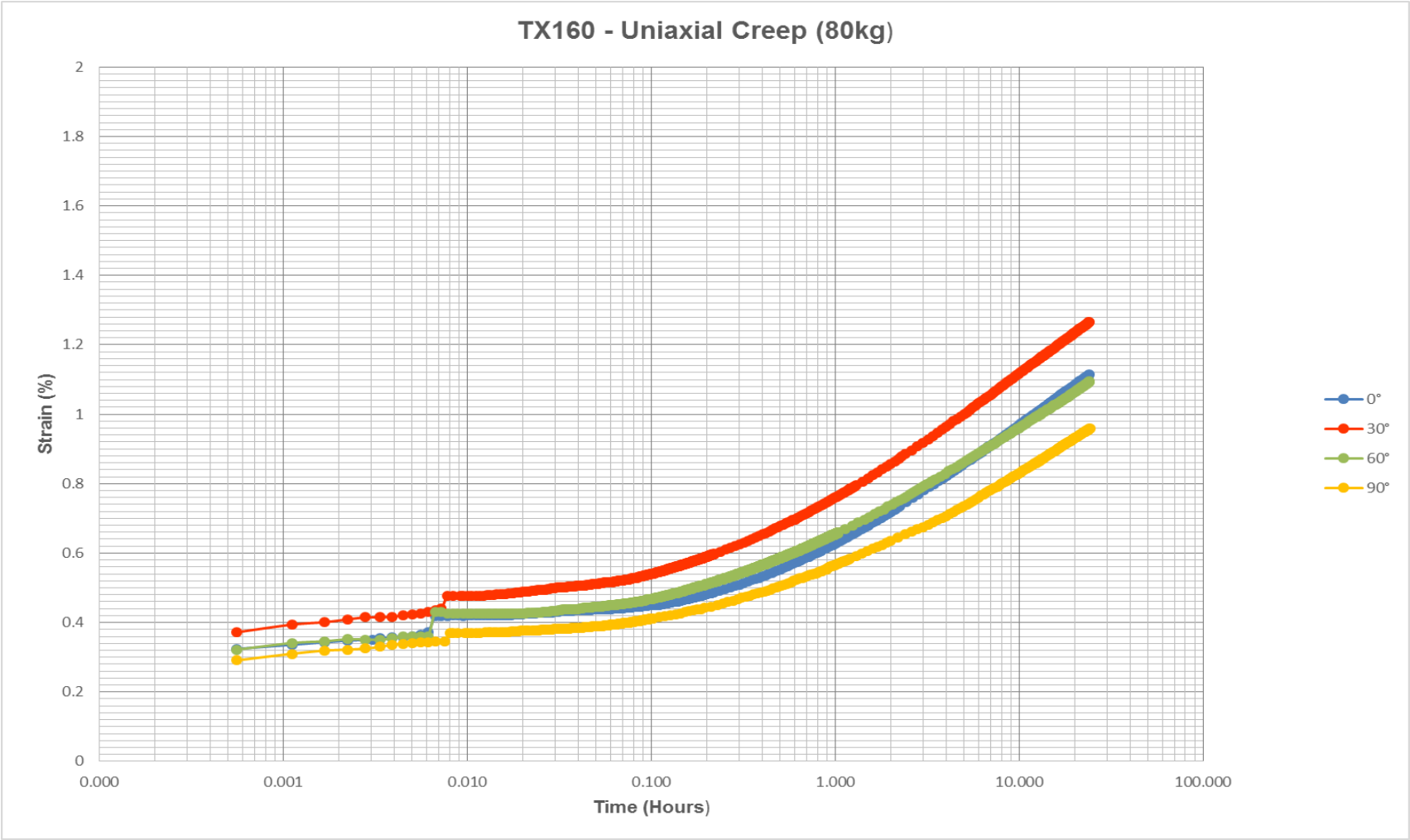


Fig 5.40 – TX160 creep curves in four directions tested uniaxially at 80kg load.



Fig 5.41 – TX160 creep curves of the first 10 seconds, in four directions, tested uniaxially at 80kg load.

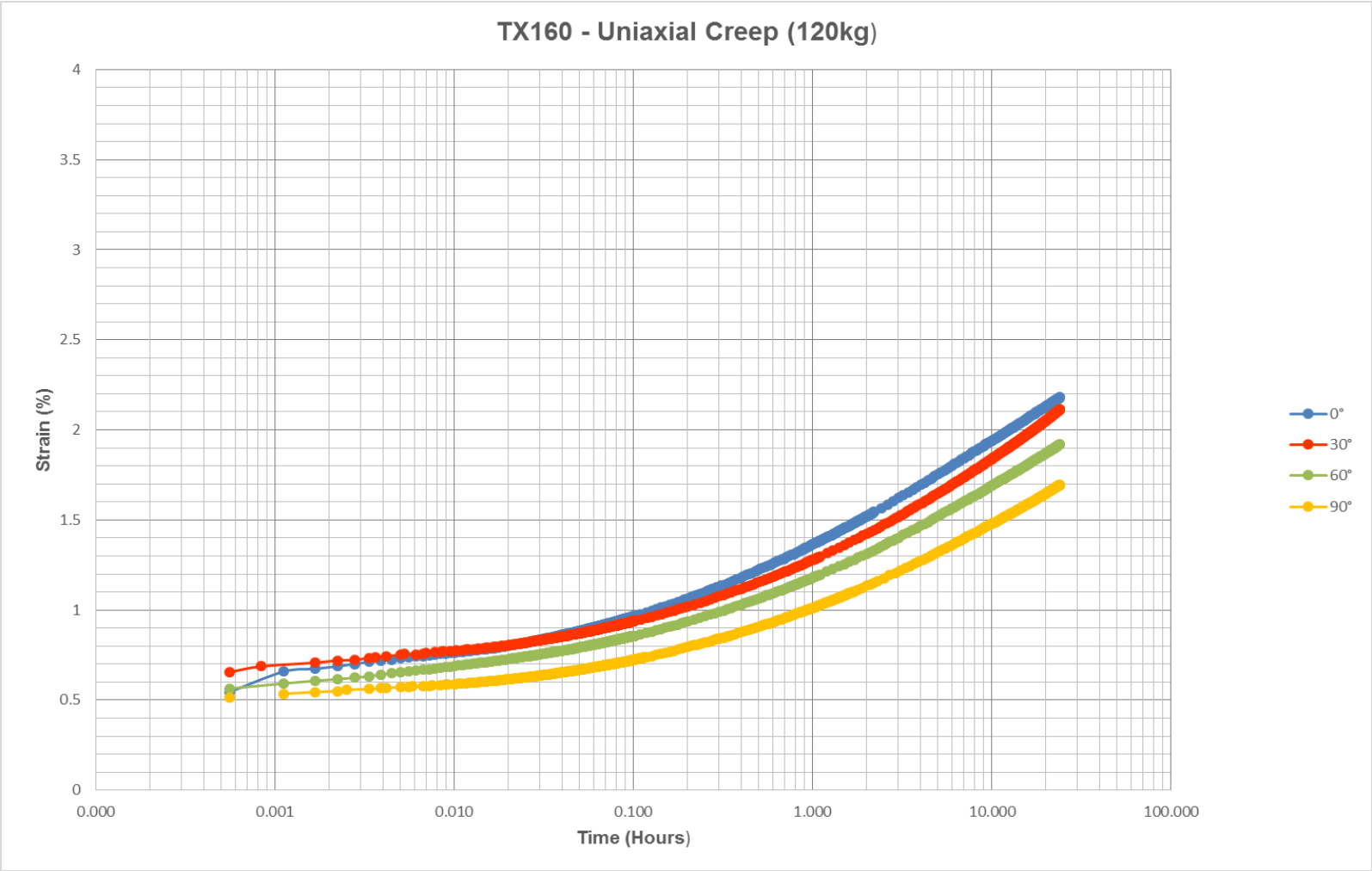


Fig 5.42 – TX160 creep curves in four directions tested uniaxially at 120kg load.

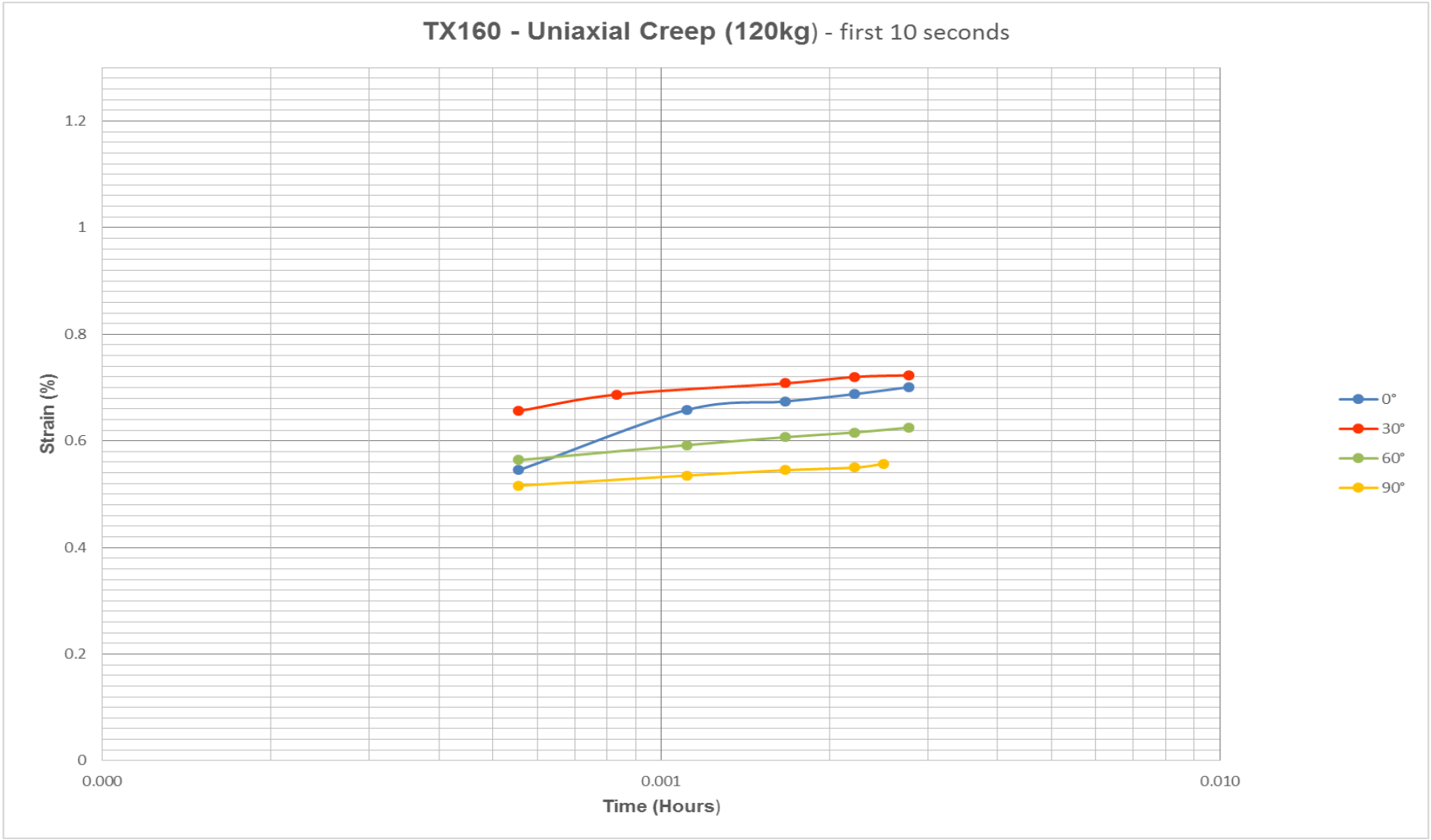


Fig 5.43 – TX160 creep curves of the first 10 seconds, in four directions, tested uniaxially at 120kg load.

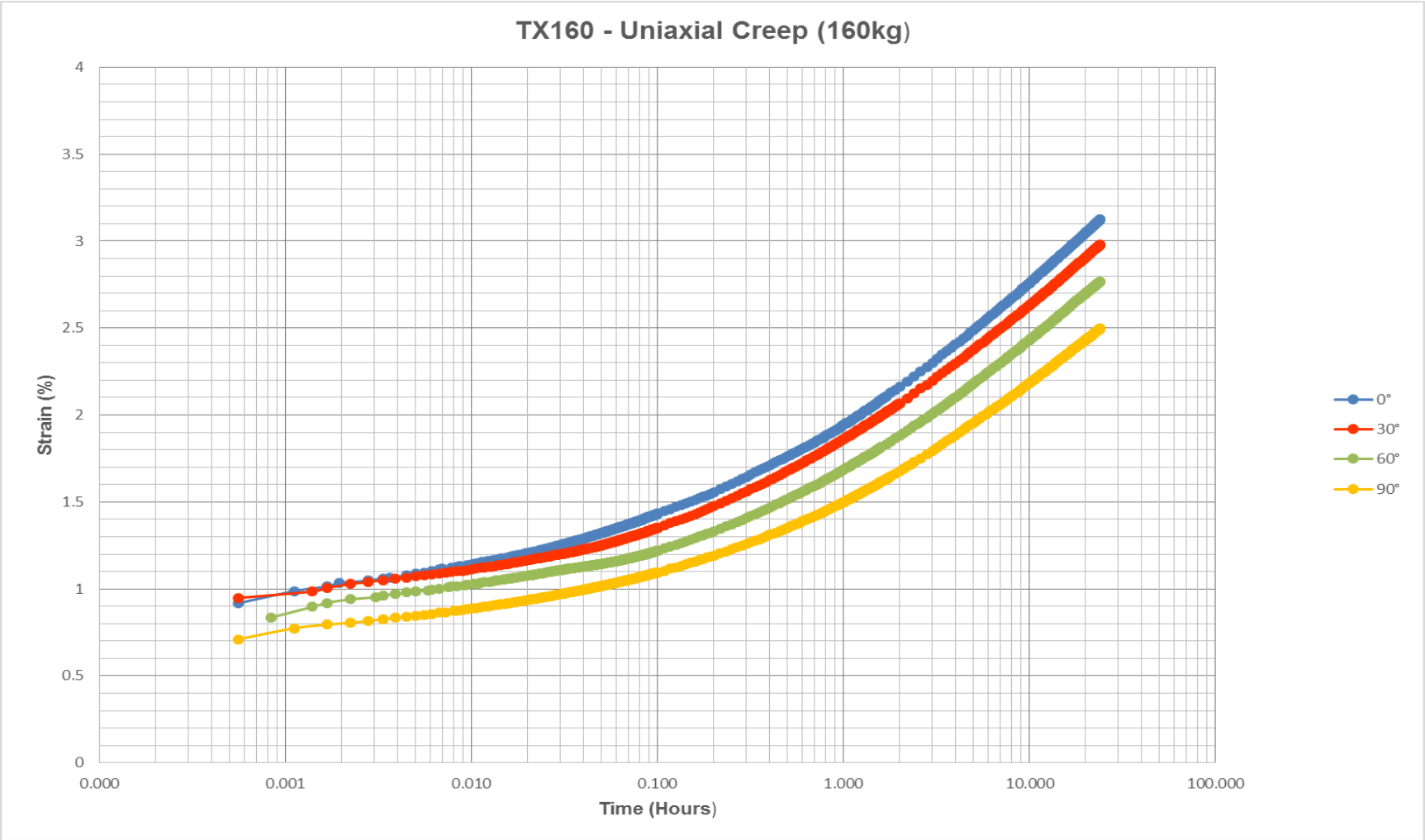
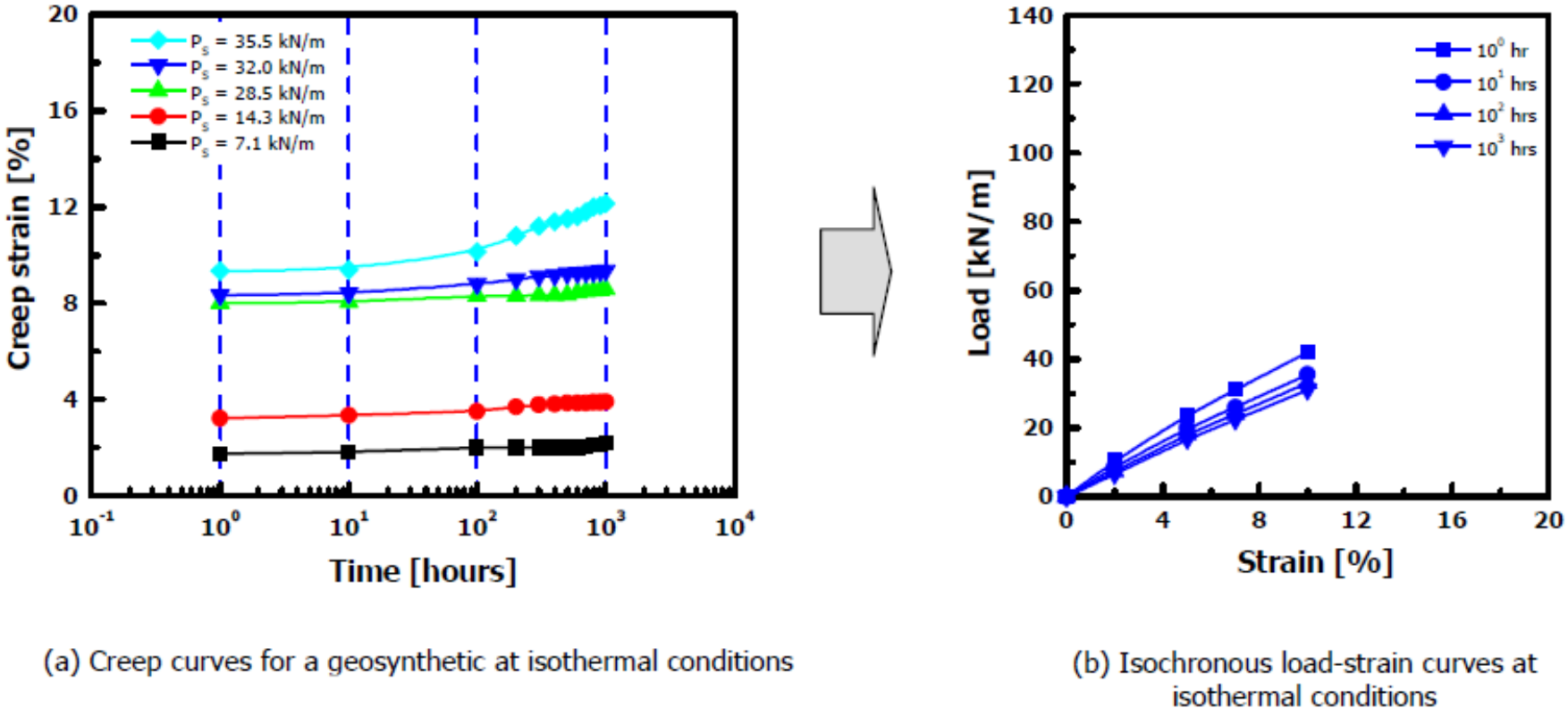


Fig 5.44 – TX160 creep curves in four directions tested uniaxially at 160kg load.



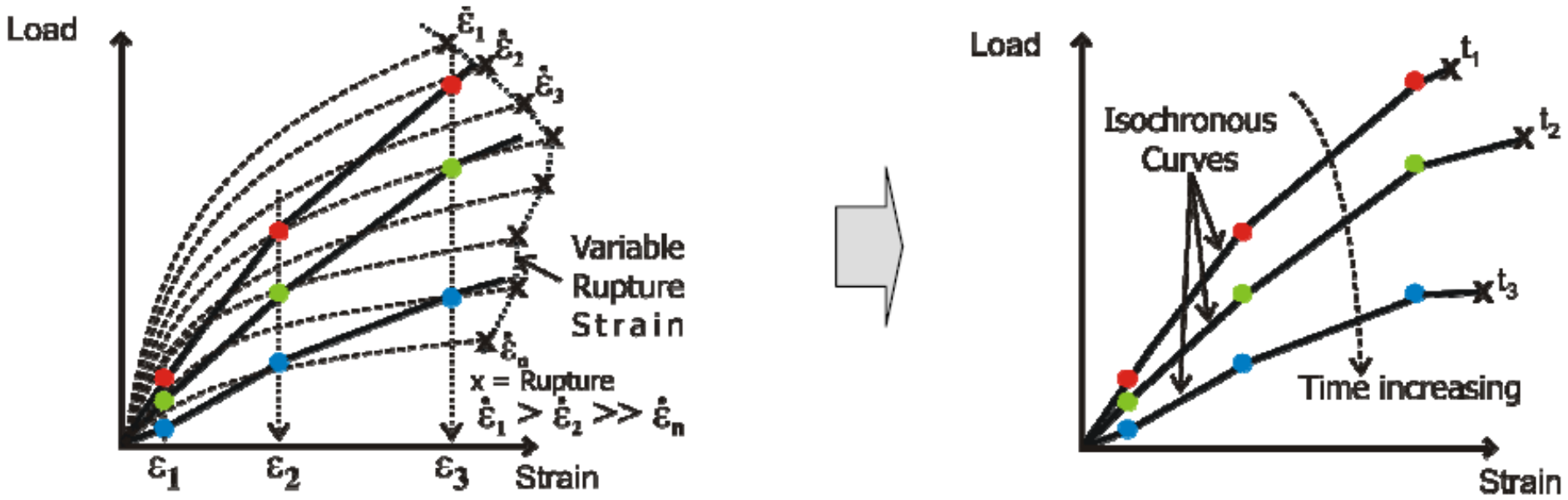
Fig 5.45 – TX160 creep curves of the first 10 seconds, in four directions, tested uniaxially at 160kg load.



(a) Creep curves for a geosynthetic at isothermal conditions

(b) Isochronous load-strain curves at isothermal conditions

Fig 5.46 – Derivation of isochronous load-strain curves from sustained loading test data, after Khan (1999)



(a) Construction of isochronous load-strain curves from CRS test data

(b) Isochronous load-strain curves

Fig 5.47 – Derivation of isochronous load-strain curves from CRS test data, after Kupec (2004)

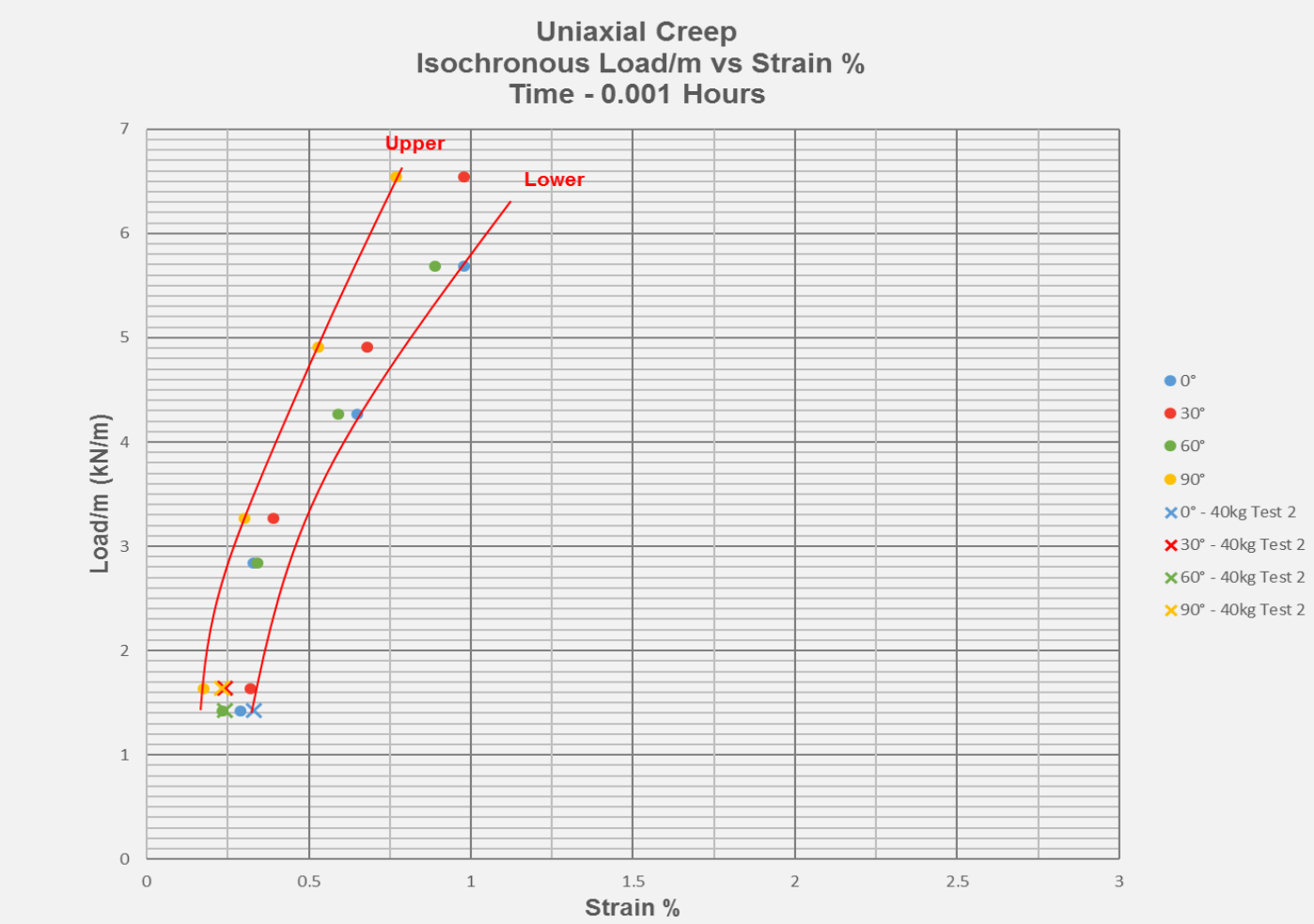


Fig 5.48 – Isochronous Load-Strain curves at 0.001 hours of TX160 creep data, tested in four directions.

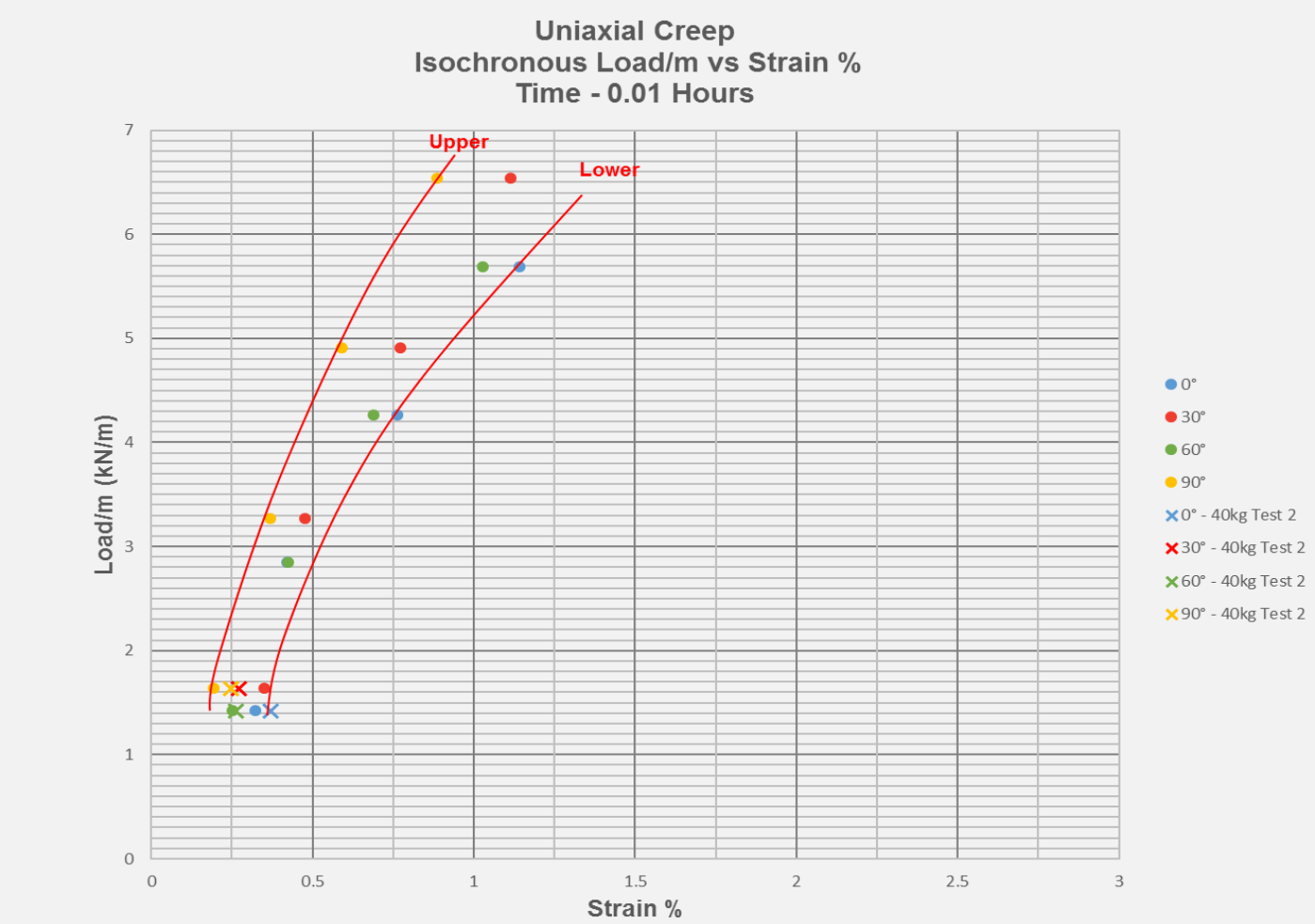


Fig 5.49 – Isochronous Load-Strain curves at 0.01 hours of TX160 creep data, tested in four directions.

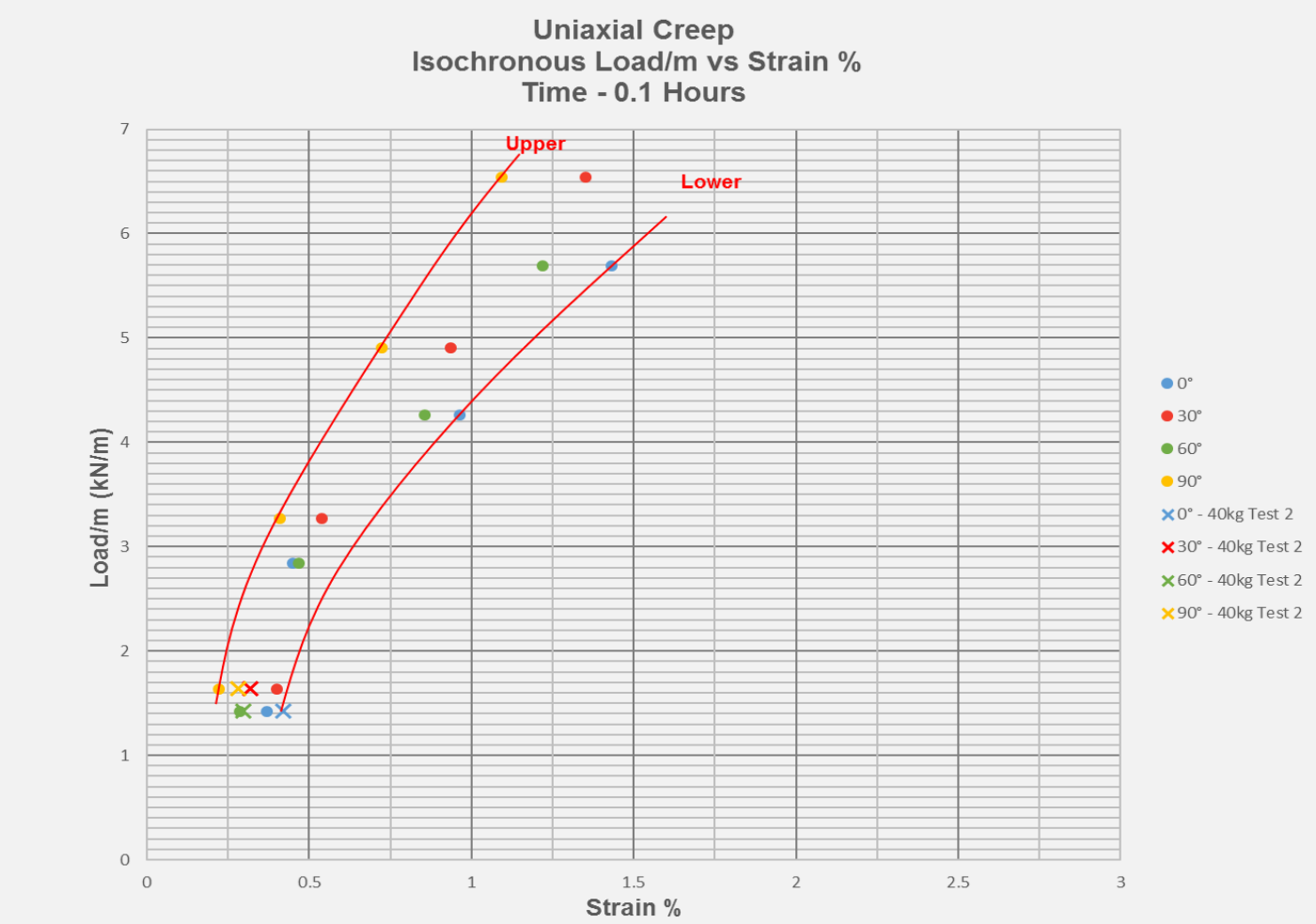


Fig 5.50 – Isochronous Load-Strain curves at 0.1 hours of TX160 creep data, tested in four directions.

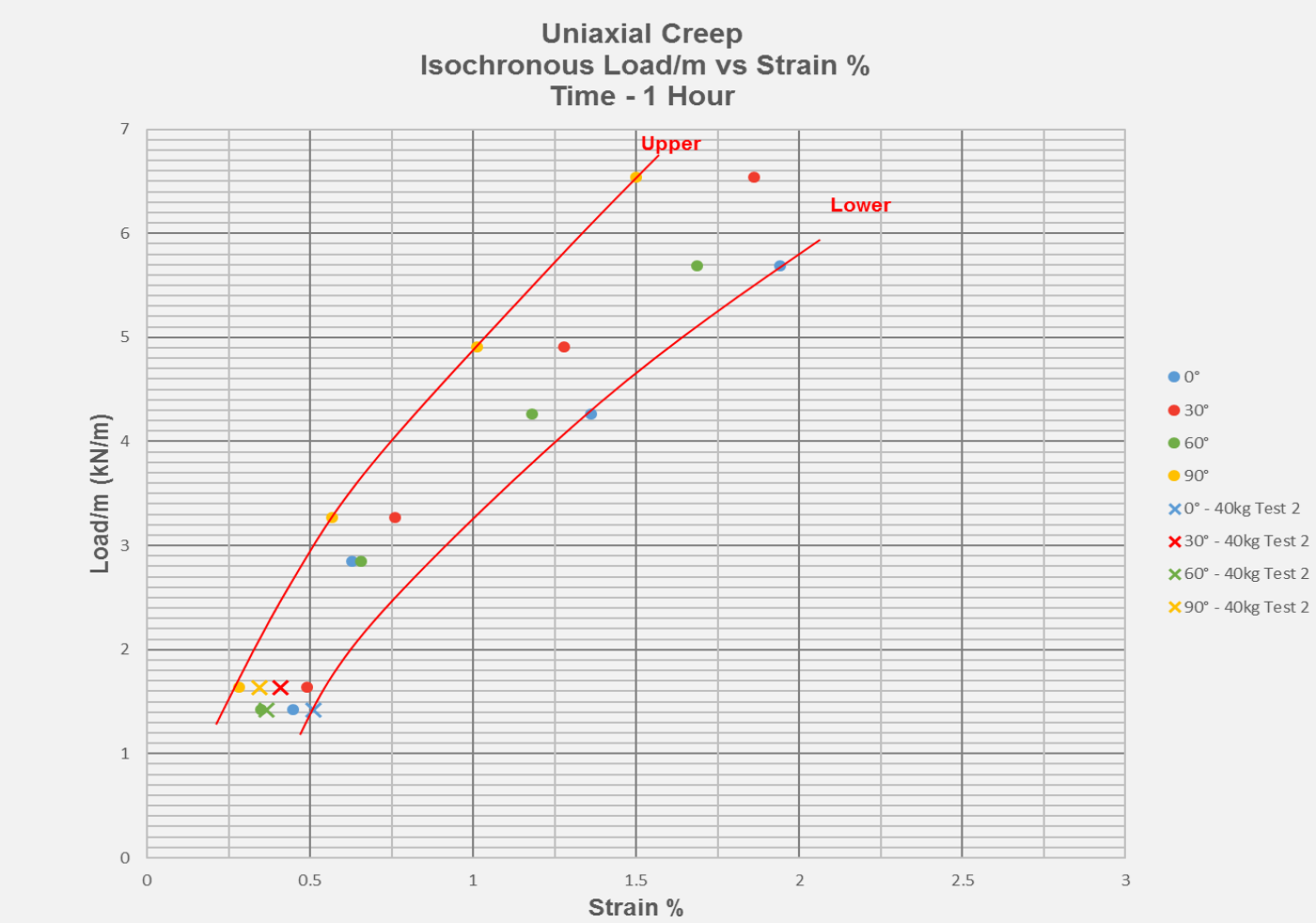


Fig 5.51 – Isochronous Load-Strain curves at 1 hour of TX160 creep data, tested in four directions.

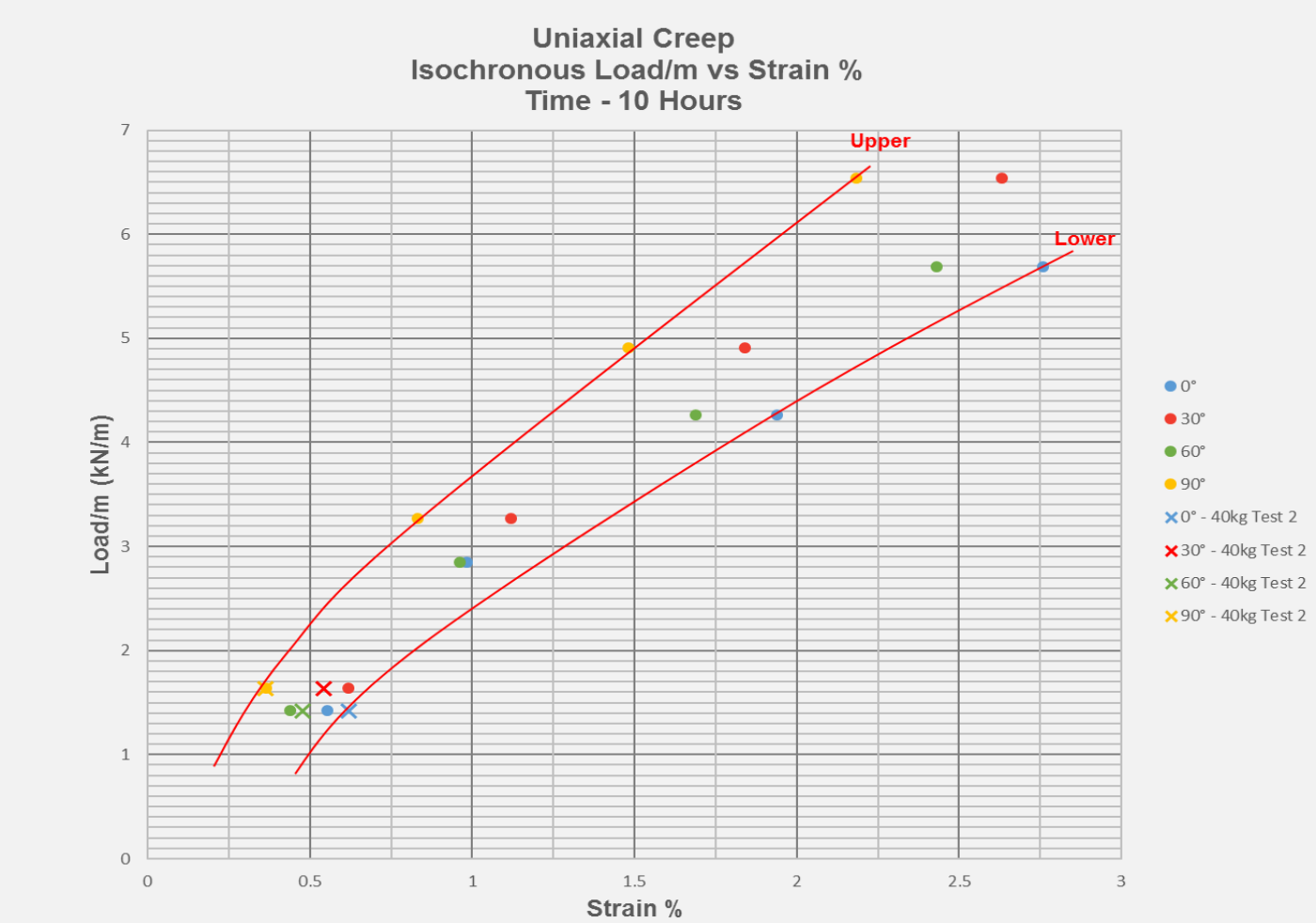


Fig 5.52 – Isochronous Load-Strain curves at 10 hours of TX160 creep data, tested in four directions.

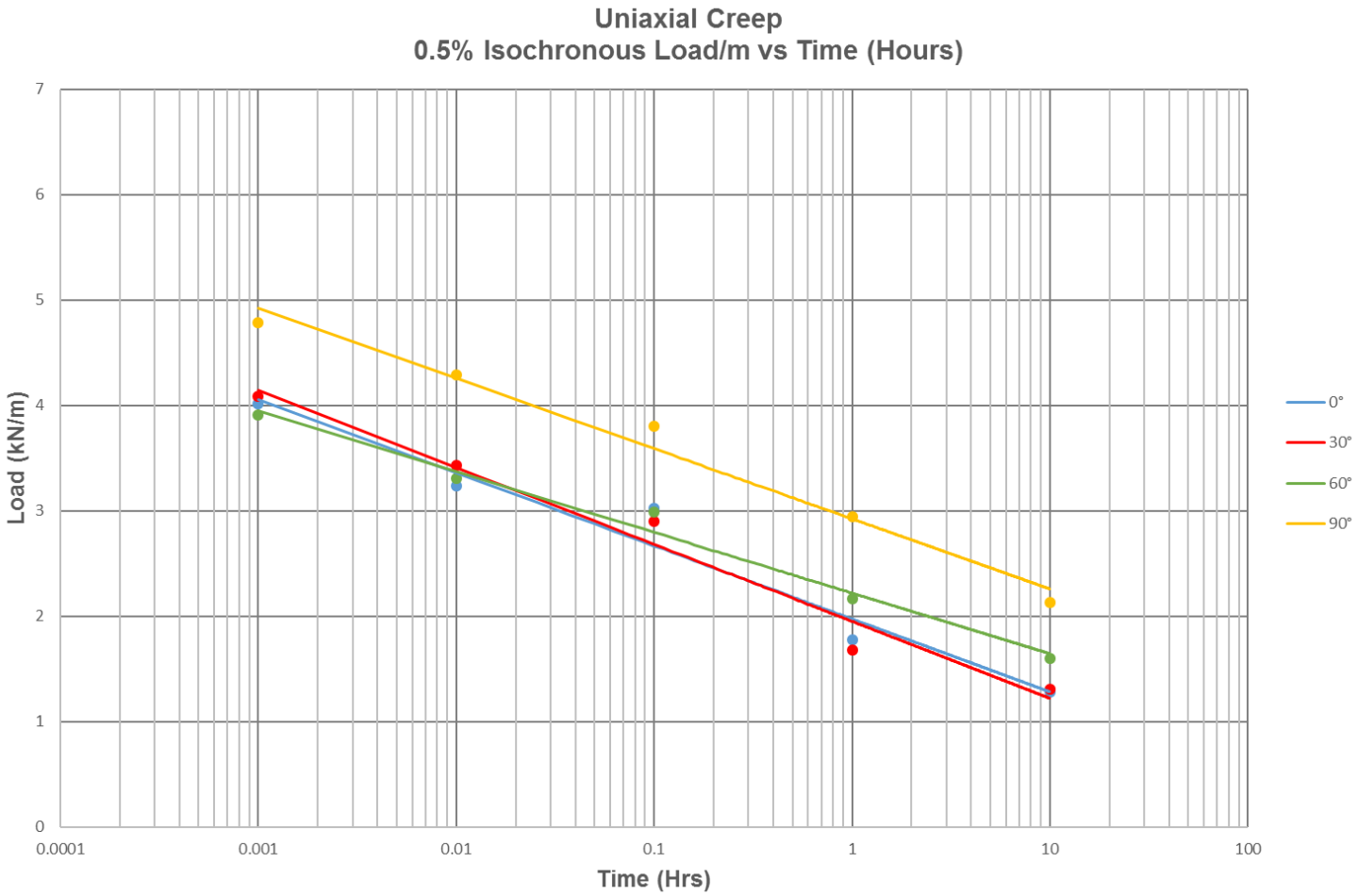


Fig 5.53 – 0.5% isochronous load versus time (best fit data) of TX160 (Batch Ref: 056218) creep data, tested in four directions.

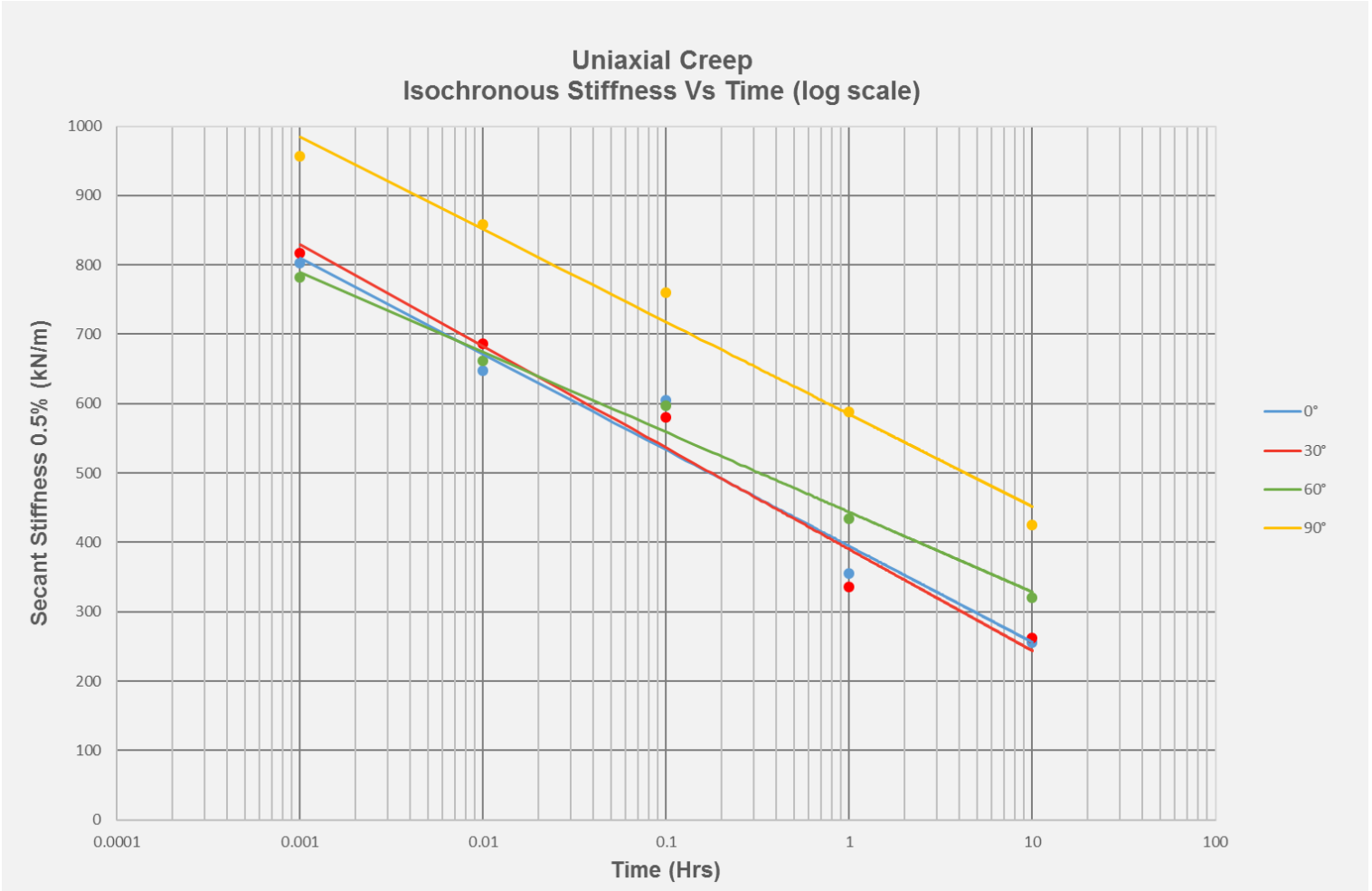


Fig 5.54 – 0.5% isochronous stiffness versus time (best fit data) of TX160 creep data, tested in four directions.

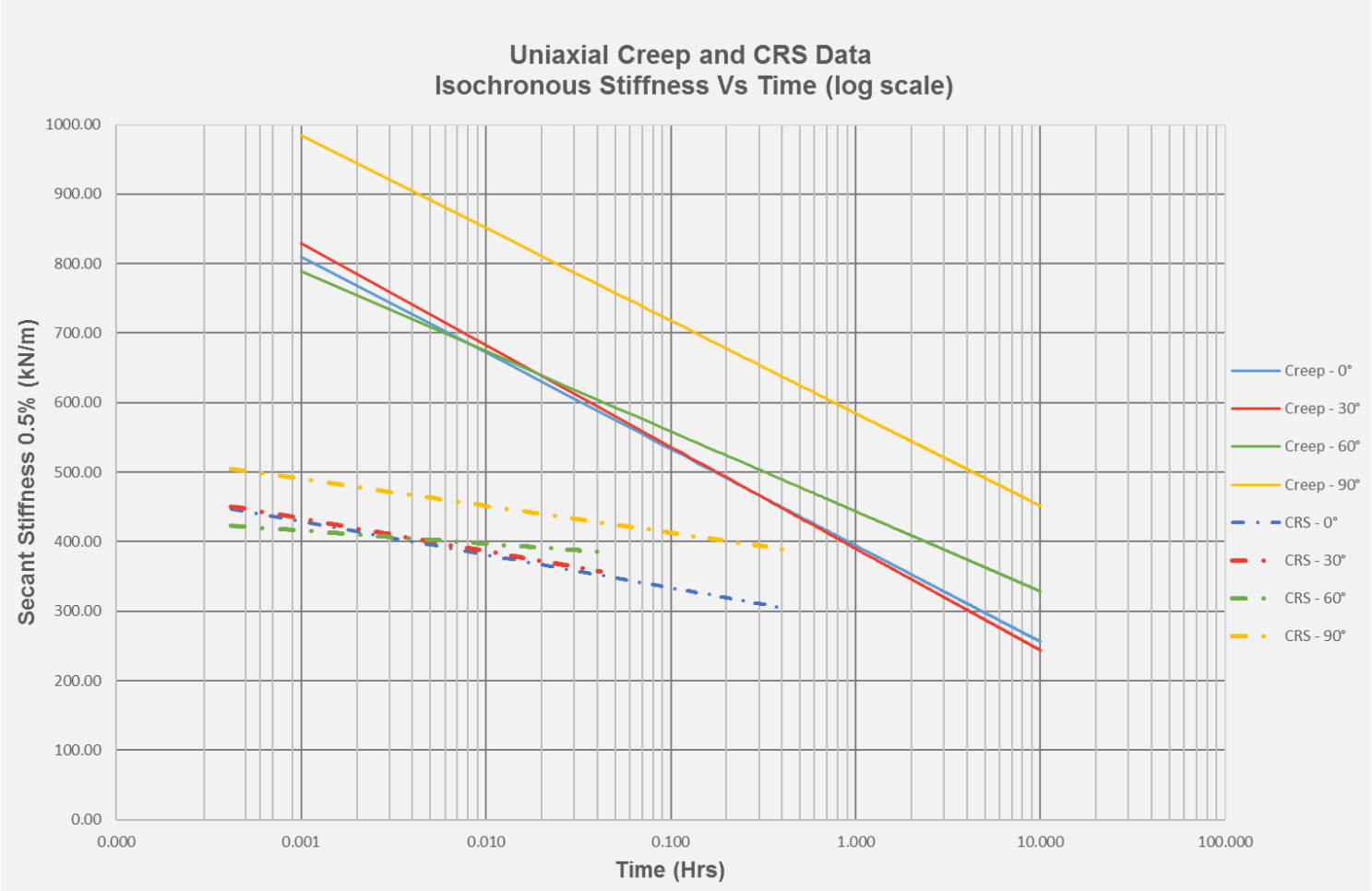


Fig 5.55 – 0.5% isochronous stiffness versus time (best fit data) of TX160 creep and CRS data tested in four directions.

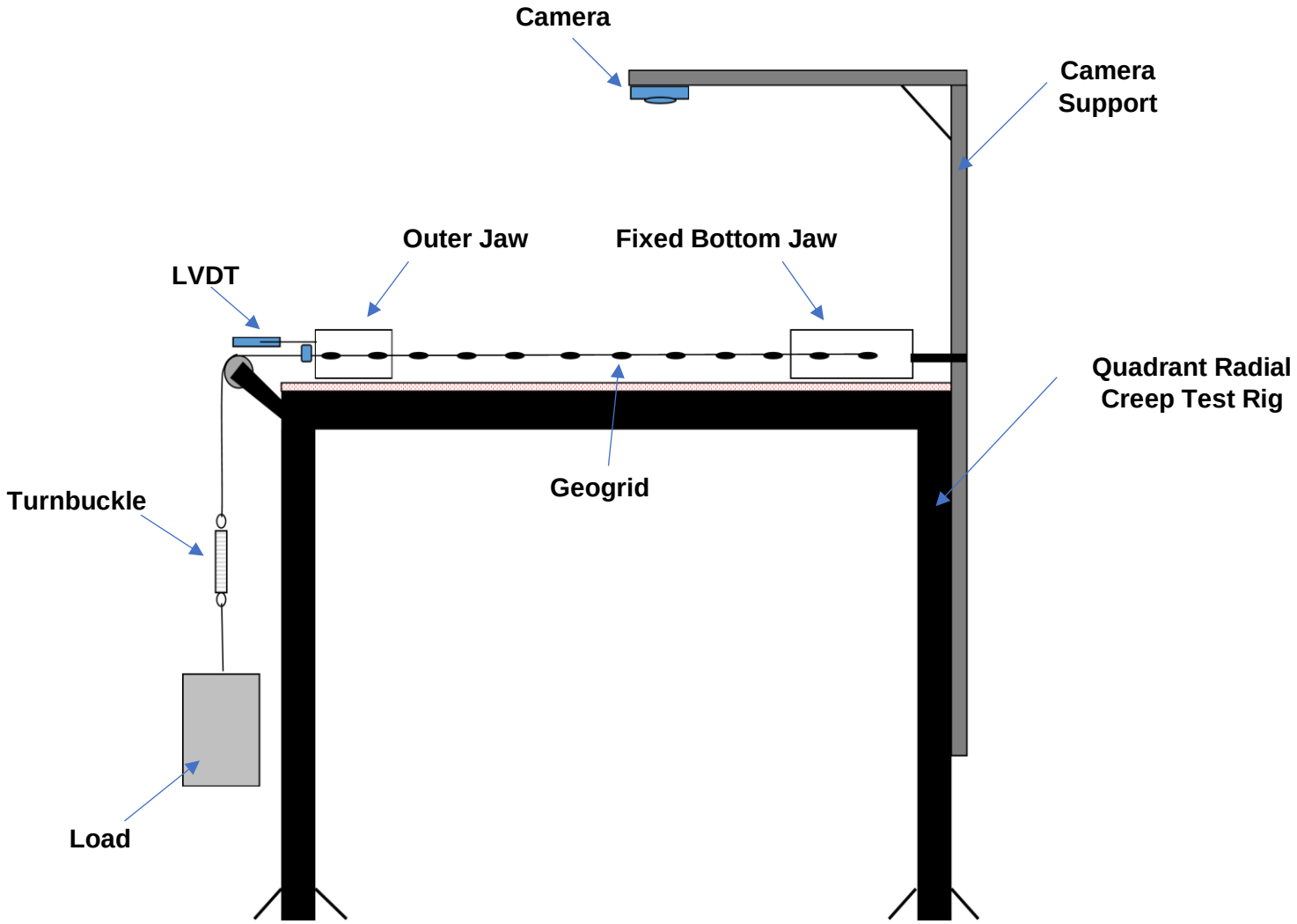


Fig 6.1 – Quadrant radial creep testing apparatus

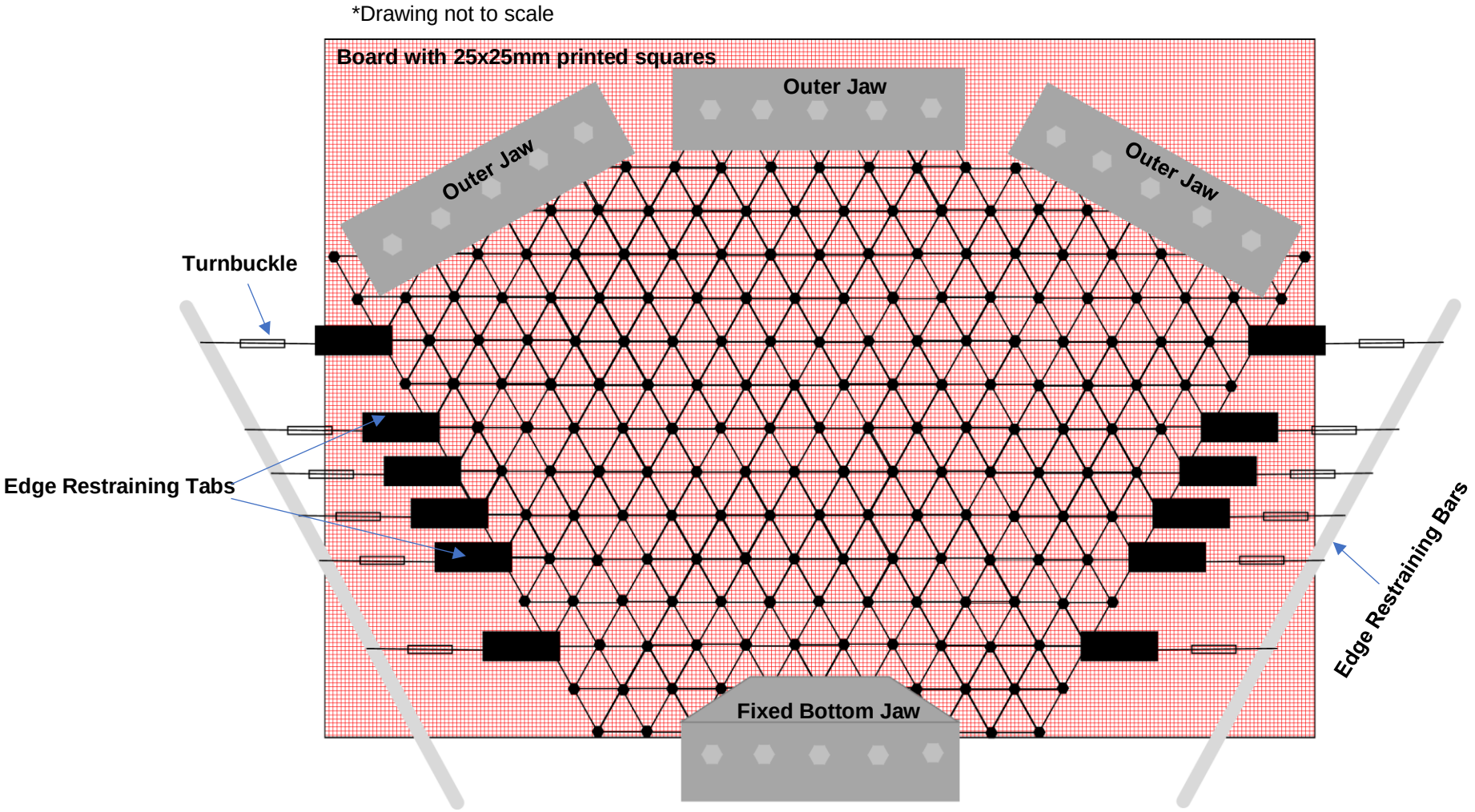


Fig 6.2 – Birds-eye-view of quadrant radial creep testing apparatus and specimen (0° & 60° Direction)

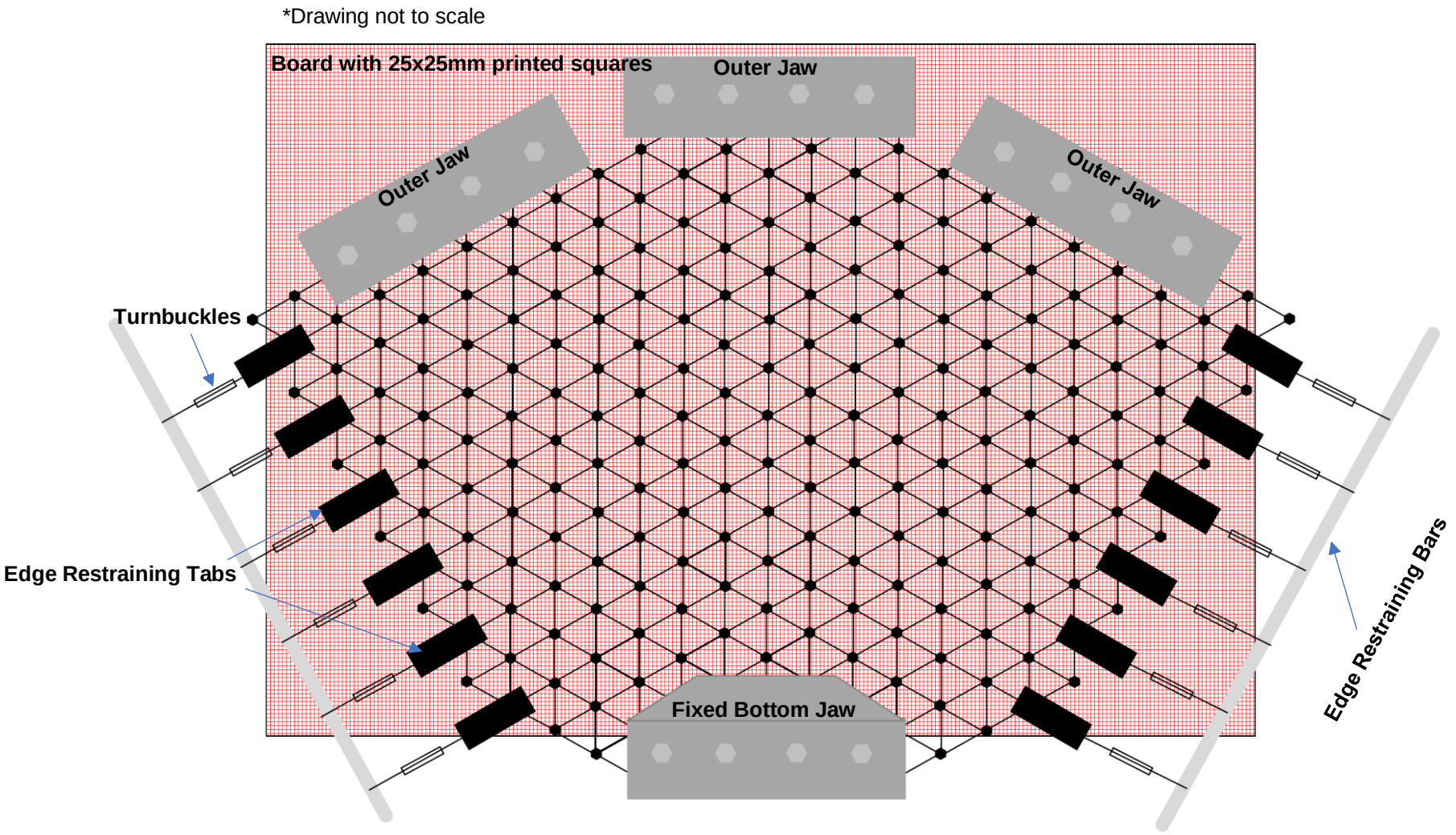


Fig 6.3 – Birds-eye-view of quadrant radial creep testing apparatus and specimen (30° & 90° Direction)

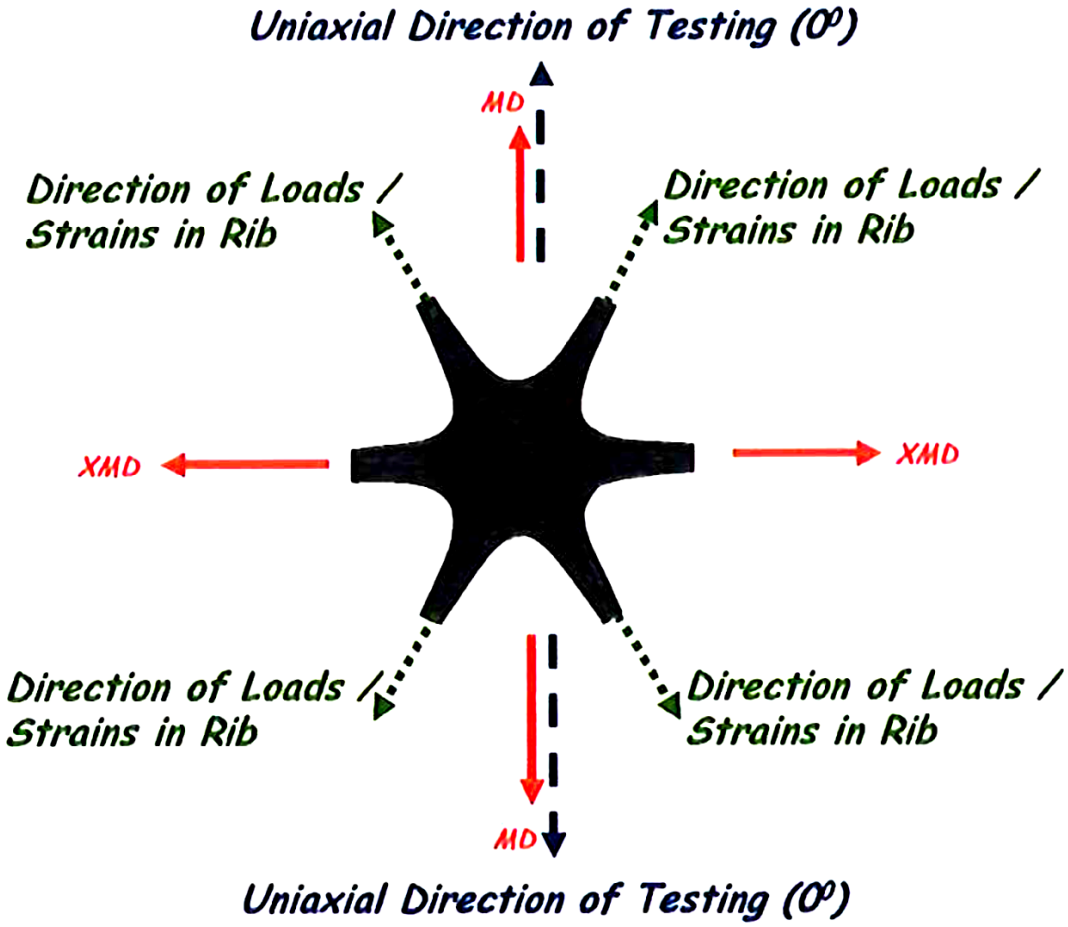


Fig 6.4 – Direction of load/strain in the ribs when tested in the 0° direction.

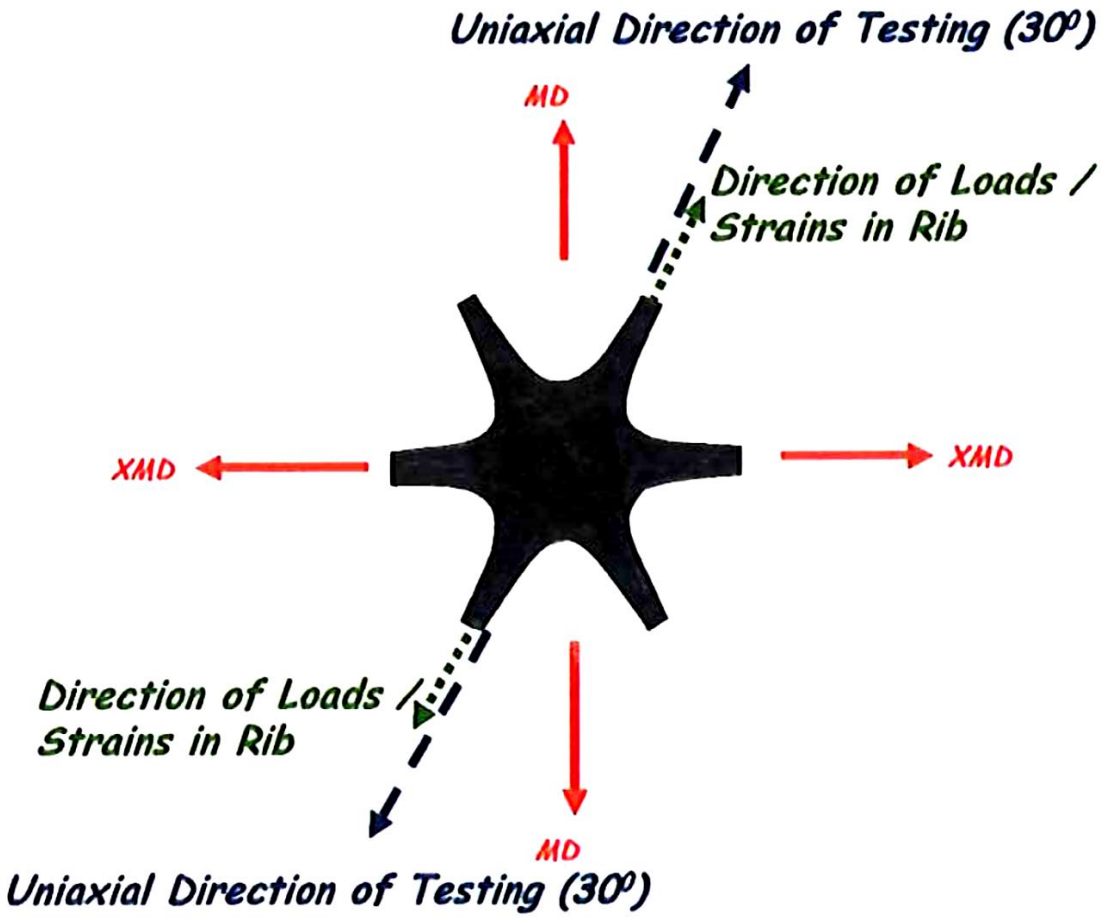


Fig 6.5 – Direction of load/strain in the ribs when tested in the 30° direction.

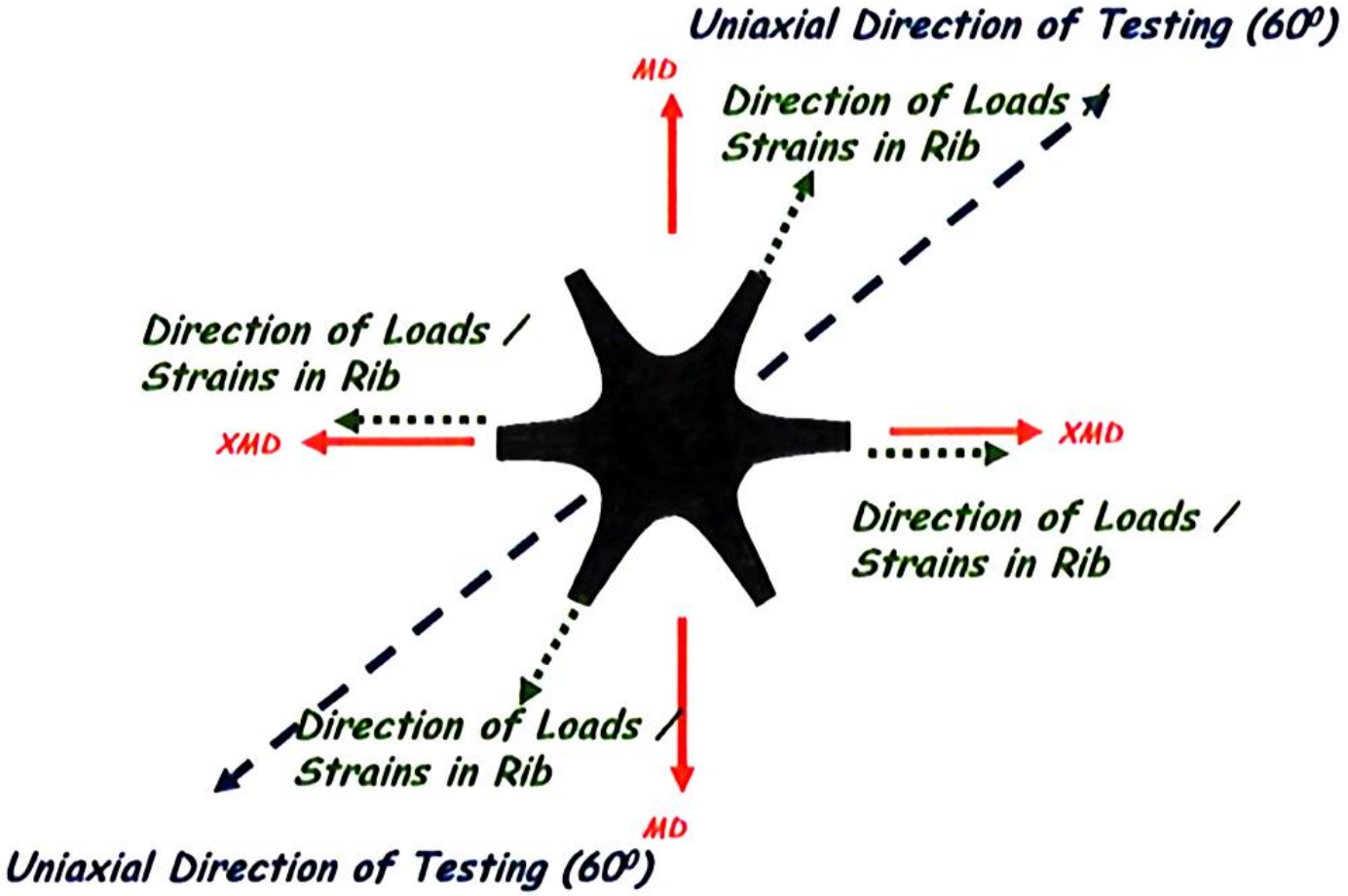


Fig 6.6 – Direction of load/strain in the ribs when tested in the 60° direction.

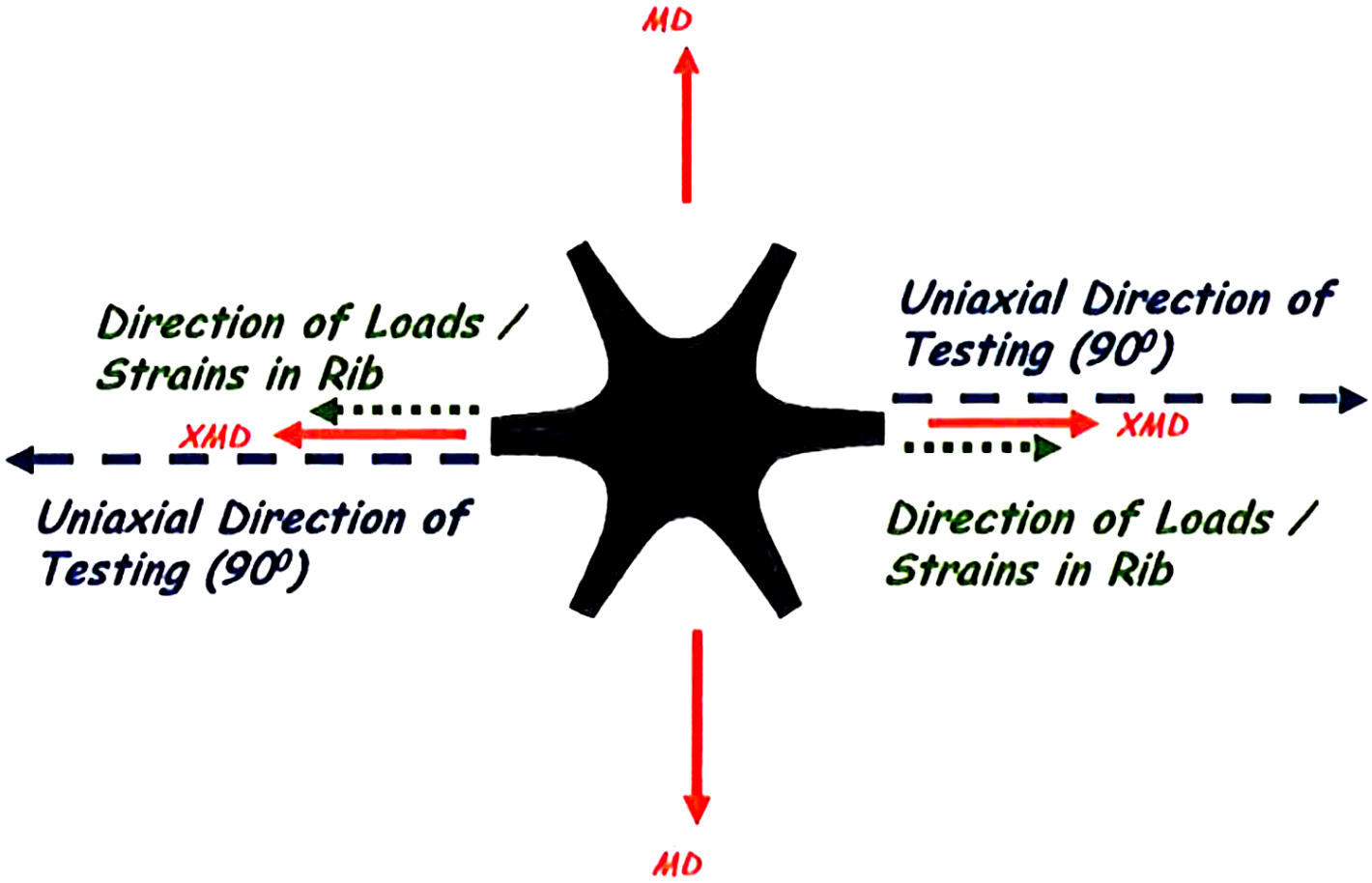


Fig 6.7 – Direction of load/strain in the ribs when tested in the 90° direction.

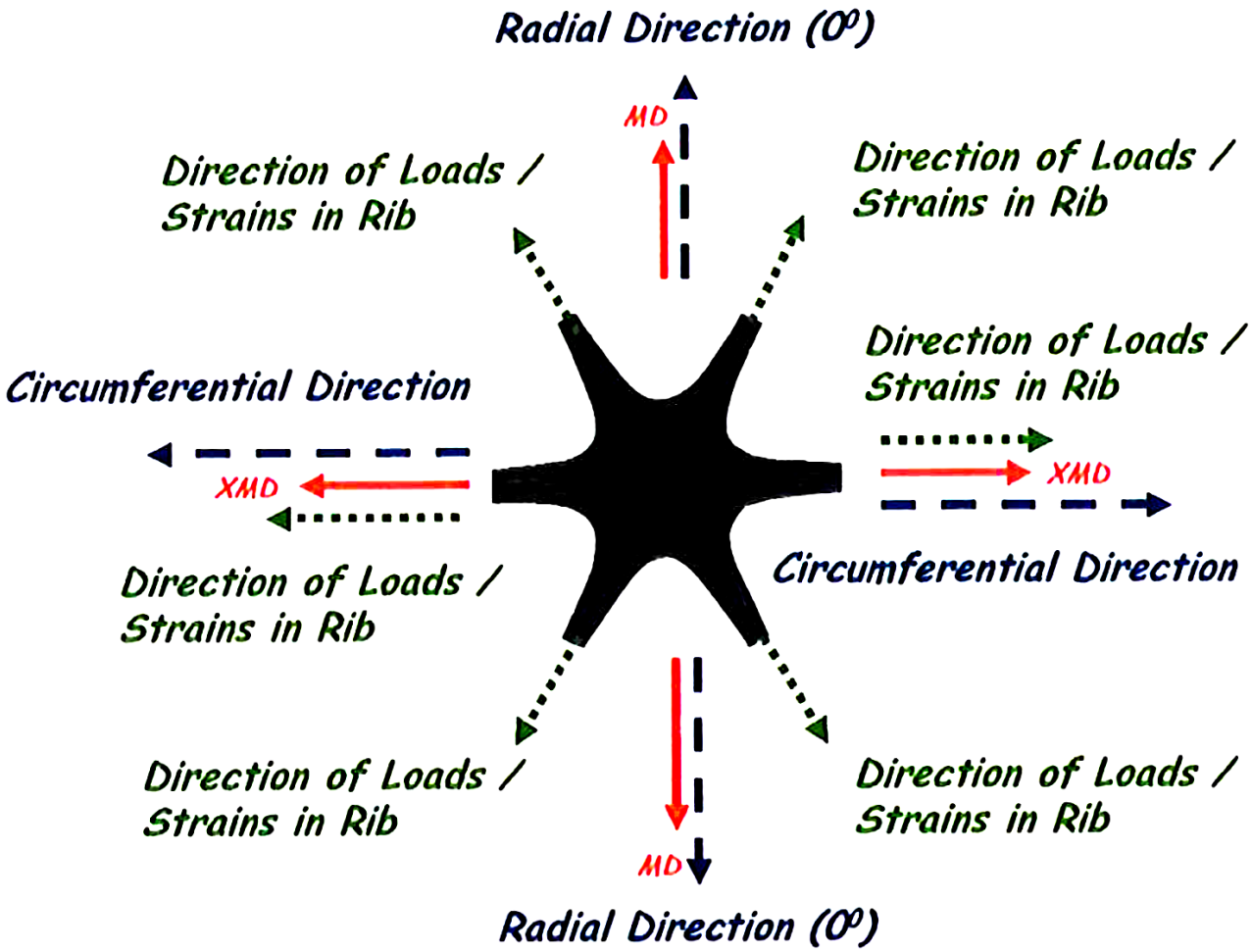


Fig 6.8 – Direction of load/strain in the ribs when tested radially in the 0° direction.

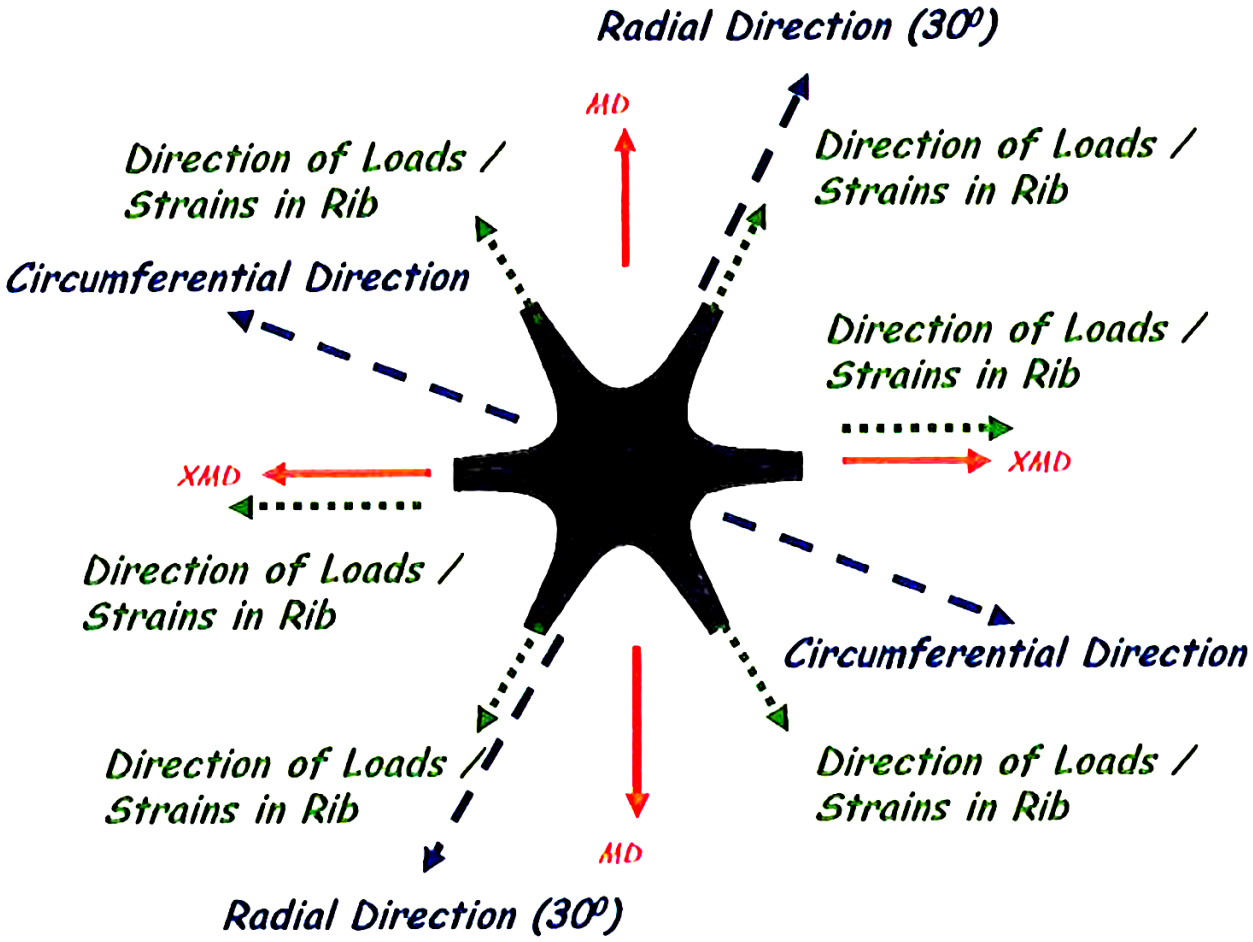


Fig 6.9 – Direction of load/strain in the ribs when tested radially in the 30° direction.

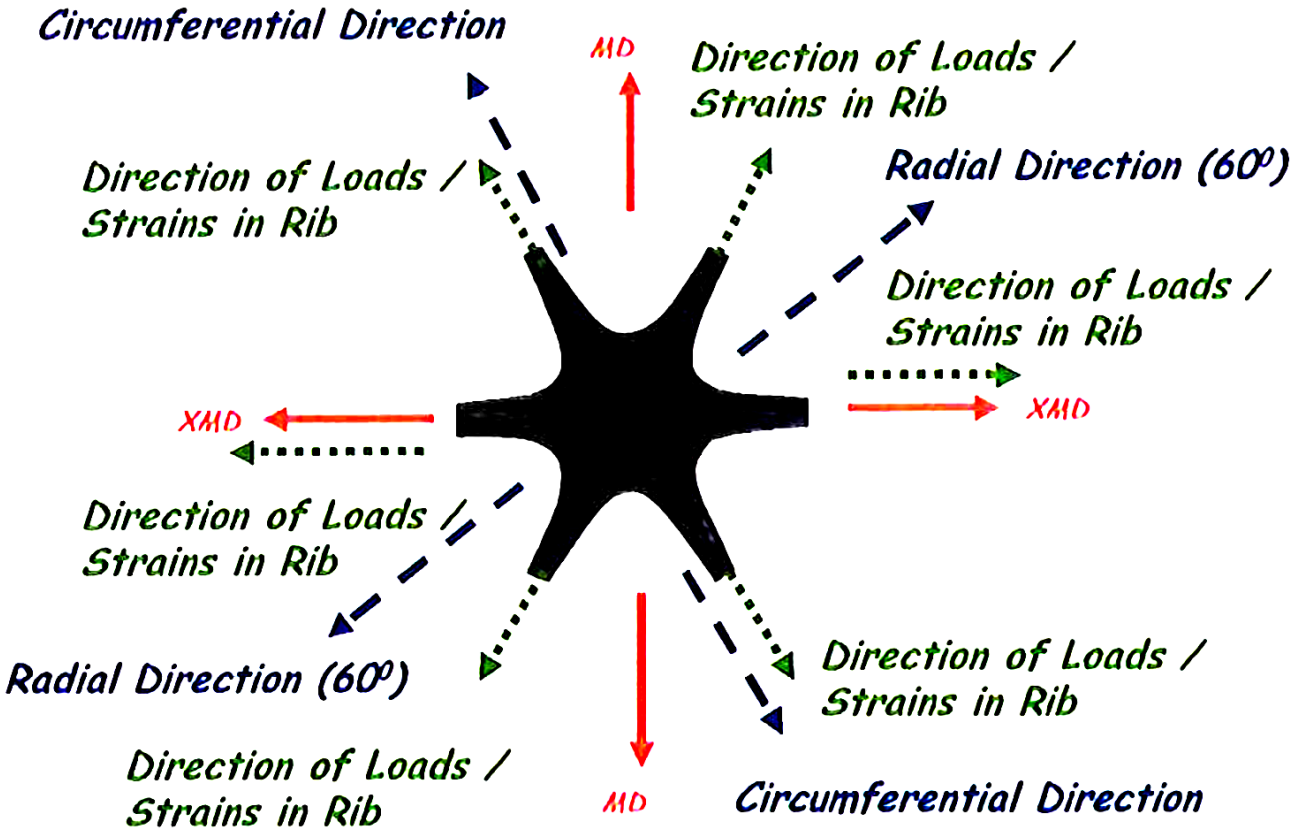


Fig 6.10 – Direction of load/strain in the ribs when tested radially in the 60° direction.

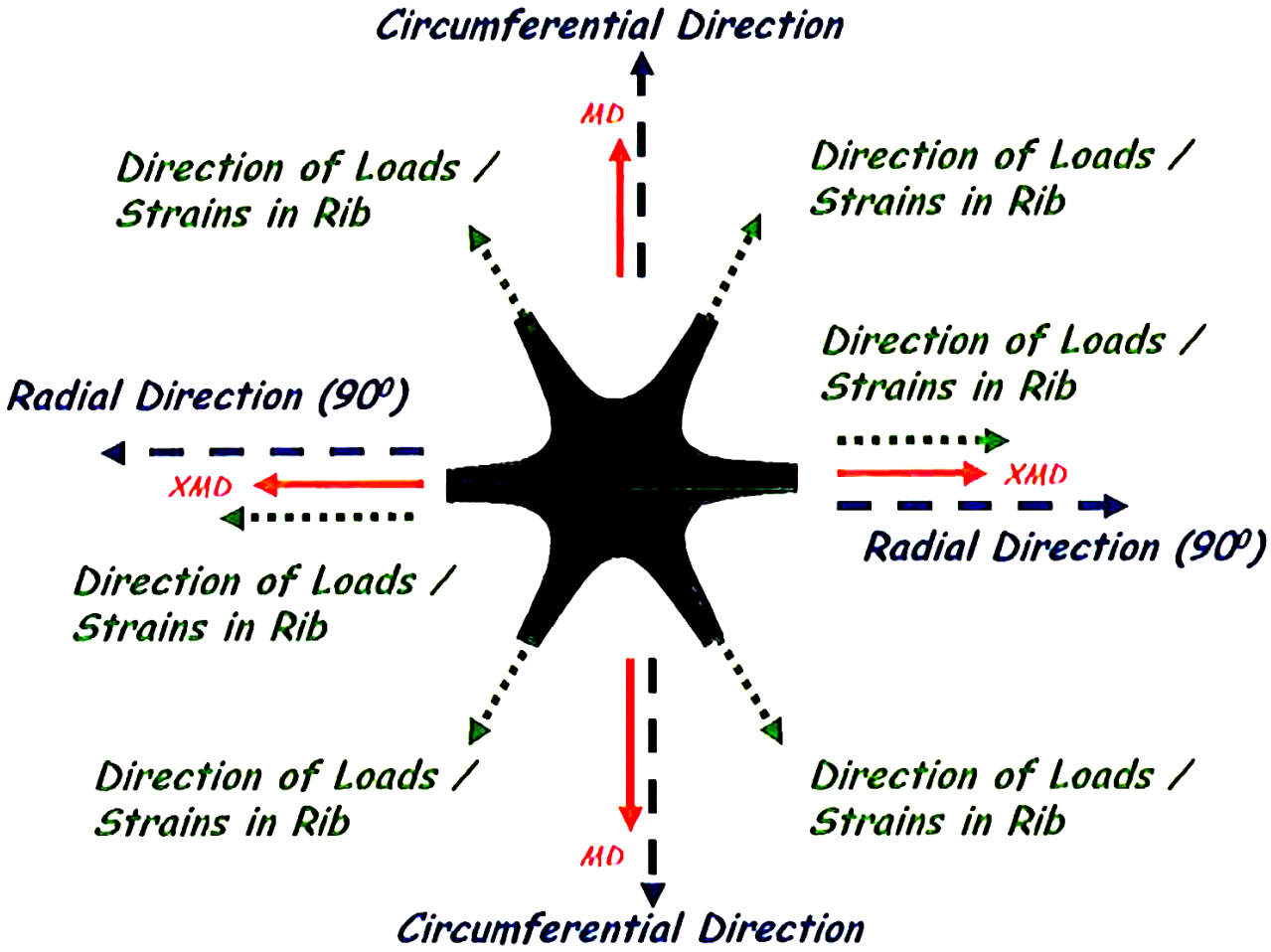


Fig 6.11 – Direction of load/strain in the ribs when tested radially in the 90° direction.

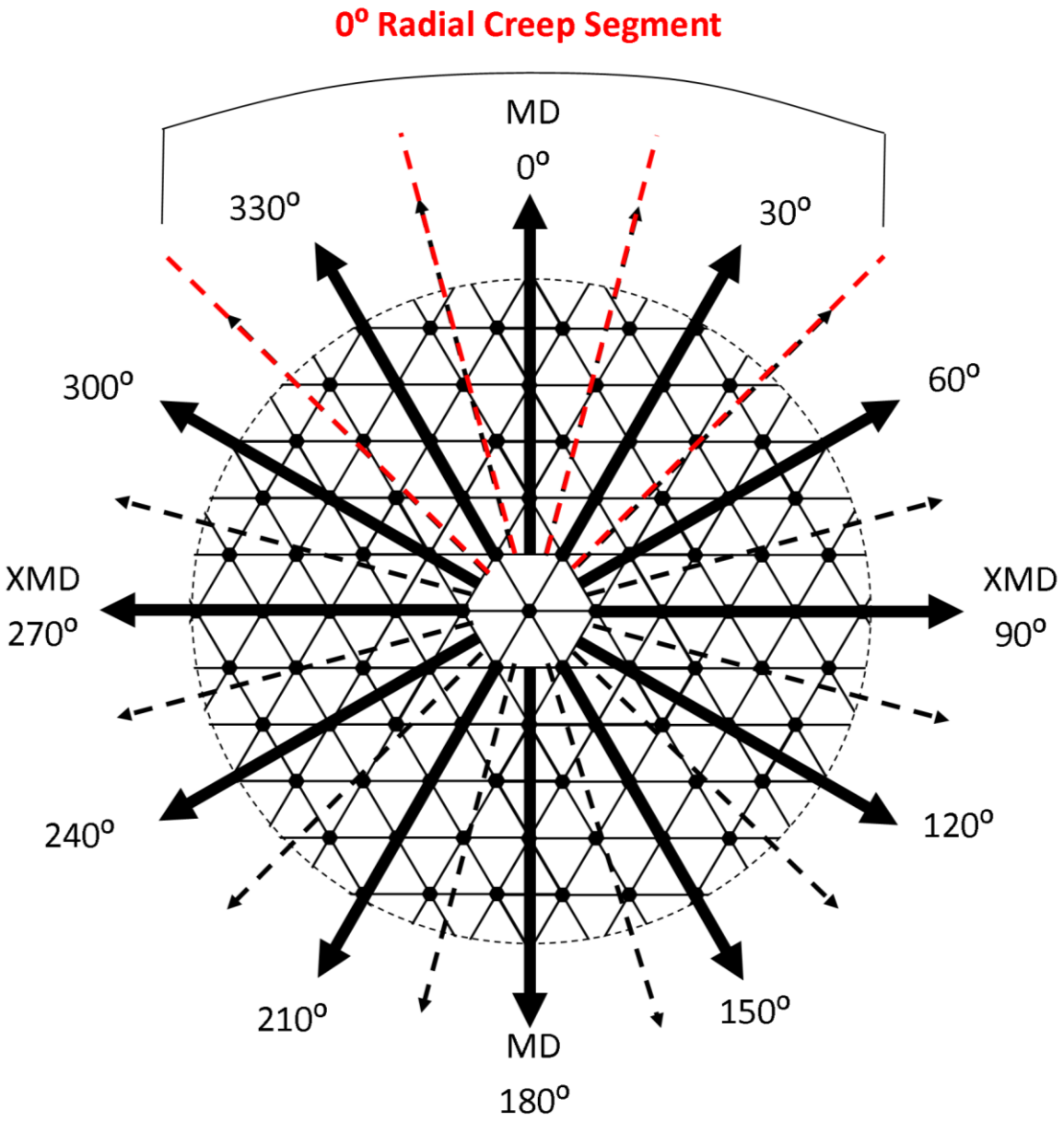


Fig 6.12 – 0° Radial creep specimen

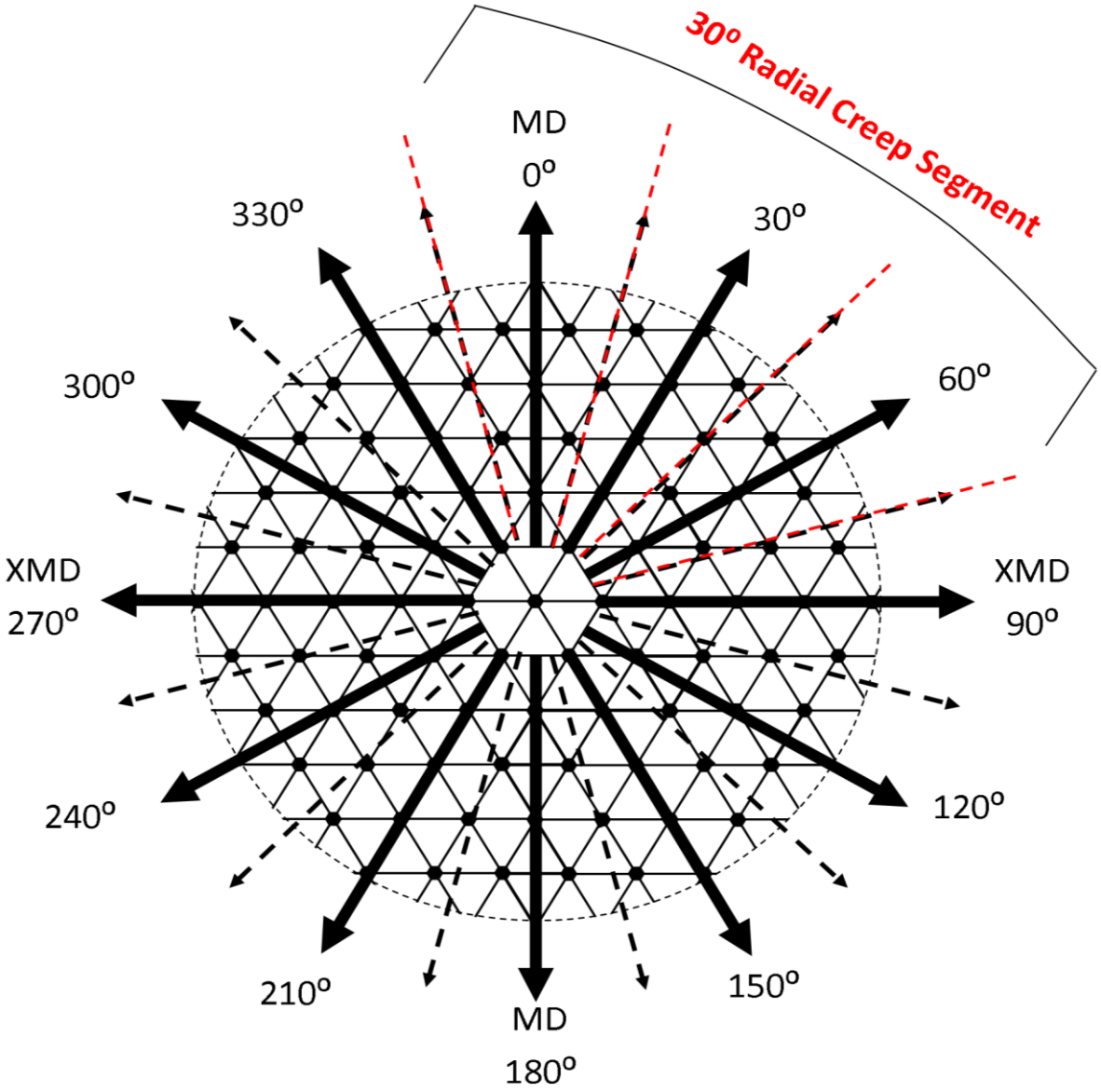


Fig 6.13 – 30° Radial creep specimen

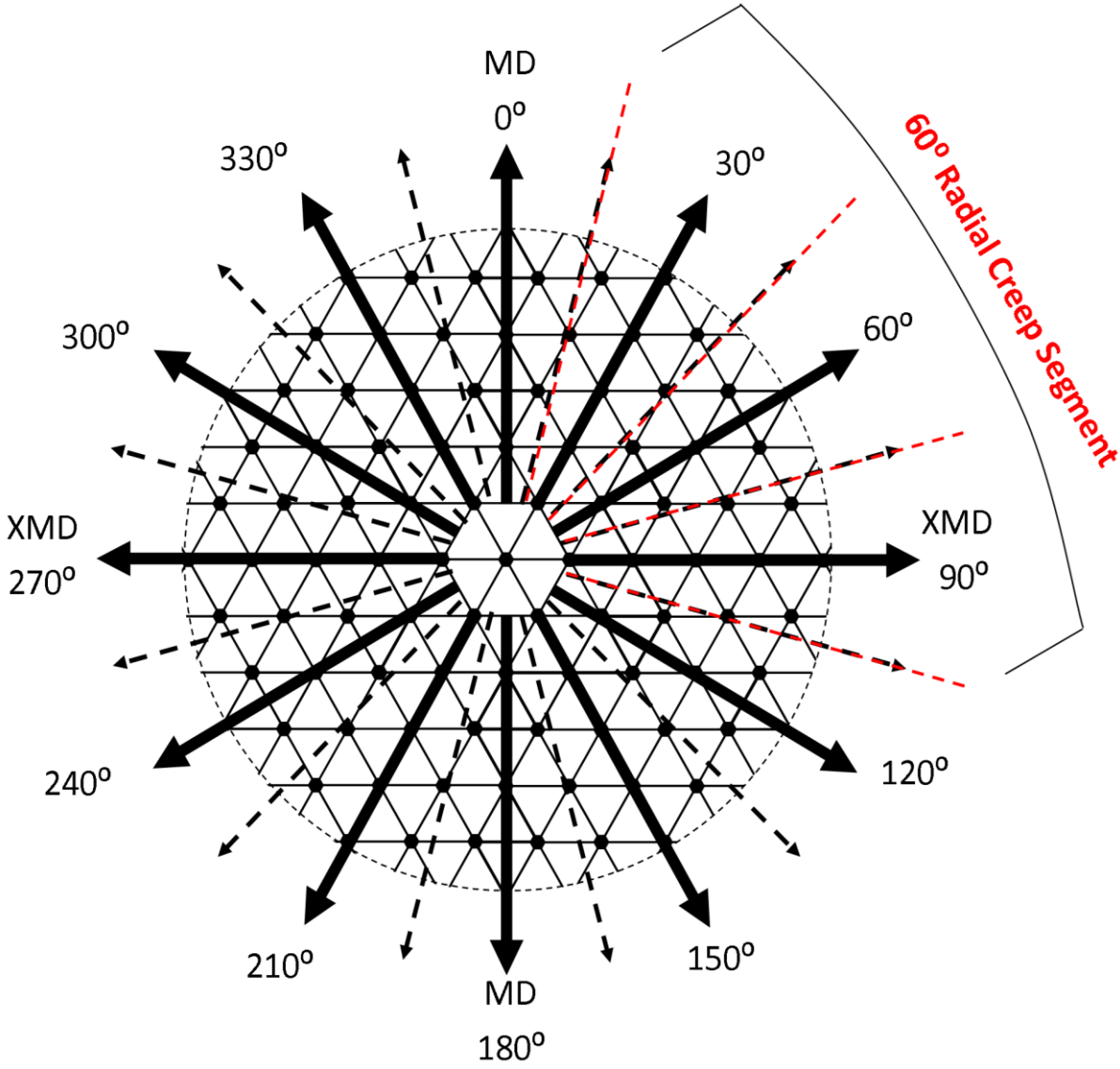


Fig 6.14 – 60° Radial creep specimen

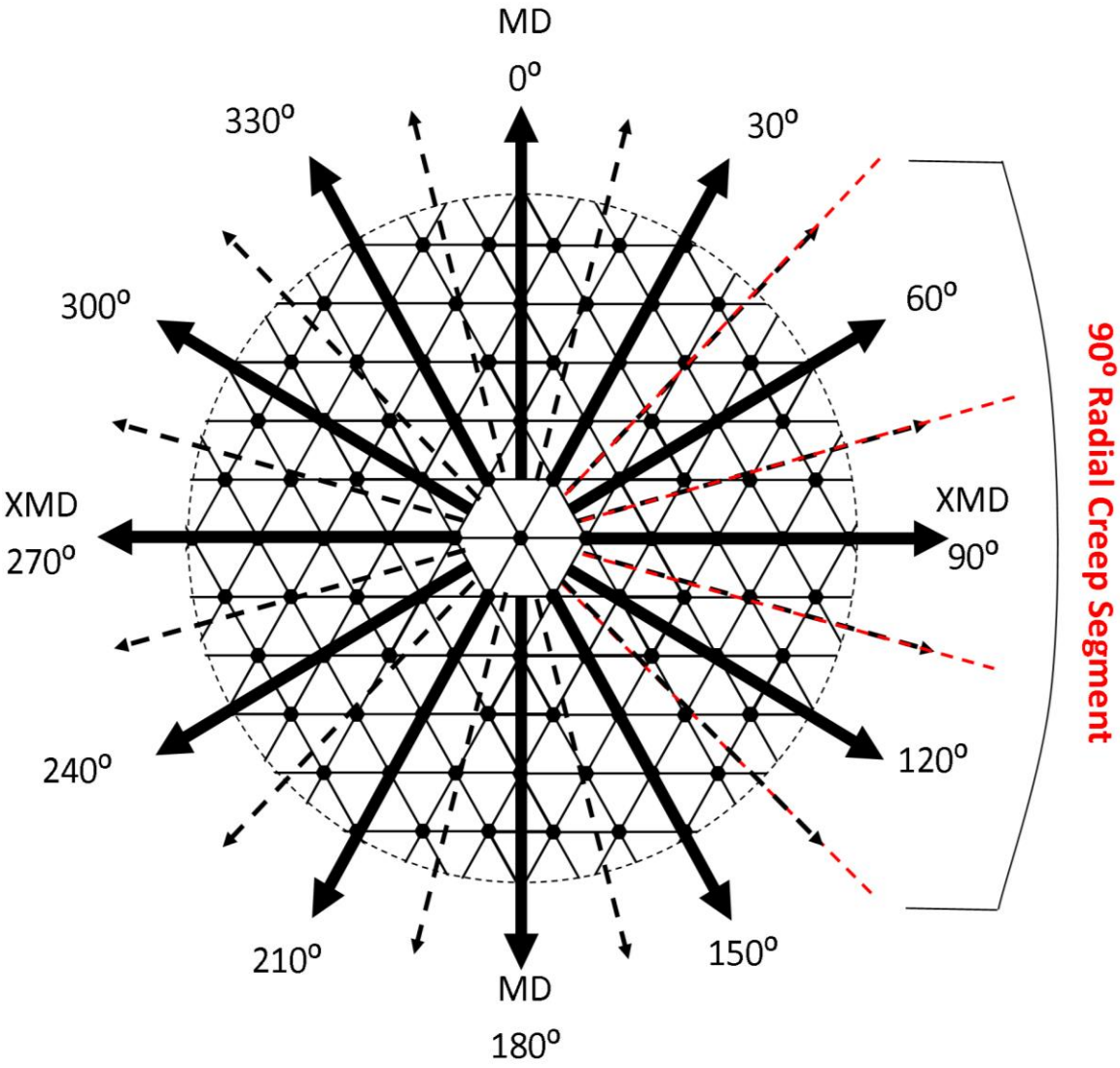


Fig 6.15 – 90° Radial creep specimen

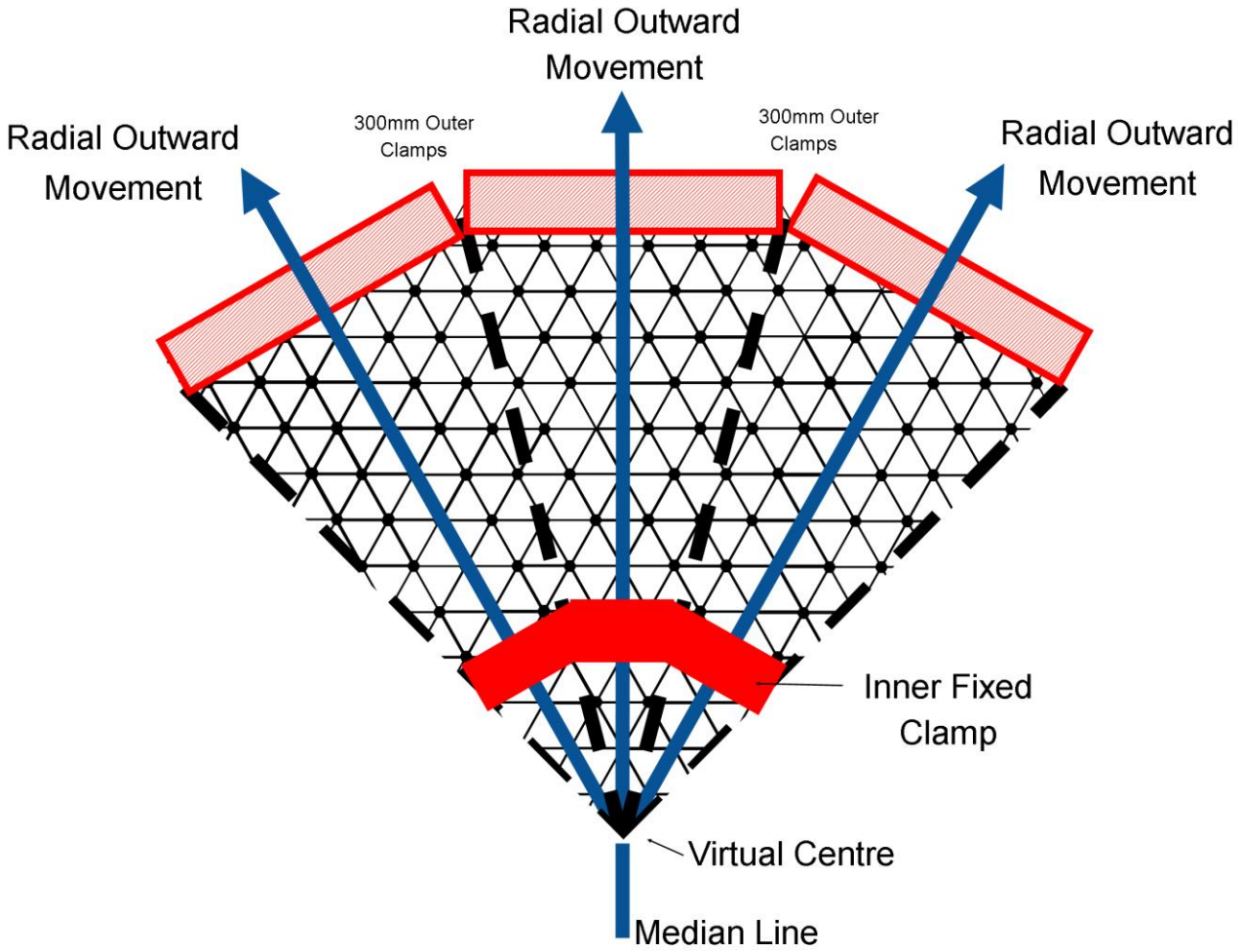


Fig 6.16 – Schematic of suggested shape and size of radial test specimen (0° & 60°)

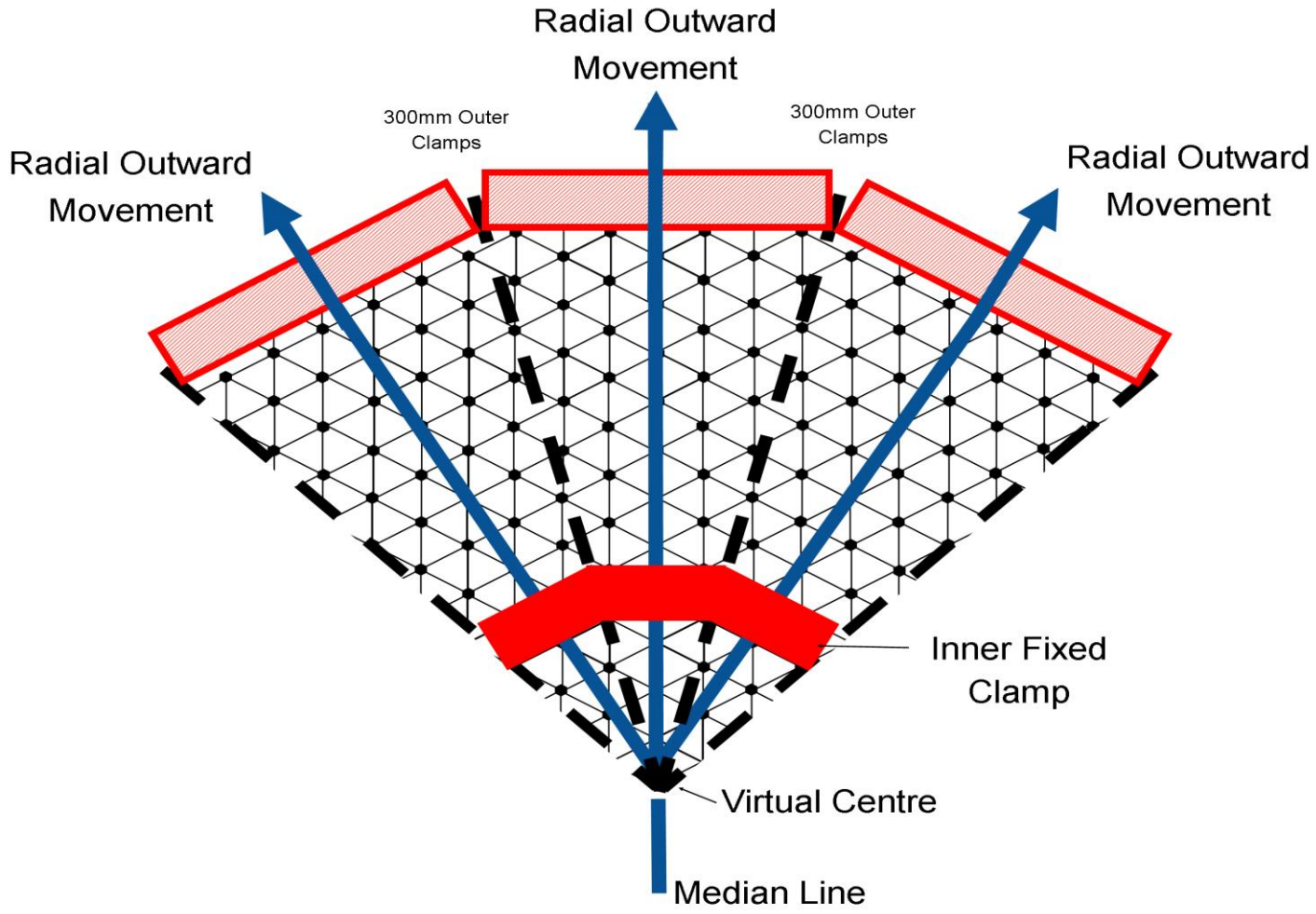
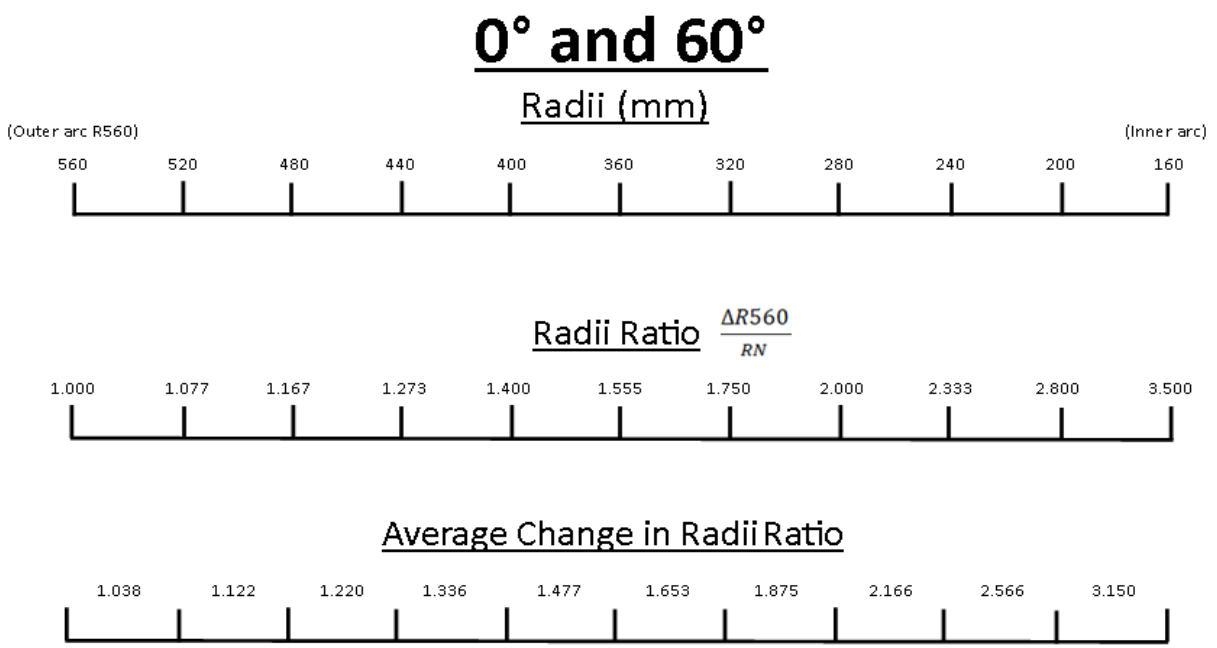


Fig 6.17 – Schematic of suggested shape and size of radial test specimen (30° & 90°)



Average change = SUM OF AVERAGE CHANGE IN RADII RATIO/10 = 17.603/10 = **1.76**

$$\text{Applied Load/m at R560 for 30kg test load} = \frac{\text{Applied loads (kg) x 9.81}}{\text{Length at outer arc}} = \frac{30 \text{ x } 3 \text{ x } 9.81}{0.880 \text{ x } 1000} = \textbf{1.00 kN/m}$$

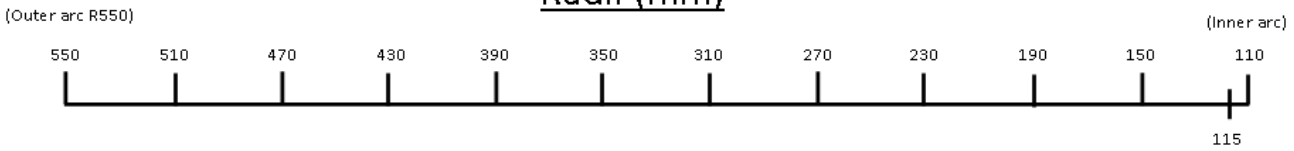
Average Load/m over gauge length = 1000 x 1.76 = **1.76 kN/m**

Radius at Average Load/m = 560/1.76 = **318mm**

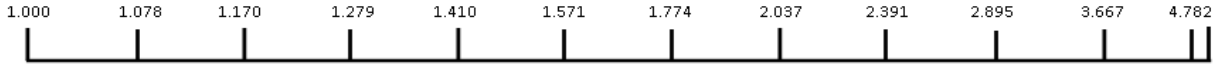
Fig 6.18 – Calculations of Applied Load/m at R560, Average Load/m Over Gauge Length and Radius at Average Load/m for 3x30kg loaded radial test specimen at 0° and 60° directions.

30° and 90°

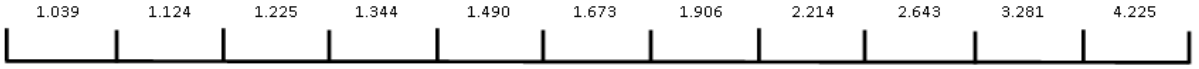
Radii (mm)



Radii Ratio $\frac{\Delta R550}{RN}$



Average Change in Radii Ratio



Average change = SUM OF AVERAGE CHANGE IN RADII RATIO/10.875 = 22.164/10.875 = **2.04**

$$\text{Applied Load/m at R550 for 30kg test load} = \frac{\text{Applied loads (kg) x 9.81}}{\text{Length at outer arc}} = \frac{30 \times 3 \times 9.81}{0.871 \times 1000} = \mathbf{1.01\ kN/m}$$

Average Load/m over gauge length = 1.01 x 2.04= **2.06 kN/m**

Radius at Average Load/m = 550/2.04 = **270mm**

Fig 6.19 – Calculations of Applied Load/m at R550, Average Load/m Over Gauge Length and Radius at Average Load/m for 3x30kg loaded radial test specimen at 30° and 90° directions.

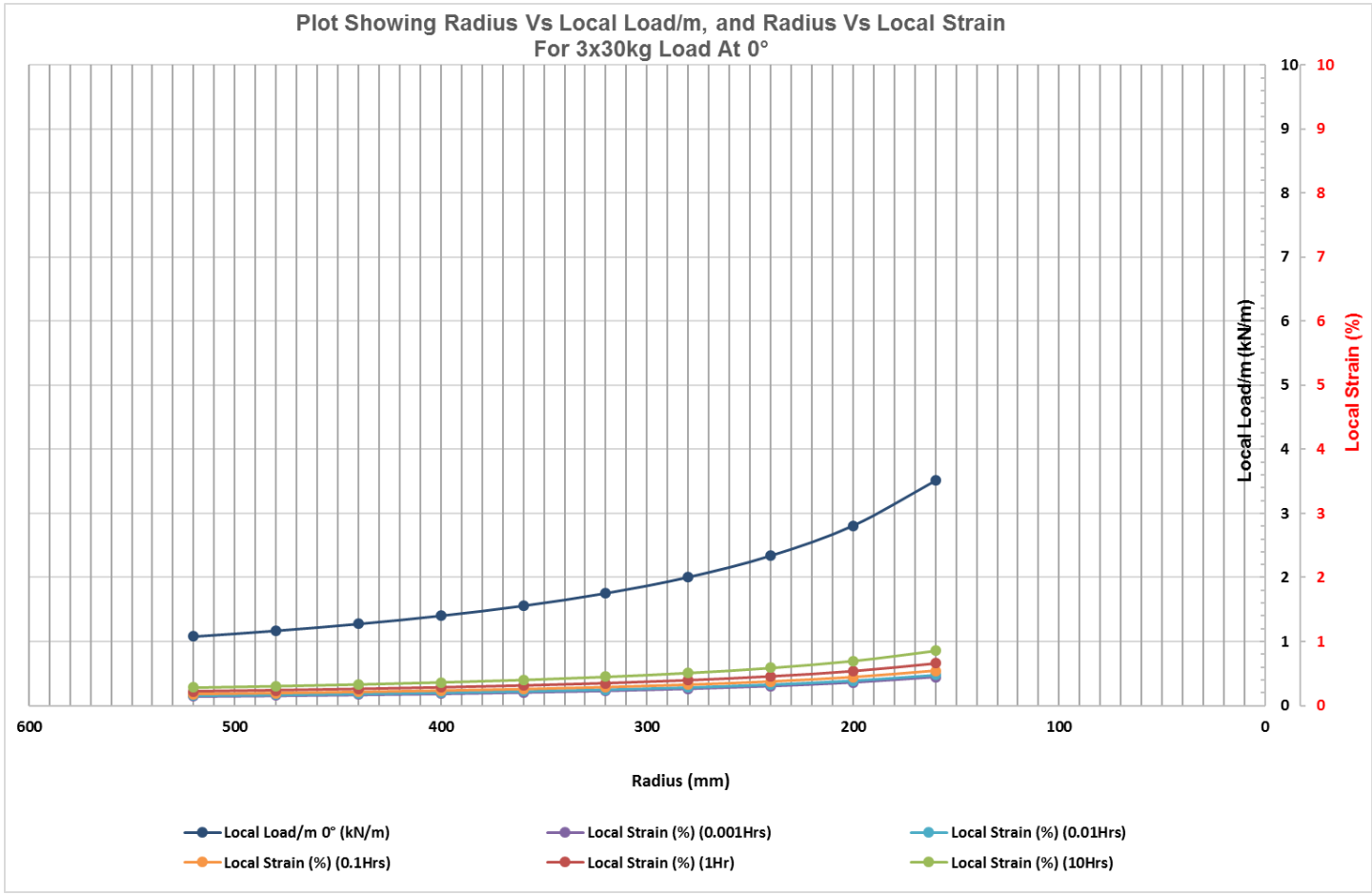


Fig 6.20 – Plot Showing Radius Vs Local Load/m and Radius Vs Local Strain for Test Loaded at 30kg and tested in the 0° direction.

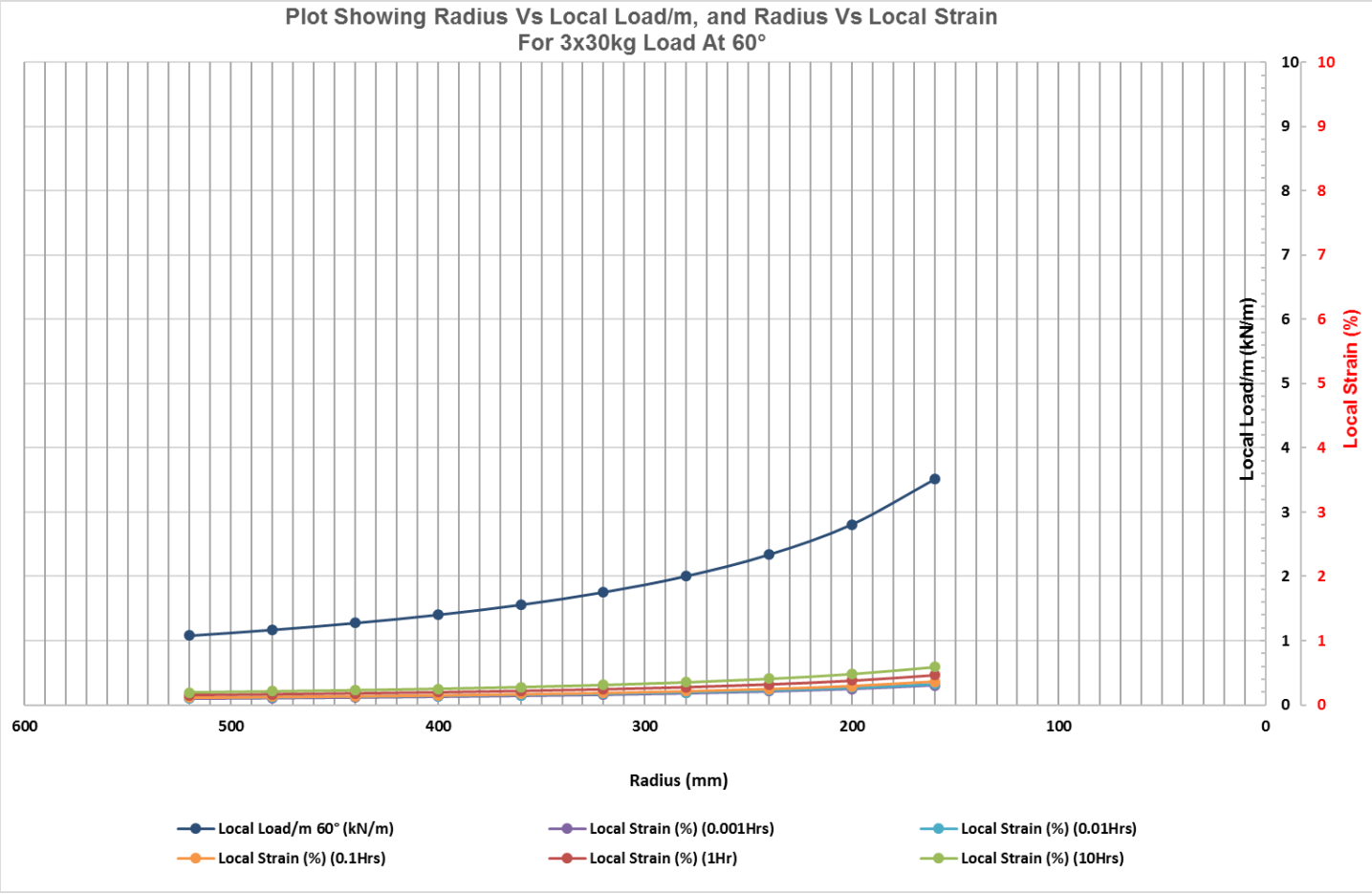


Fig 6.21 – Plot Showing Radius Vs Local Load/m and Radius Vs Local Strain for Test Loaded at 30kg and tested in the 60° direction.

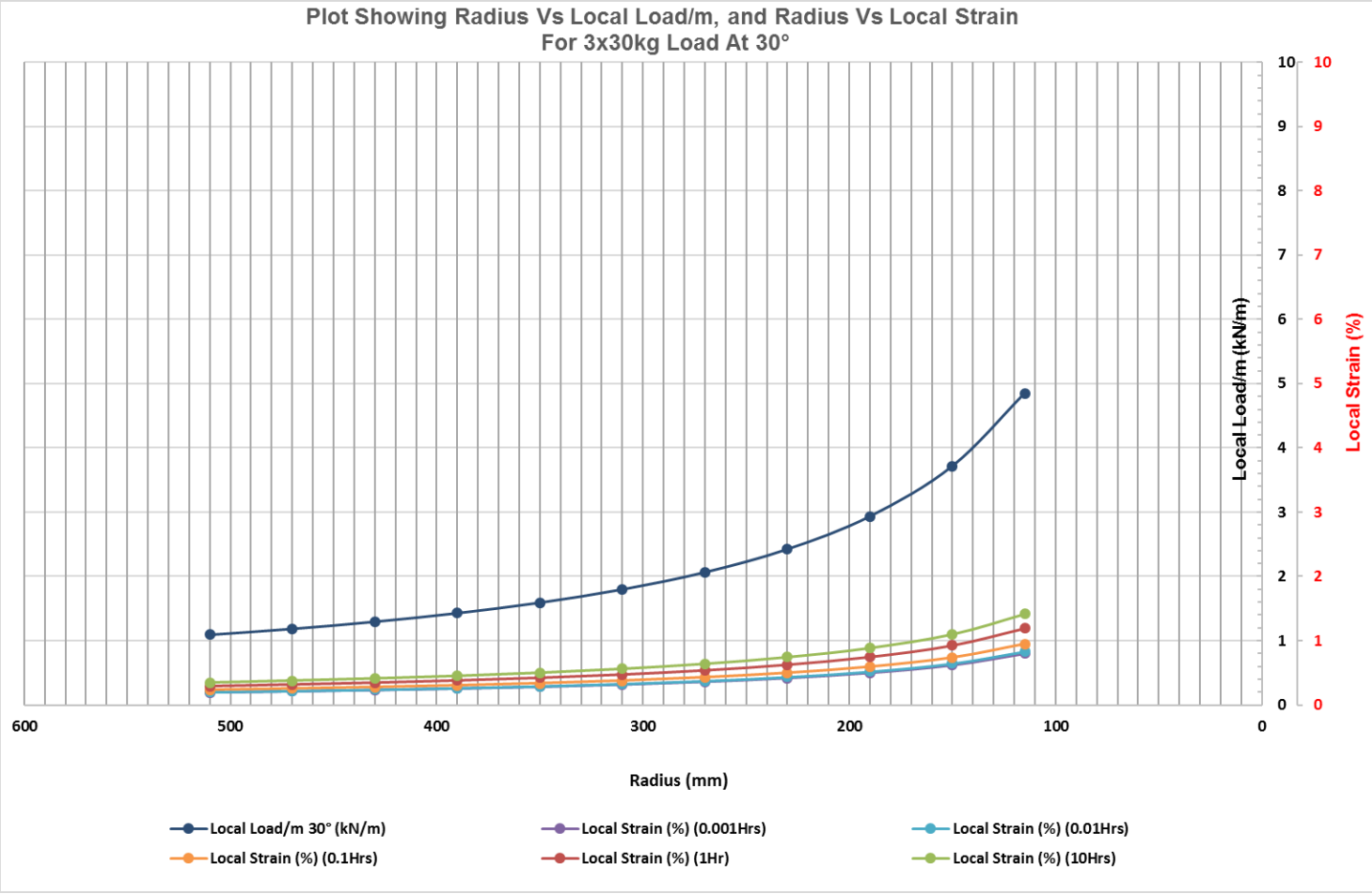


Fig 6.22 – Plot Showing Radius Vs Local Load/m and Radius Vs Local Strain for Test Loaded at 30kg and tested in the 30° direction.

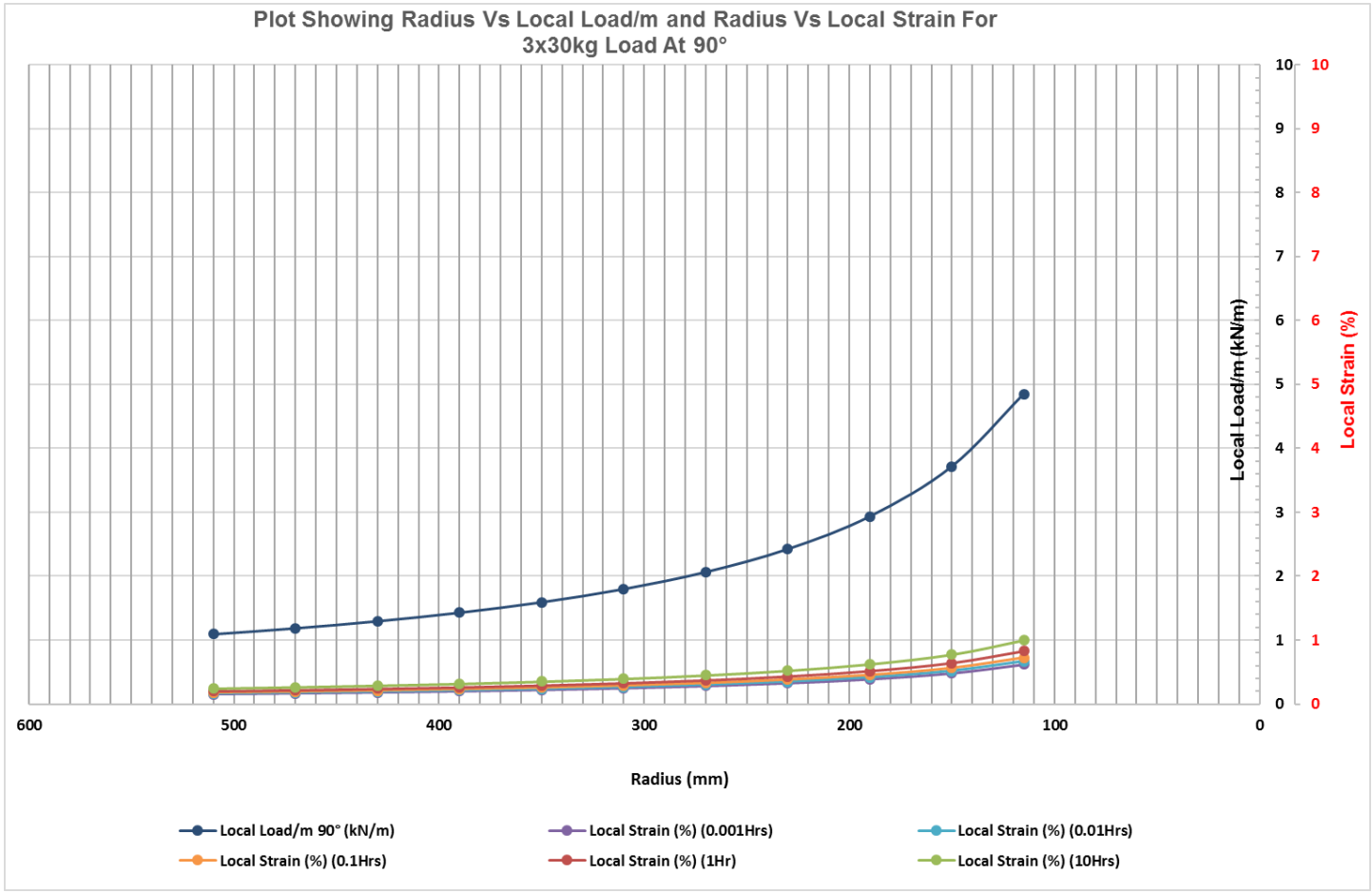


Fig 6.23 – Plot Showing Radius Vs Local Load/m and Radius Vs Local Strain for Test Loaded at 30kg and tested in the 90° direction.

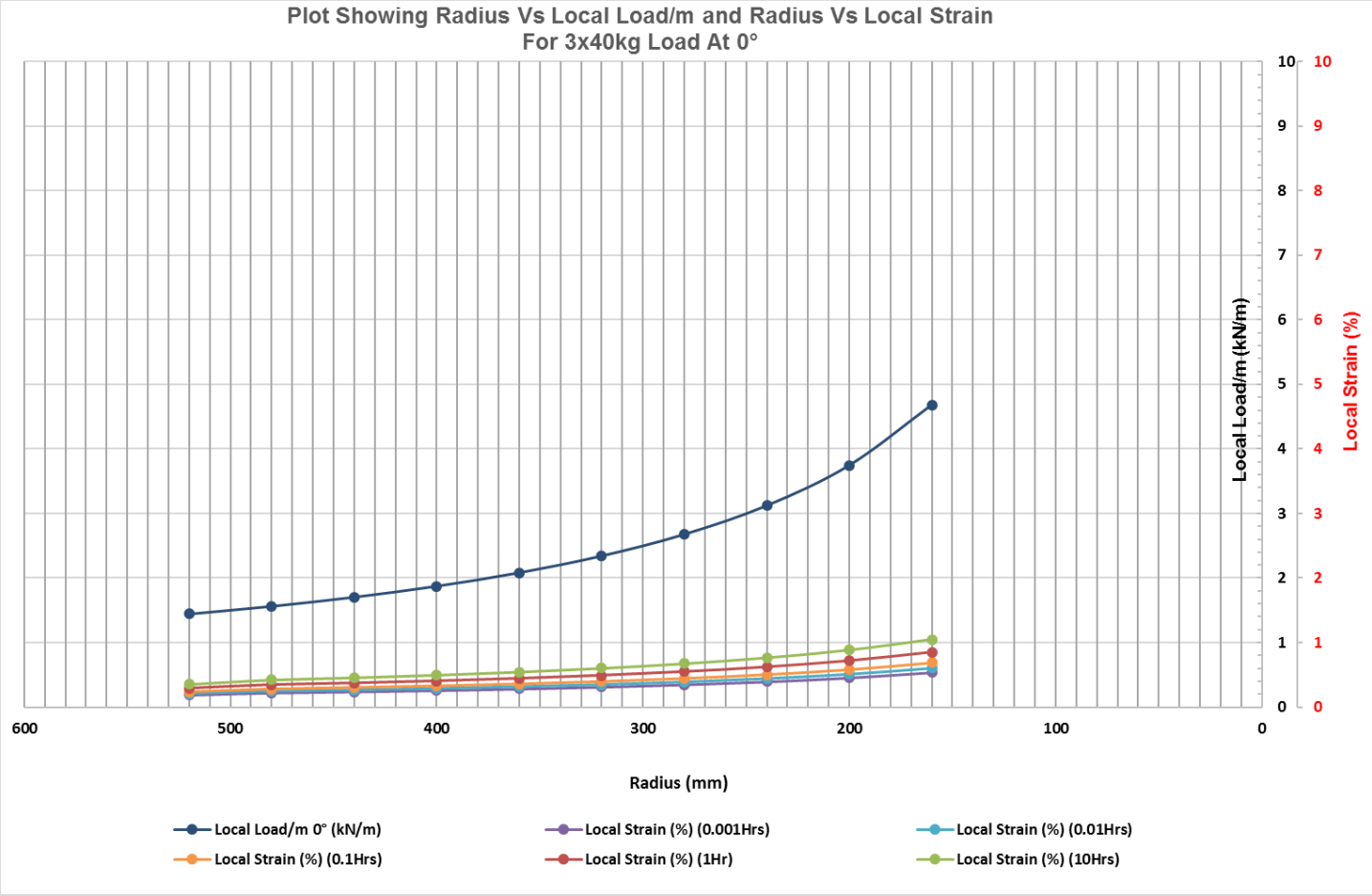


Fig 6.24 – Plot Showing Radius Vs Local Load/m and Radius Vs Local Strain for Test Loaded at 40kg and tested in the 0° direction.

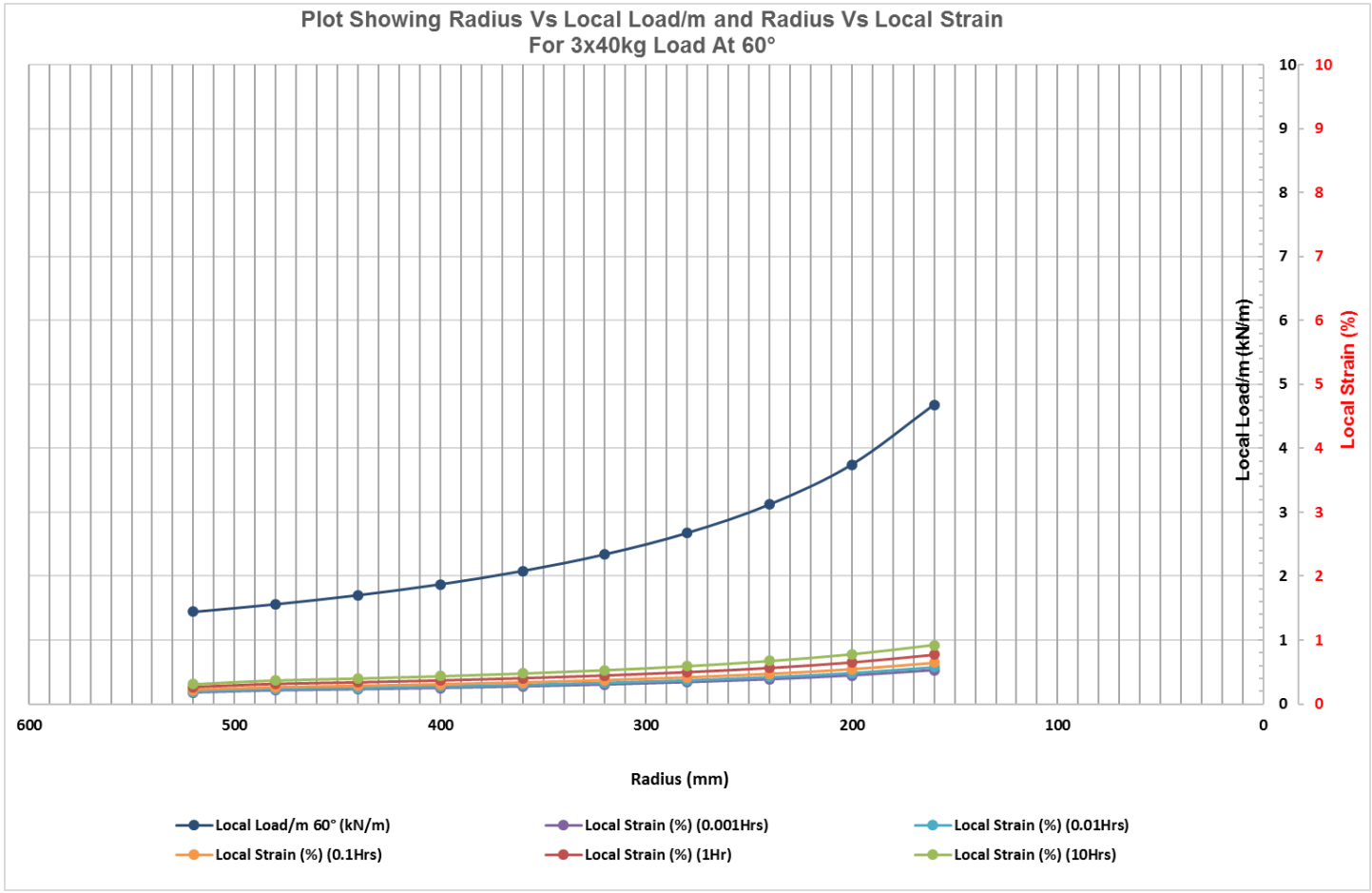


Fig 6.25 – Plot Showing Radius Vs Local Load/m and Radius Vs Local Strain for Test Loaded at 40kg and tested in the 60° direction.

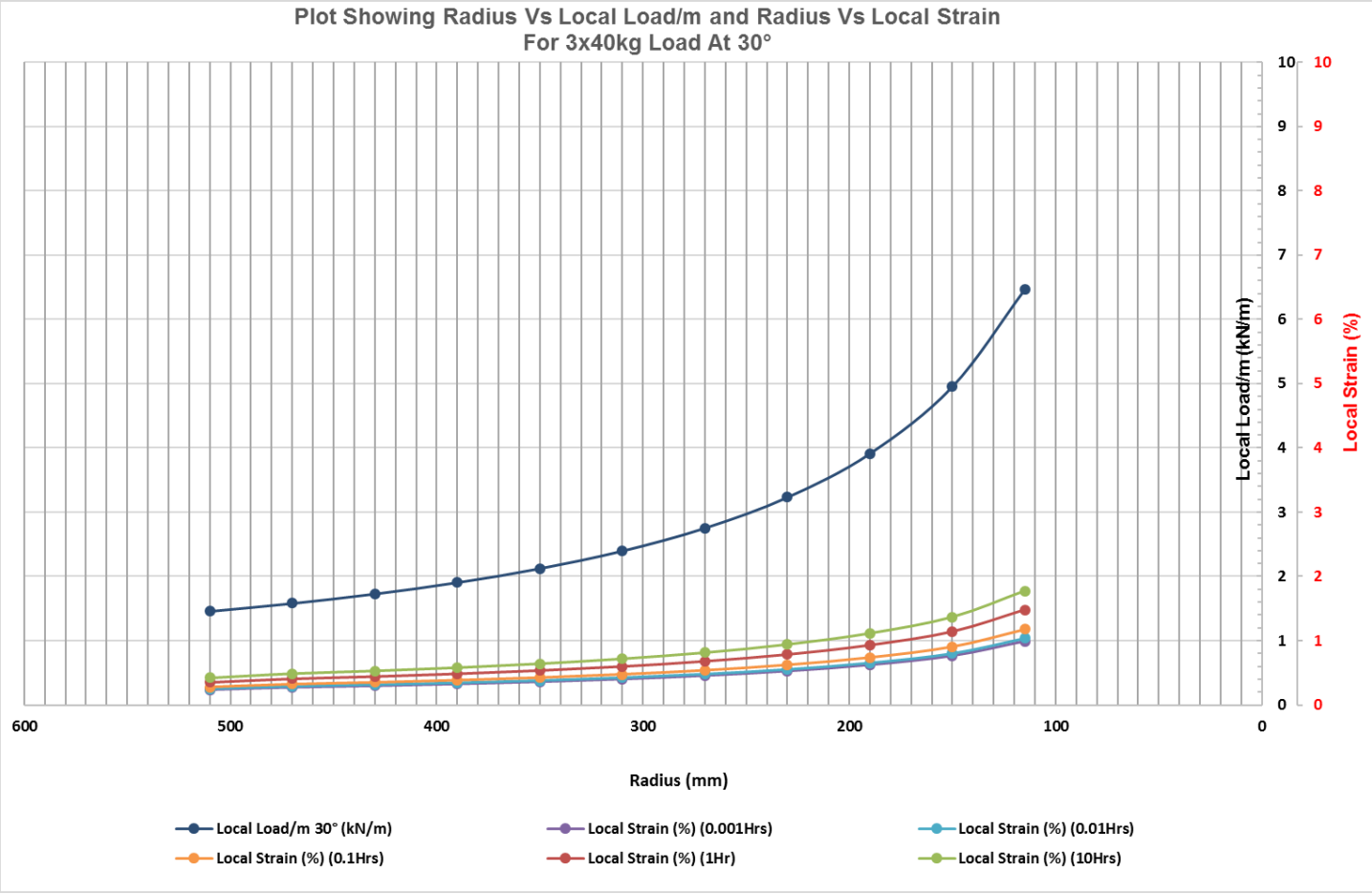


Fig 6.26 – Plot Showing Radius Vs Local Load/m and Radius Vs Local Strain for Test Loaded at 40kg and tested in the 30° direction.

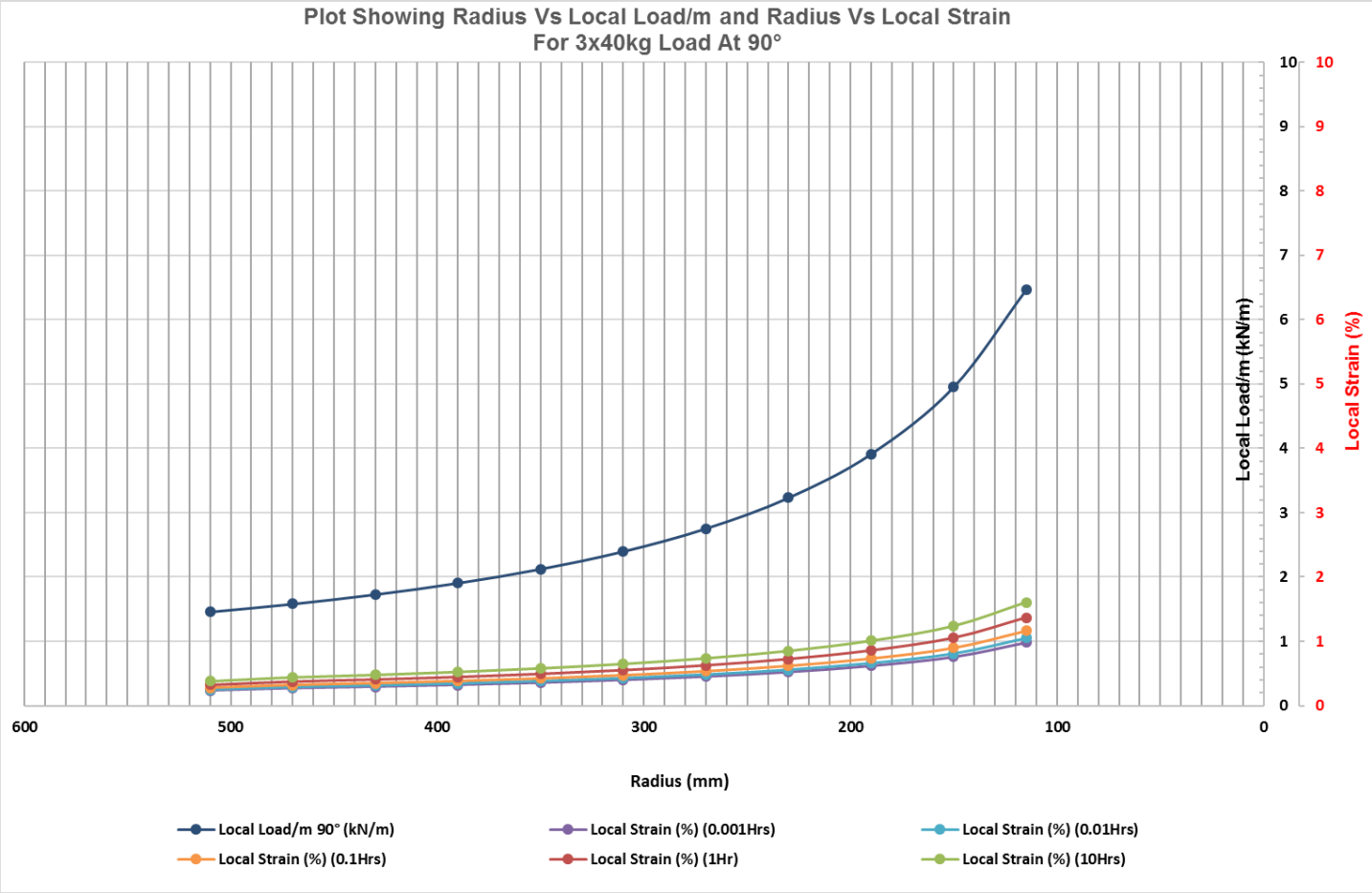


Fig 6.27 – Plot Showing Radius Vs Local Load/m and Radius Vs Local Strain for Test Loaded at 40kg and tested in the 90° direction.

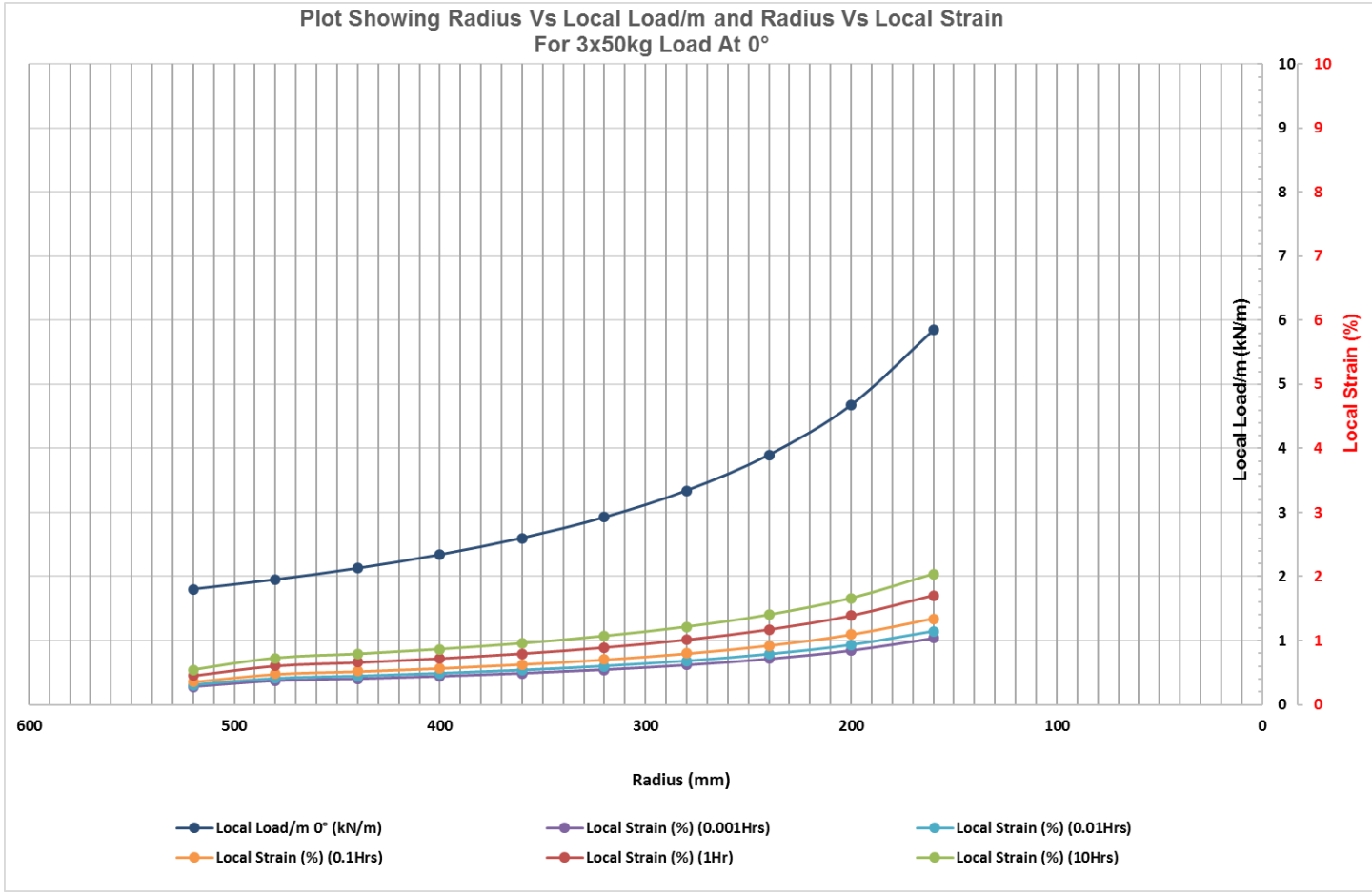


Fig 6.28 – Plot Showing Radius Vs Local Load/m and Radius Vs Local Strain for Test Loaded at 50kg and tested in the 0° direction.

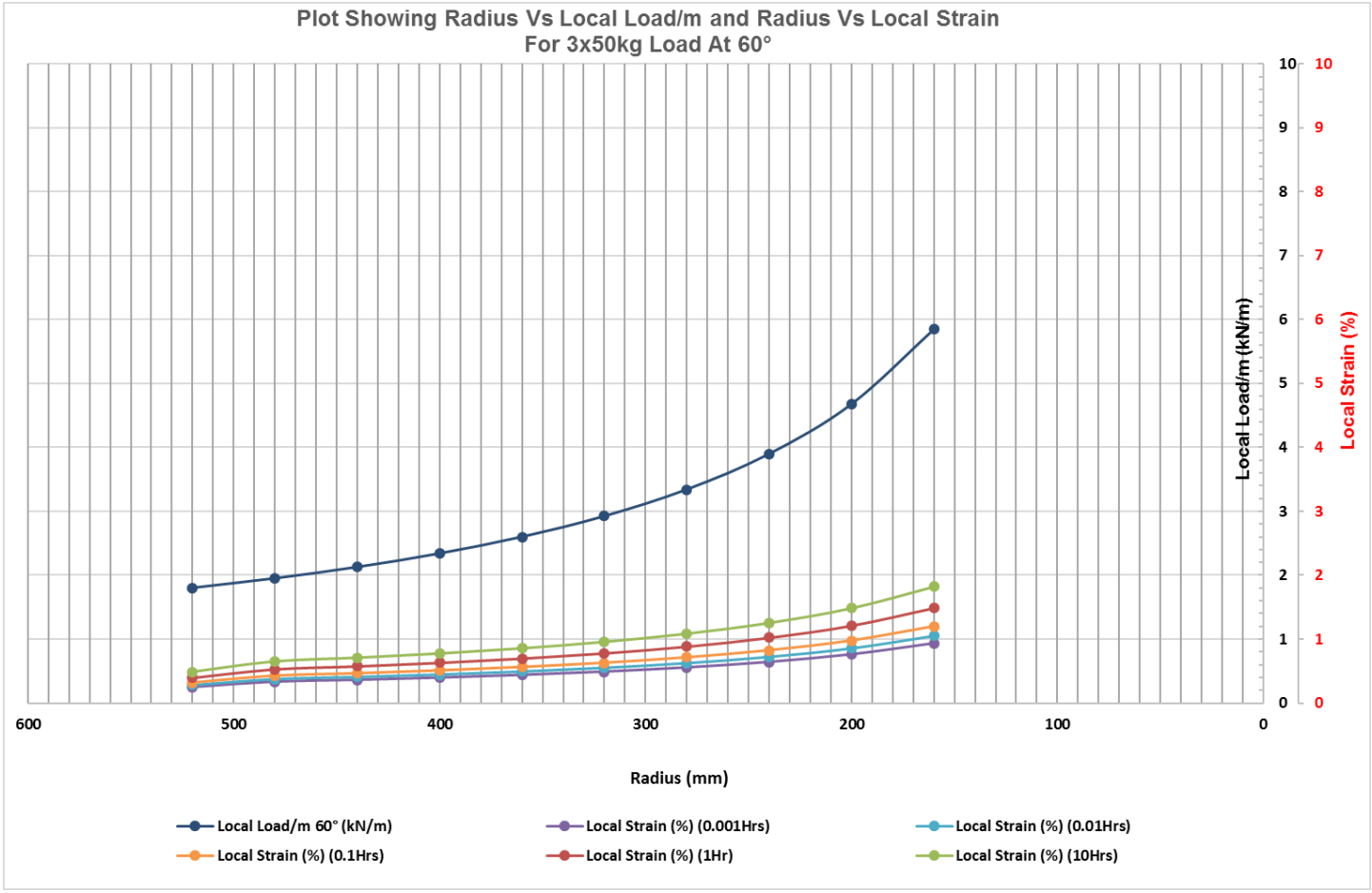


Fig 6.29 – Plot Showing Radius Vs Local Load/m and Radius Vs Local Strain for Test Loaded at 50kg and tested in the 60° direction.

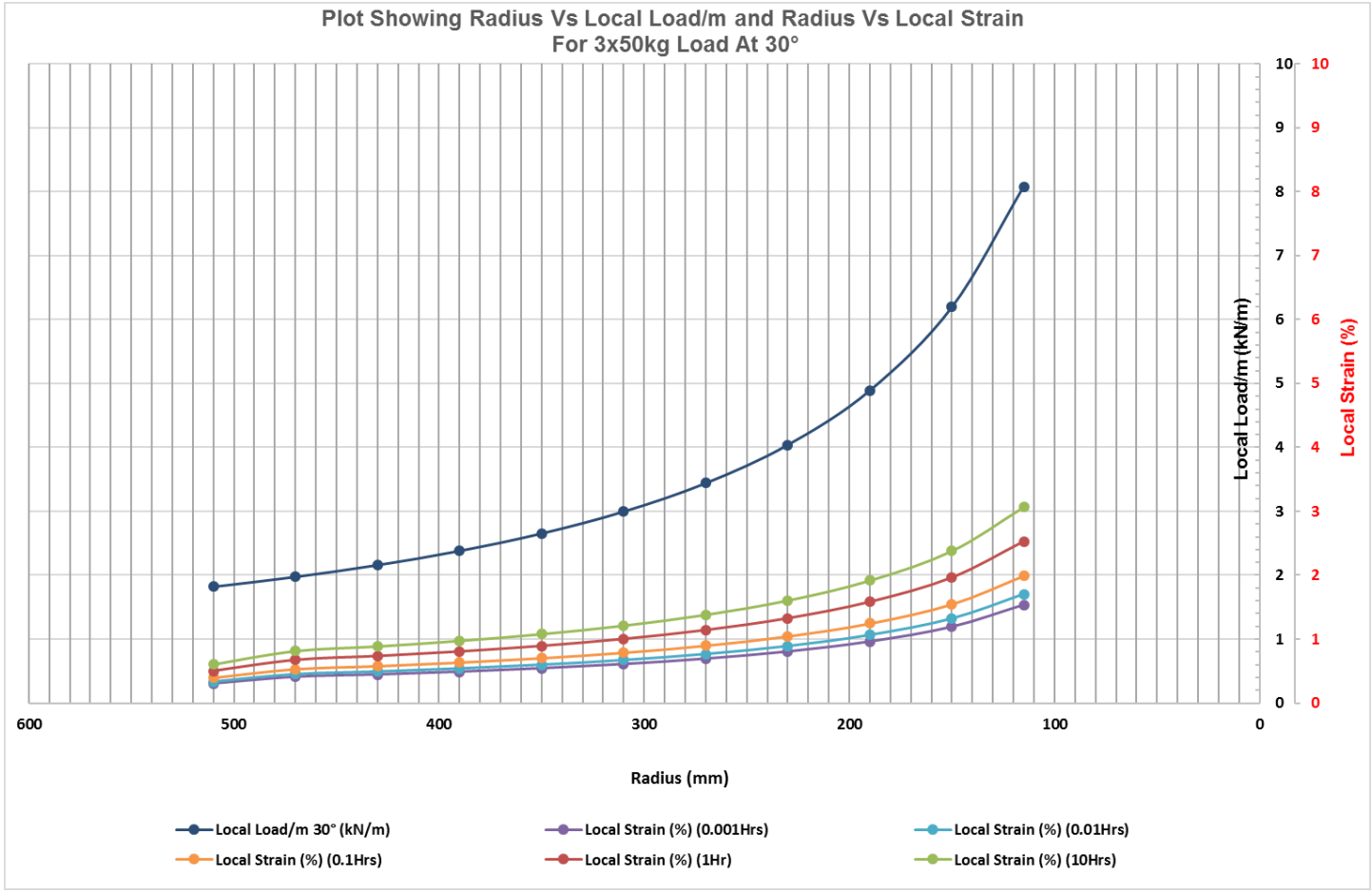


Fig 6.30 – Plot Showing Radius Vs Local Load/m and Radius Vs Local Strain for Test Loaded at 50kg and tested in the 30° direction.

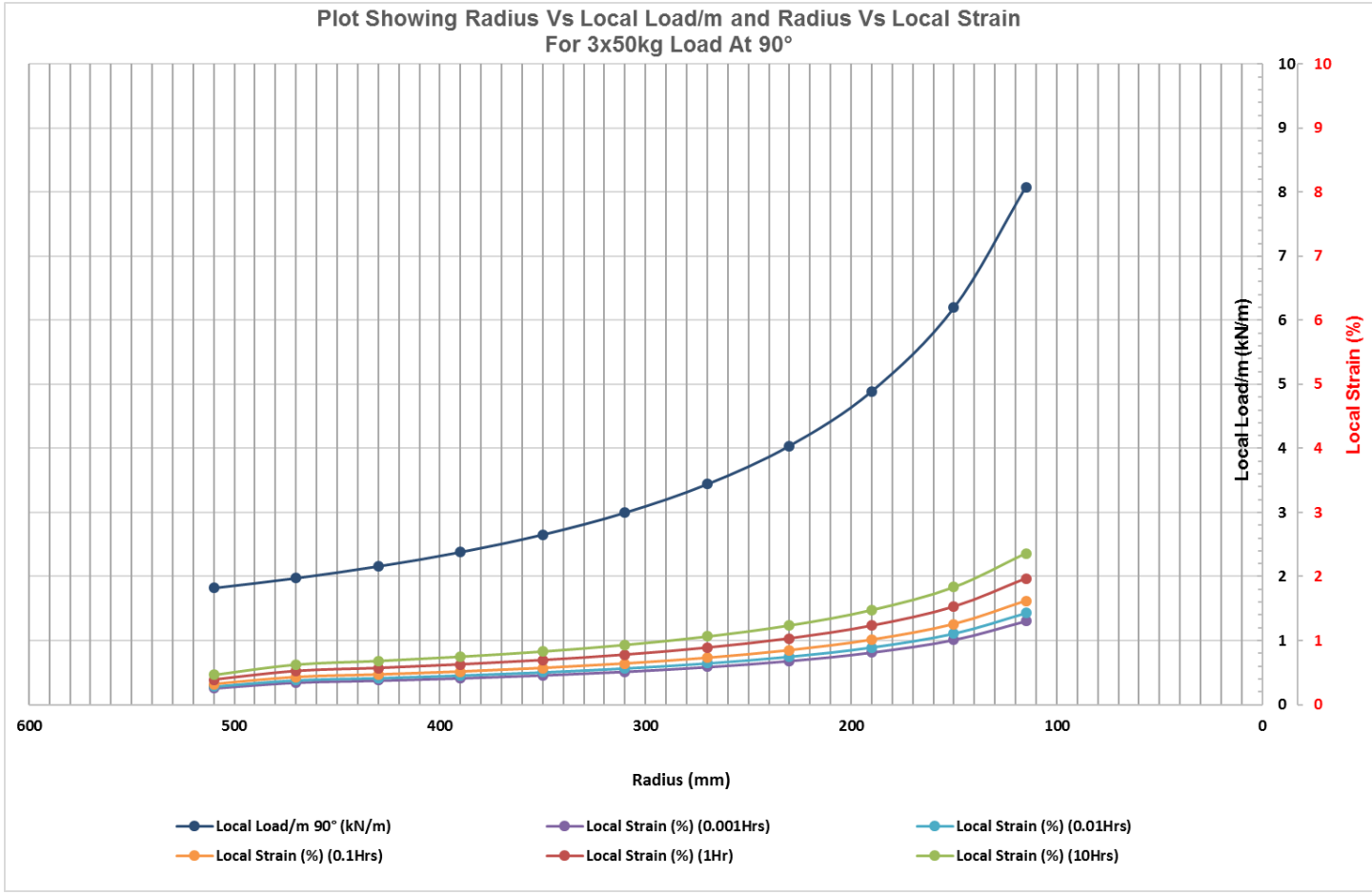


Fig 6.31 – Plot Showing Radius Vs Local Load/m and Radius Vs Local Strain for Test Loaded at 50kg and tested in the 90° direction.

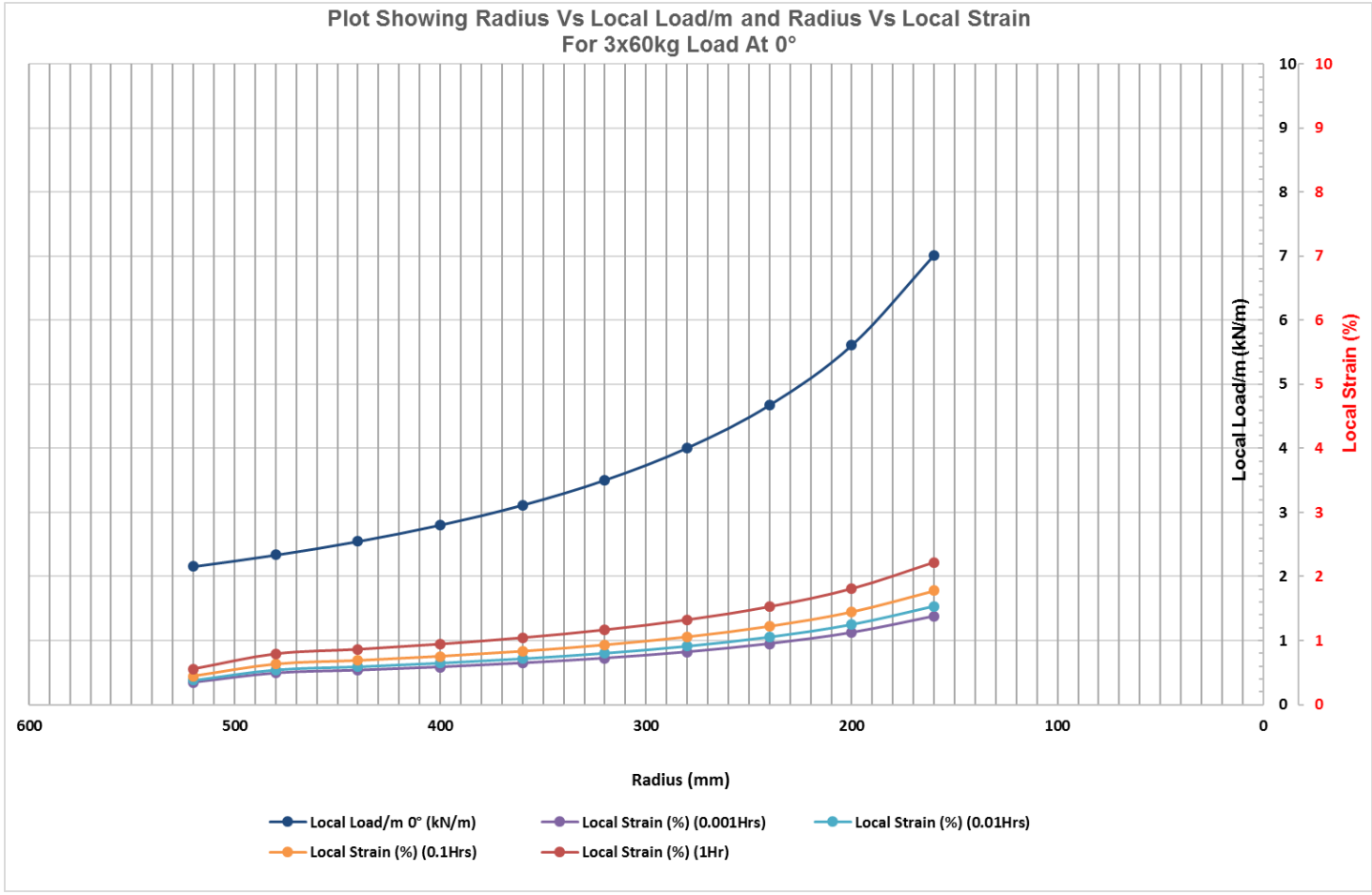


Fig 6.32 – Plot Showing Radius Vs Local Load/m and Radius Vs Local Strain for Test Loaded at 60kg and tested in the 0° direction.

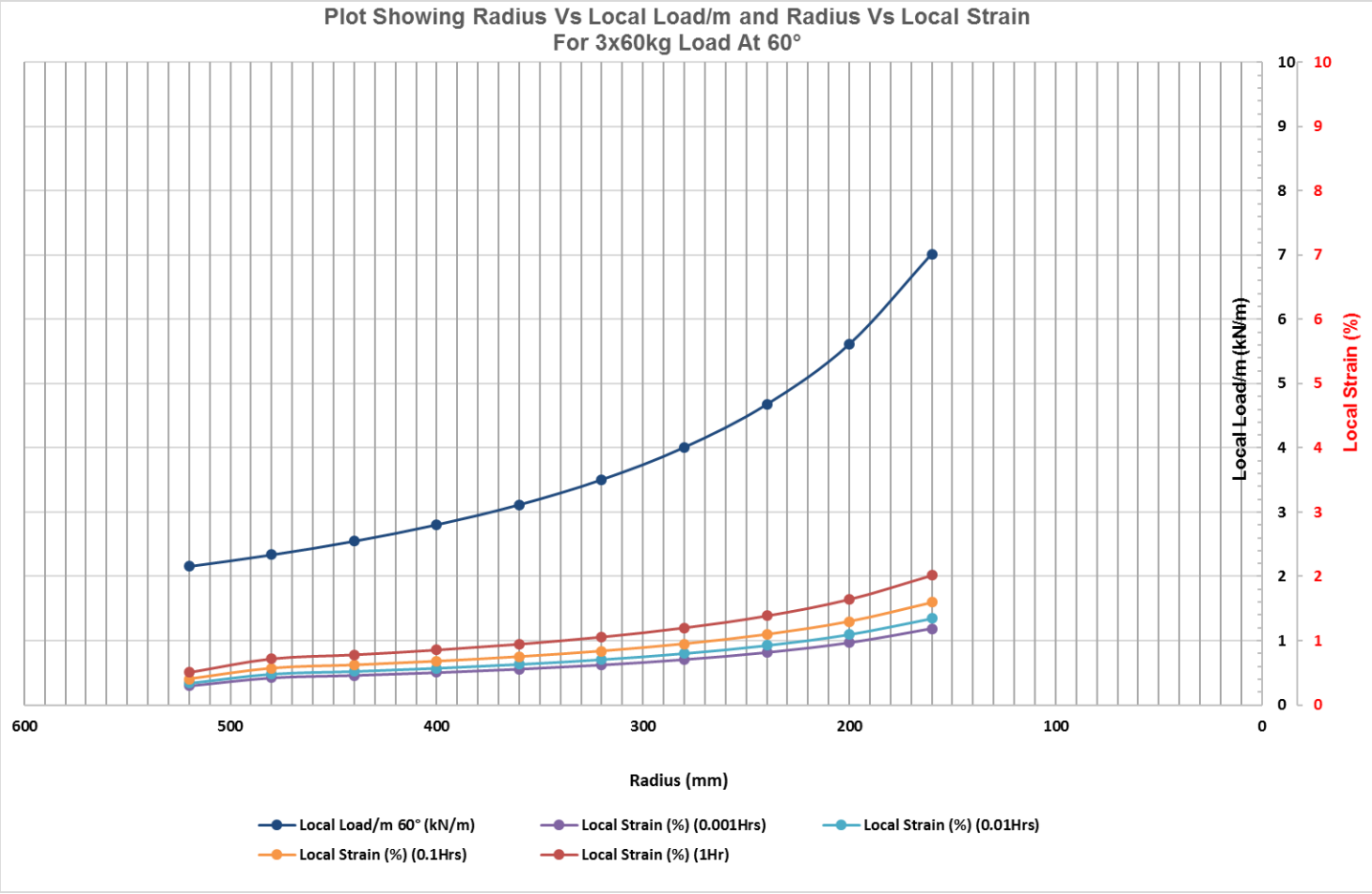


Fig 6.33 – Plot Showing Radius Vs Local Load/m and Radius Vs Local Strain for Test Loaded at 60kg and tested in the 60° direction.

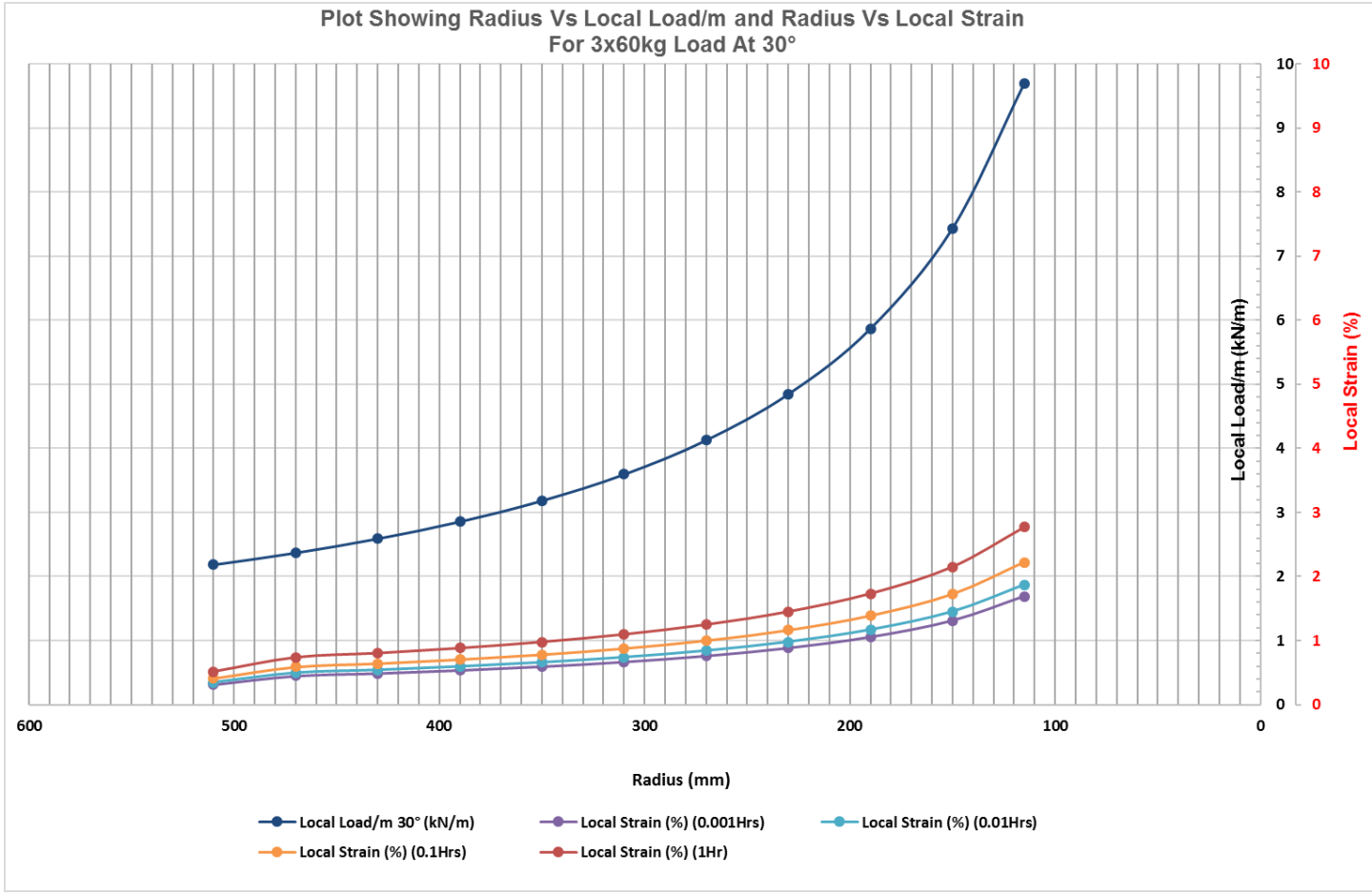


Fig 6.34 – Plot Showing Radius Vs Local Load/m and Radius Vs Local Strain for Test Loaded at 60kg and tested in the 30° direction.

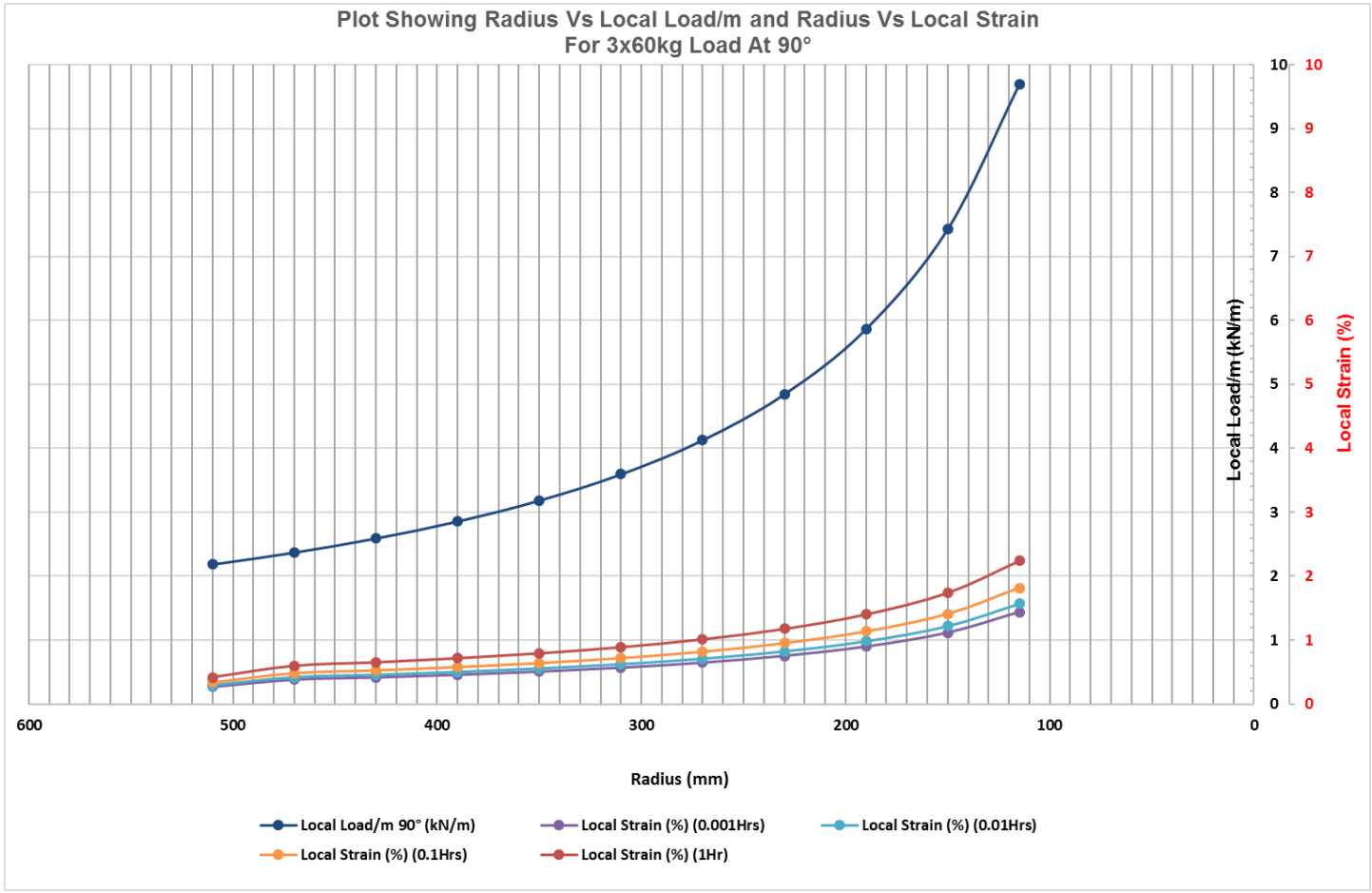


Fig 6.35 – Plot Showing Radius Vs Local Load/m and Radius Vs Local Strain for Test Loaded at 60kg and tested in the 90° direction.

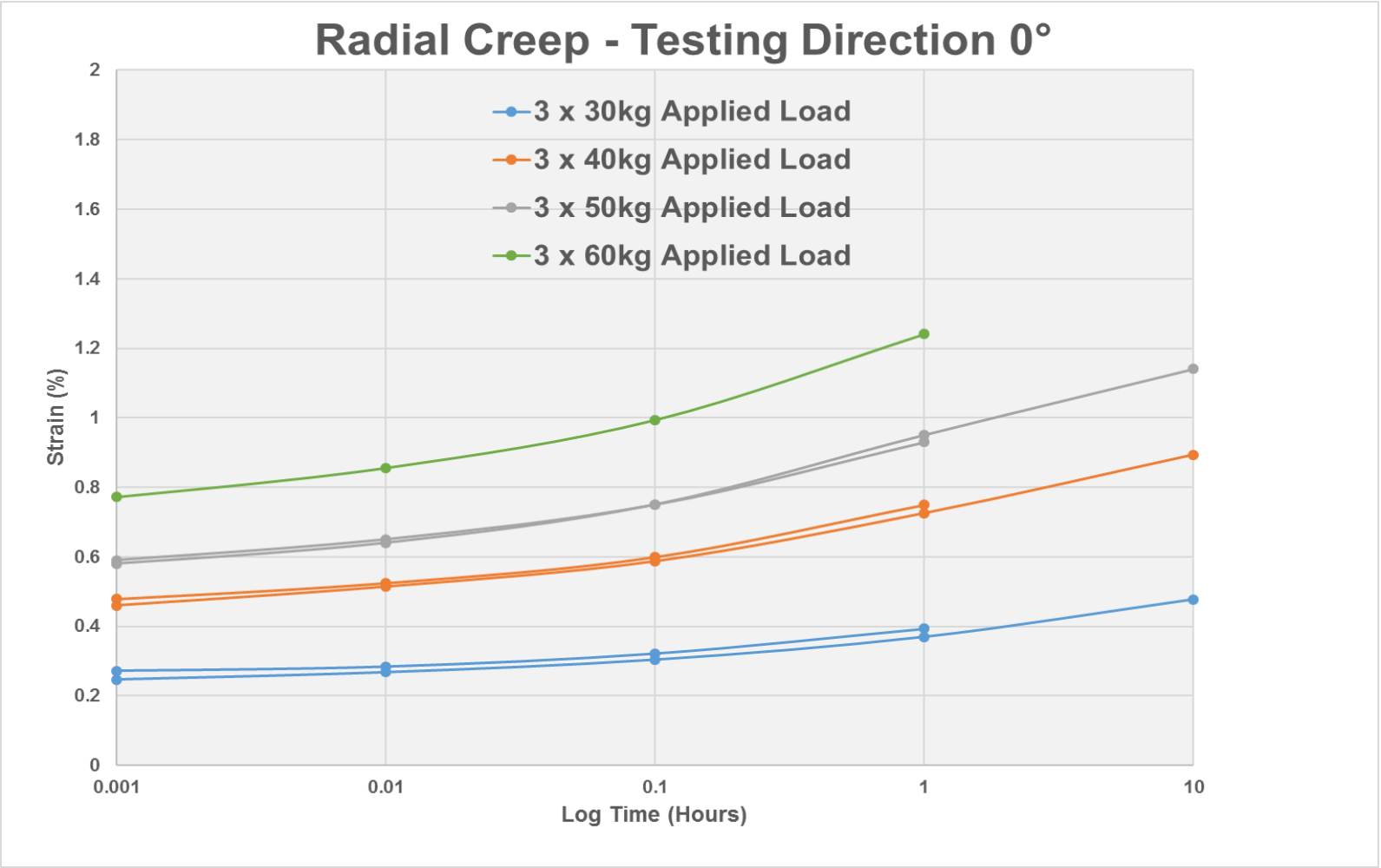


Fig 6.36 – TX160 creep curves obtained from radial creep testing in the 0° direction.

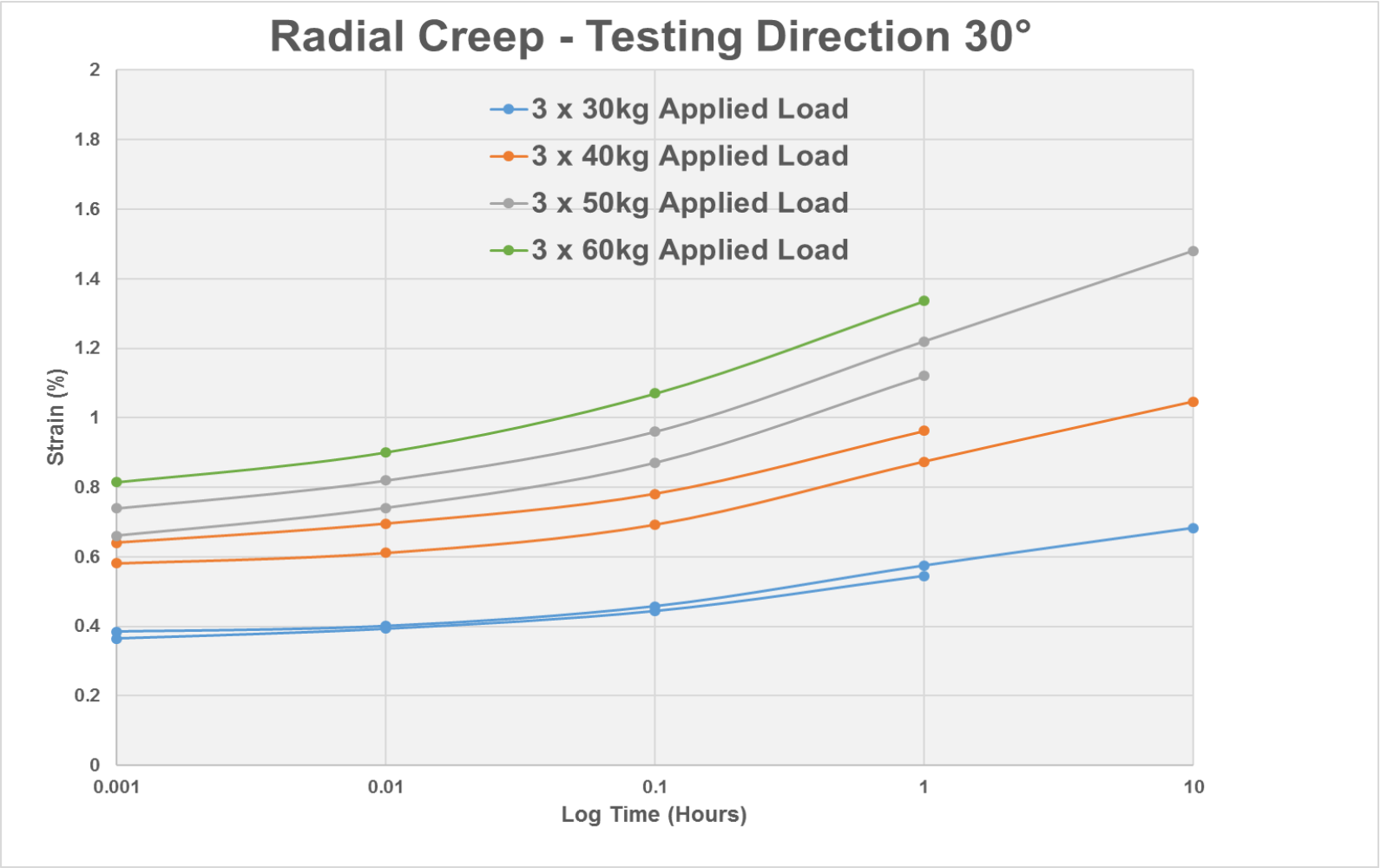


Fig 6.37 – TX160 creep curves obtained from radial creep testing in the 30° direction.

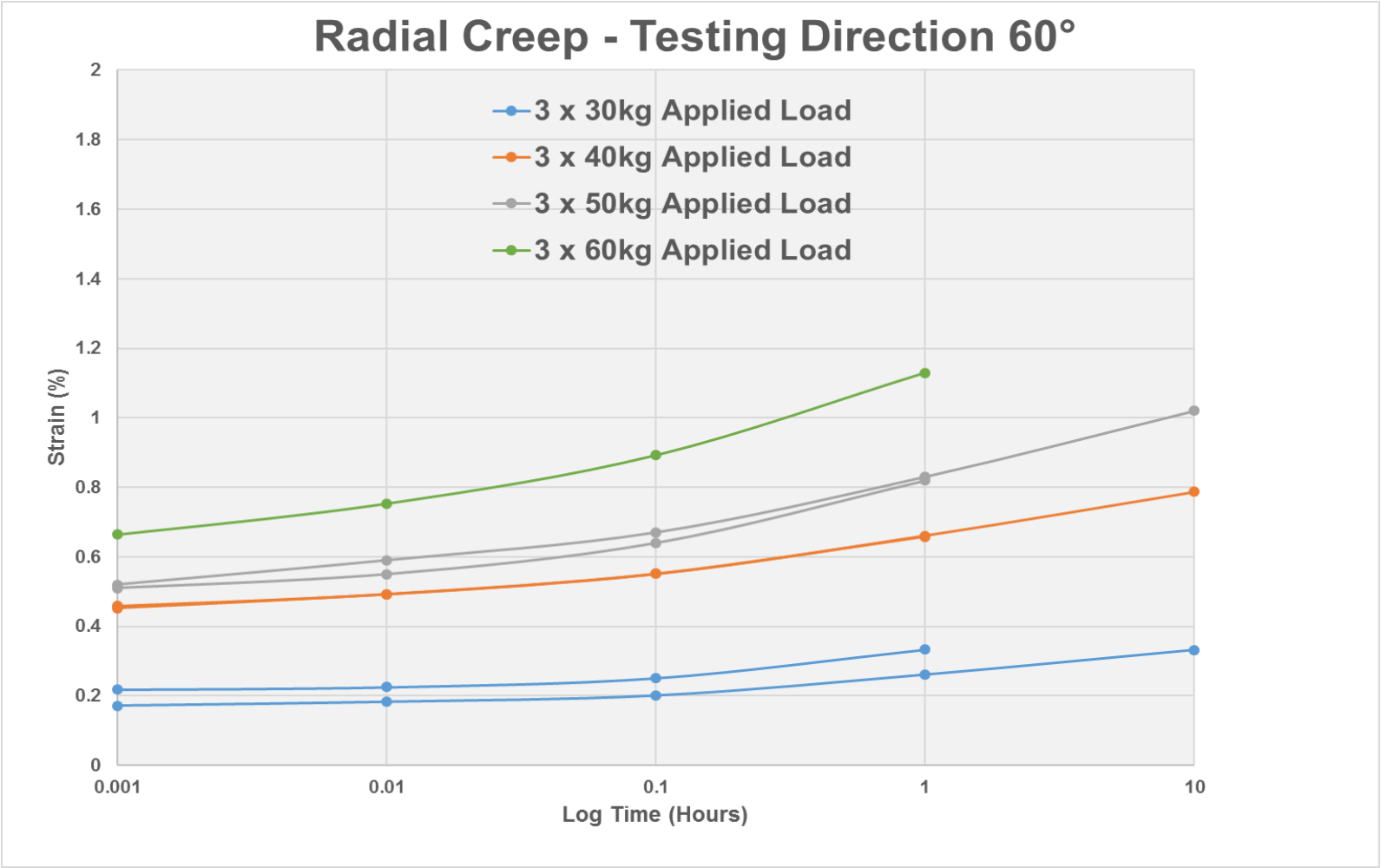


Fig 6.38 – TX160 creep curves obtained from radial creep testing in the 60° direction.

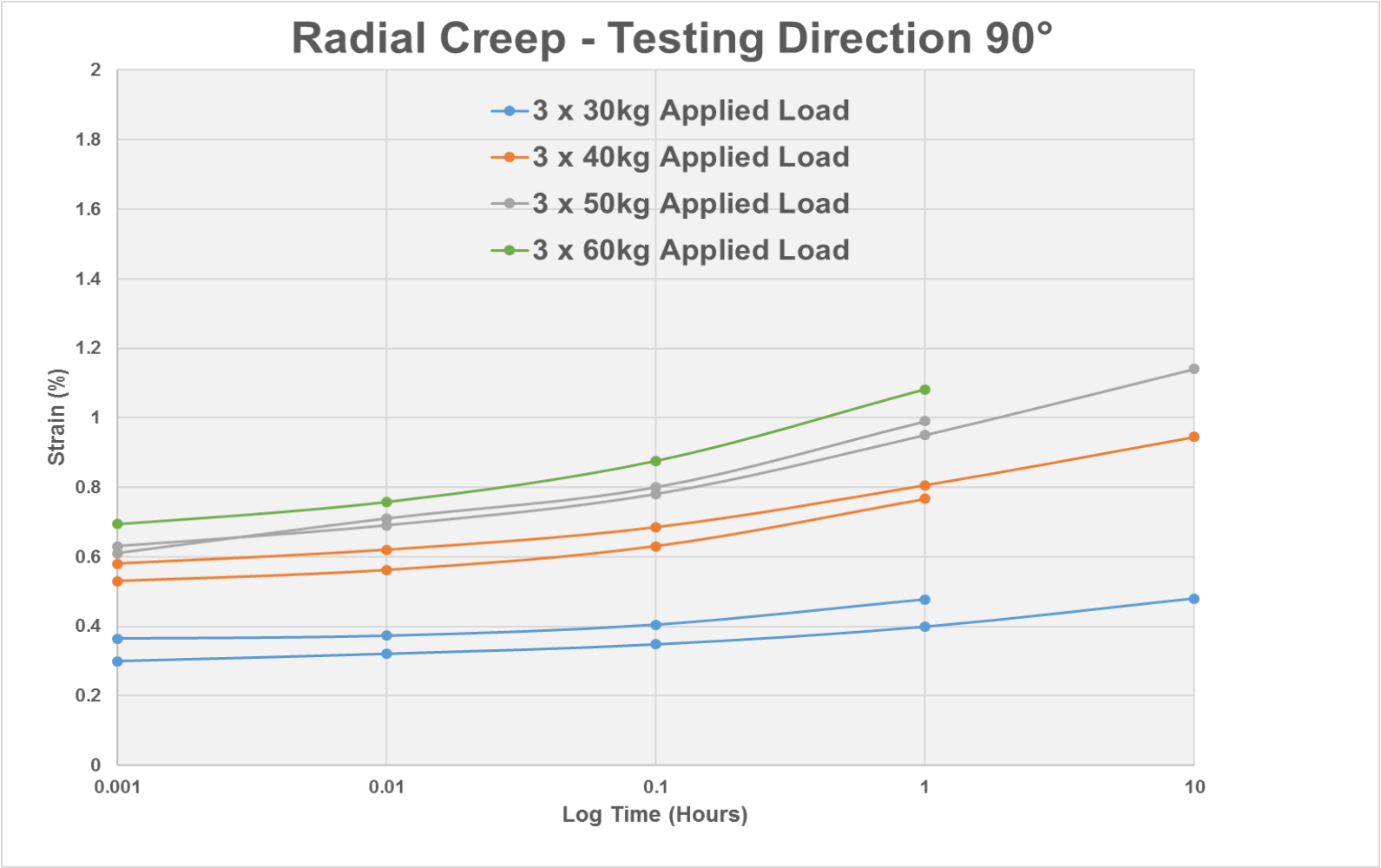


Fig 6.39 – TX160 creep curves obtained from radial creep testing in the 90° direction.

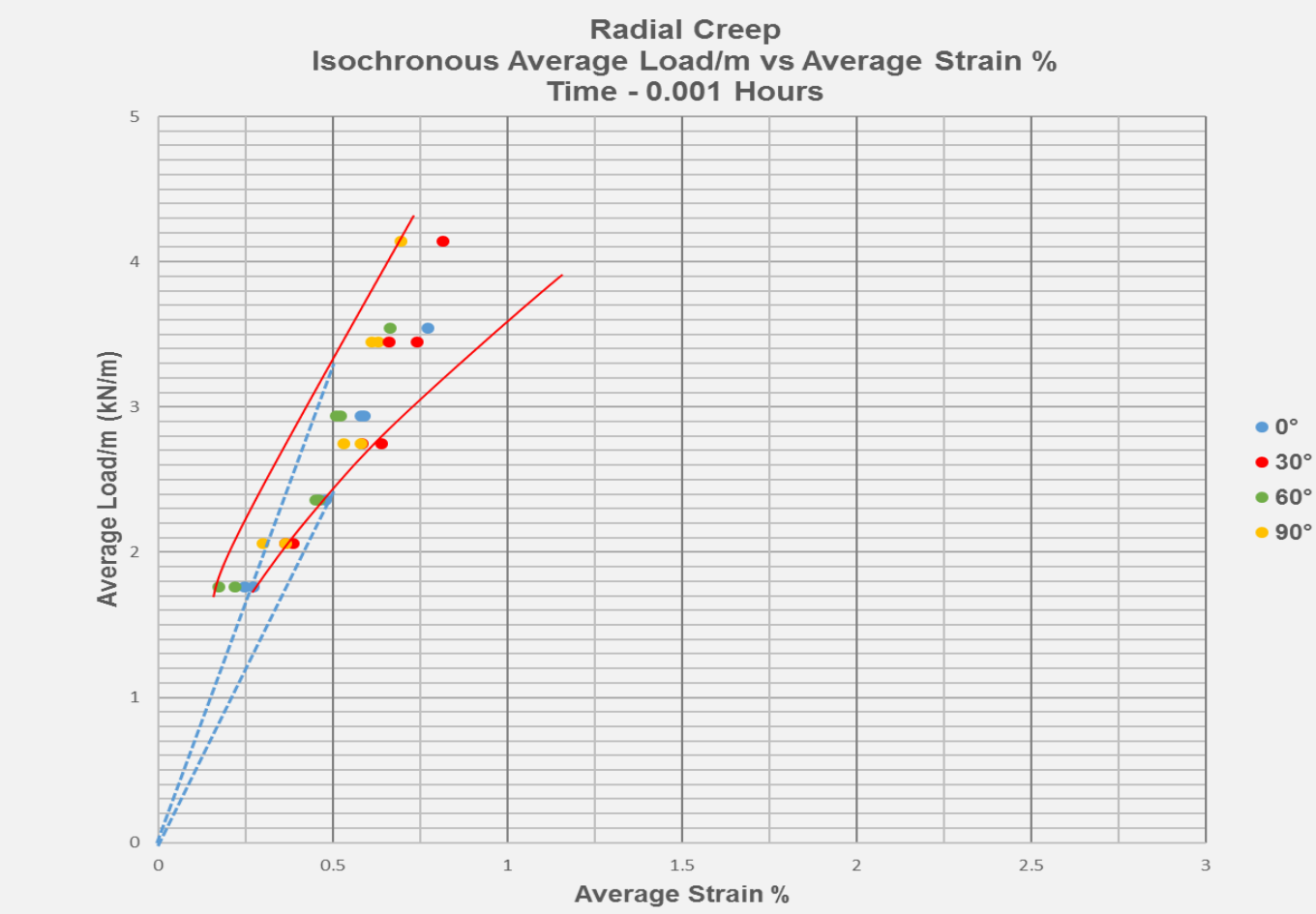


Fig 6.40 – Radial Creep, Isochronous Load-Strain curves at 0.001 hours of TX160 creep data, tested in four directions.

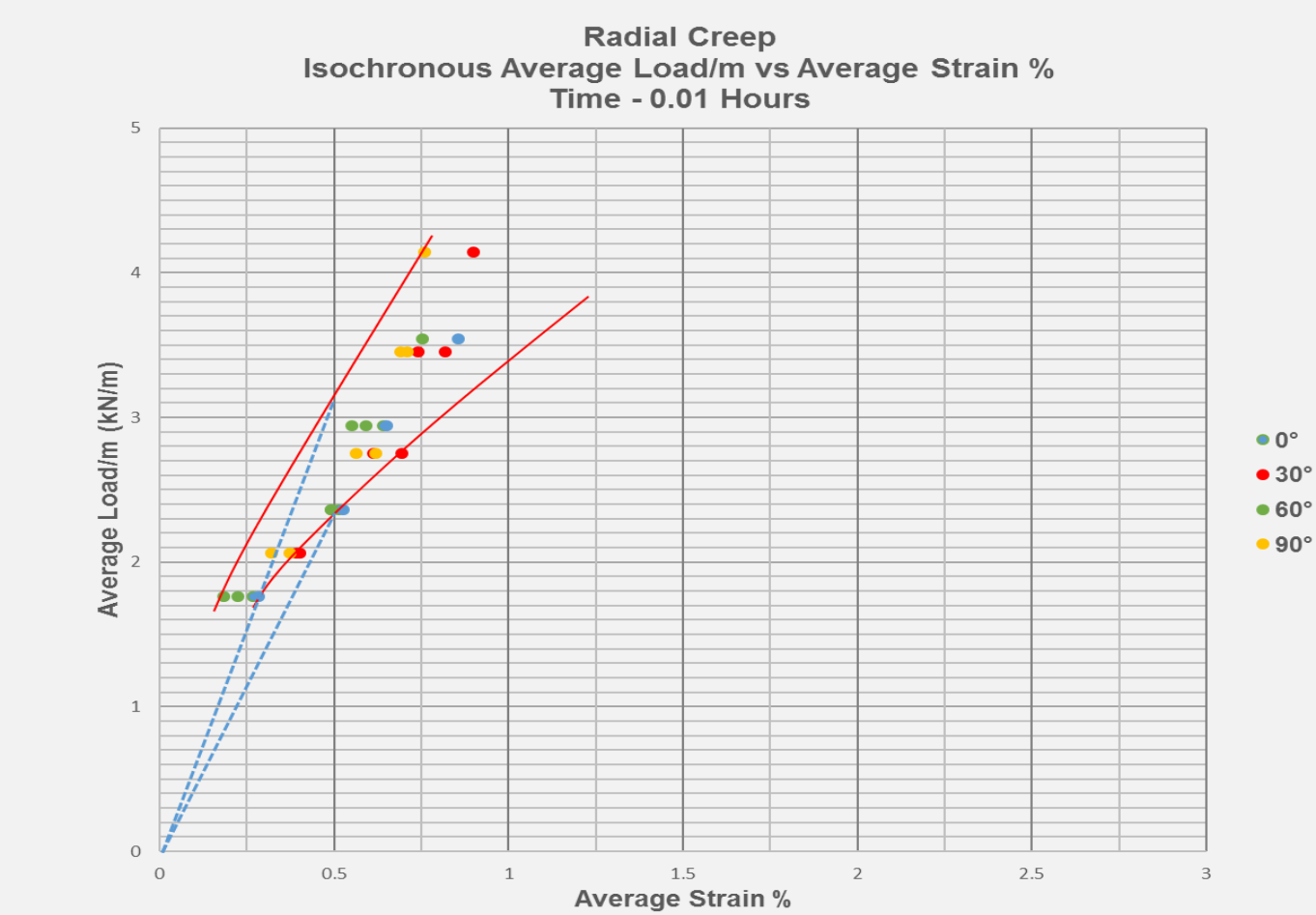


Fig 6.41 – Radial Creep, Isochronous Load-Strain curves at 0.01 hours of TX160 creep data, tested in four directions.

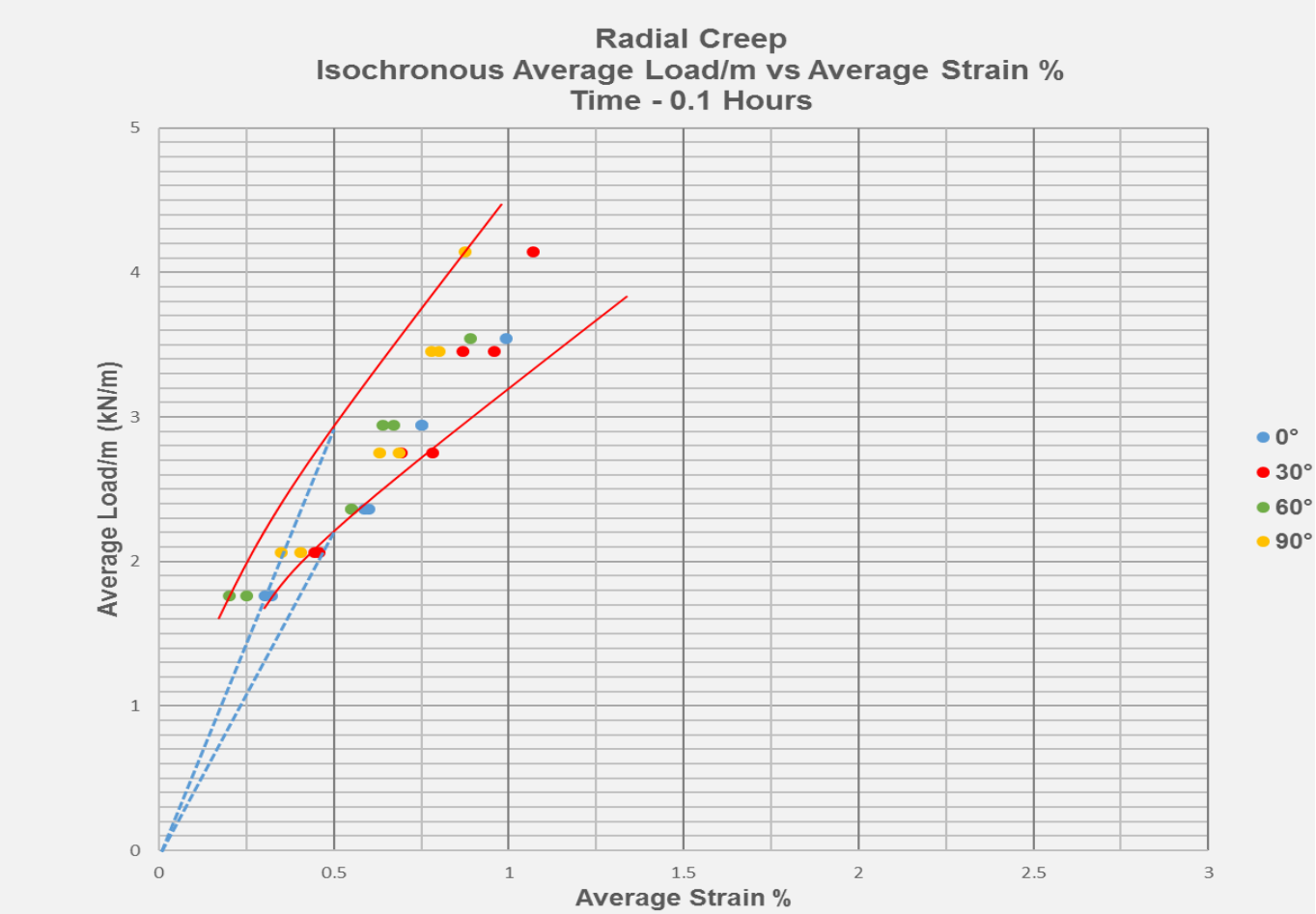


Fig 6.42 – Radial Creep, Isochronous Load-Strain curves at 0.1 hours of TX160 creep data, tested in four directions.

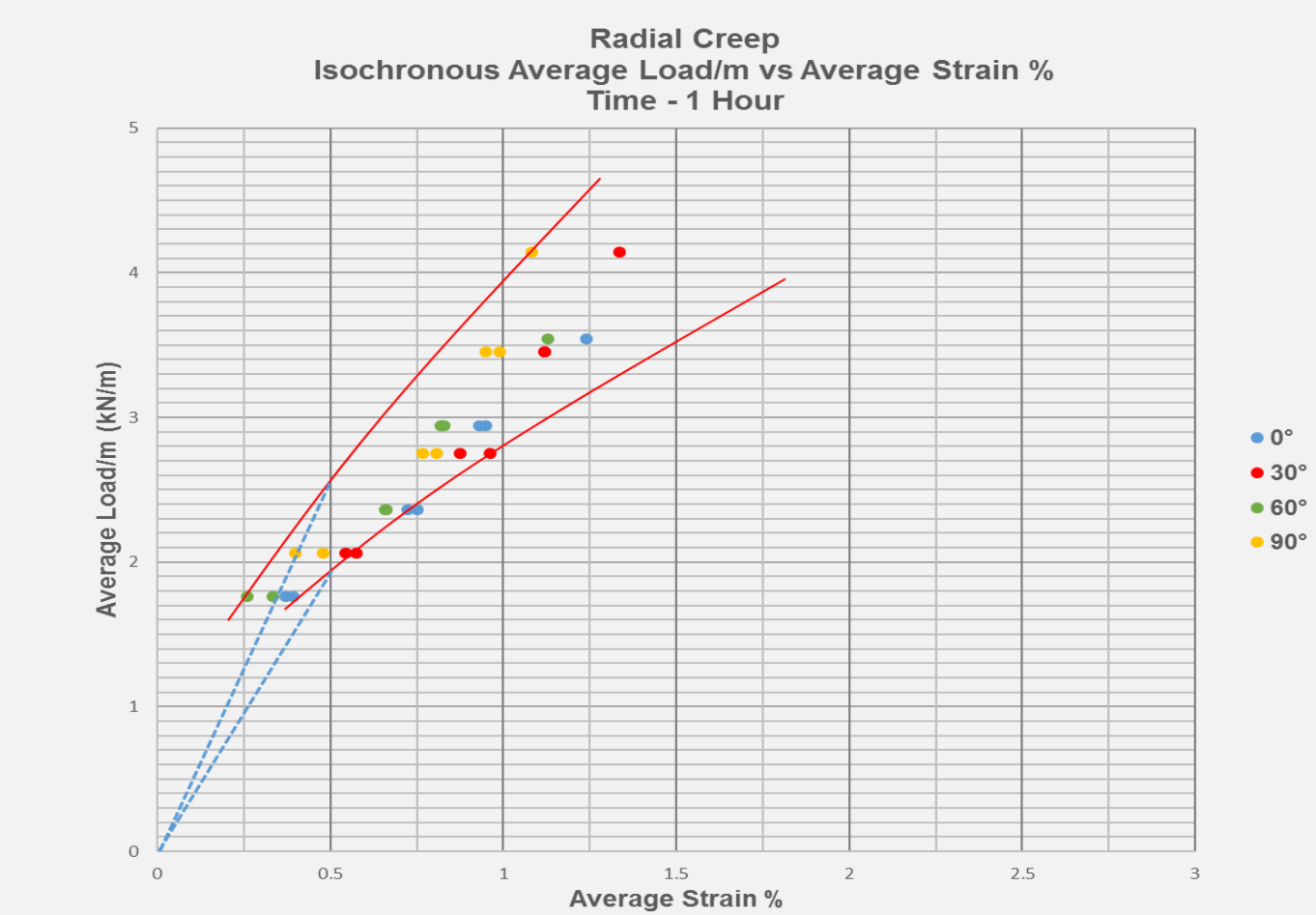


Fig 6.43 – Radial Creep, Isochronous Load-Strain curves at 1 hour of TX160 creep data, tested in four directions.

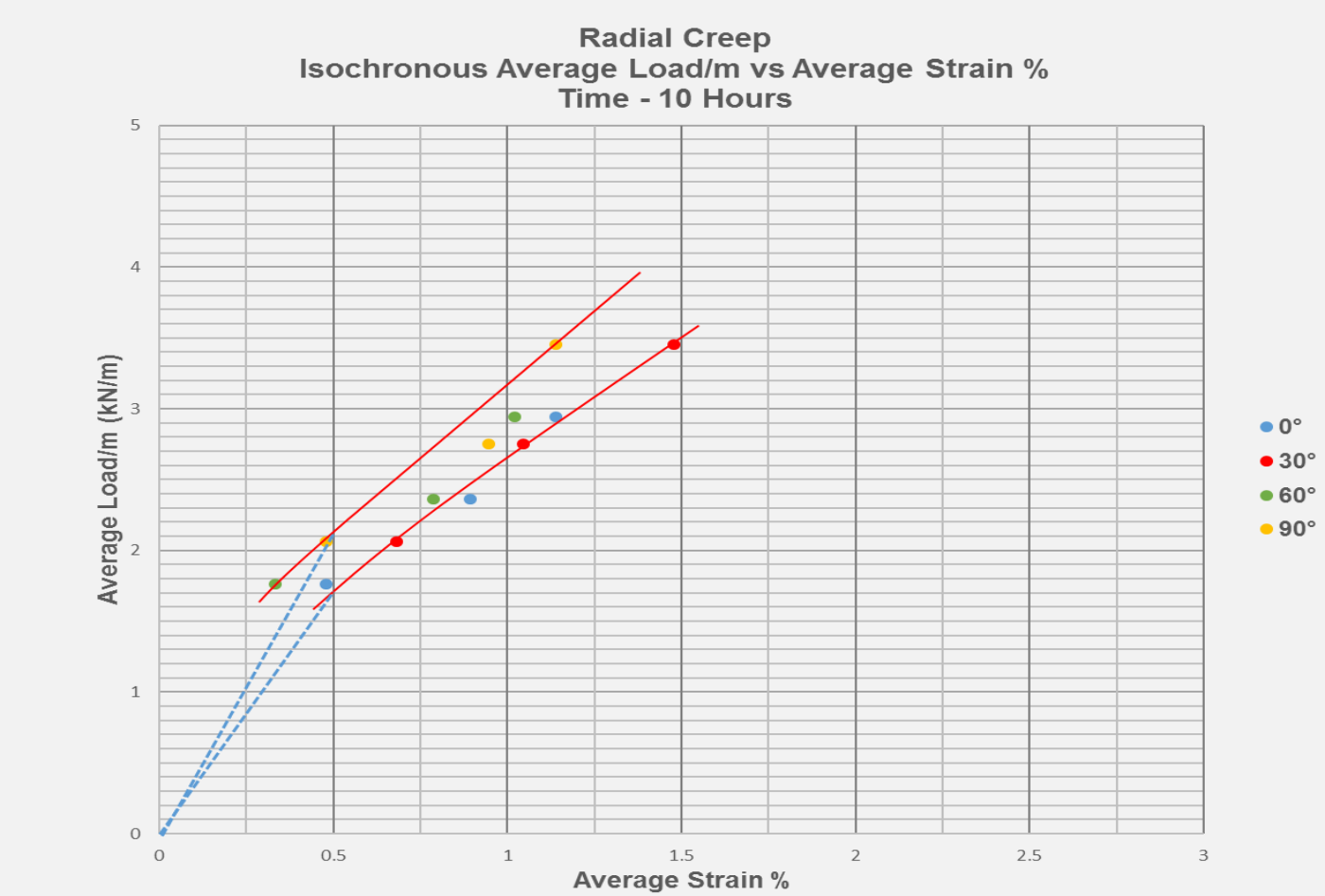


Fig 6.44 – Radial Creep, Isochronous Load-Strain curves at 10 hours of TX160 creep data, tested in four directions.

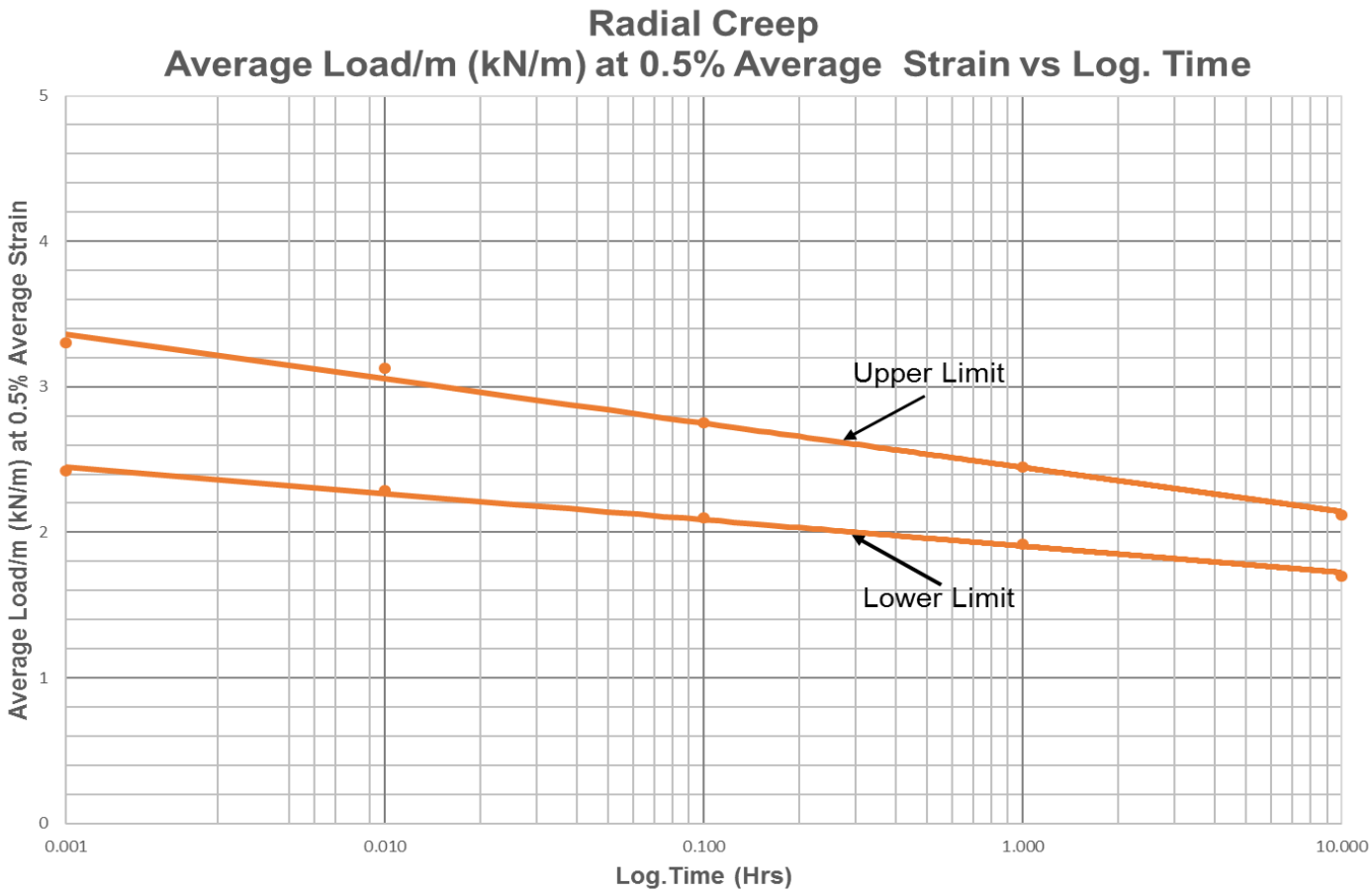


Fig 6.45 – Radial Creep, Average load at 0.5% average strain versus time (upper and lower boundaries) of TX160, tested in four directions.

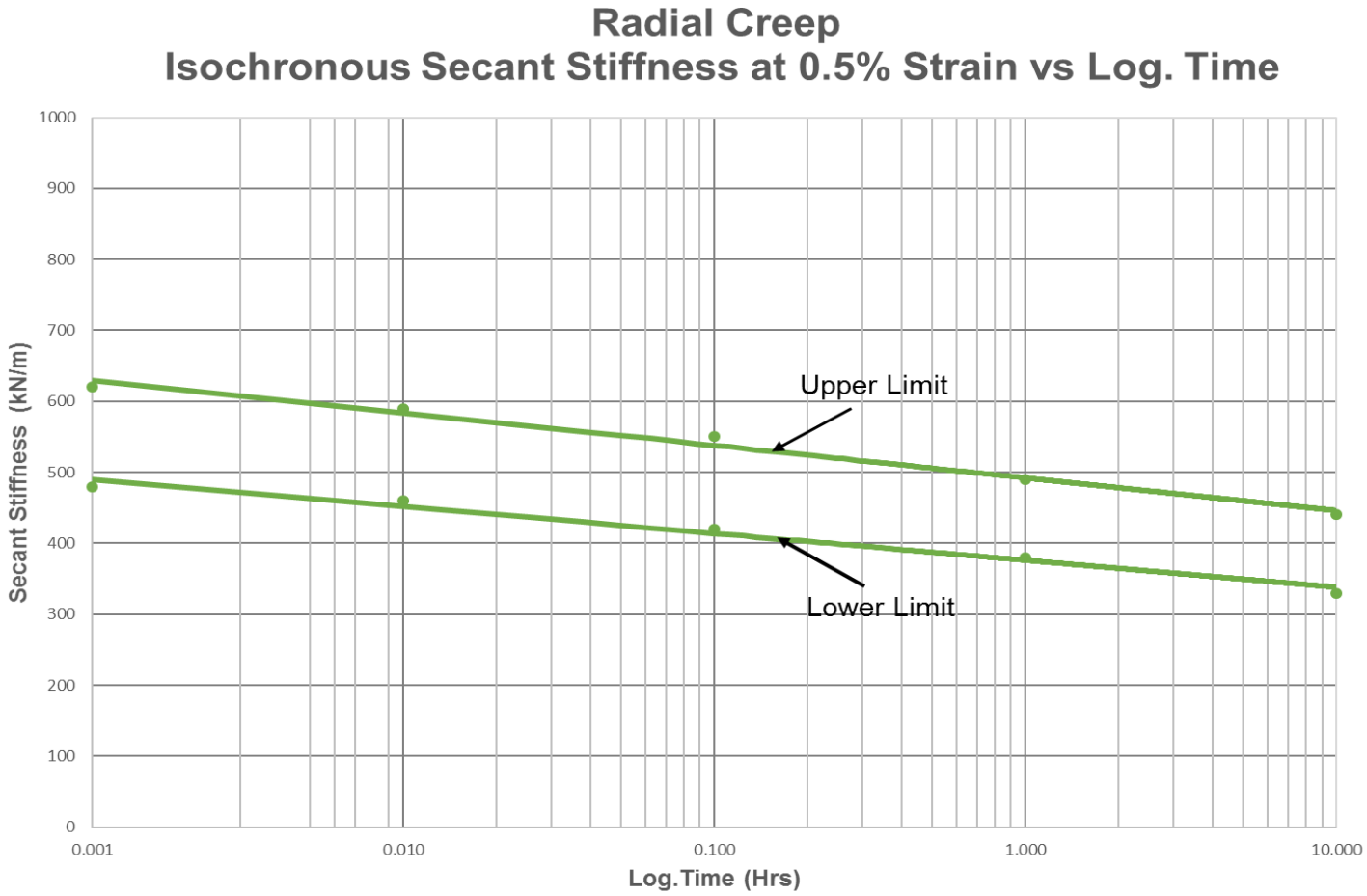


Fig 6.46 – Radial Creep, isochronous stiffness at 0.5% strain versus time (upper and lower boundaries) of TX160, tested in four directions.

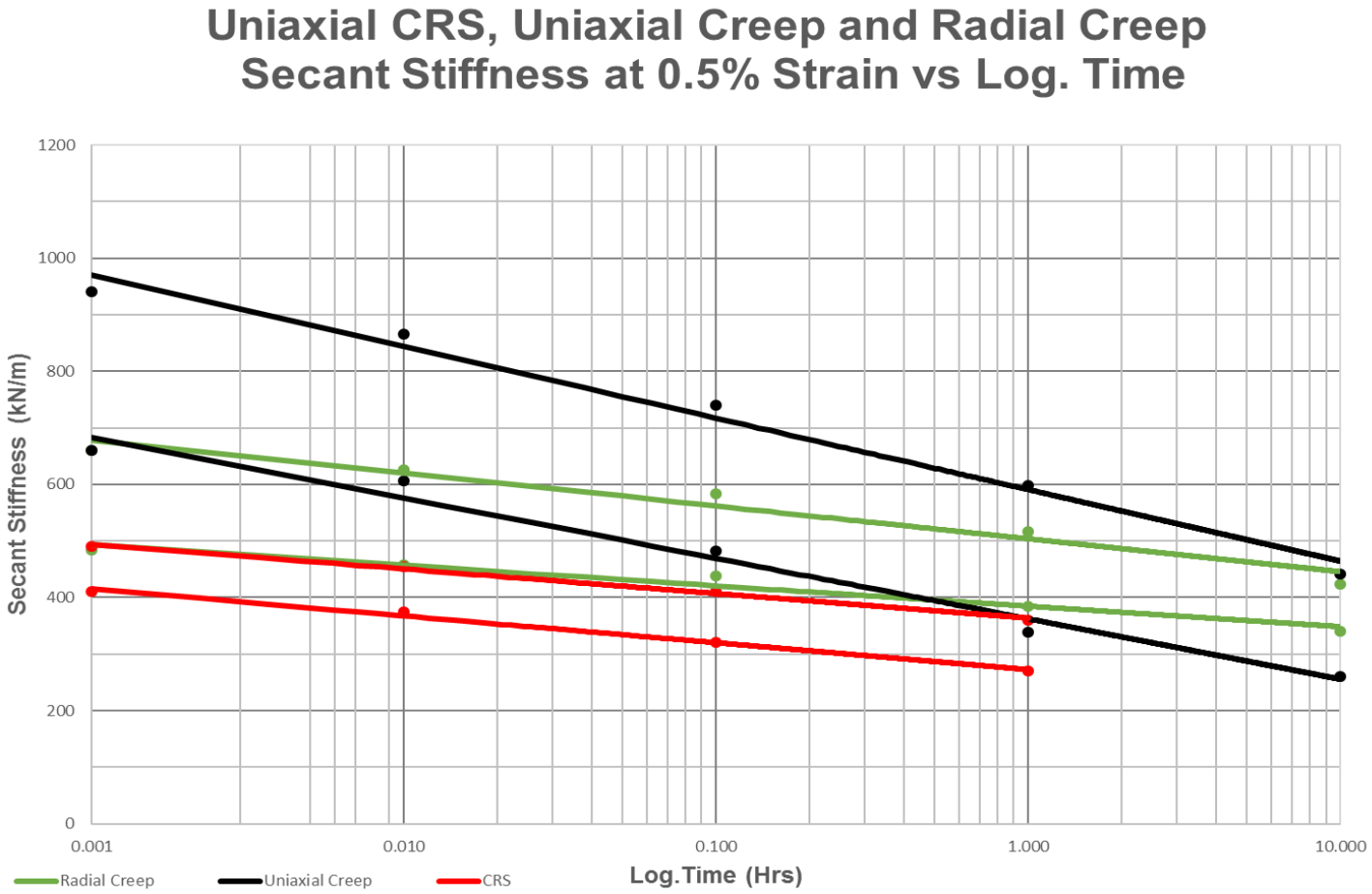


Fig 7.1 – Comparison of Secant Stiffness at 0.5% Strain vs Log Time of Uniaxial CRS, Uniaxial Creep, and Radial Creep test data.

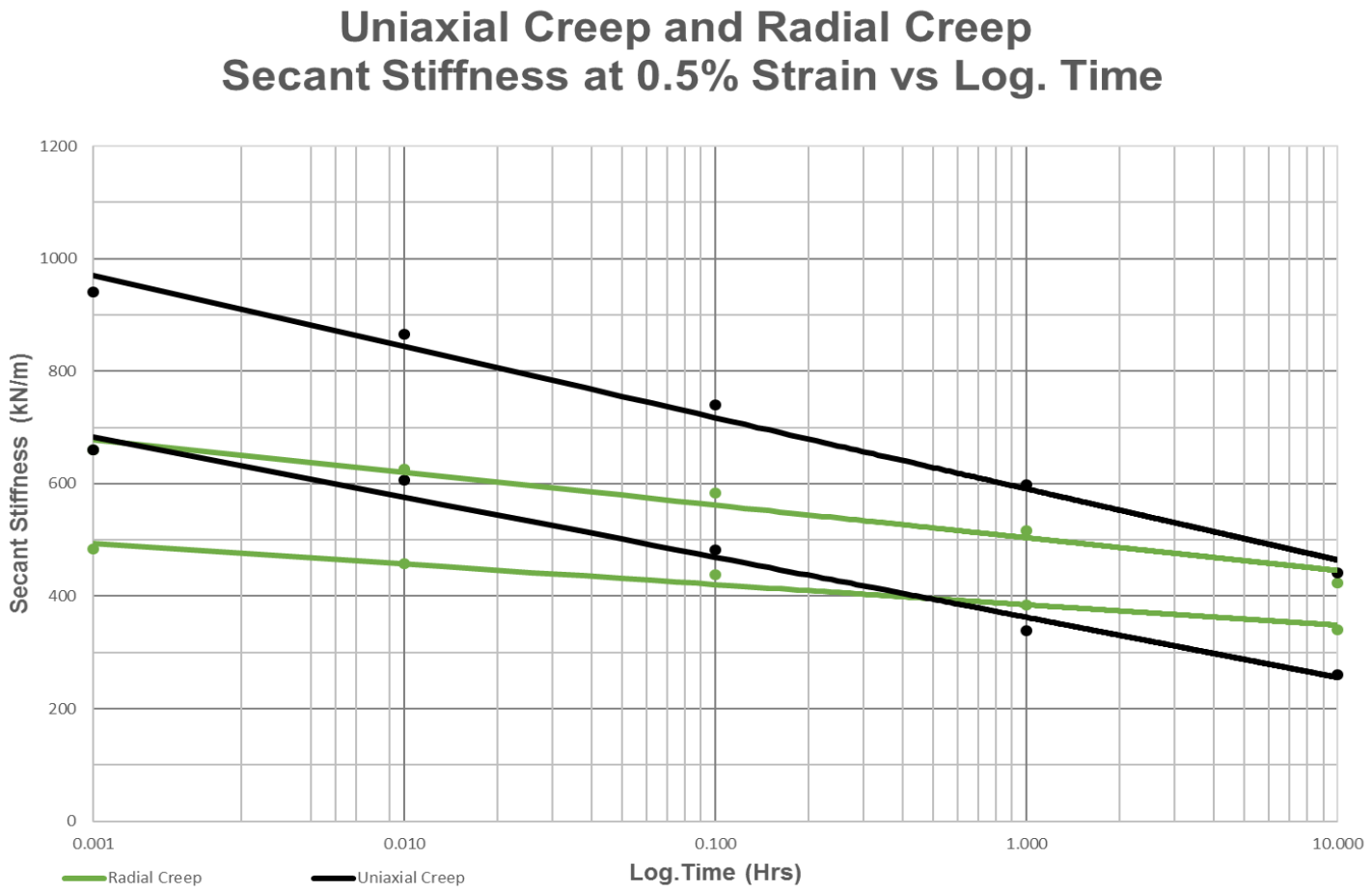


Fig 7.2 – Comparison of Secant Stiffness at 0.5% Strain vs Log Time Uniaxial Creep, and Radial Creep test data.

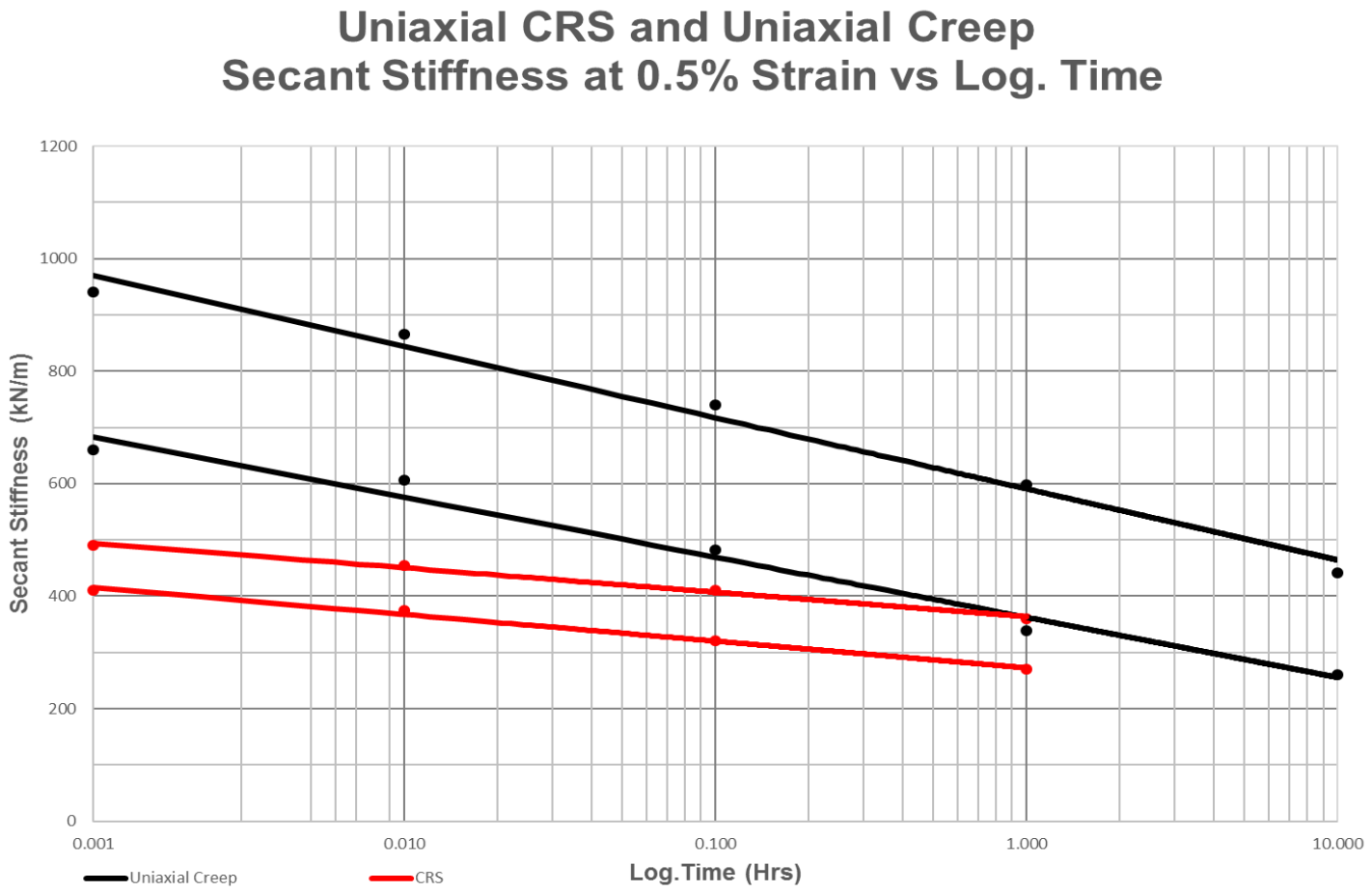


Fig 7.3 – Comparison of Secant Stiffness at 0.5% Strain vs Log Time Uniaxial CRS and Uniaxial Creep test data.

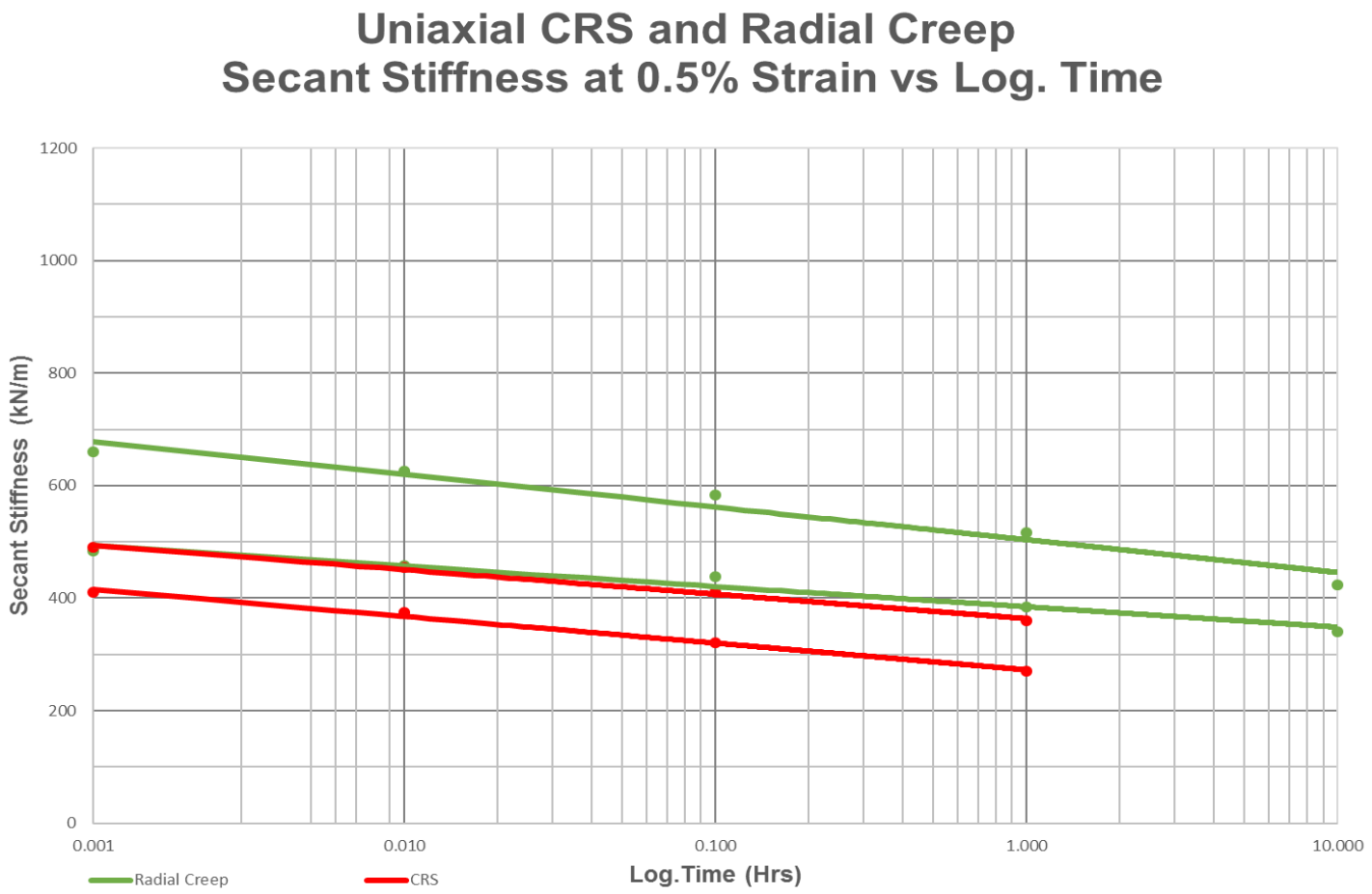


Fig 7.4 – Comparison of Secant Stiffness at 0.5% Strain vs Log Time Uniaxial CRS, and Radial Creep test data.

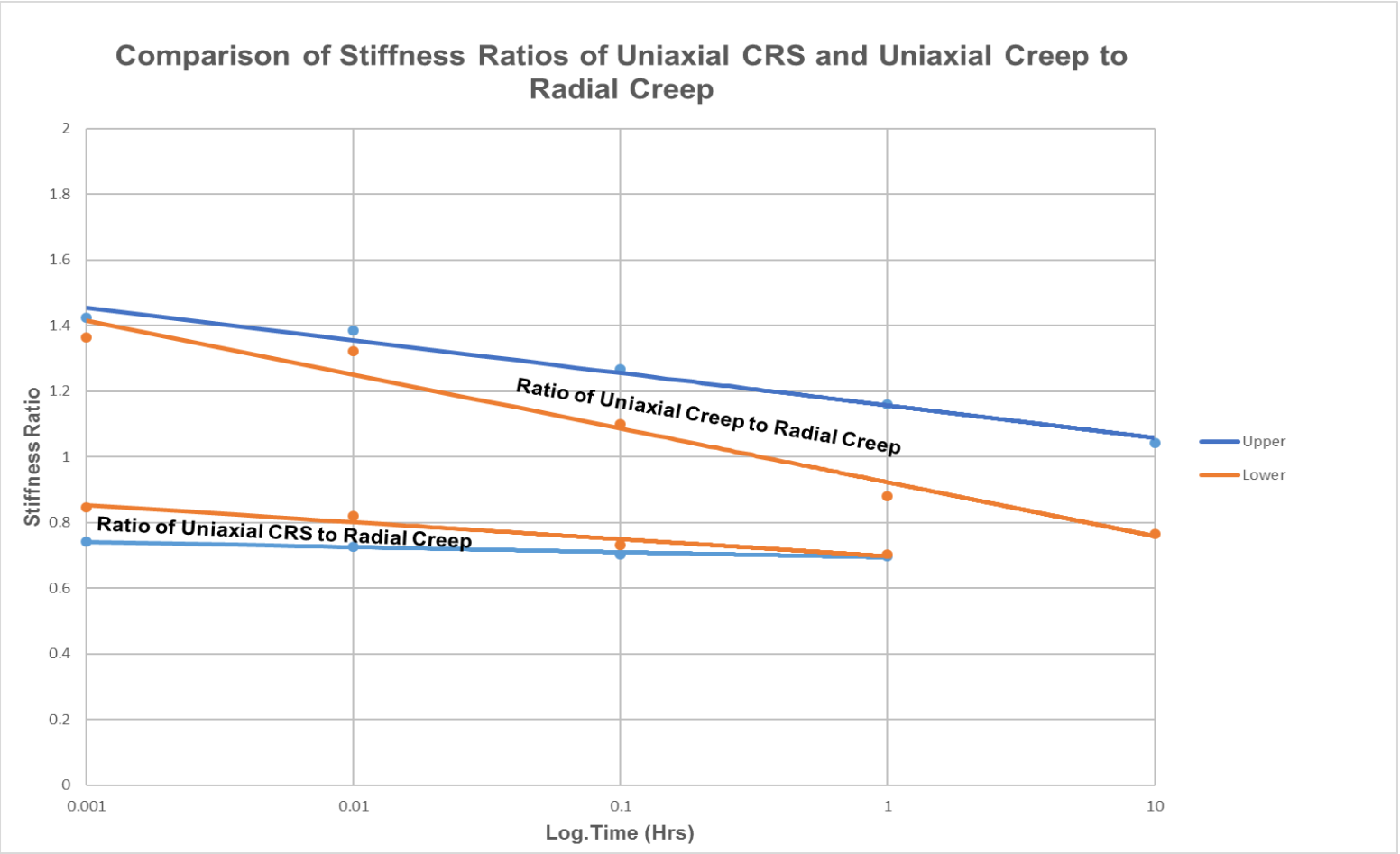


Fig 7.5 – Comparison of Stiffness Ratios of Uniaxial Creep-to-Radial Creep and Uniaxial CRS-to-Radial Creep.

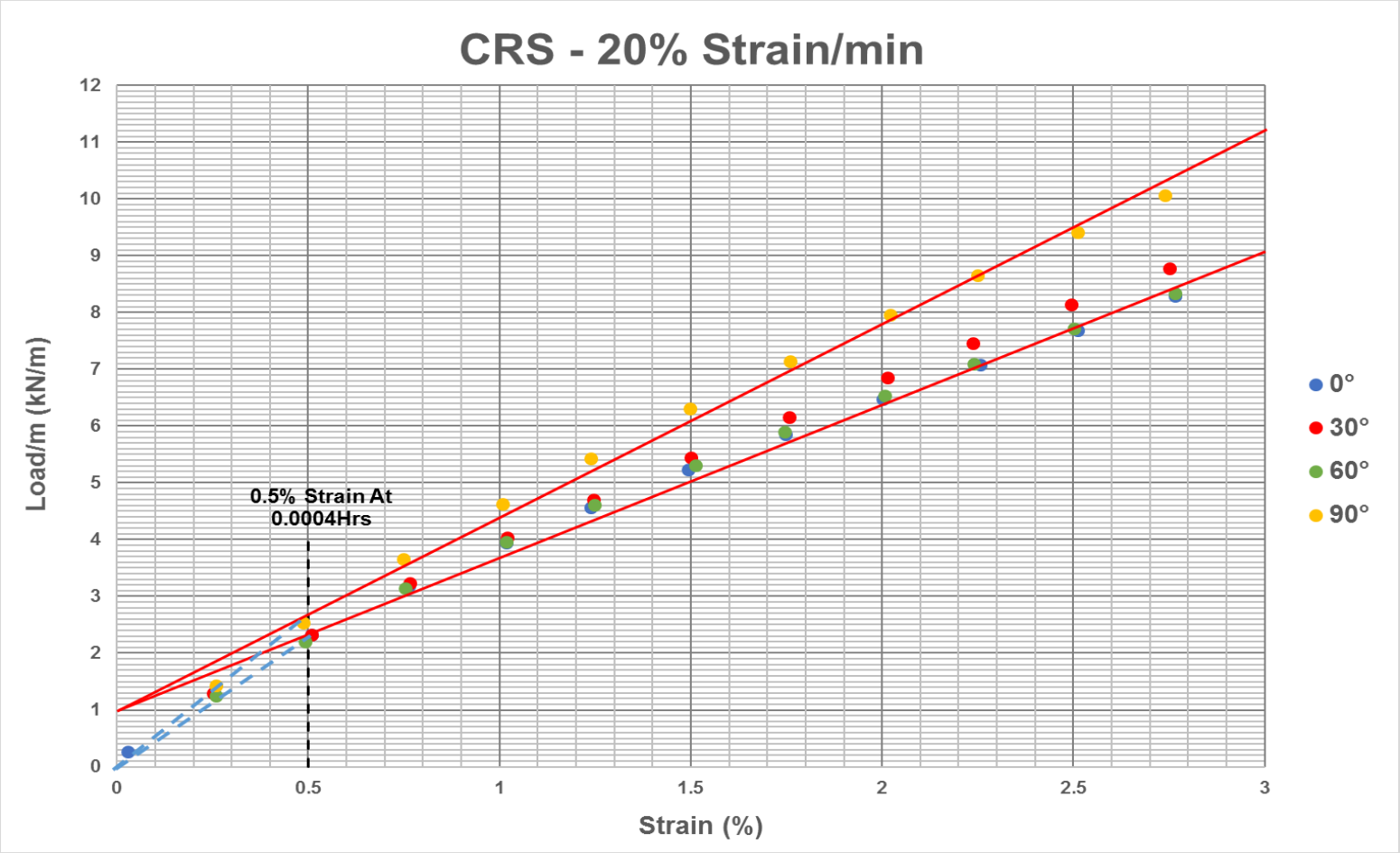


Fig 7.6 – CRS, Load/m vs Strain plot of TX160 tested at 20% strain/min in all four directions, with best fit upper and lower boundaries lines passing through locked-in stress of 1kN/m.

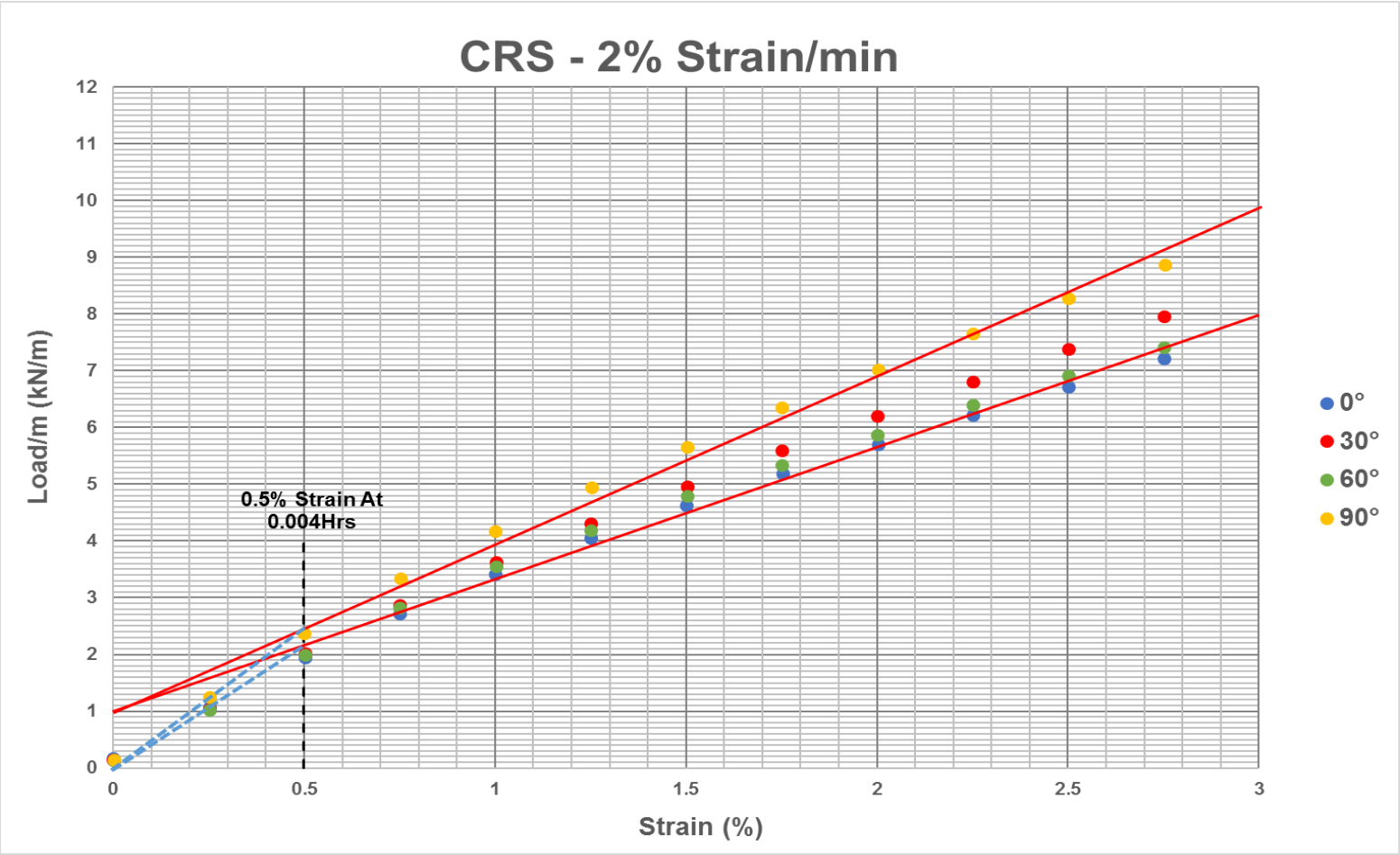


Fig 7.7 – CRS, Load/m vs Strain plot of TX160 tested at 2% strain/min in all four directions, with best fit upper and lower boundaries lines passing through locked-in stress of 1kN/m.

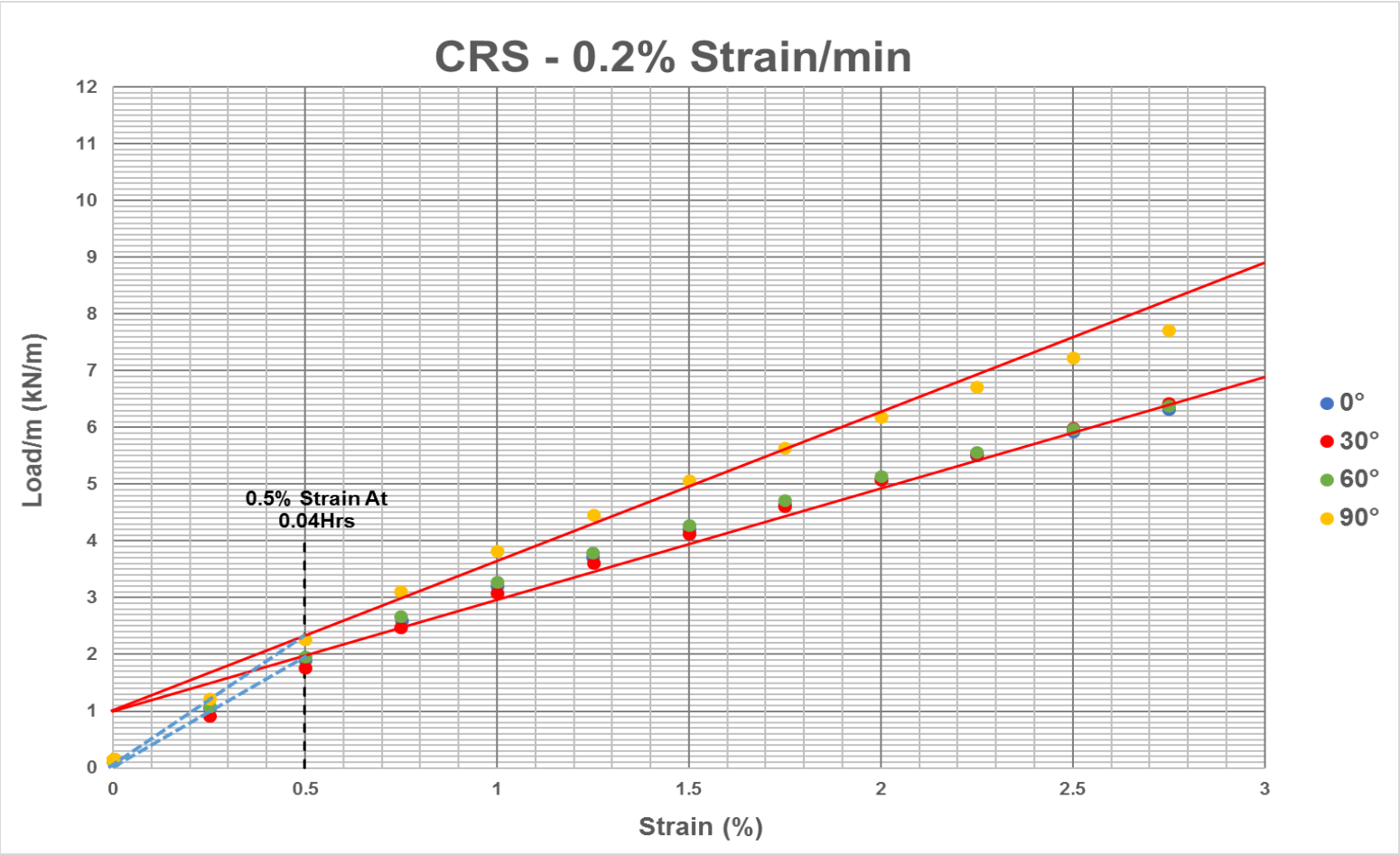


Fig 7.8 – CRS, Load/m vs Strain plot of TX160 tested at 0.2% strain/min in all four directions, with best fit upper and lower boundaries lines passing through locked-in stress of 1kN/m.

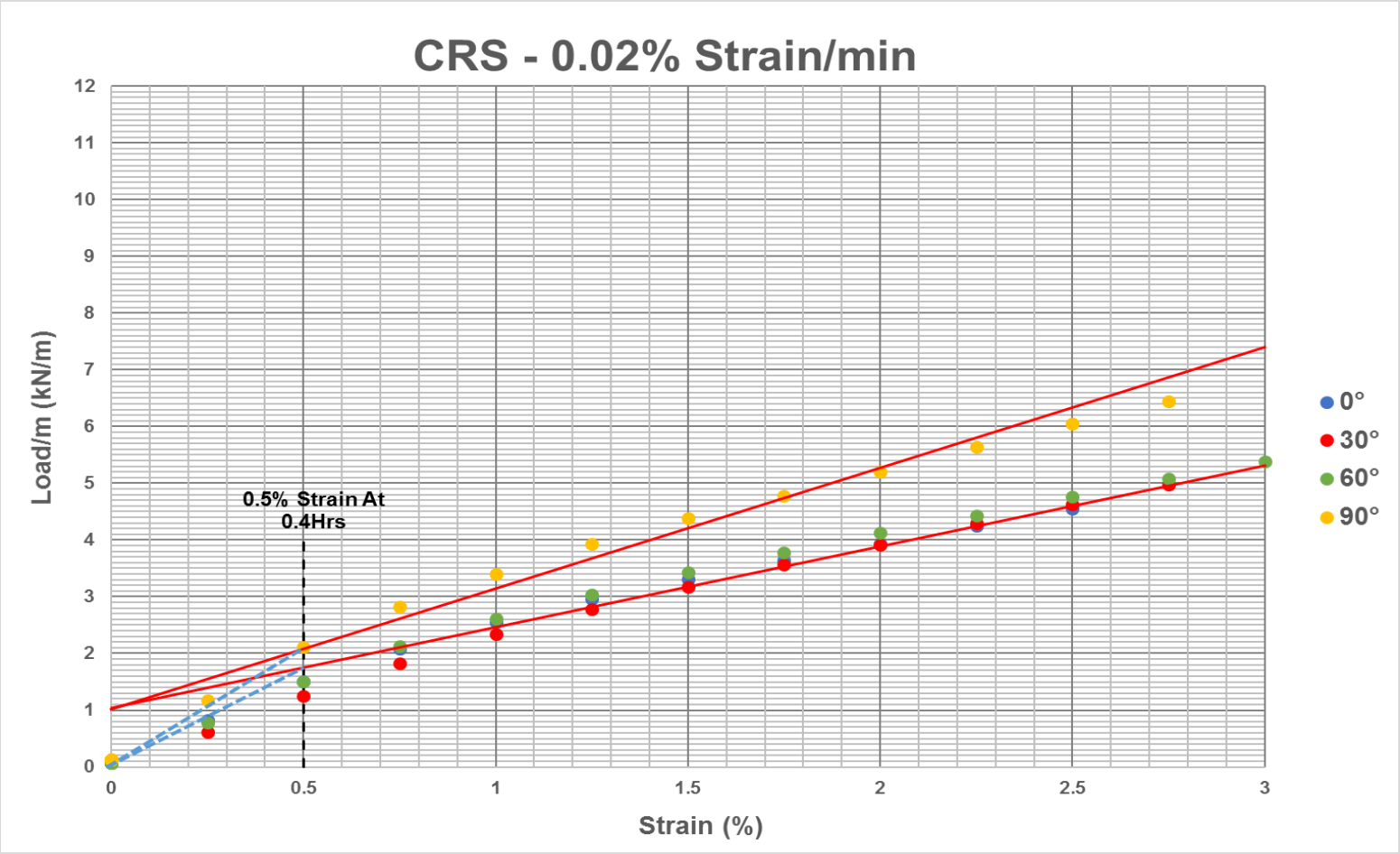


Fig 7.9 – CRS, Load/m vs Strain plot of TX160 tested at 0.02% strain/min in all four directions, with best fit upper and lower boundaries lines passing through locked-in stress of 1kN/m.

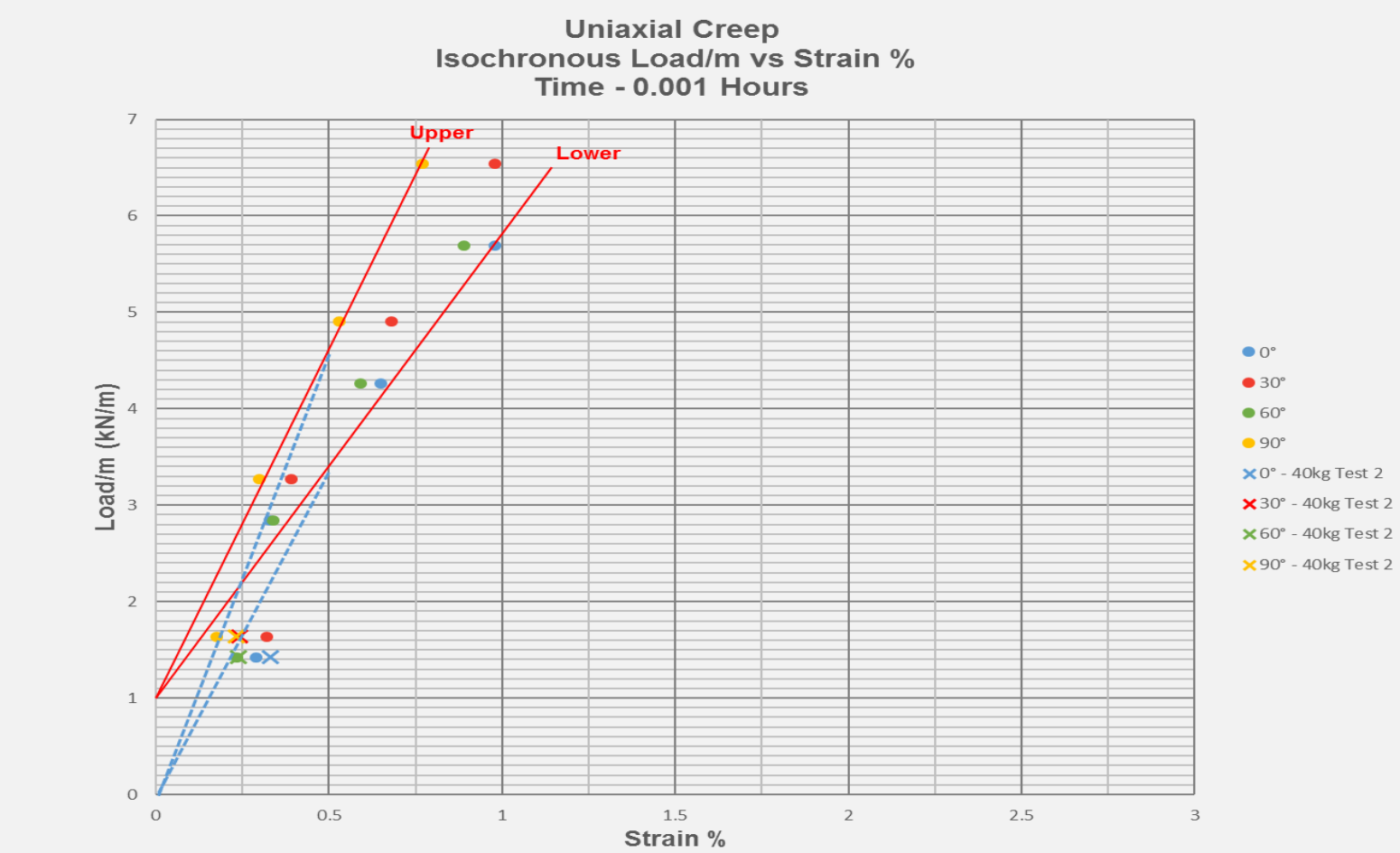


Fig 7.10 – Uniaxial Creep, Isochronous Load-Strain curves at 0.001 hours of TX160 creep data, tested in four directions with best fit upper and lower boundaries passing through locked-in stress of 1kN/m.

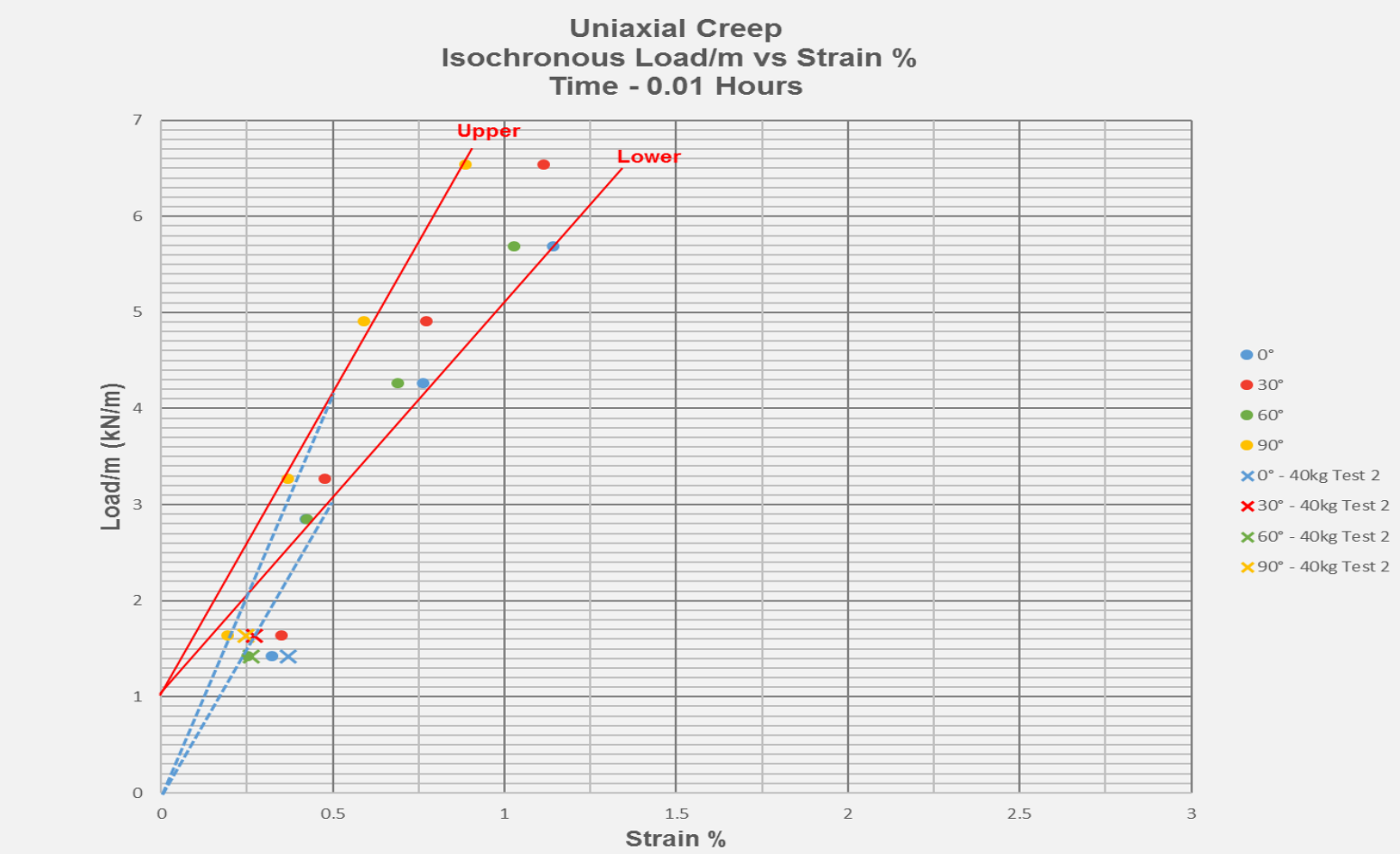


Fig 7.11 – Uniaxial Creep, Isochronous Load-Strain curves at 0.01 hours of TX160 creep data, tested in four directions with best fit upper and lower boundaries passing through locked-in stress of 1kN/m.

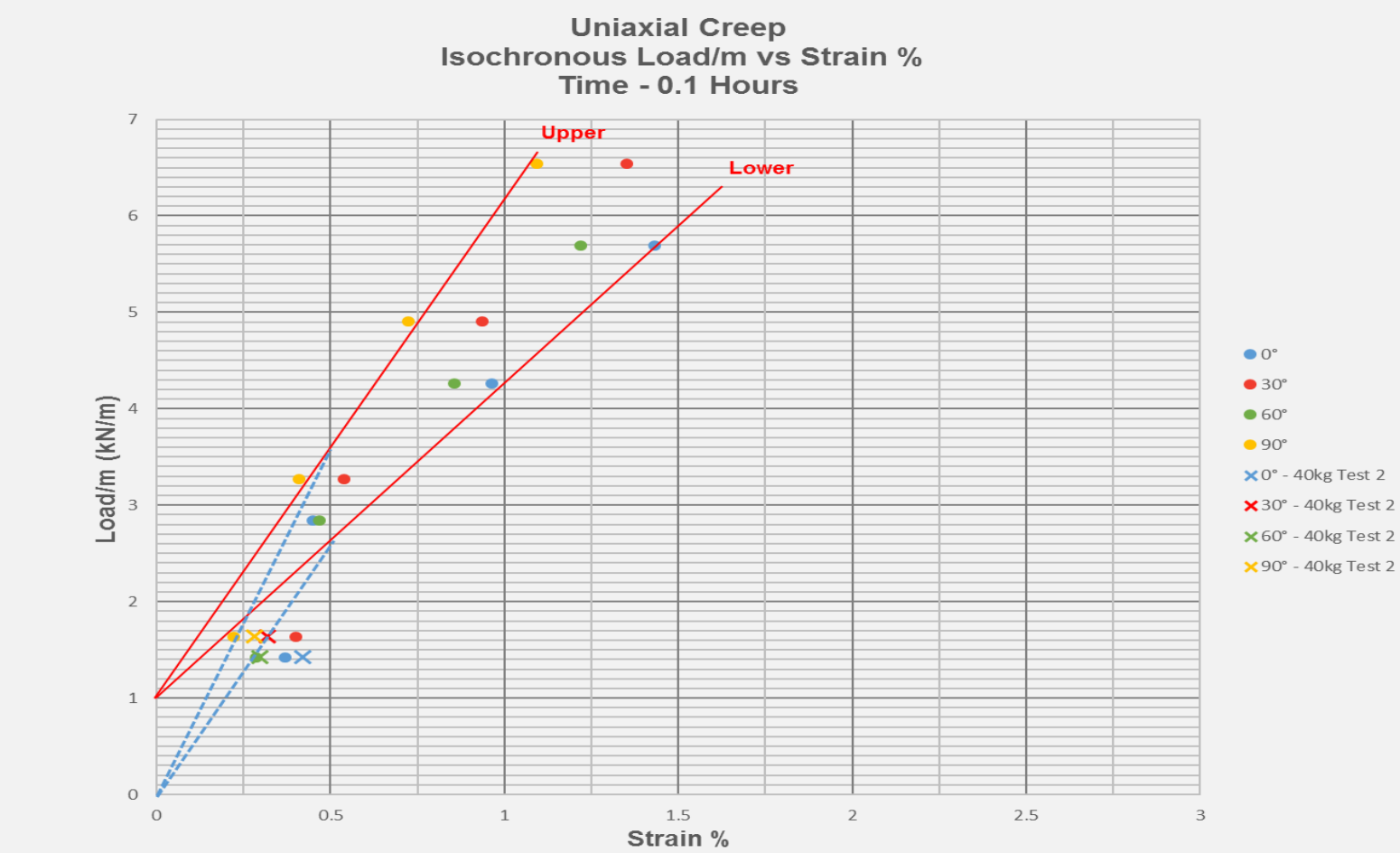


Fig 7.12 – Uniaxial Creep, Isochronous Load-Strain curves at 0.1 hours of TX160 creep data, tested in four directions with best fit upper and lower boundaries passing through locked-in stress of 1kN/m.

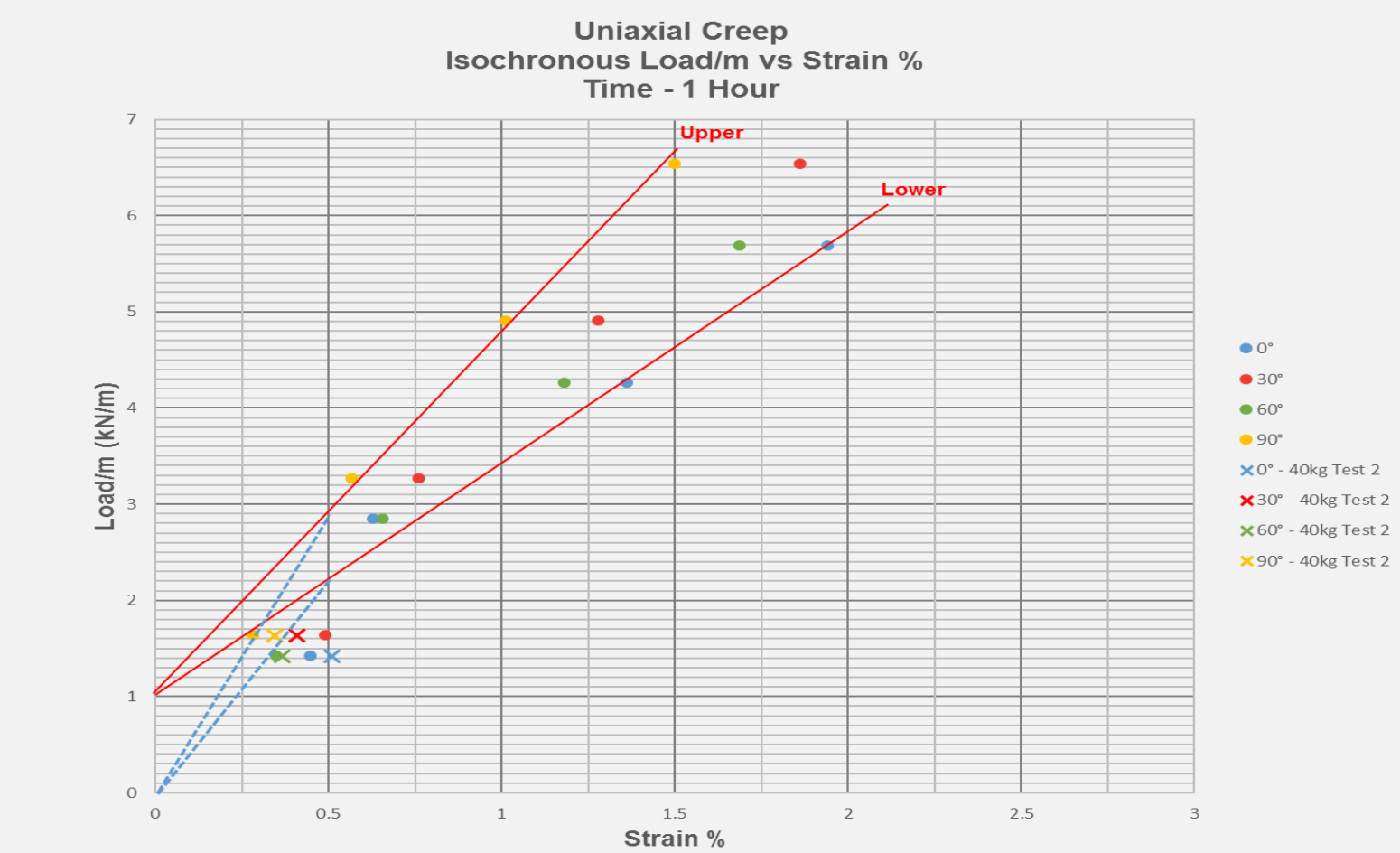


Fig 7.13 – Uniaxial Creep, Isochronous Load-Strain curves at 1 hour of TX160 creep data, tested in four directions with best fit upper and lower boundaries passing through locked-in stress of 1kN/m.

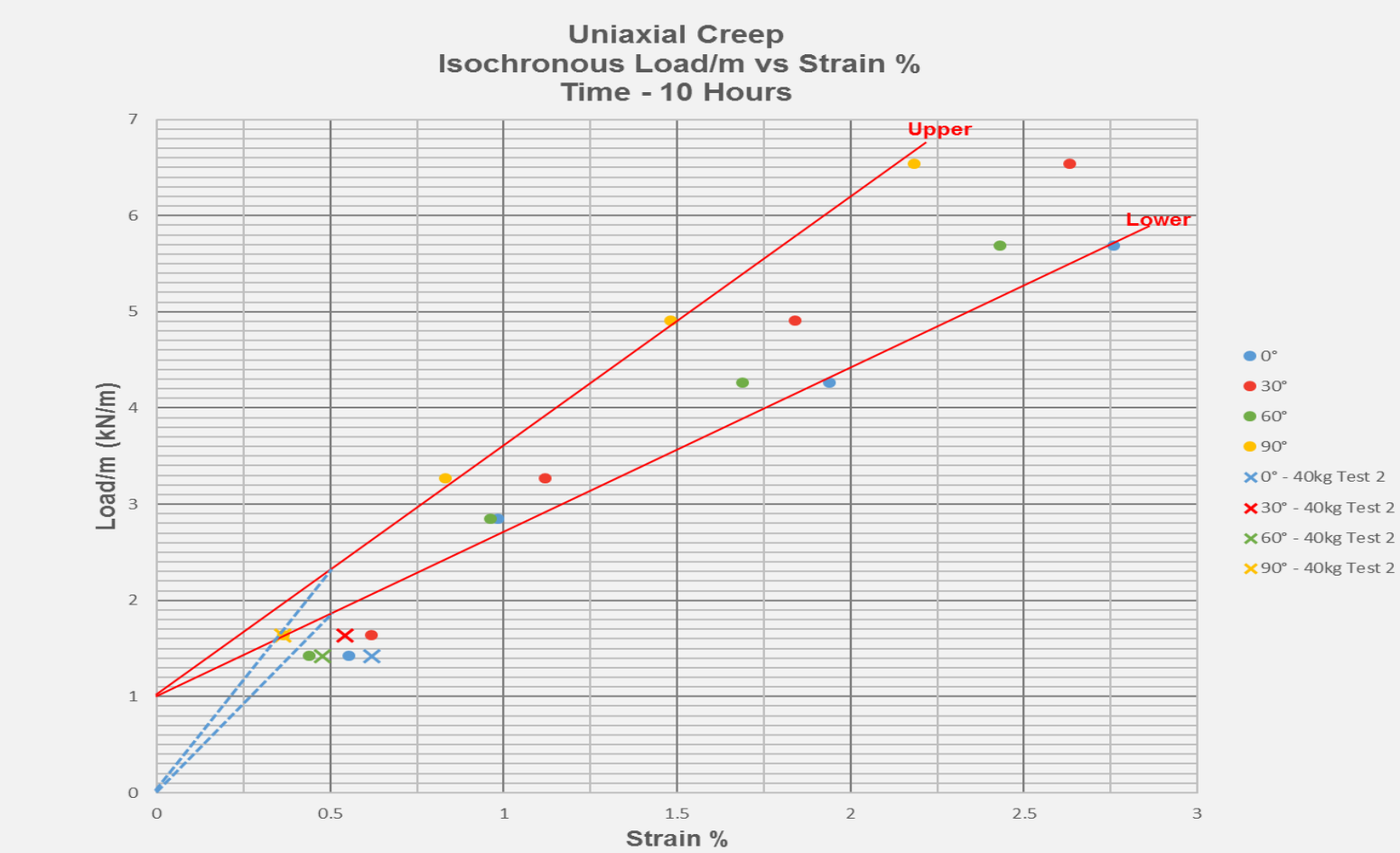


Fig 7.14 – Uniaxial Creep, Isochronous Load-Strain curves at 10 hours of TX160 creep data, tested in four directions with best fit upper and lower boundaries passing through locked-in stress of 1kN/m.

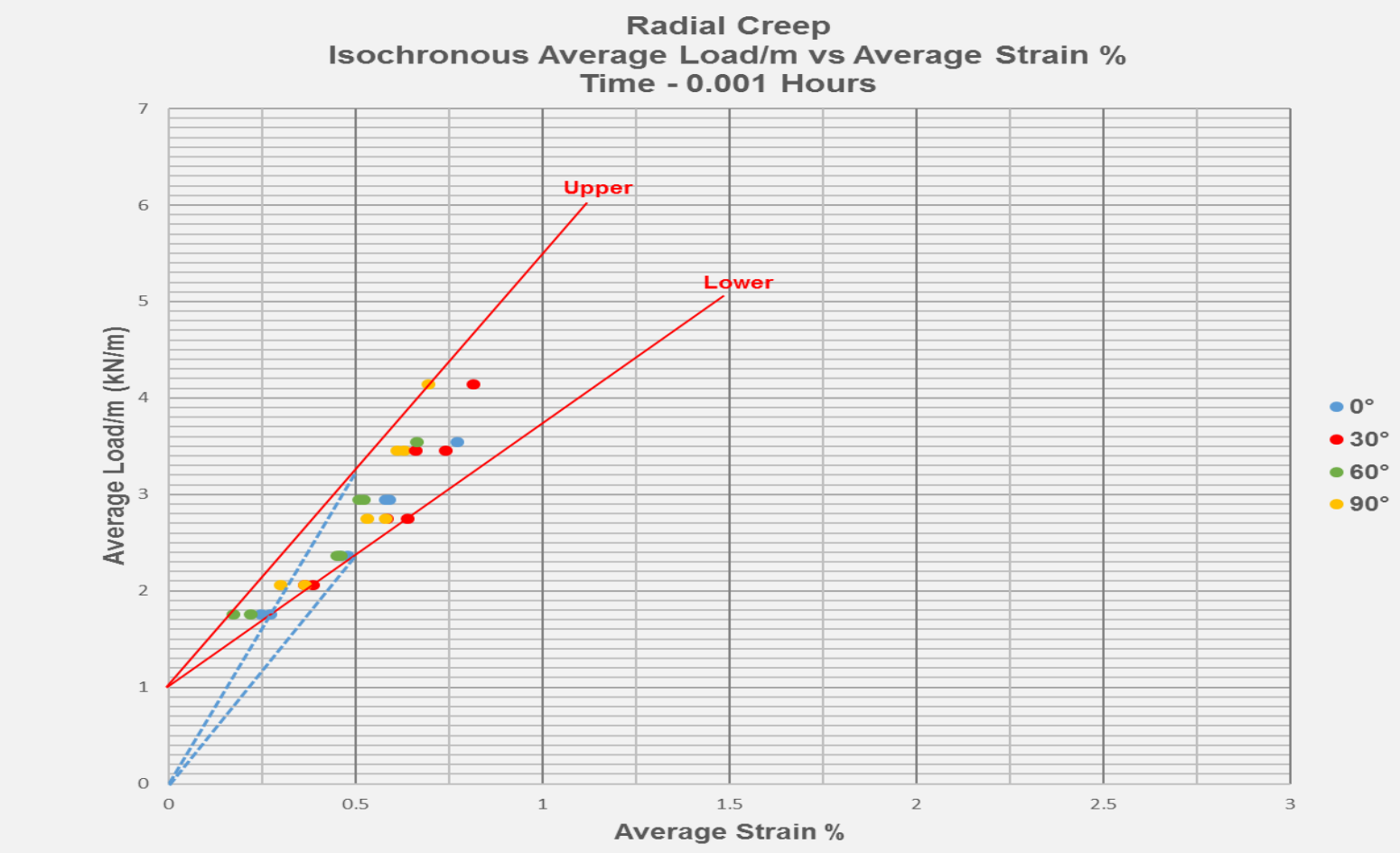


Fig 7.15 – Radial Creep, Isochronous Load-Strain curves at 0.001 hours of TX160 creep data, tested in four directions with best fit upper and lower boundaries passing through locked-in stress of 1kN/m.

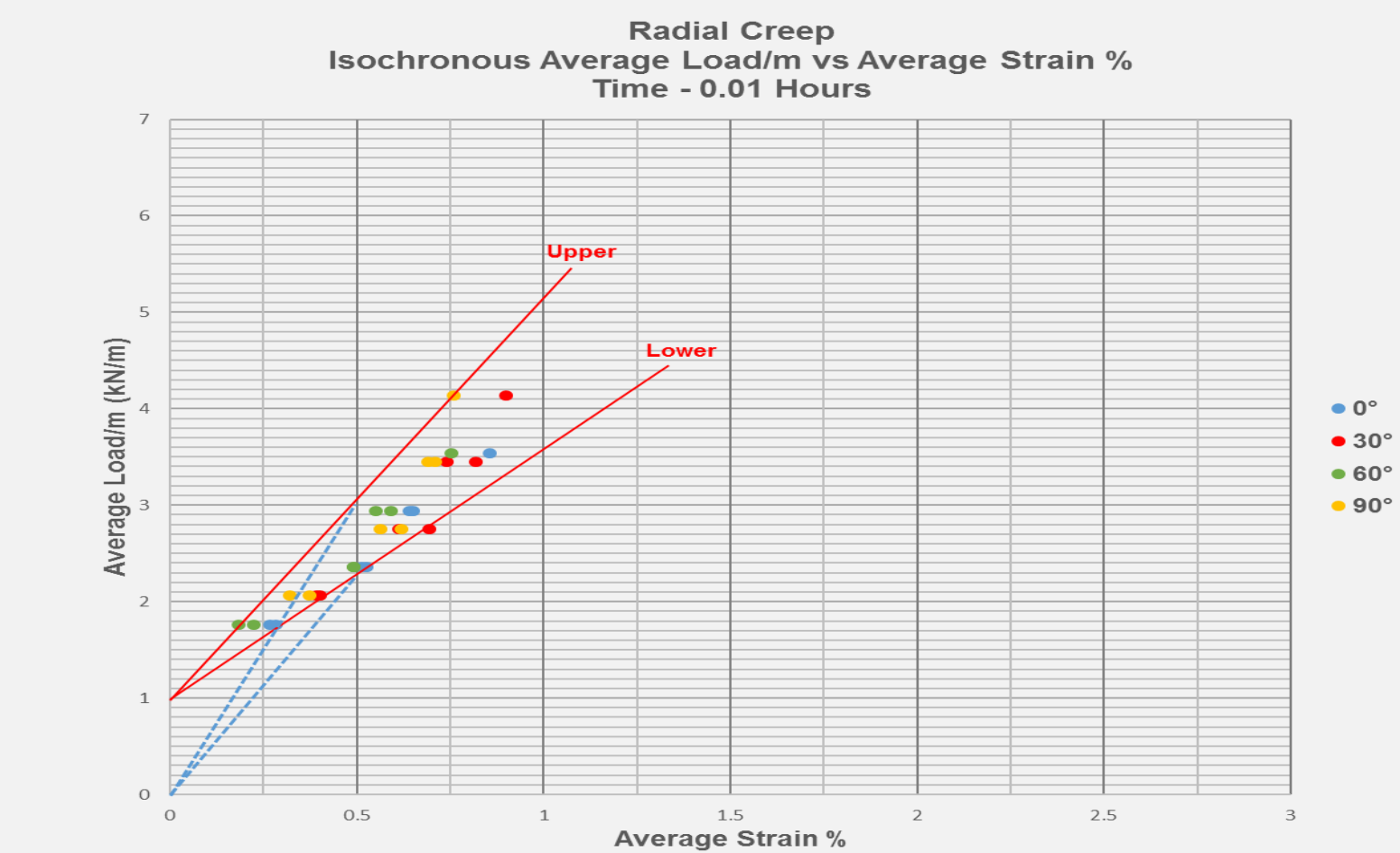


Fig 7.16 – Radial Creep, Isochronous Load-Strain curves at 0.01 hours of TX160 creep data, tested in four directions with best fit upper and lower boundaries passing through locked-in stress of 1kN/m.

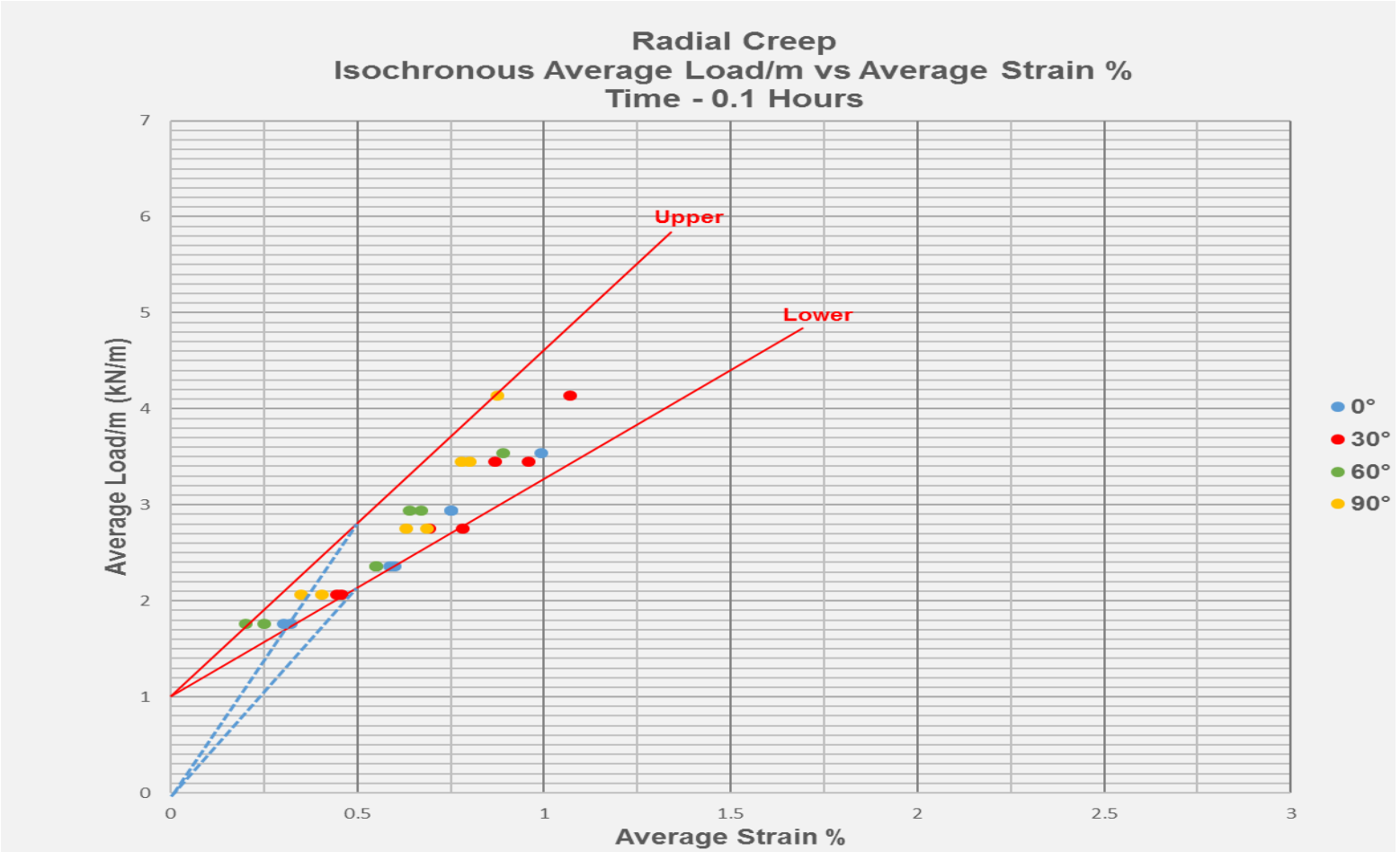


Fig 7.17 – Radial Creep, Isochronous Load-Strain curves at 0.1 hours of TX160 creep data, tested in four directions with best fit upper and lower boundaries passing through locked-in stress of 1kN/m.

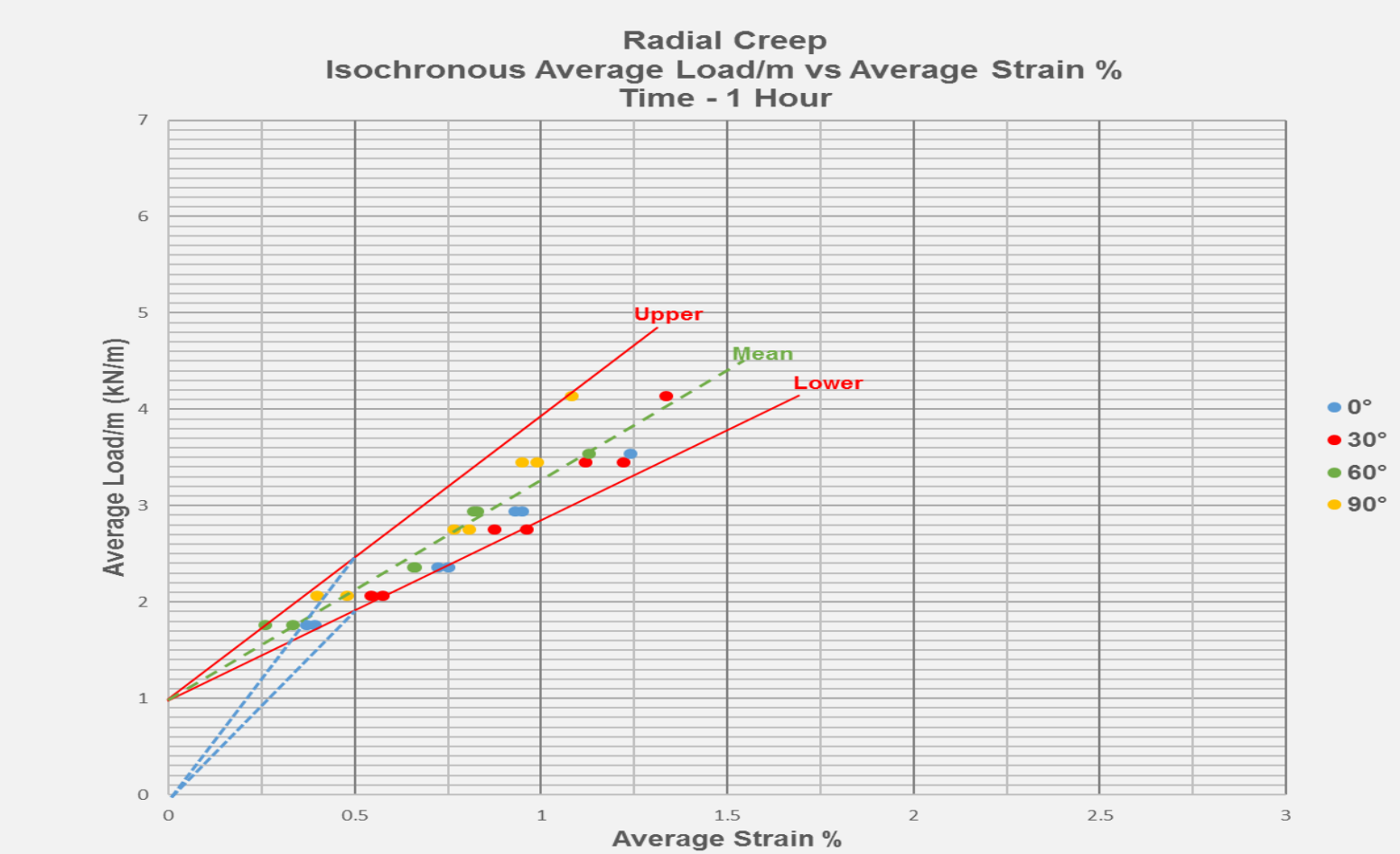


Fig 7.18 – Radial Creep, Isochronous Load-Strain curves at 1 hour of TX160 creep data, tested in four directions with best fit upper and lower boundaries passing through locked-in stress of 1kN/m.

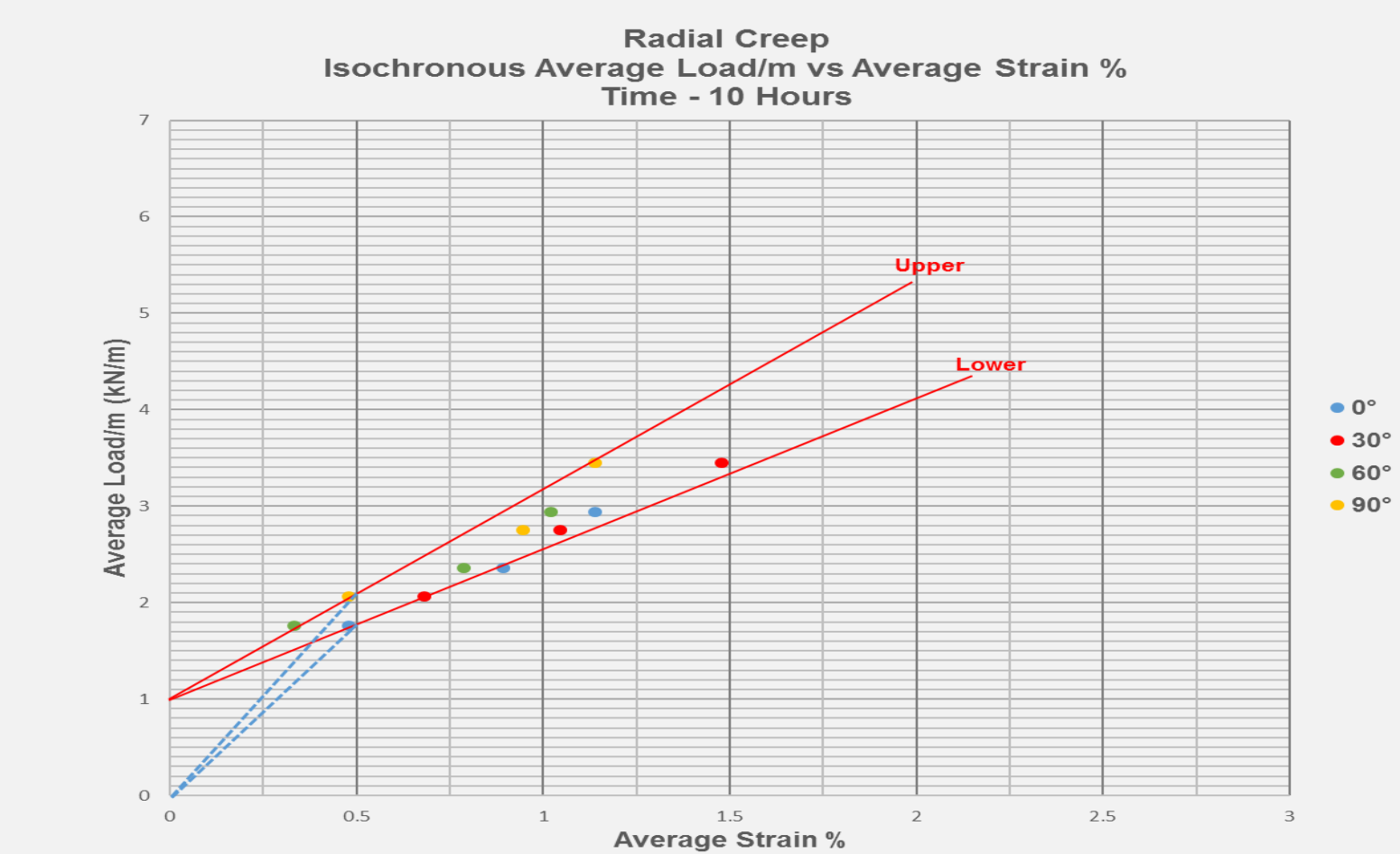


Fig 7.19 – Radial Creep, Isochronous Load-Strain curves at 10 hours of TX160 creep data, tested in four directions with best fit upper and lower boundaries passing through locked-in stress of 1kN/m.

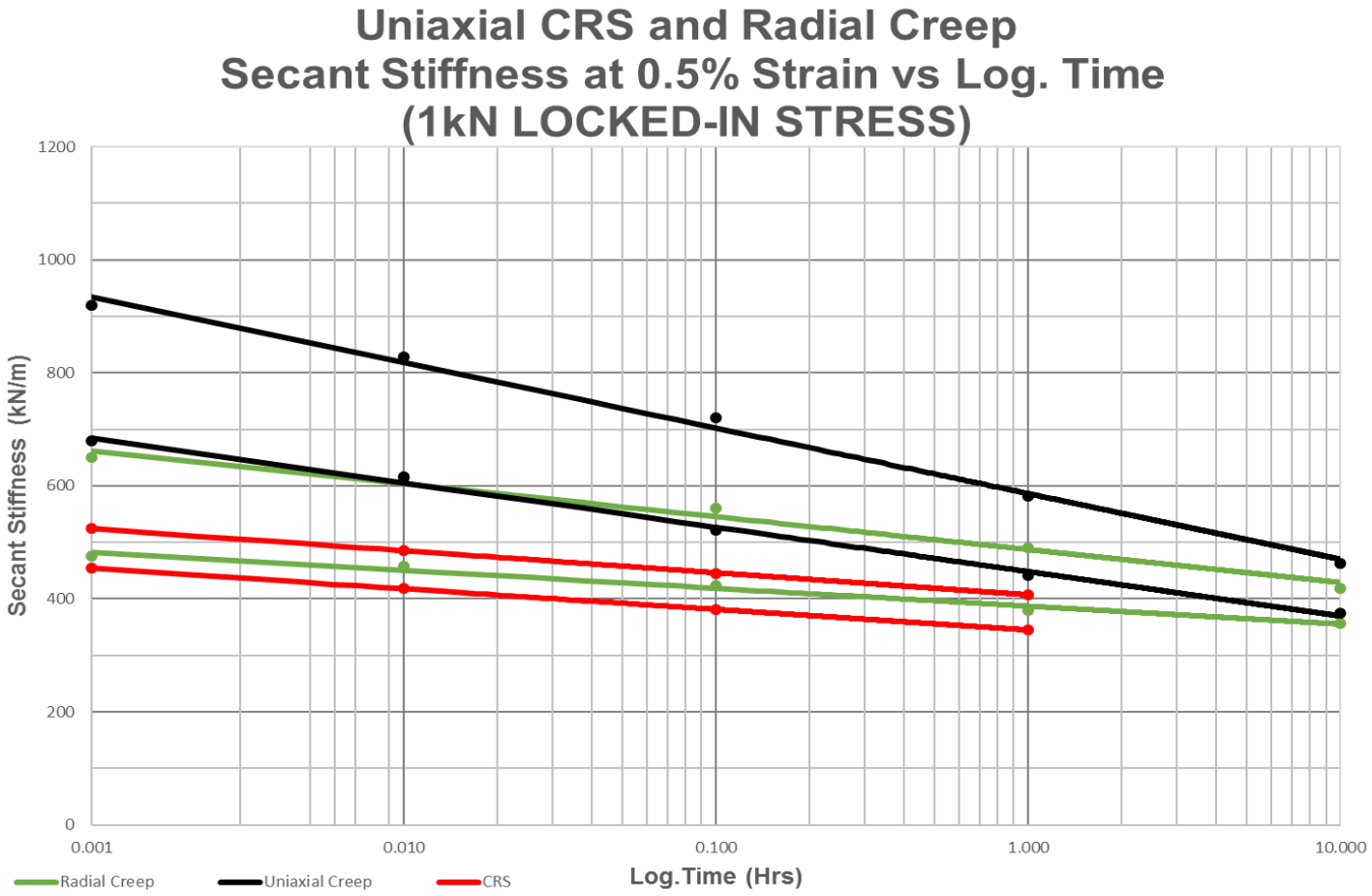


Fig 7.20 – Comparison of Secant Stiffness at 0.5% Strain vs Log Time of Uniaxial CRS, Uniaxial Creep, and Radial Creep test data.

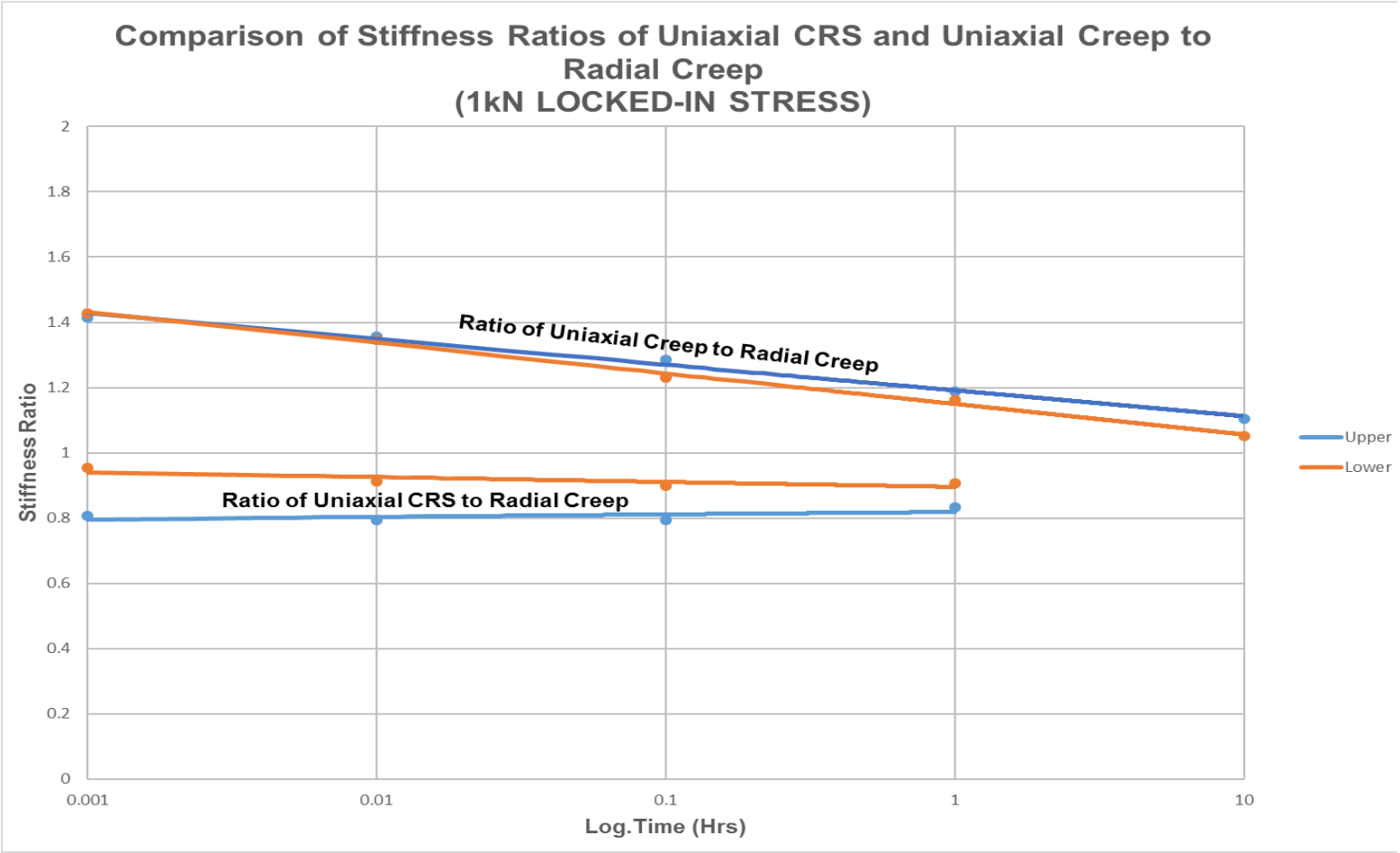


Fig 7.21 – Comparison of Stiffness Ratios of Uniaxial Creep-to-Radial Creep and Uniaxial CRS-to-Radial Creep when using a 1kN/m locked-in stress.

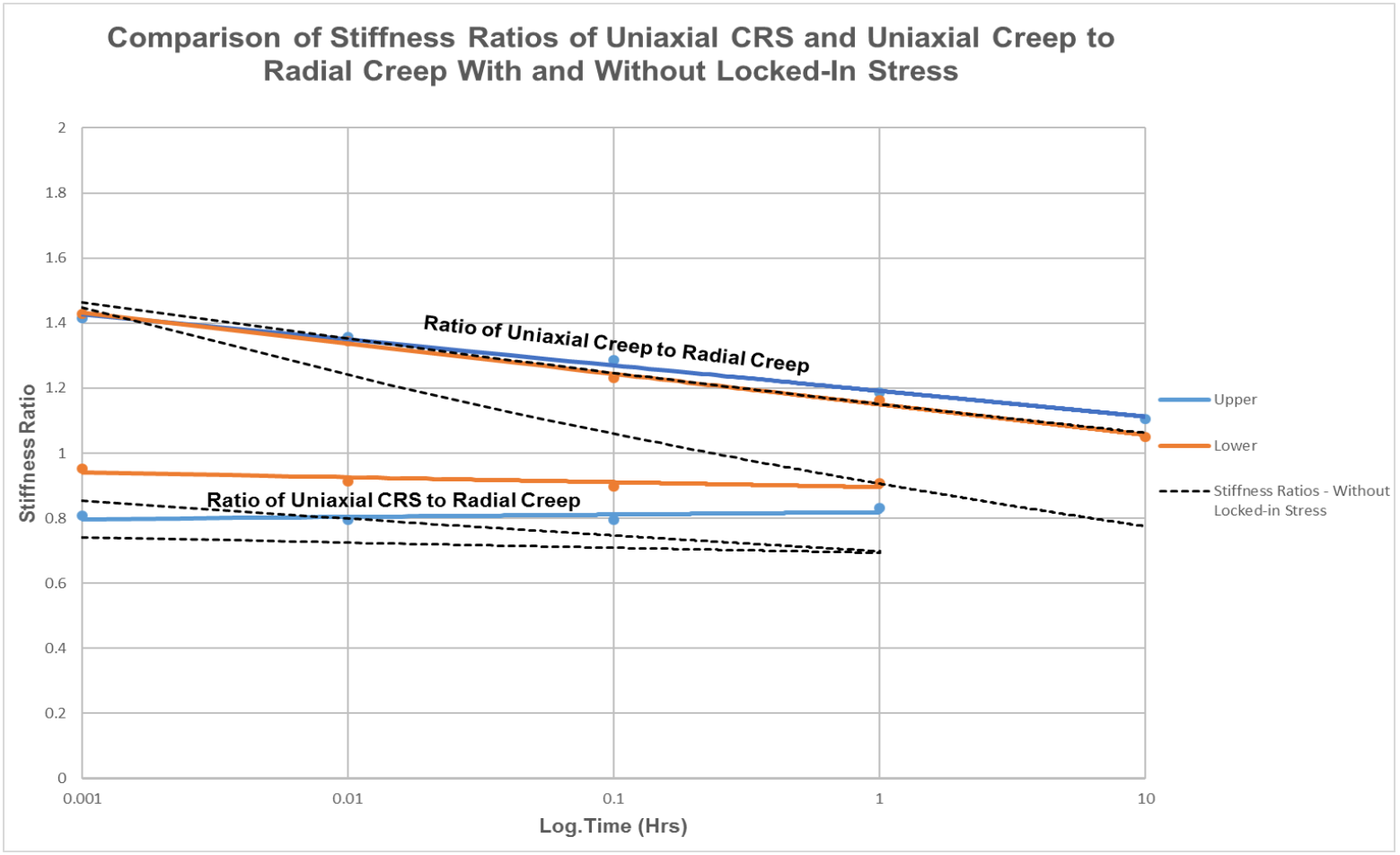


Fig 7.22 – Comparison of Stiffness Ratios of Uniaxial Creep-to-Radial Creep and Uniaxial CRS-to-Radial Creep with and without locked-in stress.

PLATES

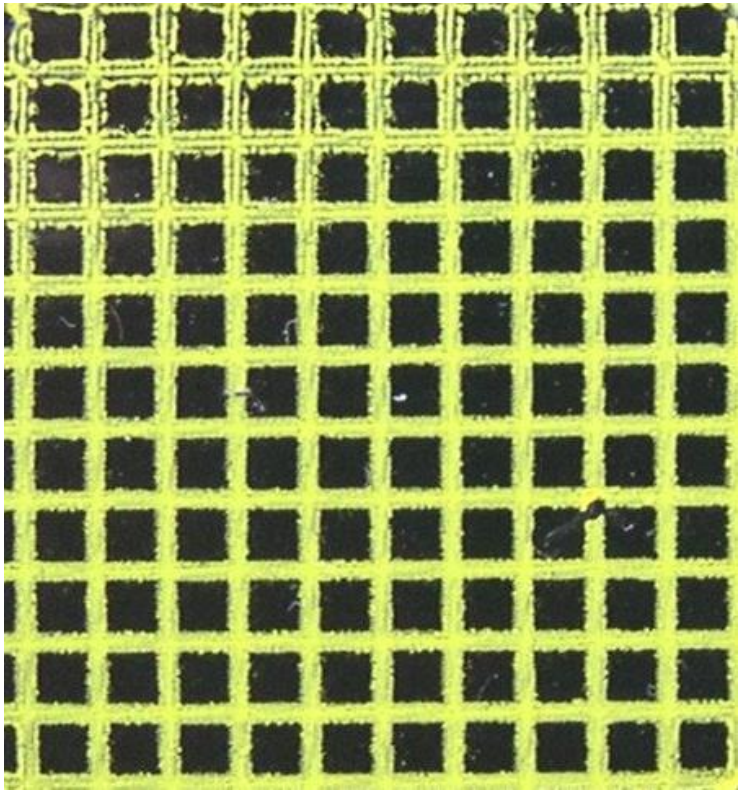


Plate 2.1 – Close up of 1mm x 1mm screen printed regular orthogonal lines.

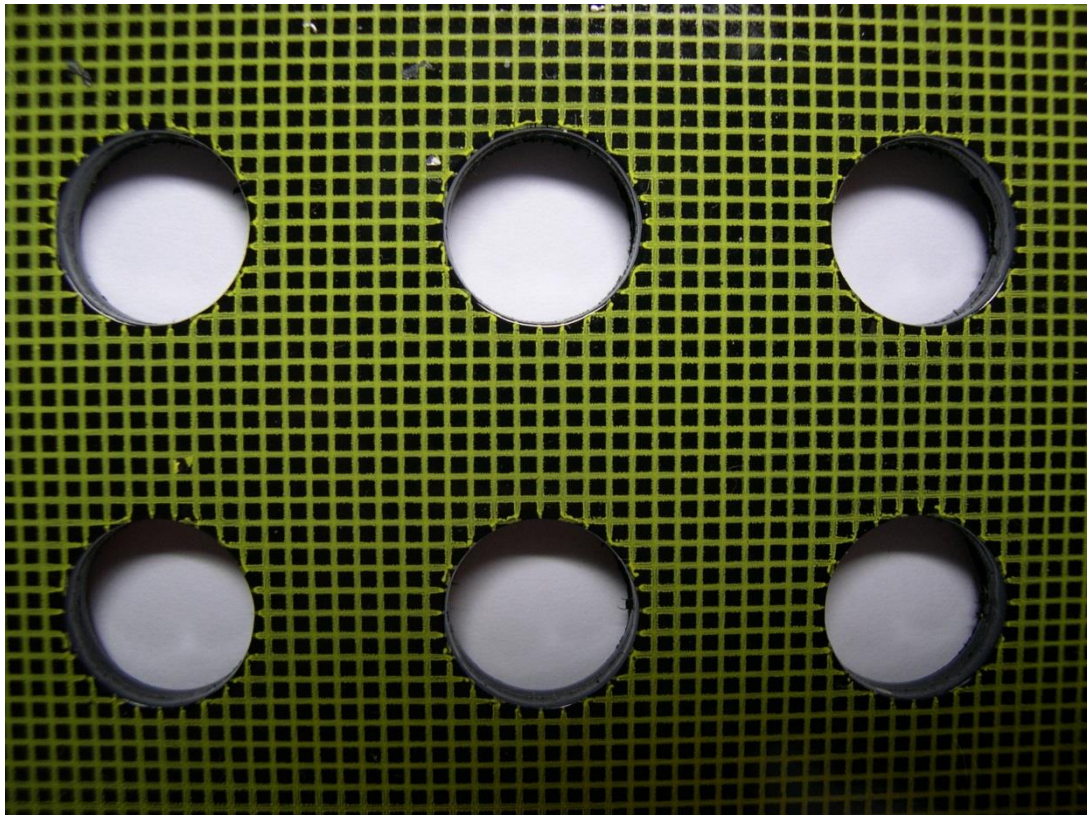


Plate 2.2 – A 1mm x 1mm screen printed punched sheet.

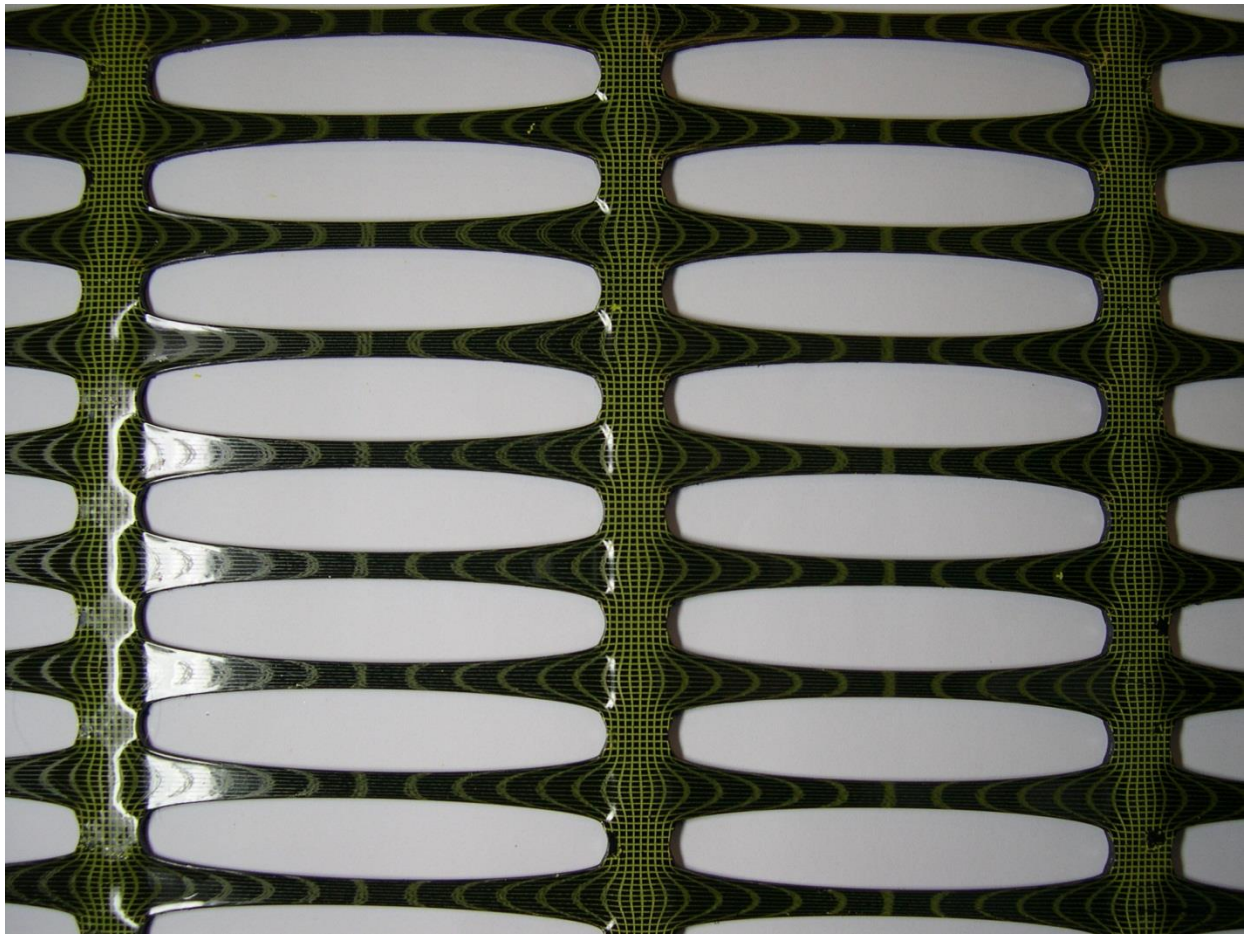


Plate 2.3 – Stretched screen printed sample of Tensar SR2.

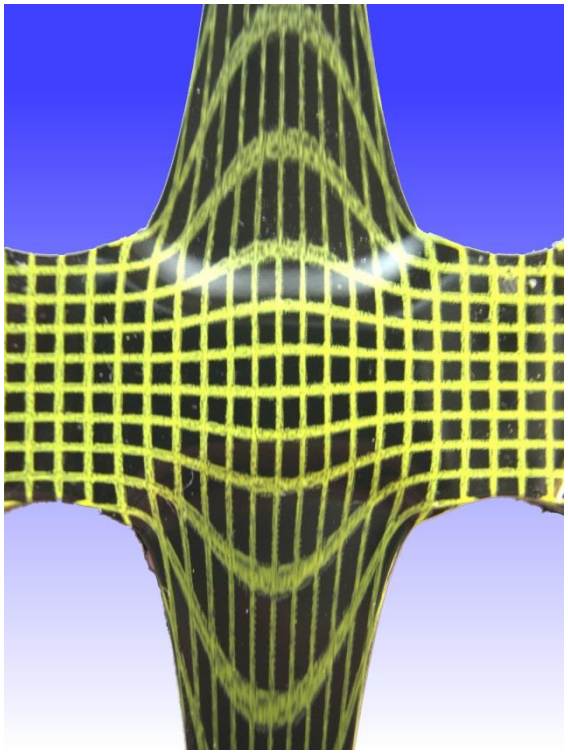


Plate 2.4 – Detail of the screen printing at the junction after stretching.

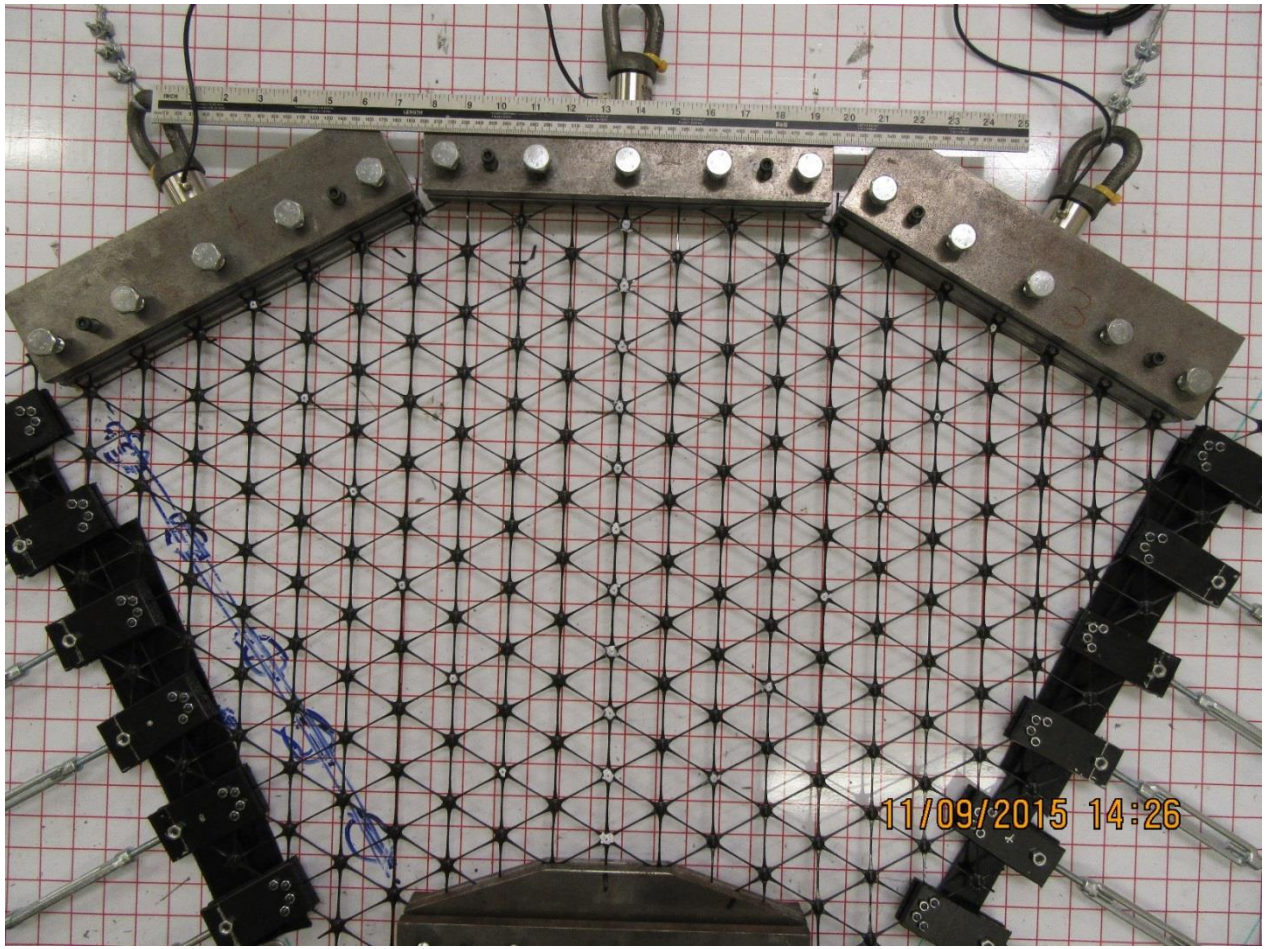


Plate 6.1 – Trial quadrant radial creep test example (for 30° & 90° direction), no load applied.

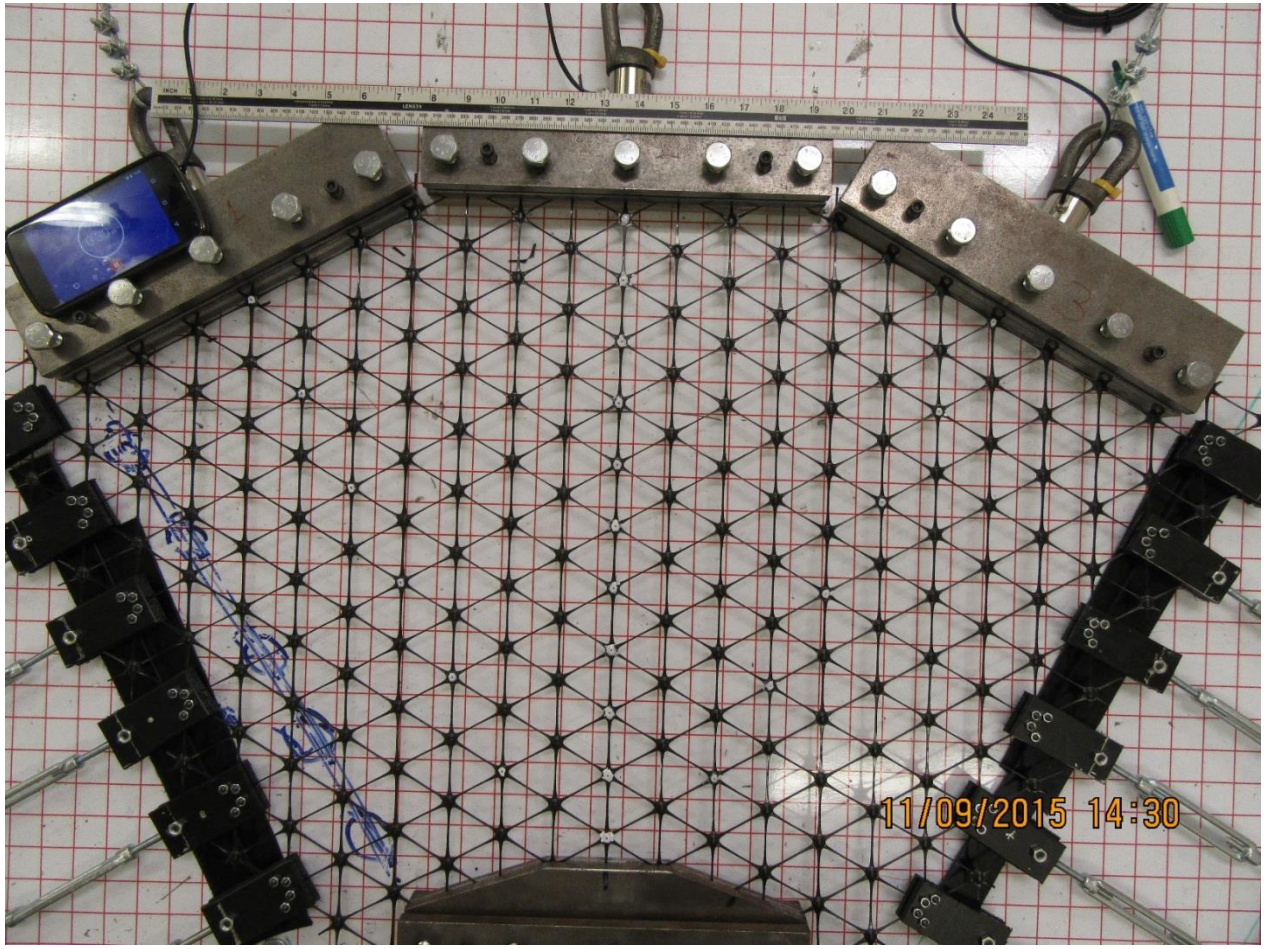


Plate 6.2 – Trial quadrant radial creep test example (for 30° & 90° direction), 40kg load applied to each outer clamp. 30 second interval.

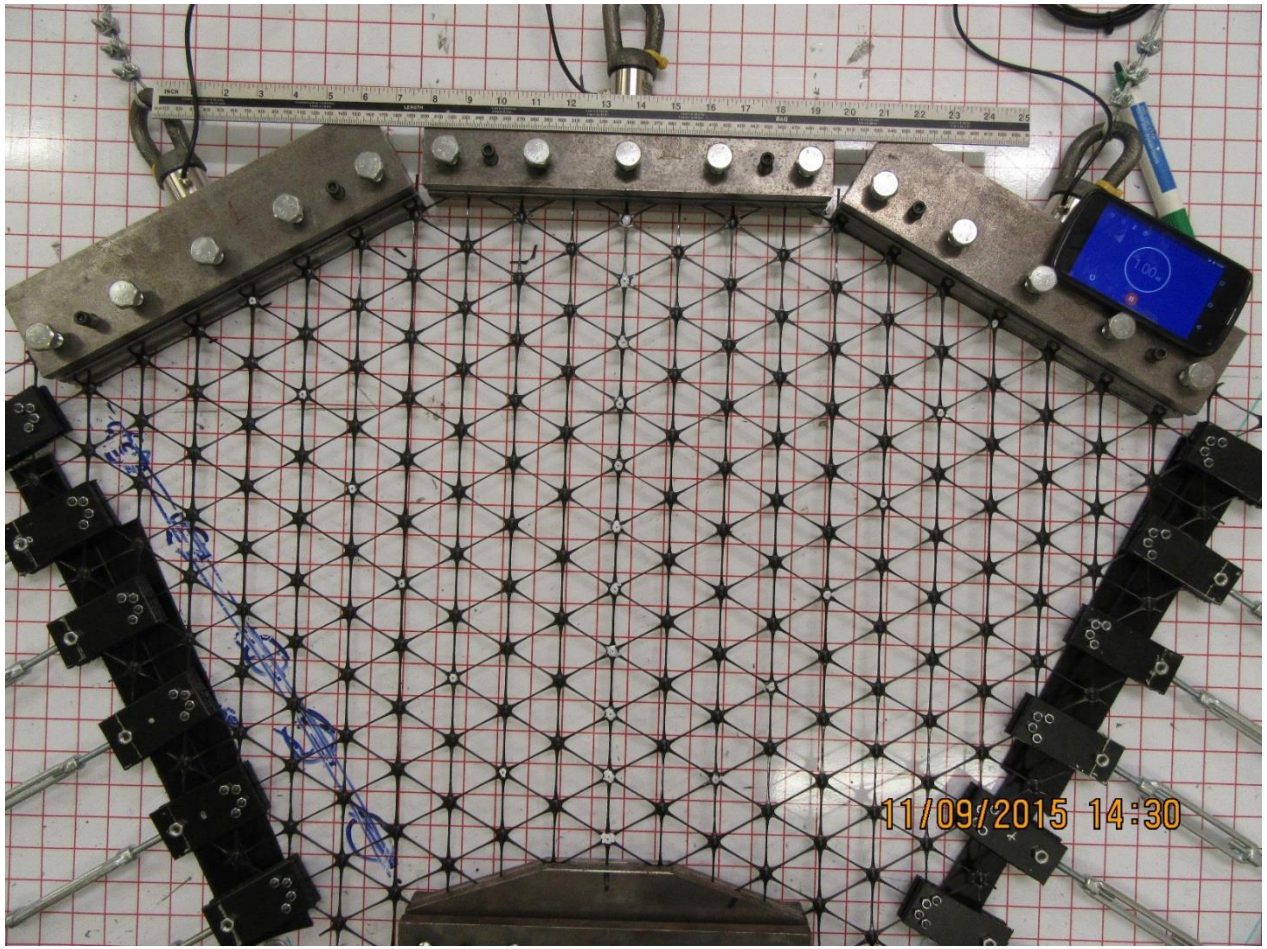


Plate 6.3 – Trial quadrant radial creep test example (for 30° & 90° direction), 40kg load applied to each outer clamp. 1 minute interval.

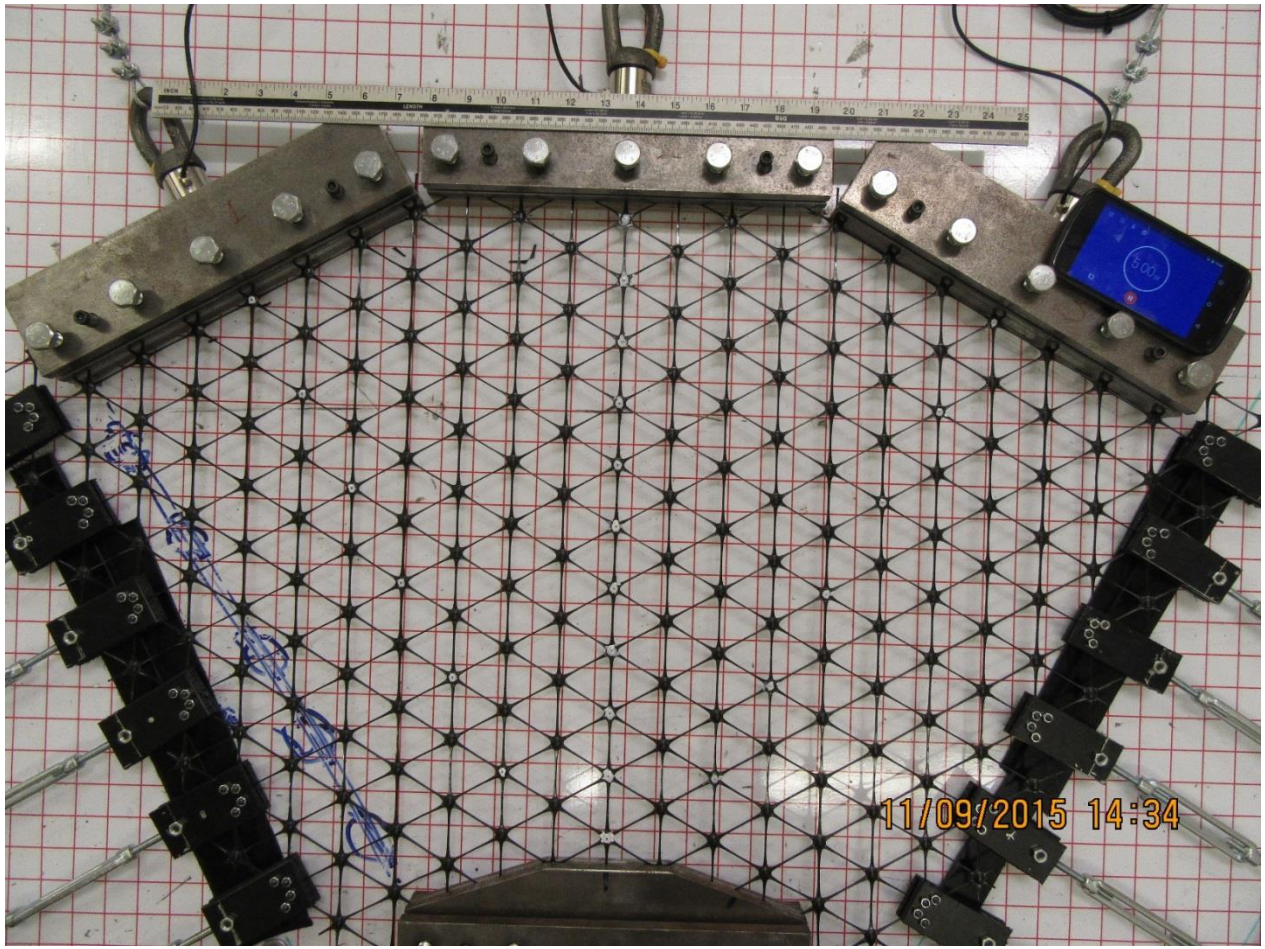


Plate 6.4 – Trial quadrant radial creep test example (for 30° & 90° direction), 40kg load applied to each outer clamp. 5 minute interval.

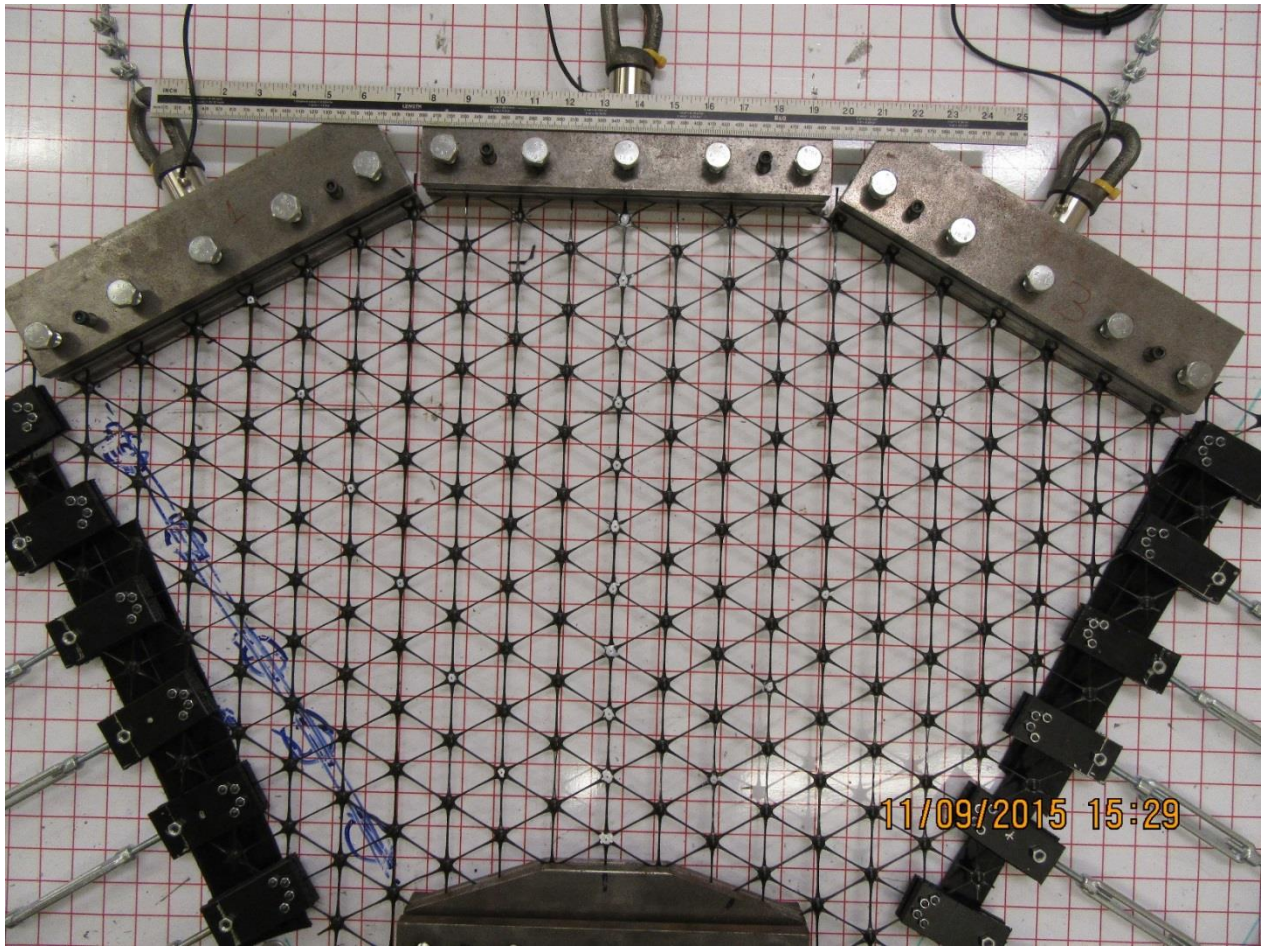


Plate 6.5 – Trial quadrant radial creep test example (for 30° & 90° direction), 40kg load applied to each outer clamp. 1 hour interval.

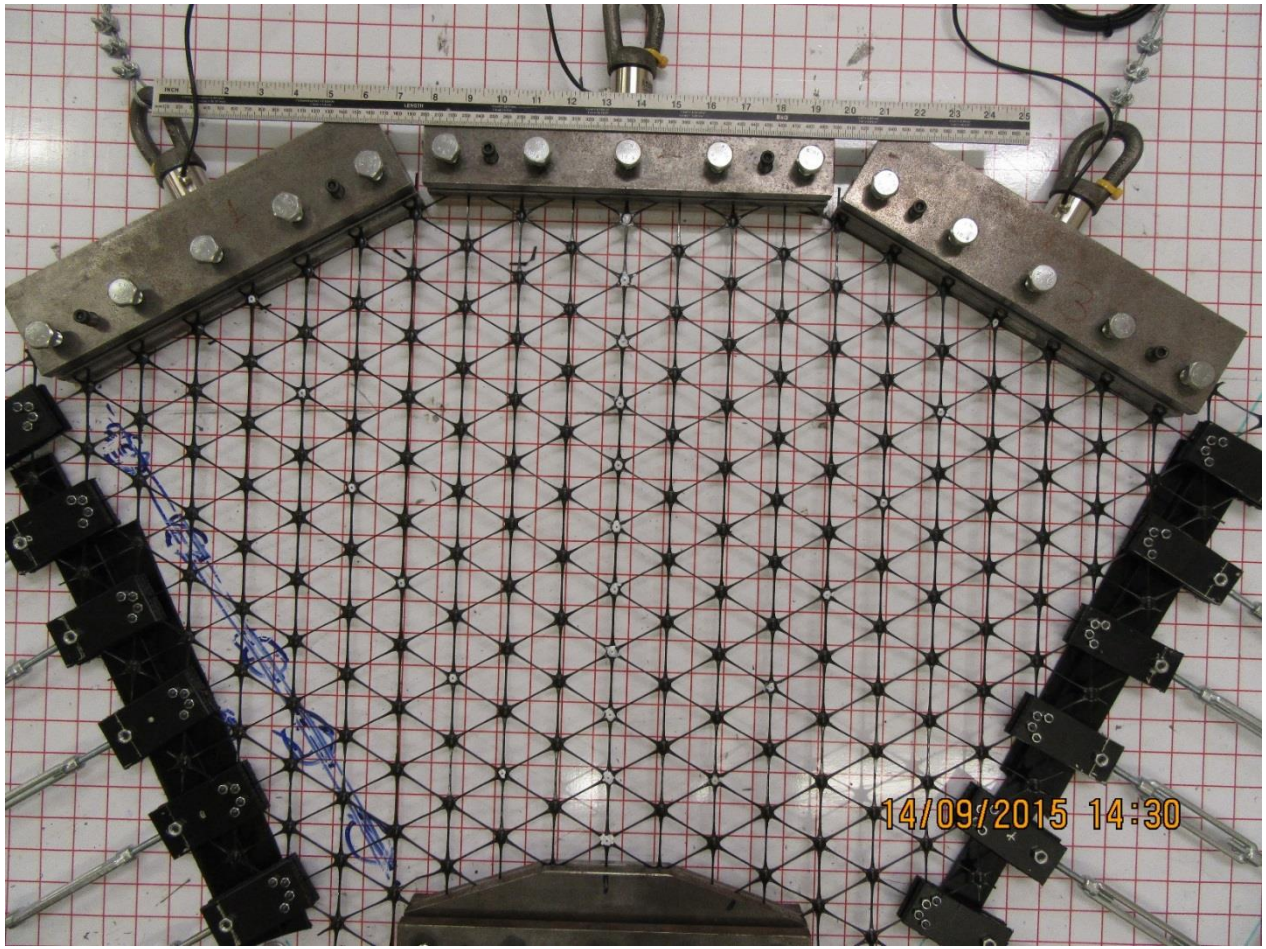


Plate 6.6 – Trial quadrant radial creep test example (for 30° & 90° direction), 40kg load applied to each outer clamp. 72 hour interval.